# PTTG, PBF AND p53 IN HEAD AND NECK CANCER

By

Bhavika Modasia

A thesis presented to the College of Medical and Dental Sciences at the University of Birmingham for the Degree of Doctor of Philosophy

Institute of Metabolism and Systems Research

School of Clinical and Experimental Medicine

College of Medical and Dental Sciences

September 2016

# ABSTRACT

Head and neck squamous cell carcinoma (HNSCC) is the 6$^{th}$ most common cancer worldwide and poses a significant health burden due to its rising incidence. The proto-oncogene PTTG is overexpressed in HNSCC and correlates with poor patient prognosis. A recent unpublished GEO profile cDNA array analysis has further suggested a potential upregulation of its binding partner PBF in HNSCC. PTTG and PBF cause transformation *in vitro* and tumour formation *in vivo*, both effects thought to be partly mediated by their interactions with the tumour suppressor protein p53. Dysregulation of the p53 pathway is frequently observed in HNSCC, thus alluding to the importance of functionally active p53 in the suppression of HNSCC initiation and progression. The work presented in this thesis describes the functional relationship between PTTG, PBF and p53 in HNSCC. Initial studies confirmed that PTTG and PBF are overexpressed in HNSCC tumours compared to matched normal tissue. In addition, high tumoural PTTG expression correlated with HPV status, whereas high tumoural PBF expression was associated with a significant gender bias. Further investigations established that PTTG and PBF functionally interact with p53 and cooperate to reduce p53 protein stability in HNSCC cells. Moreover, attenuation of PTTG or PBF expression led to dysregulated expression of p53-related genes involved in DNA repair and apoptosis, indicating that both proto-oncogenes may serve to promote genomic instability and HNSCC cell survival. Functionally, depletion of PTTG or PBF significantly repressed cellular migration and invasion, and impaired colony formation in HNSCC cells.

Overall, this research has provided novel insights into the roles of PTTG and PBF in HNSCC tumour initiation and progression, through modulation of p53 activity and function.

# DEDICATION

To my parents and sister.

# ACKNOWLEDGMENTS

I would like to thank my supervisors Professor Chris McCabe and Professor Hisham Mehanna for their excellent support and guidance throughout this PhD project. I would also like to express thanks to Dr Martin Read, Dr Vicki Smith and Dr Kristien Boelaert for their time, patience and invaluable advice, Dr Gavin Ryan for his guidance and helpfulness in teaching me new techniques, Dr Grant Stewart and Dr Kabir Khan for their guidance on lentiviral RNAi expression systems, Dr Rasoul-Amel Kashipaz for assisting in the evaluation of the tissue microarray slides and Mrs Hannah Nieto for her medical insight and advice. Acknowledgments must also be made to the inHANSE team for providing the tissue specimens, use of their immunohistochemistry facilities, and their endless support and guidance.

I am also grateful to all my friends in Birmingham for their great support and friendship, as well as everyone else on the 2nd floor IBR for making my Ph.D a memorable experience. I would particularly like to thank Lorna, Pushpa, Alice and Waraporn for helping me through some difficult times and for keeping me sane.

Finally I would like to dedicate a special thank you to my parents and my sister for their love, support and perseverance. I would not have been able to complete this Ph.D without you.

This research was funded by the Wellcome Trust.

# TABLE OF CONTENTS

# LIST OF FIGURES

# LIST OF TABLES

# LIST OF ABBREVIATIONS

| | |
|---|---|
| **APC/C** | Anaphase promoting complex/cyclosome |
| **BAX** | BCL-2 associated protein X |
| **BCL-2** | B-cell lymphoma 2 |
| **BRCA1** | Breast cancer type 1 susceptibility protein |
| **BSA** | Bovine serum albumin |
| **Cas9** | CRISPR-associated protein 9 |
| **CDK** | Cyclin-dependent kinase |
| **CHEK1** | Checkpoint kinase 1 |
| **ChIP** | Chromatin immunoprecipitation |
| **co-IP** | Co-immunoprecipitation |
| **CRISPR** | Clustered regularly interspaced short palindromic repeats |
| **CTTN** | Cortactin |
| **DDR** | DNA damage response |
| **DNA** | Deoxyribonucleic acid |
| **DNA-PK** | DNA-dependent protein kinase |
| **DSB** | DNA double-strand break |
| **EBV** | Epstein-Barr virus |
| **ECM** | Extracellular matrix |
| **EGFR** | Epidermal growth factor receptor |
| **EMT** | Epithelial-to-mesenchymal transition |
| **ERE** | Oestrogen response element |
| **ERα** | Oestrogen receptor α |
| **ESCC** | Oesophageal squamous cell carcinoma |
| **FFPE** | Formalin-fixed, paraffin-embedded |
| **FGF** | Fibroblast growth factor |
| **GST** | Glutathione-S-transferase |
| **HDM2** | Human double minute 2 homologue |
| **HNSCC** | Head and neck squamous cell carcinoma |
| **HPV** | Human papillomavirus |
| **HR** | Homologous repair |
| **LB** | Lysogeny broth |
| **LSCC** | Laryngeal squamous cell carcinoma |
| **MAPK** | Mitogen activated protein kinase |
| **MDM2** | Mouse double minute 2 homologue |
| **miRNA** | microRNA |
| **MMP** | Matrix metalloproteinase |
| **mRNA** | Messenger RNA |

| | |
|---|---|
| **MYC** | Myelocytomatosis viral oncogene homologue |
| **NF-d$H_2O$** | Nuclease-free deionised water |
| **NHEJ** | Non-homologous end joining |
| **NLS** | Nuclear localisation signal |
| **NSCC** | Nasopharyngeal squamous cell carcinoma |
| **OPSCC** | Oropharyngeal squamous cell carcinoma |
| **OSCC** | Oral squamous cell carcinoma |
| **PBF** | PTTG-binding factor |
| **PBS** | Phosphate buffered saline |
| **PCR** | Polymerase chain reaction |
| **PhI** | Phosphatase inhibitor |
| **PI** | Protease inhibitor |
| **PI3K** | Phosphatidylinositol 3-kinase |
| **PIK3CA** | Phosphatidylinositol-4,5-bisphosphate 3-kinase |
| **PLA** | Proximity ligation assay |
| **PTEN** | Phosphatase and tensin homologue |
| **PTTG** | Pituitary tumor transforming gene |
| **RNAi** | RNA interference |
| **shRNA** | Short hairpin RNA |
| **siRNA** | Short interfering RNA |
| **STR** | Short tandem repeat |
| **SUMO** | Small ubiquitin-like modifier |
| **SV40** | Simian virus 40 |
| **TBS** | Tris-buffered saline |
| **TMA** | Tissue microarray |
| **TNM** | Tumour, Node, Metastasis |
| **UTR** | Untranslated region |
| **v/v** | Volume to volume ratio |
| **VEGF** | Vascular endothelial growth factor |
| **VO** | Vector only |
| **w/v** | Weight to volume ratio |
| **WT** | Wild-type |

# Chapter 1

# General Introduction

## 1.1 Head and neck cancer

### 1.1.1 Basic anatomy of the head and neck

Head and neck cancers are a heterogeneous group of malignancies originating from one of the many anatomical sites within the head and neck region. The anatomical sub-sites are presented in Figure 1.1 and include the nasal cavity, nasopharynx, oropharynx, hypopharynx, oral cavity and larynx. Approximately 90 % of head and neck cancers are of squamous cell origin and arise in the mucosal epithelium lining of the upper aerodigestive tract (Argiris et al. 2008). Collectively, they are termed head and neck squamous cell carcinoma (HNSCC). The remaining tumours are of non-squamous cell origin and include salivary gland tumours, malignant melanoma and sarcomas of the soft tissue or jawbone (Argiris et al. 2008).

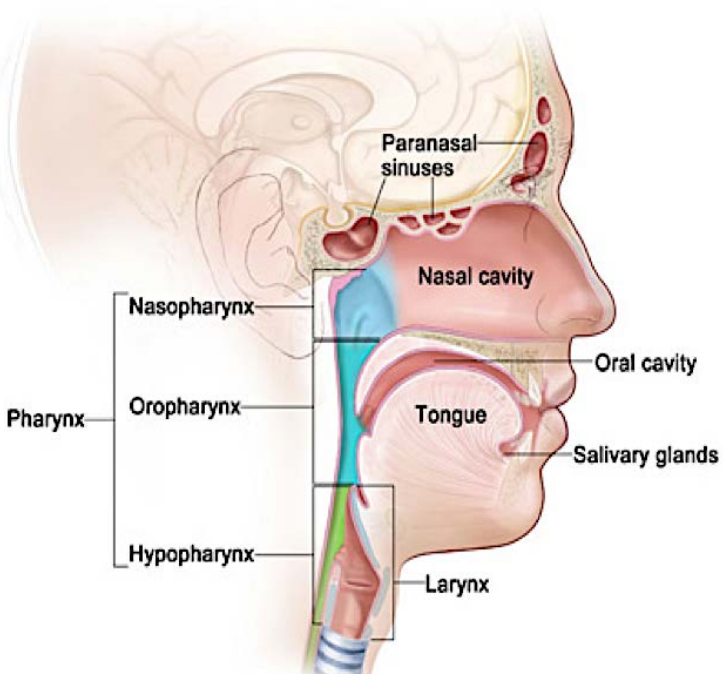


*Figure 1.1 Anatomical sites and sub-sites of the human head and neck. Illustration showing the sites and sub-sites of head and neck cancer (figure from National Cancer Institute 2013).*

### 1.1.2 Epidemiology and incidence of head and neck cancer

Head and neck cancer is the sixth most common cancer by incidence worldwide, with approximately 687,000 new cases diagnosed in 2015 alone (Torre et al. 2015, Ferlay et al. 2015). However, there is considerable geographical variation in the incidence and anatomical distribution of HNSCC. This variation has mainly been attributed to differences in lifestyle factors, such as tobacco and alcohol consumption, which are common risk factors (Blot et al. 1988, Franceschi et al. 1990). For example, the highest incidence rates are found in Southeast Asia and India (Siegel et al. 2016). In these regions, HNSCC represents 40-50 % of all diagnosed malignancies and is due to increased consumption of betel quid and tobacco (Siegel et al. 2016). Additional risk factors, such as HPV infection, which are unique to specific anatomical sub-sites, have also contributed to differing trends in geographical incidence.

In the UK, the overall incidence appears to be on the rise, having increased by 92 % in Great Britain alone since the 1970s (Figure 1.2) (Cancer Research UK 2016). However significant differences in HNSCC incidence have been reported for the various anatomical sub-sites. For example, the incidence rates for oral squamous cell carcinoma (OSCC) and OPSCC in England increased by 39 % and 67 %, respectively between 1995 and 2011 (Louie et al. 2015). Conversely, the incidence of laryngeal (LSCC) and nasopharyngeal (NSCC) squamous cell carcinoma decreased over the same period of time (Louie et al. 2015). In addition, HNSCC appears to affect older individuals, with approximately 45 % of annual cases being diagnosed in patients aged 65 years and above (Cancer Research UK 2016). Men also have a 3-times greater risk of developing HNSCC than females, although the rate of incidence in females has increased at a similar rate (Ferlay et al. 2015).

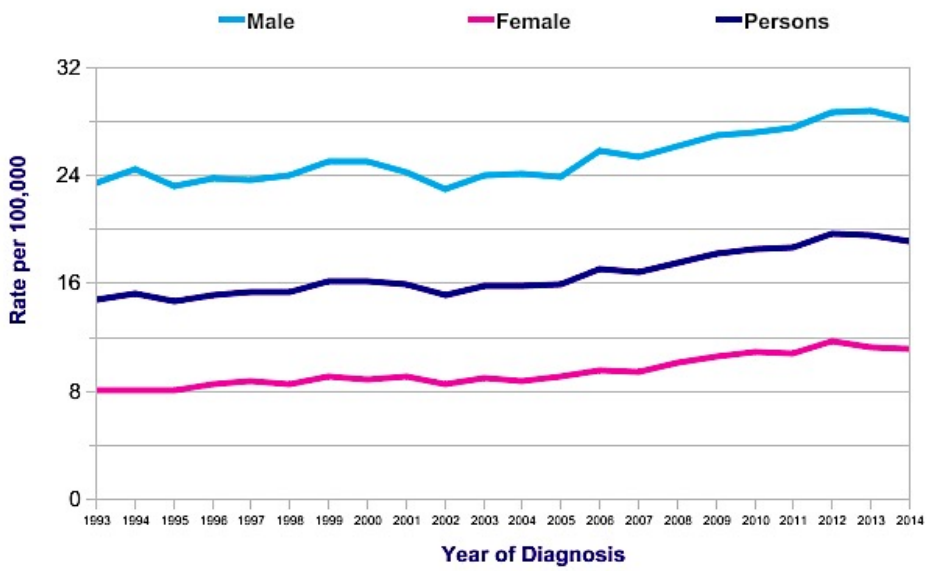


*Figure 1.2 Head and neck cancer incidence in the UK. European age-standardised head and neck cancer (ICD-10 C00-C14 C30-C32) incidence rates per 100,000 population between 1993 and 2014 in the UK.*

### 1.1.3 Risk factors for developing head and neck cancer

#### *1.1.3.1 Tobacco and alcohol*

There are several well-documented risk factors for developing HNSCC. Tobacco and excessive alcohol consumption represent the most important risk factors, together accounting for more than 75 % of all diagnosed HNSCC cases (Blot et al. 1988). As a result, their relative contributions have been extensively examined. Blot et al. were the first to describe an association between cigarette smoking and head and neck cancer (Blot et al. 1988). This was more recently confirmed in a pooled analysis of 15 case-control studies involving 10,244 head and neck cancer case subjects, which demonstrated a 2-fold increased risk of head and neck cancer in cigarette smokers compared to never users (Hashibe et al. 2007). Importantly, a strong dose-response relationship was observed, with the risk of developing HNSCC rising with the frequency, duration and number of pack-years of cigarette smoking (Hashibe et al. 2007).

The risk of HNSCC is not just limited to cigarette smoking. Cigar and pipe smoking impact upon the risk of developing HNSCC, with an odds ratio (OR) of 2.54 (95 % CI: 1.93, 3.34) and 2.08 (95 % CI: 1.55, 2.81) reported for cigar smokers and pipe smokers, respectively (Wyss et al. 2013). The use of smokeless tobacco, particularly chewing of betel quid, has become an increasing international problem and has also been linked to the development of oral cancer (Travasso 2013). Betel quid is widely consumed in the Indian subcontinent and is a combination of betel leaf, areca nut, slaked lime and, often tobacco too. The OR of OSCC or OPSCC was 7.74 (95 % CI: 5.38, 11.13) for betel quid with tobacco, whereas, the OR was reduced to 2.56 (95 % CI: 2.00, 3.28) for betel quid without tobacco (Travasso 2013).

Heavy alcohol consumption (> 3 drinks per day) has also been implicated as an independent aetiological factor in HNSCC, displaying a dose-response relationship similar to that observed with cigarette smoking (Blot et al. 1988, Hashibe et al. 2007, Purdue et al. 2009). However this association was limited to oropharyngeal, hypopharyngeal and laryngeal cancers only (OR: 2.04, 95 % CI: 1.29, 3.21) (Blot et al. 1988, Hashibe et al. 2007). Interestingly, the effects of tobacco and alcohol consumption appear to be multiplicative, increasing the risk of developing HNSCC by more than 35-fold (Blot et al. 1988).

*1.1.3.2 Viral infection*

Viral infection is also recognised as an important aetiological factor in HNSCC. The first reported association was between the Epstein-Barr virus (EBV) and undifferentiated nasopharyngeal squamous cell carcinoma (Old et al. 1966). Antibodies to EBV were detected in the sera of African and American patients with nasopharyngeal cancer (Old et al. 1966). Further investigations demonstrated the presence of circulating EBV DNA in approximately 96 % of nasopharyngeal cancer patients compared to only 7 % of healthy control patients (Lo

et al. 1999). Moreover, higher levels of circulating EBV DNA were significantly correlated with poorer prognosis (Lo et al. 2000).

In recent years, mucosotropic high-risk human papilloma viruses (HPV), in particular HPV-16, have been implicated as an independent factor in the aetiology of HNSCC. Whilst HPV infection has been associated with cancers of the oral cavity, the strongest association is with OPSCC (OR: 6.2, 95 % CI: 3.1, 12.1) (Schwartz et al. 1998, Gillison et al. 2000). HPV genomic DNA has frequently been detected in the nuclei of OPSCC tumour cells, as well as lymph node metastases, but not in the surrounding pathologically normal tissue (Gillison et al. 2000, Kreimer et al. 2005). Active transcription of the viral oncogenes E6 and E7 has also been documented in OPSCC tumours (van Houten et al. 2001). Furthermore, serum antibodies against these viral oncogenes have been detected in up to 65 % of OPSCC tumours (D'Souza et al. 2007).

*1.1.3.3 Genetic factors*

Although HNSCC tends to occur sporadically, a familial history has been described, thus demonstrating that genetic predisposition may contribute to HNSCC susceptibility (Negri et al. 2009). Furthermore, the risk of developing HNSCC appears to be increased in individuals with cancer susceptibility syndromes, such as Li-Fraumeni syndrome, Fanconi's anaemia and ataxia telangiectasia (Foulkes et al. 1996). Genetic polymorphisms have been identified in key DNA repair genes and enzymes required for the metabolism of tobacco and alcohol (Varela-Lema et al. 2008, McKay et al. 2011, Cadoni et al. 2012). For example, a meta-analysis of 30 case-control studies has demonstrated a significant association between certain polymorphisms in the metabolic enzymes, Glutathione S-Transferase Mu 1(GSTM1) and Cytochrome P450 family member A1 (CYP1A1) and OPSCC (Varela-Lema et al. 2008).

### 1.1.4 Diagnosis of head and neck cancer

To make a definitive diagnosis of head and neck cancer, patients usually undergo an endoscopy under anaesthetic to allow further clinical examination of the primary tumour. A histological diagnosis in most cases is mandatory and so a core biopsy is also taken for histological examination. Ultrasound-guided fine needle aspiration cytology (FNA) may also be performed as part of the diagnostic assessment of patients presenting with neck lumps or to diagnose lymph node metastases (Roland et al. 2016). Following confirmation of the suspected diagnosis of head and neck cancer, additional imaging is required to complete assessment, classification and staging of the patient's tumour. Investigations usually include computed tomography (CT) and/or magnetic resonance imaging (MRI) scans of the head, neck and chest regions, to delineate the size and extent of the primary tumour and to assess and locate nodal metastases (Roland et al. 2016).

### 1.1.5 Management of head and neck cancer

#### *1.1.5.1 Staging*

In the UK, head and neck cancers are staged according to the TNM classification, which describes the **T**umour size, **N**odal status and the presence or absence of **M**etastases. The TNM classification for head and neck cancer varies depending on the primary tumour site and sub-site. However, an example of the TNM staging for oropharyngeal cancer is provided in Table 1.1.

| Stage | Description |
|---|---|
| ***Primary tumour (T)*** | |
| **TX** | Primary tumour cannot be assessed |
| **T0** | No evidence of primary tumour |
| **Tis** | Carcinoma in situ |
| **T1** | Tumour ≤ 2 cm in greatest dimension |
| **T2** | Tumour > 2 cm but not more than 4 cm in greatest dimension. |
| **T3** | Tumour > 4 cm in greatest dimension or extension to lingual surface of the epiglottis |
| **T4a** | Tumour invades the larynx, deep/extrinsic muscle of the tongue, medial pterygoid, hard palate or mandible. |
| **T4b** | Tumour invades lateral pterygoid plates, lateral nasopharynx or skull base, or encases the carotid artery. |
| ***Regional lymph nodes (N)*** | |
| **NX** | Regional nodes cannot be assessed |
| **N0** | No regional lymph node metastasis |
| **N1** | Metastasis in a single ipsilateral lymph node ≤ 3 cm in greatest dimension |
| **N2** | Metastasis in a single ipsilateral lymph node > 3 cm but not more than 6 cm in greatest dimension; or in bilateral or contralateral lymph nodes, none > 6 cm in greatest dimension |
| **N2a** | Metastasis in a single ipsilateral lymph node > 3 cm but no more than 6 cm in greatest dimension |
| **N2b** | Metastasis in multiple ipsilateral lymph nodes, none > 6 cm in greatest dimension |
| **N2c** | Metastasis in bilateral or contralateral lymph nodes, none > 6 cm in greatest dimension |
| **N3** | Metastasis in a lymph node > 6 cm in greatest dimension |
| ***Distant metastasis (M)*** | |
| **M0** | No distant metastasis |
| **M1** | Distant metastasis |

*Table 1.1 TNM classification for oropharyngeal cancer (from Mehanna et al. 2016).*

#### *1.1.5.2 Treatment*

For head and neck cancers, the most frequently used treatment modalities are surgery and radiotherapy (Mehanna et al. 2010). However, the specific treatment strategy will depend on the primary tumour site/sub-site, the TNM staging and individual factors, for example the general health of the patient and patient preferences (Nutting 2016). Single modality treatment is most often used for early-stage tumours. Surgical excision and radiotherapy provide similar cure rates (Nutting 2016). Surgical excision usually achieves complete microscopic clearance

of the tumour, although for cancers where physical function is important, radiotherapy offers better organ preservation and future quality of life (Nutting 2016). For advanced tumours, the single modality approach usually leads to poor clinical outcome (Bhalavat et al. 2003). In these cases, chemoradiotherapy or a combination of surgery and post-operative radiotherapy tend to provide a better cure rate (Wolf et al. 1991, Bhalavat et al. 2003). For patients presenting with recurrent or metastatic disease, treatment options are limited and usually palliative (Mehanna et al. 2010). However, a recent phase III randomised trial involving recurrent HNSCC patients whose disease had progressed within six months of receiving platinum-based chemotherapy found that treatment with the therapeutic anti-PD-1 monoclonal antibody Nivolumab significantly extended the median overall survival by two months when compared with standard, single-agent therapy (methotrexate, docetaxel or Cetuximab) (Ferris et al. 2016). Furthermore, treatment with Nivolumab was associated with reduced toxicity grading and with improvements in patient-reported quality-of-life measures (Ferris et al. 2016).

### 1.1.6 Prognosis

The prognosis for patients with head and neck cancer is generally poor, although it varies considerably depending on the anatomical site of the primary tumour and the TNM classification (Mehanna et al. 2010). Patients with squamous cell carcinoma of the lip generally display the most favourable outcome, with a 5-year survival rate of approximately 90 %, whereas patients with squamous cell carcinoma of the hypopharynx tend to have the poorest outcome, with a 5-year survival rate of only 32 % (Siegel et al. 2016). Details of the 5-year survival rates for different head and neck cancer sites are presented in Table 1.2.

| Tumour site | 5-year survival rate (%) |
|---|---|
| Lip | 90 |
| Salivary gland | 73 |
| Oral cavity | 66 |
| Floor of mouth | 51 |
| Tongue | 49 |
| Oropharynx | 63 |
| Hypopharynx | 32 |

*Table 1.2 Survival rates for patients with head and neck cancer. 5-year survival rates (%) for patients diagnosed with head and neck cancer in the USA between 2005-2011 (from Siegel et al. 2016).*

Fewer than a third of head and neck cancer patients are diagnosed at early stage and approximately 50 % of patients who present with locally advanced disease will develop regional or distant relapses (Argiris et al. 2008, Ferlay et al. 2015). Furthermore, it is expected that ~55 % of patients diagnosed with head and neck cancer will die from their disease (Ferlay et al. 2015). Last year alone, there were 376,665 head and neck cancer-related deaths worldwide (Ferlay et al. 2015). In the UK, the age-standardised mortality rate has risen by 21 % over the last decade (Cancer Research UK 2016), with more than 9,600 deaths reported in 2015 (Ferlay et al. 2015).

## 1.2 Oropharyngeal squamous cell carcinoma

### 1.2.1 Basic anatomy of the oropharynx

The oropharynx is a subdivision of the pharynx and is located between the soft palate and superior border of the epiglottis. The structure comprises the soft palate, base of tongue (posterior one third of the tongue), palatine tonsils, lingual tonsils, the tonsillar pillars and posterior pharyngeal wall (Figure 1.3).

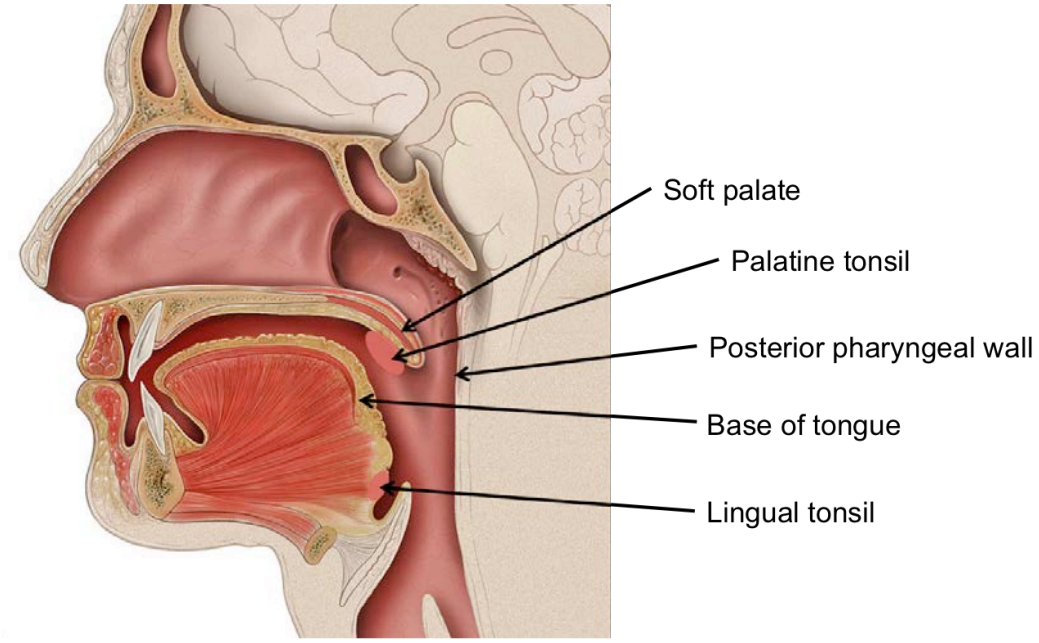


*Figure 1.3 Anatomical sub-sites of the human oropharynx. Illustration showing the sub-sites of the oropharynx (adapted from Lynch 2006).*

### 1.2.2 Epidemiology and incidence of oropharyngeal squamous cell carcinoma

Several studies have reported a dramatic rise in the prevalence of OPSCC, most notably among younger individuals (Chaturvedi et al. 2008, Chaturvedi et al. 2013). In the UK, the incidence of OPSCC has more than doubled between 1990 and 2006 (Price et al. 2010). A significant increase in OPSCC incidence has also been observed in other economically developed countries, including the US, Australia, Japan, Canada and Slovakia (Chaturvedi et al. 2013).

This global increase in OPSCC incidence has mainly been attributed to oral HPV infection. Consistent with this, several studies have demonstrated a relatively high prevalence of HPV-16, particularly among younger HNSCC patients who are less likely to have a history of tobacco or heavy alcohol consumption and are also less likely to harbour TP53 mutations (Gillison et al. 2000, Kreimer et al. 2005, D'Souza et al. 2007, Chaturvedi et al. 2008, Mehanna et al. 2012, Chaturvedi et al. 2013). Furthermore, the majority of HPV-positive

HNSCC cases were found to be OPSCCs, with HPV-16 prevalence varying depending on OPSCC sub-site (Gillison et al. 2000, Kreimer et al. 2005, Attner 2013). However, a meta-analysis of 269 studies and 19,368 patients demonstrated that the overall HPV prevalence in OPSCC increased from 40 % in 2000 to 71 % in 2009 (Mehanna et al. 2012).

Importantly, tumour HPV status has been revealed to be a strong independent factor determining OPSCC patient prognosis (Gillison et al. 2000, Chaturvedi et al. 2008, Ang et al. 2010). Retrospective analyses have consistently demonstrated that HPV-positive OPSCC patients have considerably higher overall survival rates than HPV-unrelated OPC patients (3-year survival: 82 % vs. 57 %) (Gillison et al. 2000, Chaturvedi et al. 2008, Ang et al. 2010). Furthermore, HPV-positive OPSCC patients have been shown to respond better to a number of different treatment modalities and strategies when compared with HPV-negative OPSCC patients (Licitra et al. 2006, Fakhry et al. 2008, Ang et al. 2010).

Oral HPV infection is thought to be a sexually transmitted disease. A pooled analysis of eight separate multinational studies found that the risk of developing OPSCC was increased in participants who had a history of six or more lifetime sexual partners (OR: 1.25, 95 % CI: 1.01, 1.54), four or more lifetime oral sexual partners (OR: 2.25, 95 % CI: 1.42, 3.58) and, in males participants, an earlier age at sexual debut (OR: 1.59, 95 % CI: 1.09, 2.33) (Heck et al. 2010). It is therefore thought that the increasing incidence of HPV-positive OPSCC may be due to changes in sexual behaviour and practices.

### 1.2.3 Human papilloma virus

Human papilloma viruses are a diverse group of non-enveloped, circular double-stranded DNA viruses that infect the mucosal and cutaneous epithelia (Figure 1.4A). To date, most of the knowledge regarding the normal productive life cycle of these viruses has been obtained

from studies conducted on human foreskin keratinocytes and cervical cancer cell lines. HPV viral infection is thought to occur at the basal cell layer of keratinocytes through micro-wounding or micro-abrasion of the epithelium (Doorbar et al. 2012). Following successful infection of a basal keratinocyte, the early viral replication proteins E1 and E2 maintain the viral genome at low copy numbers in episomal form to avoid immune detection (Angeletti et al. 2002, Doorbar et al. 2012). As the basal keratinocytes migrate up in to the parabasal layers they begin to differentiate and lose their nuclei, at which point they are no longer able to proliferate. Viral genome amplification, however, is entirely dependent on the host replication machinery. The virus therefore initiates the expression of the early E6 and E7 oncoproteins, which drive proliferation of keratinocytes in the parabasal layers, thus enabling continued viral genome replication (Betiol et al. 2013). As the infected keratinocytes continue to differentiate, expression of the late viral L1 and L2 proteins is induced to allow packaging of the viral genome into infectious particles (Doorbar et al. 2012). The early viral E4 and E5 proteins are thought to support viral replication and maturation.

The two principal oncoproteins E6 and E7 disrupt critical cellular processes, such as cell proliferation, differentiation and apoptosis, thus retaining cells in a state favourable for virus replication. As such, they represent a crucial component in HPV-induced malignant transformation and progression. The most well known functions of E6 and E7 are their associations with the host tumour suppressor proteins p53 and Retinoblastoma (pRb), respectively (Figure 1.4B).

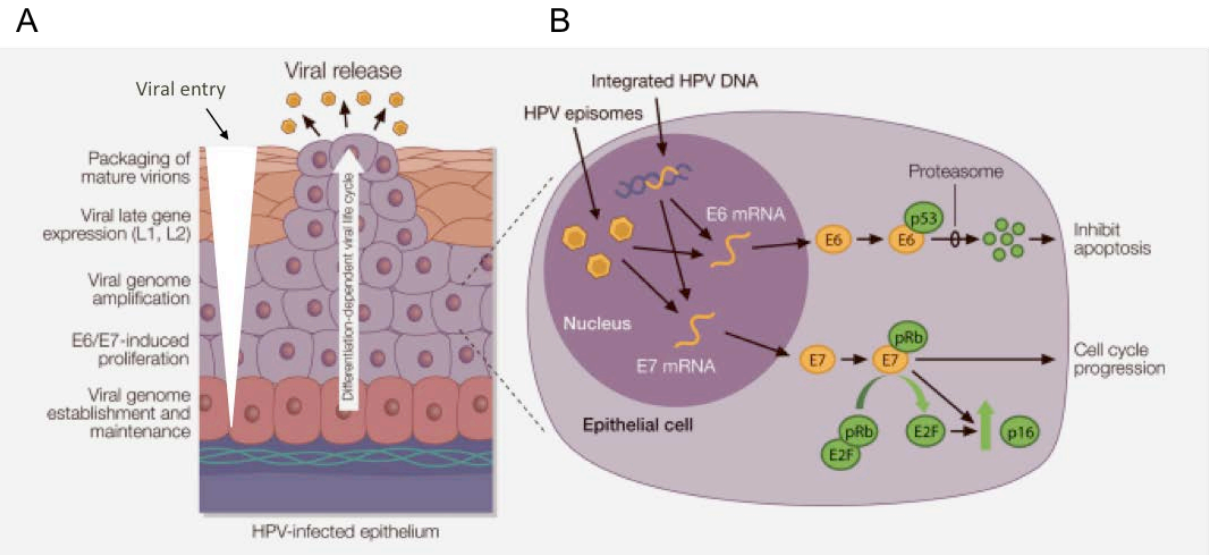


*Figure 1.4 The productive life cycle of HPV.* ***A*** *– HPV gains access to the basal cell layer of keratinocytes through a micro-wound in the epithelium. Following successful infection, the HPV genome is maintained at a low copy number. As the keratinocytes begin to differentiate and migrate in to the parabasal layers, expression of the viral oncoproteins E6 and E7 is induced to maintain keratinocytes in a proliferative state. Viral genome amplification and expression of the late viral proteins L1 and L2 is also induced as the keratinocytes continue to differentiate, thus allowing packaging of the amplified viral genomes in to infectious viral particles. The viral particles are thought to be released by natural tissue desquamation.* ***B*** *– The viral oncoproteins E6 and E7 target the tumour suppressor proteins p53 and pRb, respectively, for ubiquitination and subsequent proteasomal degradation. Degradation of pRb induces cell cycle progression and cell proliferation. Degradation of p53 prevents cell apoptosis, triggered by aberrant cell growth signals (adapted from Andersen et al. 2014).*

p53 is arguably one of the most critical 'cellular gatekeepers' owing to its ability to regulate cellular responses to DNA damage, deregulated cell growth and cell stress. It is a sequence-specific transcription factor that binds to p53 response elements upstream of numerous target genes, the majority of which encode proteins involved in cell cycle regulation, apoptosis, senescence, DNA repair and angiogenesis (Vogelstein et al. 2000, Levine, Oren 2009). The E6 oncoprotein is able to functionally inactivate p53 via two distinct mechanisms, thus inhibiting p53-mediated apoptosis. It associates with the HECT domain ubiquitin ligase E6-associated protein (E6AP) to induce the ubiquitination and subsequent proteasomal degradation of p53 (Scheffner et al. 1990, Scheffner et al. 1993). In addition, an

interaction between E6AP-bound E6 and the transcriptional co-activator CBP/p300 has been reported (Zimmermann et al. 1999). CBP/p300 is required for effective acetylation of p53, a post-translational modification that enhances p53 stability and transcriptional activity (Xie et al. 2013, Zimmermann et al. 1999).

The nuclear phosphoprotein pRb constitutes another major cell cycle regulator and is responsible for the regulation of the host-encoded E2F transcription factors. In the hypophosphorylated state, pRb represses transcription of E2F-responsive genes required for cell cycle progression (Giacinti, Giordano 2006). The pRb-E2F complex also recruits histone deacetylase 1 (HDAC1), which further represses gene transcription by deacetylating nucleosomes, leading to chromosome compaction (Brehm et al. 1998). Phosphorylation of pRb by the cyclin D1-CDK4/6 complex (whose activity is tightly regulated by the CDK inhibitor, p16/INK4) inactivates pRb resulting in the release of E2F and the subsequent transcription of S-phase genes (Giacinti, Giordano 2006). The viral E7 oncoprotein associates with the CUL2 multi-subunit ubiquitin ligase complex and targets pRb for proteasomal degradation, leading to deregulated cell proliferation (Munger et al. 1989, Huh et al. 2007). Aberrant cell proliferation usually triggers p53-mediated apoptosis. However, due to E6 inactivation of p53, cell apoptosis is inhibited, thus allowing further deregulated cell proliferation. However, whilst both viral oncoproteins act in concert to promote tumourigenesis, expression of E6 and E7 alone are insufficient for malignant progression (Munger et al. 1992). Given that not all HPV-infected individuals develop cancer, additional genetic alterations must be required.

## 1.3 The molecular biology of head and neck cancer

### 1.3.1 Molecular heterogeneity of head and neck cancer

Several lines of investigation have demonstrated that HNSCC is a heterogeneous group of malignancies, displaying vastly different biological and clinical features (Chung et al. 2004, Walter et al. 2013, Rampias et al. 2013, Keck et al. 2015, Cancer Genome Atlas Network 2015). Genetic profiling studies have identified numerous subclasses of HNSCC based upon their gene expression profiles. Chung et al. were the first to report four distinct HNSCC subtypes, which were associated with differing prognoses (Chung et al. 2004). These disease subtypes were later validated in an independent cohort of HNSCC patients and were referred to as basal (BA), mesenchymal (MS), atypical (AT) and classical (CL), based upon their molecular and morphological characteristics (Walter et al. 2013). Interestingly, these subtypes were consistent with gene expression patterns previously identified in squamous cell carcinomas of the lung (Cancer Genome Atlas Research Network 2012).

HNSCC patients who fell into the BA subgroup displayed the poorest clinical outcome and were associated with elevated expression of the growth factor and receptor TGFα and EGFR (Chung et al. 2004, Walter et al. 2013). On the other hand, gene expression in the AT subgroup was associated with a strong HPV-positive signature, with increased expression of CDKN2A (Chung et al. 2004, Walter et al. 2013). The subgroup also demonstrated the best clinical outcome (Chung et al. 2004, Walter et al. 2013). CL tumours had a gene expression pattern consistent with exposure to cigarette smoking, frequently demonstrating overexpression of the xenobiotic metabolism genes AKR1C1/3 and GPX2 (Chung et al. 2004, Walter et al. 2013). In contrast, tumours in the MS subgroup were found to overexpress several genes involved in epithelial-to-mesenchymal transition, such as the mesenchymal marker vimentin (Chung et al. 2004, Walter et al. 2013).

Further genomic analyses of datasets enriched for HPV-positive tumours have found that HPV-positive HNSCC can be further subdivided into two distinct subtypes based on differential gene expression (Keck et al. 2015). Additional HNSCC subtypes have also been identified based on unique epigenetic signatures (Lechner et al. 2013). Such heterogeneity amongst HNSCC tumours will undoubtedly have important implications, not only for tumour classification, patient prognostication and treatment planning, but also for research into the molecular mechanisms underlying HNSCC.

### 1.3.2 Pathogenesis of head and neck cancer

As with many cancers, the initiation and progression of HNSCC is thought to result from the gradual accumulation of genetic and epigenetic alterations in fundamental signalling pathways within the squamous epithelium. Many of these alterations have been identified in common premalignant lesions of HNSCC, such as oral leukoplakia, and further molecular and genetic analyses have elucidated a model of genetic progression from premalignant lesions to invasive carcinoma (Haddad, Shin 2008) (Figure 1.5). This large body of research has also highlighted the few oncogenes and tumour suppressor genes, which are frequently targeted by activating or inactivating mutations, gene expression changes and altered gene methylation in HNSCC tumourigenesis (Agrawal et al. 2011, Stransky et al. 2011, Lechner et al. 2013, Cancer Genome Atlas Network 2015). Some of the most critically altered signalling pathways are those involved in squamous epithelial cell proliferation, differentiation and survival, and are discussed in more detail below.

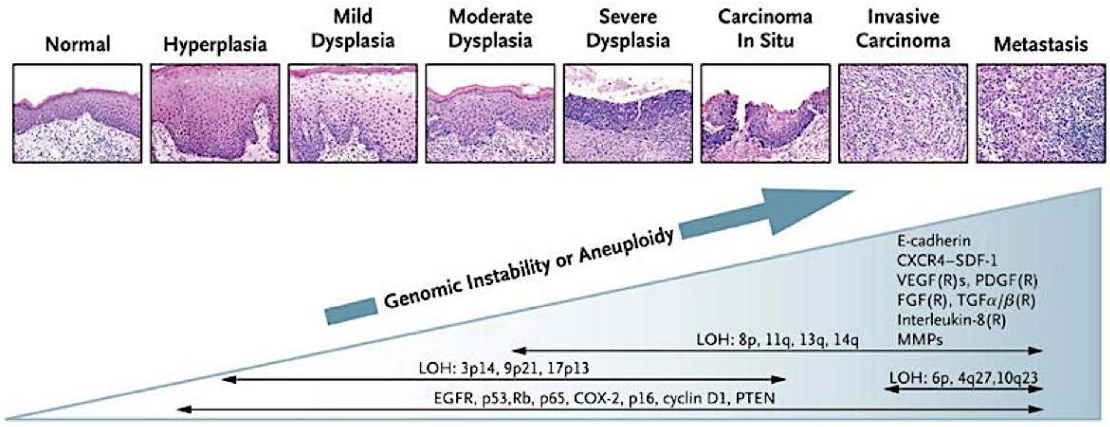


*Figure 1.5 Proposed model of the genetic progression of head and neck cancer. Head and neck cancer is thought to progress from a normal histological appearance through to metastatic carcinoma via a multi-step process, which involves the gradual accumulation of genetic and epigenetic alterations. These include loss of heterozygosity (LOH) of certain chromosomes and amplification/deletion or upregulation/downregulation of specific oncogenes and tumour suppressor genes (from Haddad, Shin 2008).*

### *1.3.2.1 Cell proliferation: p53 and pRb pathways*

The p53 and pRb tumour suppressor pathways play a vital role in the regulation of the cell cycle and dysregulation of both pathways remains a crucial early event in HNSCC tumourigenesis. TP53 mutations represent one of the most common genetic alterations in HNSCC. Next-generation sequencing efforts have found that TP53 mutations exist in approximately 50-80 % of HNSCC cases (Agrawal et al. 2011, Stransky et al. 2011). Furthermore, loss of p53 function through its interaction with the HPV E6 oncoprotein or loss of heterozygosity (LOH) is thought to occur in an additional 20 % of HNSCC tumours (Scheffner et al. 1990, Agrawal et al. 2011, Stransky et al. 2011). In the remaining tumours harbouring wild-type TP53, disruption of the p53 pathway may be achieved by specific targeting of p53-related genes. For example, gene amplification or upregulation of MDM2, a negative regulator of p53, is often found in HNSCC tumours (Denaro et al. 2011). Alternatively, these tumours may undergo p53-independent malignant progression (Leemans et al. 2011).

Similarly, inactivating mutations in the pRb pathway are often observed in HNSCC tumours. For example, the CCDN1 gene, which encodes cyclin D1, is frequently amplified or overexpressed in HPV-negative HNSCC tumours (Leemans et al. 2011). Furthermore, the CDKN2A gene, which is located on chromosome 9p21, is often inactivated through loss of heterozygosity and/or mutation or methylation (Reed et al. 1996). The CDKN2A gene encodes two cell cycle regulators, p16/INK4A and p14/ARF, which are involved in the negative regulation of the CDK4/6 cyclin-dependent kinases and MDM2, respectively. Loss of CDKN2A therefore promotes MDM2-mediated degradation of p53 and enables cells to bypass the cell cycle inhibitory effects of pRb. Functional inactivation of both p53 and Rb pathways in oral keratinocytes therefore leads to deregulated cell proliferation and cellular immortalisation (Smeets et al. 2011).

*1.3.2.2 Cell differentiation: NOTCH signalling pathway*

NOTCH signalling has been implicated in numerous biological processes, including regulation of the cell cycle, self-renewal capacity and cell survival (Rothenberg, Ellisen 2012). NOTCH signalling has also been reported to play a crucial role in regulating cell-fate decisions and has been proposed to modulate keratinocyte differentiation and maturation (Rangarajan et al. 2001, Nickoloff et al. 2002). Whole-exome sequencing studies have recently identified a significant number of inactivating NOTCH1 mutations in HNSCC tumours, with mutations present in approximately 15 % of patients (Agrawal et al. 2011, Stransky et al. 2011). Furthermore, additional mutations were identified in downstream NOTCH signalling pathway genes and NOTCH family members (Agrawal et al. 2011, Stransky et al. 2011). As the majority of genetic alterations were classified as inactivating mutations, it was hypothesised that NOTCH may act as a tumour suppressor in HNSCC (Agrawal et al. 2011).

Consistent with this finding, abrogation of NOTCH1 led to the formation of basal cell carcinoma-like tumours in NOTCH1-deficient mice following topical treatment with a chemical carcinogen (Nicolas et al. 2003). In addition, NOTCH1 has been shown to inhibit HPV E6 and E7 expression, further demonstrating a role for NOTCH1 in tumour suppression (Talora et al. 2002). However, recent investigations have uncovered a series of activating NOTCH1 mutations in Chinese patients with OSCC, thus suggesting that NOTCH signalling may promote malignant progression in a subset of HNSCC patients (Song et al. 2014, Sun et al. 2014). Activating mutations were present in 32-43 % of HNSCC tumours and were significantly correlated with lymph node metastasis and poor overall clinical outcome (Song et al. 2014, Sun et al. 2014).

*1.3.2.3 Cell survival: EGFR signalling pathway*

The epidermal growth factor (EGF) receptor (EGFR) is a member of the HER family of cell surface tyrosine kinase receptors, which acts upstream of the Ras/MAPK and PI3K/PTEN/Akt signalling pathways to orchestrate a number of biological functions, including cell proliferation and survival. The EGFR is ubiquitously overexpressed in HNSCC and has been associated with loco-regional recurrence and a reduction in overall and disease-free survival in HNSCC patients (Rubin Grandis et al. 1998, Ang et al. 2002, Keren et al. 2014). Furthermore, retroviral transduction of EGFR has been demonstrated to induce the *in vitro* transformation of normal oral keratinocytes (Goessel et al. 2005).

Genetic alterations in EFGR are relatively uncommon in HNSCC tumours. TCGA data analyses have detected EGFR gene alterations in only 14 % of HNSCC patients (Cerami et al. 2012, Gao et al. 2013). However, a variant of the receptor, known as EGFRvIII, has been reported in 42 % of HNSCC tumours (Sok et al. 2006). EGFRvIII is a constitutively active truncation mutant, which has been described in several other cancer types (Sok et al. 2006).

By contrast, genetic alterations in the downstream signalling effectors are much more common in HNSCC. PIK3CA encodes a positive regulator of the PI3K signal transduction pathway. The TCGA data revealed PIK3CA activating mutations and/or gene amplification in 37 % of HNSCC tumours (Cerami et al. 2012, Gao et al. 2013). The PI3K negative regulator PTEN is also targeted in up to 40 % of HNSCC tumours through loss of heterozygosity or inactivating mutation (Shao et al. 1998, Rothenberg, Ellisen 2012).

## 1.4 Pituitary Tumor Transforming Gene (PTTG)

### 1.4.1 The PTTG gene

PTTG was initially characterised by Pei et al. through mRNA differential display PCR to identify mRNAs highly expressed in rat pituitary tumour $GH_4$ cells but not expressed in normal pituitary tissue (Pei, Melmed 1997). The human homologue (hPTTG) was subsequently cloned and was found to be expressed in the thymus (Dominguez et al. 1998), foetal liver (Zhang et al. 1999) and testis (Kakar, Jennes 1999). The hPTTG gene is located on chromosome 5q33 and encodes a 202 amino acid protein, which shares significant homology with rat PTTG (89 % homology at protein level) (Zhang et al. 1999). Further investigations revealed that both rat and human PTTG are transforming *in vitro* and tumourigenic *in vivo,* thus implying PTTG may function as a proto-oncogene (Pei, Melmed 1997, Zhang et al. 1999, Wang, Melmed 2000).

#### *1.4.1.1 PTTG protein structure*

Human PTTG is very hydrophilic and comprises a predominantly basic amino acid-rich regulatory amino (N)-terminal region (from position 58 to 101) and a largely acidic amino acid-rich functional carboxyl (C)-terminal region (Zhang et al. 1999) (Figure 1.6). The N-terminal regulatory domain is rich in lysine residues and consists of a KEN box and

Destruction (D-box) box (RKALG(T or N)VN) (Zhang et al. 1999, Zou et al. 1999). These two conserved motifs target PTTG for ubiquitination by the anaphase-promoting complex/cyclosome (APC/C) E3 ubiquitin ligase, thus promoting the degradation of PTTG by the 26S proteasome during mitosis (Zou et al. 1999, Zur, Brandeis 2001). On the other hand, the C-terminal functional domain contains two proline-rich PXXP motifs, which form an Src-homology (SH-) 3-binding site (Kakar, Jennes 1999). These PXXP motifs appear to be critical for PTTG function (Zhang et al. 1999, Pei 2000, Boelaert et al. 2004). Mutation of the key proline residues abrogates its transforming and tumour-inducing properties, as well as its ability to stimulate basic fibroblast growth factor (bFGF) expression and secretion (Zhang et al. 1999, Pei 2000). Other important domains include the DNA binding and transactivation domains, both of which appear to be critical for PTTG transcriptional activity (Pei 2000, Dominguez et al. 1998).

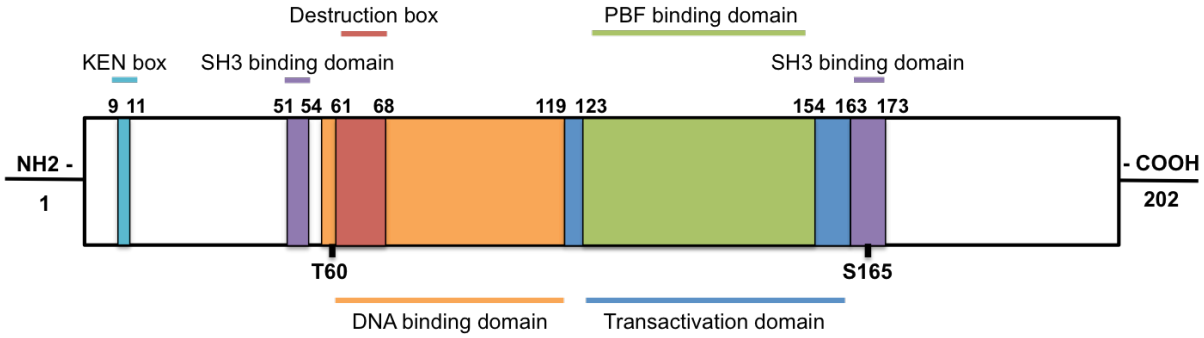


*Figure 1.6 Schematic representation of the human PTTG protein structure. PTTG comprises a predominantly regulatory N-terminus, consisting of a KEN box domain and a Destruction box (D-box) domain. The functional C-terminus is composed of a DNA binding domain, a transactivation domain (PBF binding domain also within this region), and an SH3-binding site. Regulatory and functional domains, SH3-binding sites and important amino acid residues are indicated.*

### *1.4.1.2 Expression and subcellular localisation of PTTG*

In normal adult tissue, abundant PTTG mRNA expression is present in the thymus and testis (Dominguez et al. 1998, Zhang et al. 1999, Kakar, Jennes 1999). Lower levels of

expression have also been observed in the colon, small intestine, brain, placenta and lung (Dominguez et al. 1998, Zhang et al. 1999). Elevated expression of PTTG has been noted in a number of human cancer cell lines and tumours (see section 1.4.3 below) (Zhang et al. 1999). In contrast, in human foetal tissue, PTTG mRNA expression is only detectable in the liver (Zhang et al. 1999).

The precise subcellular localisation of PTTG remains controversial. Initial reports suggested that PTTG was mainly cytoplasmic, although partial nuclear staining was evident (Dominguez et al. 1998, Stratford et al. 2005). However, further immunofluorescent and subcellular fractionation studies have demonstrated predominantly nuclear localisation (Yu et al. 2000b). PTTG was detectable in JEG-3 cells transfected with wild type, FLAG- or EGFP-tagged PTTG constructs throughout the cell but was found to be more concentrated within the nucleus (Yu et al. 2000b).

*1.4.1.3 Regulation of PTTG gene expression*

Oestrogen was the first reported regulator of PTTG mRNA expression. Rat pituitary PTTG mRNA expression was found to be significantly upregulated following oestrogen treatment in rat pituitary somato-lactotroph GH3 cells, both in a time- and dose-dependent manner (Heaney et al. 1999). *In vivo* administration of oestrogen in Fischer 344 rats was also associated with the induction of PTTG mRNA expression, with expression levels remaining elevated throughout the 14-week treatment schedule (Heaney et al. 1999). Importantly, co-treatment with a selective inhibitor of oestrogen, ICI-182780, abrogated oestrogen-induced pituitary PTTG expression *in vivo* (Heaney et al. 2002).

Insulin and insulin-like growth factor-1 (IGF-1) have also been implicated in regulating PTTG expression. Expression of either hormone or growth factor resulted in a 2.5-fold induction of PTTG mRNA and protein expression in MCF-7 human breast cancer cells

(Thompson, Kakar 2005). This effect was mediated through activation of both Ras-mitogen-activated protein kinase (MAPK) and phosphatidylinositol 3-kinase (PI3K)-Akt pathways (Thompson, Kakar 2005). Interestingly, these same signalling pathways have also been implicated in the upregulation of PTTG expression by epidermal growth factor (EGF) and transforming growth factor-α (TGFα) in U87 human glioma cells (Tfelt-Hansen et al. 2004) and K1/TPC-1 thyroid cells (Lewy et al. 2013).

Transcription factors including, specific protein-1 (Sp1), and, to a lesser degree, nuclear factor-Y (NF-Y), are critical regulators of basal PTTG transcription (Clem et al. 2003). Site-directed mutagenesis of the Sp1 binding site within the PTTG promoter region led to a 70 % reduction in PTTG promoter activity (Clem et al. 2003). Mutation of the NF-Y consensus sequence resulted in a 25 % decrease in transcriptional activation of the PTTG promoter (Clem et al. 2003). Screening of the PTTG promoter region revealed a putative T-cell factor-4 (TCF4) binding site, suggesting PTTG may also be a target for the β-catenin/TCF pathway (Zhou et al. 2005). Luciferase reporter assays demonstrated that the PTTG promoter, containing the TCF4 binding element, was activated in the presence of β-catenin but was inhibited by a dominant-negative form of TCF (Zhou et al. 2005). In addition, PTTG mRNA and protein levels appeared to be elevated in HEK293 cells overexpressing β-catenin and positively correlated with β-catenin subcellular localisation in human oesophageal squamous cell carcinoma (Zhou et al. 2005).

### 1.4.2 The molecular functions of PTTG

#### *1.4.2.1 The human securin*

Several lines of evidence led to the discovery that PTTG encodes the human securin. Analysis of HeLa cells arrested in various stages of the cell cycle demonstrated cell cycle-

dependent expression of PTTG, with protein expression peaking during mitosis (Zou et al. 1999, Ramos-Morales et al. 2000). Furthermore, PTTG was preferentially phosphorylated in mitosis (Figure 1.7). Securins play an important role in sister chromatid separation during the metaphase-anaphase transition in mitosis. Their proper functioning is imperative, as defects in sister chromatid separation result in aneuploidy and chromosomal instability, a major hallmark of cancer (Cahill et al. 1998, Jallepalli et al. 2001, Kim et al. 2005, Mora-Santos et al. 2013). The process is therefore rigorously regulated to ensure the timely bi-orientation of chromosomes on mitotic spindles and equal sister chromatid segregation. In eukaryotic cells, the replicated pairs of sister chromatids are held together by the multiunit cohesin complex. Two distinct mechanisms induce cohesin dissociation. During prophase, the majority of cohesin bound to chromosome arms is degraded via Aurora B and Polo-like kinase (PLK)-1 activity (Losada et al. 2002, Sumara et al. 2002, Waizenegger et al. 2000). Then during the onset of anaphase, any remaining cohesin is cleaved by the cysteine protease separase (Waizenegger et al. 2000). The latter process is tightly regulated by the APC/C (Zou et al. 1999, Zur, Brandeis 2001), which ubiquitinates, and consequently induces the degradation of, PTTG in a KEN- and D-box-dependent manner (Zur, Brandeis 2001, Zou et al. 1999). As separase function is inhibited by PTTG binding, degradation by the APC/C leads to release of separase and cleavage of cohesin, thus enabling sister chromatid separation (Zou et al. 1999, Zur, Brandeis 2001). Of note, CDK1-cyclin B1 can also regulate separase activity independently of securin, in both a positive and negative manner. Upon entry into mitosis, separase is rendered catalytically inactive by CDK1-mediated phosphorylation at position S1126 (Gorr et al. 2005). However, subsequent associations with CDK1-cyclin B1 stabilise phosphorylated separase, holding it in an inhibited, yet activatable form, which is released upon APC/C-mediated cyclin B1 degradation (Hellmuth et al. 2015).

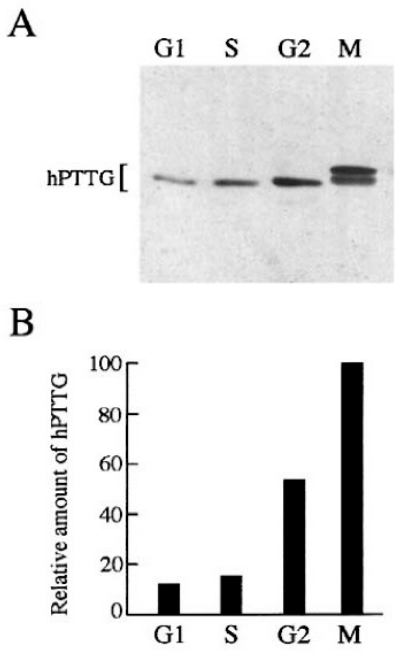


*Figure 1.7 Human PTTG expression during the cell cycle.* ***A*** *– Western blot analysis of extracts from HeLa cells arrested in the various phases of the cell cycle. Immunoblotting was performed using a polyclonal anti-hPTTG antibody, with double-banding during mitosis representing phosphorylated PTTG.* ***B*** *– Scanning densitometry of the immunoblot showing peak PTTG expression during mitosis. G1 = gap 1 checkpoint, S = synthesis, G2 = gap 2 checkpoint, M = mitosis (figure from Ramos-Morales et al. 2000).*

### *1.4.2.1 Transactivation*

The partial nuclear localisation of PTTG, as well as the presence of an acidic proline/glutamic acid-rich C-terminus, commonly associated with eukaryotic transactivation domains led to the speculation that PTTG may function as a gene transactivator (Dominguez et al. 1998, Wang, Melmed 2000). Indeed, murine PTTG exhibited transactivation activity, which positively correlated with PTTG's transforming ability in NIH3T3 cells (Wang, Melmed 2000). Accordingly, the C-terminal portion of hPTTG was capable of activating transcription of the *his3* and *lacZ* genes in *S. cerevisiae* (Dominguez et al. 1998). Further confirmation of PTTG transcriptional activity came from cDNA expression arrays. Total RNA harvested from HeLa cells, 0 hours and 24 hours post-PTTG induction, was screened

for expression of a total of 84 known gene transcripts (Pei 2001). Of these, c-Myc, MEK1 and HSP70 were identified, and subsequently confirmed by Northern blot analysis, as being differentially expressed following upregulation of PTTG (Pei 2001). More recent chromatin immunoprecipitation (ChIP)-on-ChIP assay performed in JEG-3 cells has identified a further 746 promoters enriched by PTTG, thereby suggesting a more global effect of PTTG on transcriptional regulation (Tong et al. 2007).

*1.4.2.2 DNA damage and repair*

Using a yeast two-hybrid system, the Ku-70 heterodimer was identified as a specific interacting partner of PTTG (Romero et al. 2001). Ku-70 forms the regulatory subunit of the DNA-dependent protein kinase complex (DNA-PK), an important enzyme involved in the repair of DNA double-strand breaks (DSB). Repair of DSBs in mammalian cells typically involves one of two major pathways: homologous recombination (HR), which is a highly accurate repair system, requiring the homologous sister chromosome as a template for DNA repair, and non-homologous end joining (NHEJ), which is relatively error-prone. DNA-PK is required for NHEJ repair. In response to DNA damage, Ku-70-PTTG associations are disrupted, resulting in the release of Ku-70, which is then able to bind to DNA ends and recruit the catalytic subunit of DNA-PK (DNA-PKcs) to DNA DSBs, thereby enabling repair of the damaged DNA (Romero et al. 2001, Kim et al. 2007b). DNA-PKcs is also able to phosphorylate PTTG *in vitro* (Romero et al. 2001). PTTG may therefore represent a crucial link between DNA damage pathways and sister chromatid separation by delaying the onset of mitosis to allow DNA repair to be completed.

Loss of PTTG expression has also been associated with impaired proliferative capacity and altered NHEJ repair following DNA damage in human colorectal cancer HCT116 cells (Bernal et al. 2008). Furthermore, PTTG is required for arrest of cell proliferation following

ultraviolet (UV) radiation (Romero et al. 2004). UV irradiation caused a rapid reduction in PTTG protein expression via specific inhibition of PTTG mRNA translation (Romero et al. 2004) and SKP1-CUL1-βTrCP-mediated ubiquitination and subsequent proteasomal degradation of PTTG (Romero et al. 2004, Limon-Mortes et al. 2008). Drug-induced DNA damage also results in a marked decrease in PTTG expression but requires functional p53 (Zhou et al. 2003b). Further investigation revealed that p53, activated in response to bleomycin- and doxorubicin-induced DNA damage, inhibited binding of NF-Y to the PTTG promoter, thereby repressing PTTG transcription (Zhou et al. 2003b). These data thus implicate p53 in the regulation of PTTG expression following genotoxic stress.

### 1.4.3 PTTG and tumourigenesis

Overexpression of PTTG has been well documented in several human cancer cell lines, including HepG2 hepatoma cells, haematopoietic cells (HL-60 and K-562), HeLa S3 cervical carcinoma cells, SW480 colorectal adenocarcinoma cells, breast cancer cells (MCF-7), ovarian tumour cells (CaO4, PA1, SKOV3 and VOI101) and oral squamous carcinoma cell lines (Ca9-22) (Kakar, Jennes 1999, Zhang et al. 1999, Lee et al. 1999, Laio et al. 2011). Abundant PTTG expression has also been observed in a wide range of human tumours, such as pituitary (Saez et al. 1999), colon (Heaney et al. 2000), thyroid (McCabe, Gittoes 1999), breast (Solbach et al. 2004) and head and neck cancers (Solbach et al. 2006, Zhang et al. 2014). Importantly, PTTG upregulation has been independently associated with advanced tumour stage, tumour recurrence and reduced disease-specific survival and may provide an additional prognostic marker to aid in the diagnosis and treatment of multiple cancer types (Shibata et al. 2002, Solbach et al. 2006, Solbach et al. 2004, Ito et al. 2008, Yan et al. 2009, Boelaert et al. 2003a). Together, these data suggest that PTTG may play a significant role in

tumourigenesis. Indeed, potent cellular transformation has been demonstrated in human embryonic kidney (HEK293) cells expressing wild-type PTTG (Hamid et al. 2005). Furthermore, overexpression of PTTG in NIH3T3 mouse fibroblast cells induced anchorage-independent growth in soft agar and, when subcutaneously injected in to athymic nude mice, resulted in gross tumour formation (Pei, Melmed 1997, Zhang et al. 1999). Identification of a C-terminal double PXXP motif revealed that both transactivating and transforming functions of PTTG are linked, as mutation or deletion of these putative SH3-binding sites prevented PTTG-mediated transactivation of downstream target genes *in vitro*, and inhibited *in vivo* tumour formation (Zhang et al. 1999, McCabe et al. 2002, Boelaert et al. 2004).

*1.4.3.1 PTTG as a gene transactivator*

Several mechanisms have been proposed for PTTG's role in the initiation and progression of tumours and detailed analysis has uncovered numerous genes involved in cell proliferation and angiogenesis whose expression can be transcriptionally regulated by PTTG. Expression and secretion of bFGF in response to PTTG overexpression was initially discovered in NIH3T3 cells (Zhang et al. 1999, Ishikawa et al. 2001). Interestingly, alteration of the SH3-binding site by mutagenesis disrupted both expression and secretion of bFGF, whereas a non-phosphorylatable (S165A) form of PTTG was still able to upregulate bFGF expression (Zhang et al. 1999, Ishikawa et al. 2001, Boelaert et al. 2004). In addition, conditioned medium from NIH3T3 hPTTG-transfectants stimulated proliferation, migration and tube-formation of human umbilical vein endothelial cells (HUVEC) *in vitro*. Addition of a neutralising anti-bFGF antibody to the medium prohibited these angiogenic actions (Ishikawa et al. 2001). The pro-angiogenic growth factor, vascular endothelial growth factor (VEGF), is also highly expressed in tumours demonstrating upregulated levels of PTTG (McCabe et al. 2002). Increased VEGF expression was also noted in MCF-7, JEG-3 and human foetal

neuronal NT-2 cells transfected with wild type PTTG and was again abrogated upon deletion or mutation of the PTTG SH3-binding domain (McCabe et al. 2002).

The TRβPV mouse model expresses a dominant-negative form of the thyroid hormone receptor β and spontaneously develops follicular thyroid cancer with distant metastases. Previous microarray analysis has revealed that these mice overexpress PTTG by approximately 5-fold (Ying et al. 2003). TRβPV mice lacking PTTG expression (TRβPV $PTTG^{-/-}$) exhibited a significant reduction in vascular invasion, when compared with TRβPV $PTTG^{+/+}$ control mice (Kim et al. 2007a). This effect was associated with a decrease in mortality in TRβPV $PTTG^{-/-}$ mice and was further corroborated by an observed reduction in immunohistochemical staining of the endothelial marker CD31 in the thyroids of these mice (Kim et al. 2007a). Importantly, TRβPV $PTTG^{-/-}$ mice exhibited diminished mRNA expression levels for FGF2, FGFR1 and VEGF when compared with TRβPV $PTTG^{+/+}$ mice (Kim et al. 2007a). A study conducted by Kim et al. has identified additional pro- and anti-angiogenic factors whose expression are thought to be regulated by PTTG, including ID3 and Thrombospondin (TSP)-1 (Kim et al. 2007a).

PTTGs role as a gene transactivator is not just confined to the regulation of angiogenic factors. DNA profiling of inducible PTTG cell lines revealed that c-Myc, MEK1, MEK3, PKCβ-1 and HSP70 are upregulated after induction of PTTG (Pei 2001). c-Myc is a transcription factor which has a pivotal function in cell growth, differentiation and apoptosis, and its role in tumourigenesis is well established. PTTG was shown to directly associate with the c-Myc promoter as part of a ternary complex with Upstream Stimulating Factor (USF)-1 (Pei 2001). PTTG may therefore influence cell survival and growth indirectly by targeting c-Myc. Accordingly, PTTG-mediated modulation of p53 expression and function has been shown to be mediated via regulation of c-Myc expression (Hamid, Kakar 2004).

In recent years, PTTG has also been identified as a key signature gene in tumour metastasis. Altered PTTG expression has been associated with tumour cell migration and invasion (Malik, Kakar 2006). Matrix metalloproteinases (MMP) are potent zinc-dependent endopeptidases that belong to the metzincin superfamily of proteolytic enzymes. MMP tightly regulate cell-matrix composition and remodelling. In order for cancer cells to disseminate from the primary tumour to secondary sites and form metastases, they must be able to degrade and navigate through the surrounding extracellular matrix (ECM). In light of their central role in orchestrating ECM degradation, MMP have been proposed to be involved in tumour cell invasion and migration. Among them, MMP-2 and MMP-9 have been identified as particularly important in tumour angiogenesis and metastasis (Stamenkovic 2000).

Malik et al. were first to describe a role for PTTG in the modulation of MMP-2 secretion and expression (Malik, Kakar 2006). Transient transfection of HEK293 cells with PTTG resulted in significant induction of MMP-2 gene promoter activity and MMP-2 mRNA expression (Malik, Kakar 2006). Furthermore, conditioned medium from HEK293 cells transiently or stably overexpressing PTTG also demonstrated an increase in MMP-2 secretion (Malik, Kakar 2006). Interestingly, incubation of HUVECs with this conditioned medium led to increased cell migration, invasion and tubule formation, all of which was blocked by pre-treatment with an anti-MMP-2 antibody (Malik, Kakar 2006). A role for PTTG in the transcriptional regulation of MMP-9 and MMP-13 has also been defined, with down-regulation of PTTG expression resulting in significant repression of MMP-9 and MMP-13 mRNA and protein expression in cutaneous squamous cell carcinoma and prostate cancer cell lines (Xia et al. 2013, Lin et al. 2015b). Moreover, these alterations in MMP expression were associated with reduced cell proliferation and invasion (Xia et al. 2013, Lin et al. 2015b).

Recent evidence has also linked PTTG transcriptional activity with epithelial-to-mesenchymal transition (EMT). EMT is an essential process that occurs during normal embryonic development and requires epithelial cells to shed their epithelial phenotype and acquire mesenchymal-like properties (Thiery et al. 2009). During this process cells lose polarity, assume a spindle-like morphology and become more motile (Thiery et al. 2009). As a result, EMT has been heavily implicated in tumour progression and metastasis. PTTG has been shown to regulate expression of several of the transcription factors involved in EMT (Shah, Kakar 2011b, Shah et al. 2012, Yoon et al. 2012, Li et al. 2015). In the ovarian epithelial cancer cell line A2780, overexpression of PTTG has been shown to induce expression of the EMT transcription factors Snail, Twist and Slug via upregulation of TGFβ mRNA expression and secretion (Shah, Kakar 2011b). Upregulation of these EMT transcription factors by PTTG was further associated with a reduction in the expression of the epithelial marker, E-cadherin, and a concomitant increase in the expression of the mesenchymal marker, vimentin (Shah, Kakar 2011b). PTTG has also been reported to induce EMT by regulating the expression of the integrins $\alpha_V$ and $\beta_3$, which play a crucial role in triggering cellular cytoskeletal rearrangements in response to changes in the ECM (Shah et al. 2012).

*1.4.3.2 PTTG and genetic instability*

Another mechanism by which PTTG has been shown to promote tumourigenesis is through the induction of genetic instability, via its role in mediating sister chromatid separation during mitosis. Indeed, chromosomal aberrations are frequently observed in cancers and have been implicated in tumour initiation, as well as progression (Fröhling, Döhner 2008). The first study to describe a role for PTTG in chromosomal instability demonstrated induction of aneuploidy in osteosarcoma MG-63 cells following stable

overexpression of PTTG (Yu et al. 2000a). Further single live cell imaging analysis of lung cancer H1299 cells transiently transfected with EGFP-tagged PTTG also showed signs of aneuploidy (Yu et al. 2000a). In H1299 cells transiently over-expressing low levels of EGFP-PTTG, mitosis resumed as normal due to rapid degradation of EGFP-PTTG before onset of anaphase (Figure 1.8; (Yu et al. 2003)). However, expression of higher levels of EGFP-PTTG was associated with an inability to degrade EGFP-PTTG and as a consequence, led to a marked delay in transition from metaphase to anaphase and caused asymmetrical cytokinesis, which subsequently resulted in aneuploidy (Figure 1.8; (Yu et al. 2003)).

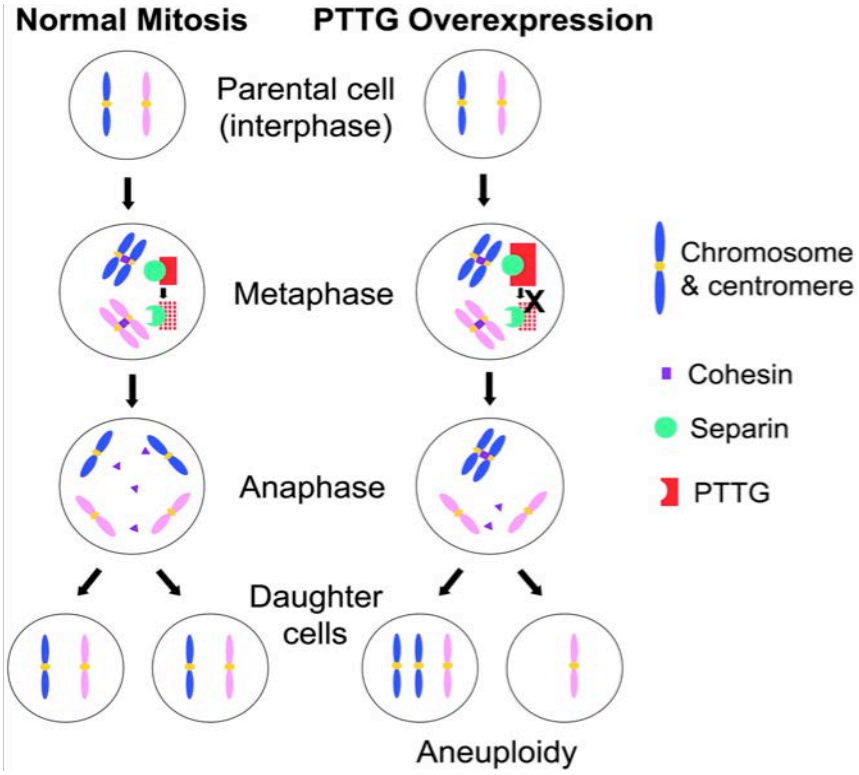


*Figure 1.8 Proposed mechanism of PTTG-induced aneuploidy.* ***Left*** *– Normal process of mitosis, whereby PTTG degradation at the end of metaphase by the APC results in release of separase, thus enabling cohesin degradation, separation of sister chromatids and their equal distribution between the daughter cells.* ***Right*** *– Abnormal mitosis due to overexpression of PTTG, which causes dysregulated sister chromatid separation and results in aneuploidy (figure from Yu et al. 2003).*

Interestingly, abnormal chromosomal separation has also been observed following PTTG depletion, thus suggesting that both over-expression and under-expression of PTTG have important implications with regard to the maintenance of genome integrity. HCT116 cells contain a stable karyotype, as well as intact DNA damage and mitotic spindle checkpoints and demonstrate no signs of aneuploidy, when assessed by fluorescent in situ hybridisation (FISH) and multiplex-FISH (M-FISH) (Jallepalli et al. 2001). In contrast, inactivation of both copies of PTTG in these cells (HCT116-PTTG$^{-/-}$) resulted in gross aneuploidy, with more than 80 % of HCT116-PTTG$^{-/-}$ cells demonstrating at least one chromosome loss (Jallepalli et al. 2001).

Further evidence indicating that PTTG induces genetic instability has come from the analysis of human normal and tumour tissue specimens via fluorescent intersimple sequence repeat PCR (FISSR-PCR), which is a technique used to measure intra-chromosomal instability. Using this technique, the level of global genetic instability was much greater in thyroid and colorectal tumours compared to normal tissues and strongly correlated with the degree of PTTG expression (Kim et al. 2005, Kim et al. 2007b). In addition, FISSR-PCR analysis of non-transformed fibroblast, follicular thyroid cancer and colorectal cancer cell lines identified a dose-dependent increase in the genetic instability index following transfection with increasing concentrations of PTTG cDNA (Kim et al. 2005, Kim et al. 2007b).

*1.4.3.3 PTTG and DNA damage repair*

As described previously (section 1.4.2.3), PTTG is capable of forming complexes with Ku-70 (Romero et al. 2001), which plays an important role in the repair of DNA double-strand breaks via the NHEJ pathway. Following DNA damage, PTTG dissociates from Ku-70, thus allowing Ku-70 to bind to DNA at the site of repair and trigger NHEJ (Romero et al. 2001).

Overexpression of PTTG in HCT116 cells has been shown to prevent Ku-70 binding to DNA, which in turn, inhibited NHEJ DNA repair activity (Kim et al. 2007b). Taken together, these data suggest that PTTG may impair critical DNA damage response mechanisms within the cell, leading to gross genetic instability. In accordance with these findings, recent research carried out by our group has revealed significant alterations in the expression of numerous p53-related DNA damage response genes in a transgenic mouse model of thyroid-specific overexpression of PTTG (PTTG-Tg) (Figure 1.9) and in human differentiated thyroid tumours (Read et al. 2016a). Many of the affected genes were downregulated, including several known to be involved in maintaining genomic integrity, such as BRCA1, CHEK1 and MUTYH (Read et al. 2016a). Importantly, PTTG-Tg thyrocytes displayed a greater level of genetic instability than primary thyrocytes derived from age- and sex-matched wild-type mice (Read et al. 2016a).

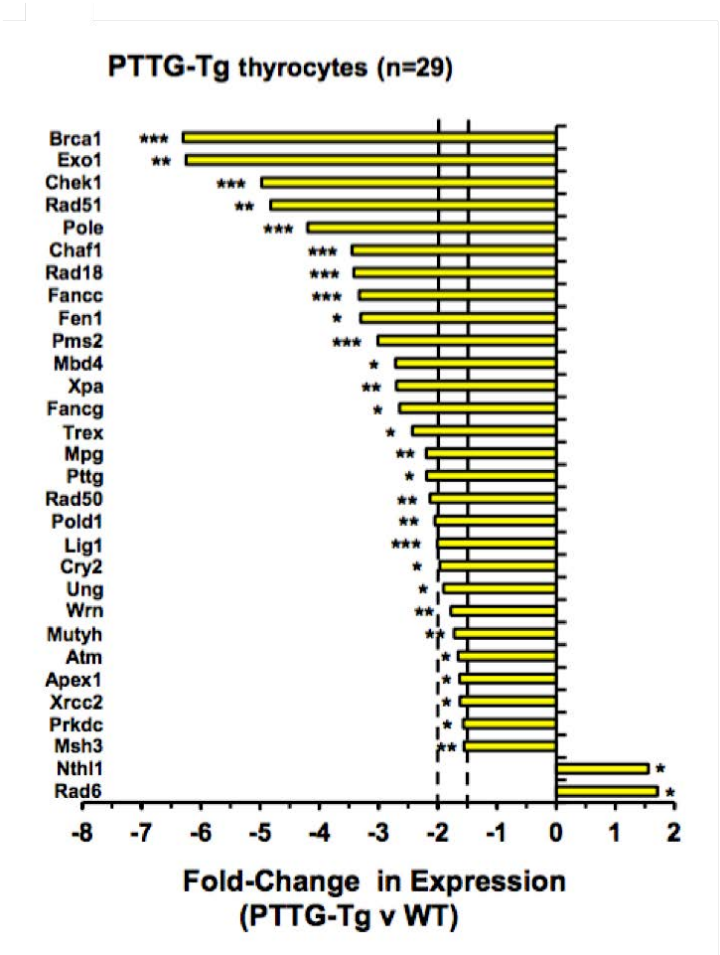


*Figure 1.9 Transcriptional profile of DNA damage response genes in PTTG-Tg thyrocytes. Gene expression analysis used a DNA damage signalling pathway-focussed RT2 Profiler PCR array in PTTG-Tg thyrocytes. Graph shows expression of DNA damage response genes altered >1.5-fold versus wild-type (WT). * p ≤0.05, ** p ≤0.01, *** p ≤0.001 (figure from Read et al. 2016a).*

### *1.4.3.4 PTTG, p53 and apoptosis*

Several reports have described an interaction between PTTG and p53 with regard to apoptosis. Initial studies demonstrated PTTG-induced apoptosis in JEG-3 cells transiently transfected with EGFP-PTTG (Yu et al. 2000b). In subsequent studies, overexpression of PTTG in breast cancer MCF-7 cells expressing wild-type p53 caused cell cycle arrest and apoptosis (Yu et al. 2000a). Furthermore, apoptosis was enhanced following co-transfection with p53 and was inhibited following co-transfection with HPV E6, thus indicating that PTTG induces apoptosis via p53-dependent mechanisms (Yu et al. 2000a). Interestingly,

overexpression of PTTG resulted in aneuploidy in MG-63 cells, which are devoid of p53, implying that p53 can inhibit PTTG induction of aneuploidy and instead promote apoptosis (Yu et al. 2000a). Hamid et al. further demonstrated that PTTG could induce apoptosis through p53-mediated upregulation of the pro-apoptotic effector BAX in HEK293 cells (Hamid, Kakar 2004).

In contrast to these findings, overexpression of PTTG and its interaction with p53 in H1299 cells blocked p53 binding to DNA, repressed p53 transcriptional activity and also inhibited p53-dependent apoptosis (Bernal et al. 2002). In addition, adenoviral-mediated knockdown of PTTG gene expression has been shown to result in activation of p53 and subsequent induction of apoptosis in SH-J1 hepatoma cells (Jung et al. 2006). The intimate relationship between PTTG and p53 is further complicated by the fact that PTTG is a direct transcriptional target of p53 (Zhou et al. 2003b). Following induction of DNA damage, p53 was able to suppress PTTG expression by impairing NF-Y binding to the PTTG gene promoter in HCT116 cells (Zhou et al. 2003b).

### 1.4.4 PTTG in head and neck cancer

Several studies have independently demonstrated overexpression of PTTG in oesophageal squamous cell carcinoma (ESCC) (Shibata et al. 2002, Zhou et al. 2005, Ito et al. 2008, Yan et al. 2009, Zhang et al. 2013). Many of these studies revealed that PTTG mRNA expression levels were significantly upregulated in human ESCC tissue specimens when compared with matched normal tissues (Shibata et al. 2002, Zhou et al. 2005). Furthermore, high tumoural PTTG mRNA expression has been found to strongly correlate with advanced pathological stage, extensive lymph node metastasis and reduced disease-free survival, indicating that PTTG may serve as a novel prognostic marker for ESCC (Shibata et al. 2002, Zhou et al.

2005). Elevated PTTG mRNA expression has also been detected in several ESCC cell lines, with very little detected in normal human keratinocytes (Zhou et al. 2005).

Overexpression of PTTG protein has also been documented in ESCC, with strong PTTG protein expression reported in approximately 60-70 % or tumours (Ito et al. 2008, Yan et al. 2009, Zhang et al. 2013). Notably, high levels of PTTG protein expression were also significantly associated with clinicopathological features, including TNM stage, lymph node metastasis and poor overall survival (Ito et al. 2008, Yan et al. 2009, Zhang et al. 2013). Interestingly, PTTG protein expression is not only upregulated but also appears to be differentially localised within the cell. Immunohistochemical analysis of 113 primary ESCC tumours found that PTTG staining was mainly present in the cytoplasm, with occasional nuclear staining also observed. However, in normal oesophageal tissues, only occasional nuclear PTTG staining was observed, with no cytoplasmic staining evident (Ito et al. 2008).

Importantly, upregulated PTTG expression has also been reported in HNSCC tumours (Solbach et al. 2006, Liao et al. 2011, Zhang et al. 2014). Similar to previous studies for ESCC, initial analyses performed on 89 tumour specimens derived from patients with OPSCC (n=66) or LSCC (n=23) revealed elevated levels of PTTG mRNA expression in the vast majority of tumours when compared to normal tissue derived from the same patients (Solbach et al. 2006). Additionally, higher levels of PTTG mRNA expression were independently associated with advanced disease stage, lymph node involvement and tumour recurrence (Solbach et al. 2006). Overexpression of PTTG mRNA and protein has also been documented in tissue specimens derived from patients with oral premalignant lesions and OSCC (Liao et al. 2011, Zhang et al. 2014). Interestingly, PTTG expression was found to increase with the degree of oral epithelial dysplasia and was further increased in OSCC (Liao et al. 2011).

Moreover, high tumoural PTTG protein expression strongly correlated with lymph node status and TNM staging (Liao et al. 2011, Zhang et al. 2014).

## 1.5 PTTG1-Binding Factor (PBF)

### 1.5.1 The PBF gene

PTTG1-binding factor (PBF; also known as PTTG1IP) was initially discovered using a yeast-2 hybrid system to identify interacting partners of PTTG (Chien, Pei 2000). Subsequent investigations revealed that the PBF gene, located at chromosome 21q22.3, encodes a 180 amino acid protein with a predicted molecular mass of 22 kDa (Chien, Pei 2000). It was later established that PBF had previously been cloned and was named C21*orf*3 (Yaspo et al. 1998). Whilst PBF shares no significant sequence homology with any other human protein, it is well conserved across different species, suggesting it has a unique function and is evolutionarily important (Yaspo et al. 1998).

#### *1.5.1.1 PBF protein structure*

C21*orf*3 was characterised as a type 1a integral membrane cell surface glycoprotein due to the identification of a putative N-terminal signal peptide, transmembrane domain, endocytosis motif and two putative N-glycosylation sites (Yaspo et al. 1998). Further structural studies revealed the existence of a putative N-terminal leucine-rich nuclear export signal within the signal peptide domain and a plexin-semaphorin-integrin (PSI) domain (Chien, Pei 2000). PSI domains are typically 50 amino acids in length and contain 8 cysteine residues, some of which are connected by disulphide bonds (Bork et al. 1999). They are usually found within the extracellular region and are involved in protein-protein interactions (Bork et al. 1999). Other important domains identified include the C-terminal bipartite nuclear localisation signal (NLS) and sorting signal (Figure 1.10). The NLS appears to be critical for PTTG nuclear

transport and, as such, facilitates its roles as a securin and a gene transactivator. Expression of PTTG-GFP was located mainly in the cytoplasm of transfected COS-7 cells, whereas co-transfection of PBF-HA along with PTTG-GFP resulted in marked translocation of PTTG into the nucleus (Chien, Pei 2000). The shuttling of PTTG into the nucleus was effectively blocked following co-transfection with a PBF-NLS deletion mutant (Chien, Pei 2000). Ablation of the NLS domain also prevented PTTG-mediated transactivation of FGF-2, thus demonstrating that PBF is required for the nuclear transport and transcriptional activation function of PTTG (Chien, Pei 2000).

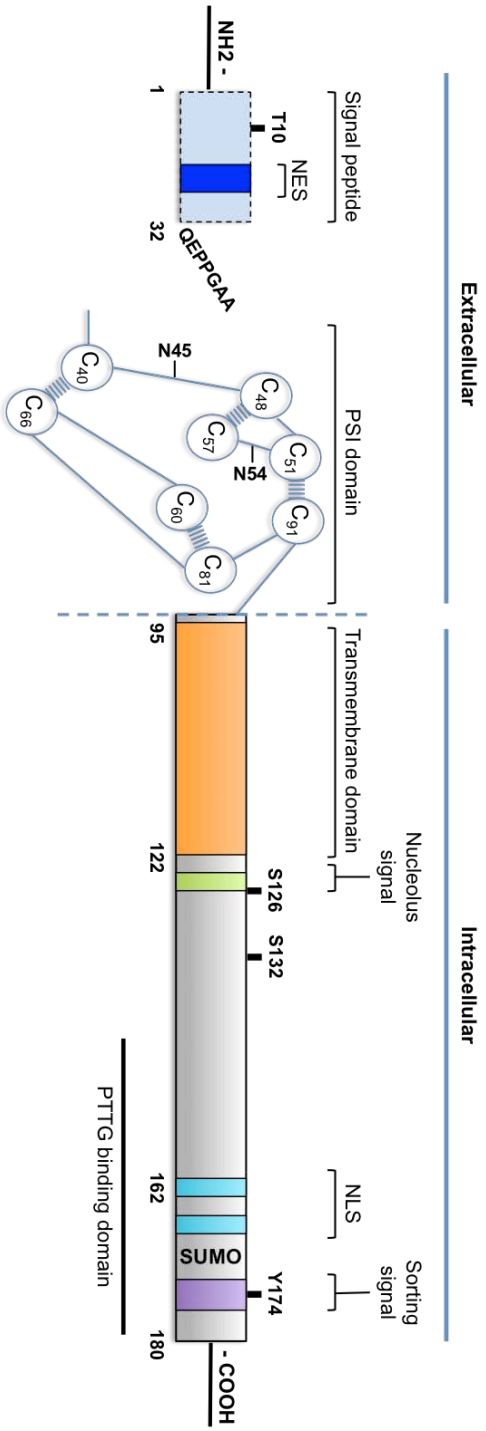


*Figure 1.10 Schematic representation of the human PBF's putative protein structure. PBF comprises an N-terminal extracellular signal peptide with a nuclear export signal (NES). This is followed by an extracellular cysteine-rich PSI domain, with disulphide bonds represented by multiple blue lines. A putative nucleolus sequence is present within the intracellular region, adjacent to the transmembrane domain. The C-terminal region contains a nuclear localisation sequence (NLS) and a sorting signal. Phosphorylation sites and the two putative N-glycosylation sites are also indicated. SUMO = predicted SUMOylation site.*

*1.5.1.2 Expression and subcellular localisation*

Initial Northern blot analysis demonstrated abundant and ubiquitous expression of PBF mRNA in all tissues examined, including the spleen, testis, ovary and colon (Yaspo et al. 1998). Additional PBF mRNA expression profiling using a human RNA master blot demonstrated high PBF mRNA expression in a selection of normal tissue specimens, suggesting widespread expression of PBF (Chien, Pei 2000). This was further supported by a comparison of the PBF nucleotide sequence with a database of expressed sequence tags (EST), which identified over 100 human ESTs corresponding to cDNAs expressed in the heart, lungs, pancreas, spleen, bone marrow, melanocytes, uterus, testis and neurons (Chien, Pei 2000).

The presence of a C-terminal NLS prompted further investigations into the subcellular localisation of PBF protein. Transfection of COS-7 cells with heamagglutinin-tagged PBF (PBF-HA) and subsequent immunofluorescence staining revealed predominantly nuclear expression of PBF, with significant cytoplasmic expression as well (Chien, Pei 2000). Interestingly, mutation of the NLS resulted in a shift in PBF expression from the nucleus to the perinuclear and cytoplasmic regions, thus implying that the NLS is required for PBF nuclear localisation (Chien, Pei 2000).

In addition to nuclear localisation, PBF expression has also been observed within intracellular vesicles, where it strongly co-localised with the late endosomal marker CD63 (Smith et al. 2009). Furthermore, deletion of the C-terminal sorting signal in PBF resulted in its accumulation at the plasma membrane, thereby supporting a role for PBF as a cell surface glycoprotein (Smith et al. 2009).

*1.5.1.3 Regulation*

The mechanisms involved in PBF regulation have not been fully elucidated. Overexpression of PTTG has been reported to induce PBF mRNA expression in primary human thyroid follicular cells and HCT116 cells (Stratford et al. 2005). Furthermore, assessment of PTTG and PBF mRNA expression in pituitary and thyroid tumour specimens has identified a significant correlation between expression of the two genes (McCabe et al. 2003, Stratford et al. 2005).

PBF has also been identified as a transcriptional target of the bone-specific transcription factor Runx2 (Stock et al. 2004). Differential hybridisation screening of mouse embryonic fibroblast cells overexpressing Runx2 demonstrated significant upregulation of PBF. Further investigations revealed direct binding of Runx2 to the PBF promoter, resulting in the subsequent transactivation of PBF in MC3T3-E1 cells (Stock et al. 2004).

Oestrogen has also been implicated in the regulation of PBF expression. PBF mRNA and protein expression was significantly induced following treatment of MCF-7 cells with the synthetic oestrogen analogues diethylstilboestrol and 17β-oestradiol (Watkins et al. 2010). Detailed analysis of the PBF promoter identified a variable number of oestrogen response elements (ERE) and co-immunoprecipitation assays subsequently confirmed oestrogen receptor α (ERα) binding to the PBF promoter (Watkins et al. 2010).

MicroRNA (miRNA) are small non-coding RNA molecules involved in the post-transcriptional regulation of gene expression (Krol et al. 2010). Recently, miRNA have been identified as important regulators of PBF expression. The liver-specific miRNA miR-122 has been reported to target PBF via a putative miR-122 complementary sequence within the 3' UTR region of the PBF sequence (Li et al. 2013). PBF-EGFP expression was repressed by miR-122 in GFP reporter assays (Li et al. 2013). Further, transfection of a miR-122 mimic

resulted in a significant reduction in PBF expression in a panel of hepatocellular carcinoma cell lines (Li et al. 2013). Another recent study has also indicated a role for miR-584 in the negative regulation of PBF expression in glioma, providing further support for miRNA-regulation of PBF (Wang et al. 2014).

### 1.5.2 PBF and tumourigenesis

As previously described, Northern blot analysis and the identification of ESTs matching the PBF nucleotide sequence in numerous tissue types established that PBF is widely expressed in normal human tissue (Yaspo et al. 1998, Chien, Pei 2000). However, further identity matches were obtained for PBF in ESTs corresponding to cDNAs overexpressed in pancreatic cancer (Yaspo et al. 1998), colon cancer, Wilms' tumour and parathyroid cancer (Chien, Pei 2000), suggesting that PBF may be frequently overexpressed in cancers. A further study conducted by our group demonstrated a 5.7-fold upregulation of PBF mRNA expression in human pituitary tumours compared with normal pituitary tissue (McCabe et al. 2003). In addition a significant positive correlation was observed between PTTG mRNA and PBF mRNA expression in the pituitary tumours but not in normal pituitary tissues (McCabe et al. 2003). Subsequent studies revealed overexpression of PBF in thyroid tumours also displaying upregulation of PTTG expression (Stratford et al. 2005), thus indicating a potential association between PTTG and PBF in pituitary and thyroid tumourigenesis. Increased expression of PBF has also been found in glioma, breast and colorectal tumours (Watkins et al. 2010, Wang et al. 2014, Read et al. 2016b). Importantly, overexpression of PBF has been independently associated with early tumour recurrence and reduced disease-free survival in patients with thyroid cancer (Stratford et al. 2005, Hsueh et al. 2013) and with Extramural

Vascular Invasion (EMVI), increased genetic instability and somatic TP53 mutations in patients with colorectal cancer (Read et al. 2016b).

These observations prompted further investigations into a potential role for PBF in tumourigenesis. Due to the strong correlation observed between expression of the two genes, the transforming potential of PTTG and PBF was examined. Stable overexpression of PTTG or PBF alone in NIH3T3 cells led to potent colony formation (Stratford et al. 2005). However, stable overexpression of PTTG deletion mutants, which were either unable to upregulate PBF mRNA expression (PBF-SH3-) or were unable to physically interact with PBF (PTTG BD-(Δ123-154)), did not induce NIH3T3 colony formation, thus demonstrating that, in addition to potentially mediating the transforming effects of PTTG, PBF in its own right is a transforming gene *in vitro* (Figure 1.11A) (Stratford et al. 2005). Additionally, injection of athymic nude mice with stable PBF-overexpressing NIH3T3 cells led to significant tumour formation, indicating that PBF is also tumourigenic *in vivo* (Figure 1.11B) (Stratford et al. 2005).

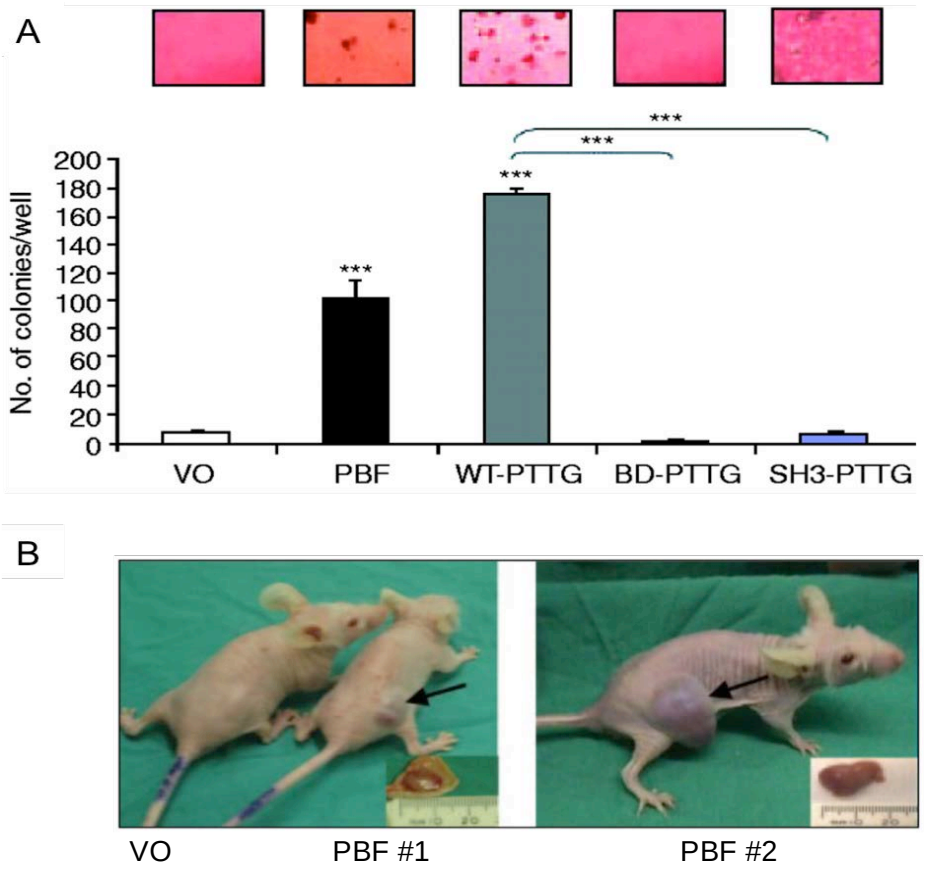


*Figure 1.11 PBF is transforming in vitro and tumourigenic in vivo.* ***A*** *– Representative images of soft agar colony formation assays performed using NIH3T3 cells stably transfected with wild-type PBF, wild-type PTTG, and PTTG with mutated PBF binding domain (BD-PTTG) or SH3 domain binding site (SH3-PTTG). The graph below shows the mean number of colonies formed per transfection condition.* ***B*** *– Tumour growth in athymic nude mice injected with stable NIH3T3 cells overexpressing PBF compared with vector only (VO) control. *** p ≤0.001 (figure from Stratford et al. 2005).*

### *1.5.2.1 PBF, NIS and iodide uptake*

Despite identifying a number of functional domains, the precise mechanisms by which PBF induces tumourigenesis have remained elusive. Research conducted by our group uncovered a role for PBF in the regulation of the sodium iodide symporter (NIS) in the thyroid. PBF represses expression of NIS in rat thyroid FRTL-5 cells and human primary thyrocytes (Boelaert et al. 2007). Additional NIS promoter studies determined that the repression of NIS by PBF was due to inhibition of the basal NIS promoter as well as disruption of a PAX8/USF1 site within the human NIS upstream enhancer element (hNUE)

(Boelaert et al. 2007). Furthermore, PBF appears to redistribute NIS from the plasma membrane into intracellular vesicles (Smith et al. 2009), providing an additional mechanism by which PBF regulates NIS. As NIS mediates the active transport of iodide into the cell, it provides an effective tool for the delivery of therapeutic doses of radioiodine to thyroid tumours to ensure their proper diagnosis and destruction. Importantly, PBF repression of NIS expression and/or alteration of its subcellular localisation are associated with a significant reduction in radioiodine uptake in FRTL-5 cells and primary cultures of thyroid cells (Boelaert et al. 2007, Smith et al. 2009, Read et al. 2011). Moreover, PBF phosphorylation by the proto-oncogene tyrosine kinase Src is essential for PBF endocytosis and abrogation of this residue results in significant retention of NIS at the plasma membrane, ultimately restoring iodide uptake in primary human thyrocytes (Smith et al. 2013). As a consequence, high tumoural expression or enhanced Y174 phosphorylation of PBF may have a profound impact on patient prognosis following radioiodine ablation therapy.

*1.5.2.2 PBF, p53 and DNA damage repair*

Recent research into the role of PBF in thyroid tumourigenesis has demonstrated that a functional interaction exists between PBF and the tumour suppressor protein p53 in thyroid and colorectal cancer (Read et al. 2014, Read et al. 2016b). Glutathione-S-transferase (GST) pull-down assays initially demonstrated that PBF binds to p53 (Read et al. 2014). Successive co-immunoprecipitation assays using protein lysates extracted from TPC-1, K1 and HCT116 cells confirmed a direct and specific interaction *in vitro* and further revealed that this interaction is enhanced following treatment of cells with ionising radiation (Figure 1.12A) (Read et al. 2014, Read et al. 2016b). The potential association between PBF and p53 was further corroborated by proximity ligation assays performed in TPC-1 cells and oligonucleotide pull-down assays (Read et al. 2014, Read et al. 2016b).

Subsequent half-life studies using anisomycin, which blocks de novo protein synthesis, found that overexpression of PBF significantly increased turnover of p53 protein when compared to vector-only control cells (Figure 1.12B) (Read et al. 2014, Read et al. 2016b). This observed reduction in p53 stability was abrogated following siRNA-mediated depletion of PBF in TPC-1 cells (Read et al. 2014). Given the diminished p53 stability, ubiquitination assays were performed following treatment with the proteasome inhibitor MG132. Several high molecular weight p53 conjugates were apparent in PBF-transfected TPC-1 and HCT116 cells, thus suggesting accumulation of ubiquitinated p53 (Read et al. 2014, Read et al. 2016b). Later investigations revealed that the reduction in p53 stability by PBF in thyroid cells occurred in an MDM2-dependent manner (Read et al. 2014).

To determine the functional consequences of p53 modulation by PBF, transient reporter assays were performed in p53-null H1299 cells. When PBF and p53 were co-expressed, PBF significantly repressed p53-mediated transactivation of the well-established p53-responsive genes p21 and MDM2/HDM2 in all three thyroid and colorectal cancer cell lines (Figure 1.12C) (Read et al. 2014, Read et al. 2016b). Furthermore, PBF was capable of altering the sensitivity of thyroid cells to irradiation in a p53-dependent manner (Read et al. 2014). Taken together, these data suggest a role for PBF in DNA damage and repair pathways through modulation of p53 stability and activity.

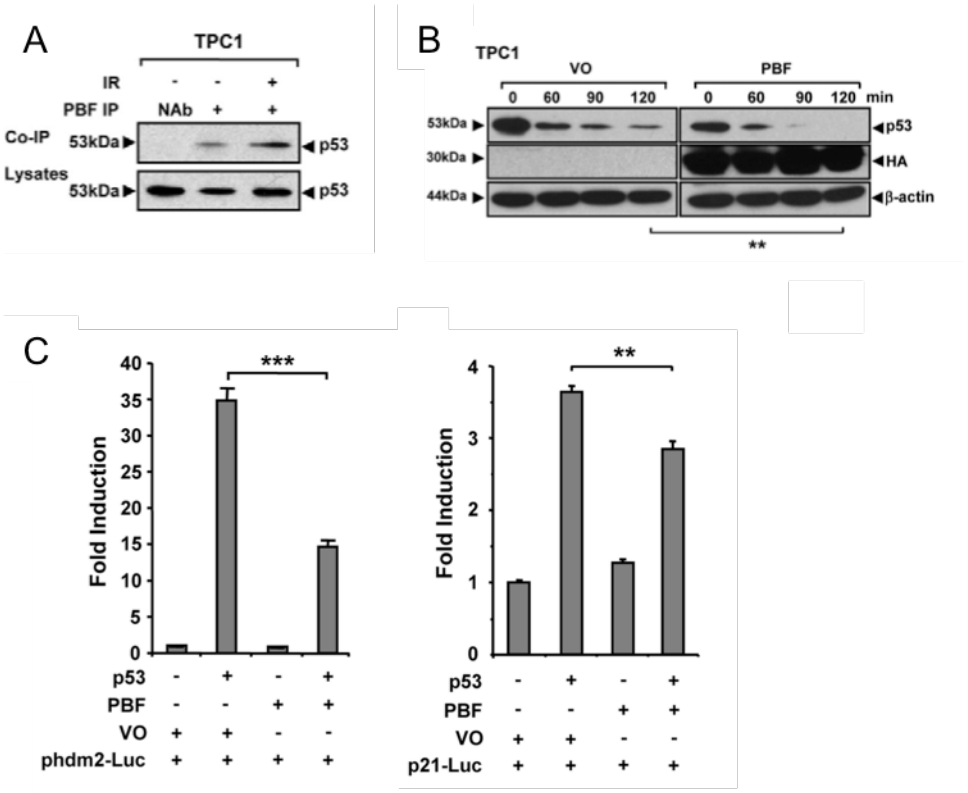


*Figure 1.12 PBF interacts with p53 in vitro and reduces p53 stability and transcriptional activity.* ***A*** *– co-immunoprecipitation of p53 with PBF in untreated (-IR) or irradiated (+IR) TPC-1 cells, NAb = no antibody control.* ***B*** *– Western blot analysis of half-life assays performed in TPC-1 cells transfected with PBF-HA and treated with 100 μM anisomycin. Protein was harvested at the indicated times post-treatment.* ***C*** *– H1299 cells were transfected with p53 luciferase reporter plasmids for HDM2 (left) or p21 (right), in conjunction with PBF and p53, or VO as indicated. Luciferase activity was measured 24 hours later (figures from Read et al. 2014 and Read et al. 2016b).*

Consistent with this, repression of p53-related DNA damage response genes was observed in primary thyrocytes obtained from a transgenic mouse model of thyroid-specific PBF overexpression (PBF-Tg) (Figure 1.13). Exposure to ionising radiation, to stabilise p53, further confirmed significant downregulation of a number of DNA damage response genes, including many involved in maintaining genomic integrity (Read et al. 2016a). Moreover, primary thyrocytes obtained from a bitransgenic mouse model of thyroid specific PTTG and PBF over-expression displayed even more extensive DNA damage response gene suppression, thus indicating that PTTG and PBF cooperate to disrupt p53 activity (Read et al.

2016a). Importantly, PBF-Tg thyrocytes also displayed a greater level of genetic instability than age- and sex-matched WT mice (Read et al. 2016a).

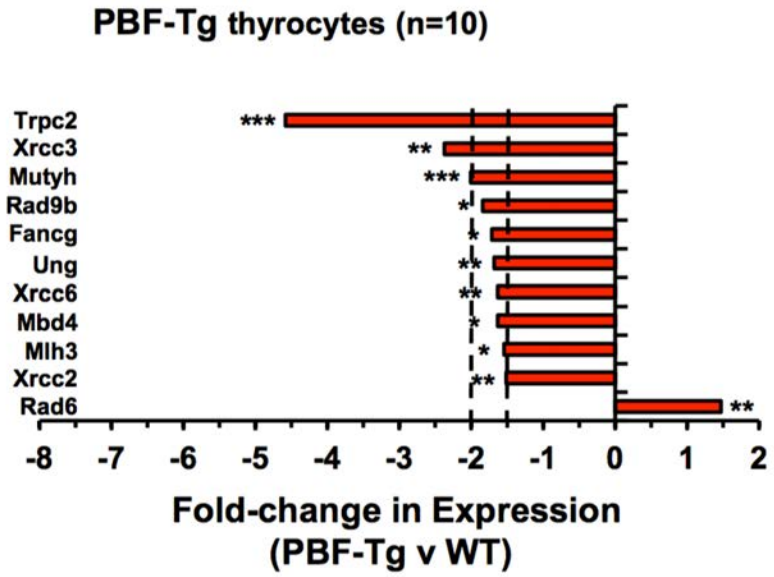


*Figure 1.13 Transcriptional profile of DNA damage response genes in PBF-Tg thyrocytes. Gene expression analysis used a DNA damage signalling pathway-focussed RT2 Profiler PCR array in PBF-Tg thyrocytes. Graph shows expression of DNA damage response genes altered >1.5-fold versus wild-type (WT). * p ≤0.05, ** p ≤0.01, *** p ≤0.001(figure from Read et al. 2016a).*

*1.5.2.3 PBF, CTTN and cell invasion*

Another mechanism by which PBF has been shown to promote tumour progression is through the induction of *in vitro* cell migration and invasion. Our group has previously shown that PBF drives breast cancer cell migration (Watkins et al. 2010). Overexpression of PBF significantly increased the invasiveness of MCF-7 cells, as determined by 2D Boyden chamber assays (Watkins et al. 2010). Critically, the observed increase in cell invasion was effectively abolished following siRNA-mediated silencing or specific mutation of the PBF gene (Watkins et al. 2010). Increased PBF promoter activity was independently correlated with poor prognosis and an increased risk of breast cancer metastasis (Xiang et al. 2012).

Consistent with our original findings, PBF overexpression has been demonstrated to induce the proliferation and invasion of hepatocellular carcinoma cells in 3D matrigel invasion assays (Li et al. 2013). In addition, work conducted by our group has recently confirmed that PBF is consistently able to induce the migration and invasion of a panel of thyroid, colorectal and breast cancer cell lines, across a variety of different *in vitro* assays (Watkins et al. 2016). A potential mechanism of PBF-induced cell invasion was also revealed. Through extensive mass spectrometry our group identified cortactin as an interacting partner of PBF (Watkins et al. 2016). Cortactin is an actin-polymerising scaffold protein, which drives the formation of specialised membrane protrusions at the leading edge of actively migrating cells (Weaver et al. 2001, Ayala et al. 2008).

Co-immunoprecipitation assays confirmed a direct interaction between PBF and cortactin *in vitro* in MCF-7 and HeLa cells (Watkins et al. 2016). This was further confirmed by proximity ligation assays, which revealed specific binding between PBF and cortactin, particularly at the periphery of the cells (Watkins et al. 2016). Importantly, siRNA-mediated knockdown of cortactin in PBF-transfected SW1736, HCT116 and MCF-7 cells significantly reduced the invasiveness of both cell lines to levels similar to or below those observed in vector-only-transfected cells (Watkins et al. 2016), thus demonstrating that cortactin depletion could ameliorate the effects of PBF overexpression. Furthermore, phosphorylation of PBF at residue Y174 was found to be critical for its functional interaction with cortactin as mutation of PBF residue Y174 (Y174A) led to a decrease in the invasive capacity of TPC-1 and MCF-7 cells, as determined by classical wound healing, 2D Boyden chamber and 3D organotypic assays (Watkins et al. 2016).

## 1.6 Hypothesis and aims

Overexpression of PTTG has been documented in several tumour types and is associated with tumour invasiveness (Zhang et al. 1999, Heaney et al. 2000, McCabe et al. 2003, Boelaert et al. 2003a, Solbach et al. 2004). PTTG encodes a multifunctional proto-oncogene, which has been implicated in numerous critical cellular processes, including mitotic regulation (Zou et al. 1999, Yu et al. 2000b), gene transactivation (Zhang et al. 1999, Pei 2001) and DNA repair (Romero et al. 2001, Kim et al. 2007b, Read et al. 2016a). PTTG has also been reported to bind to p53 and alter p53 transcriptional activity (Bernal et al. 2002).

Several high-profile studies have reported PTTG overexpression in squamous cell carcinomas of the head and neck, where elevated expression independently correlates with advanced tumour stage and poor prognosis (Shibata et al. 2002, Solbach et al. 2006, Ito et al. 2008, Yan et al. 2009). A recent unpublished GEO profile cDNA array analysis of matched normal and HNSCC samples has further suggested a potential upregulation of its interacting partner PBF in HNSCC ($p=0.026$, $n=22$). In addition, previous research conducted by our group has demonstrated that a functional interaction exists between PBF and p53 in thyroid and colorectal cancer (Read et al. 2014, Read et al. 2016b). PBF was shown to significantly reduce p53 protein stability via induction of MDM2-mediated ubiquitination and proteasomal degradation of p53 (Read et al. 2014). Furthermore, dysregulation of p53 stability by PBF significantly repressed p53-mediated transactivation of the down-stream targets p21 and HDM2 and was associated with increased genomic instability (Read et al. 2014, Read et al. 2016b).

Next-generation sequencing efforts have confirmed that mutation of the TP53 gene is one of the most common genetic alterations in HNSCC (Petitjean et al. 2007). Furthermore, p53 inactivation in tumours harbouring wild-type p53 may be achieved by additional mechanisms,

such as expression of HPV E6 and overexpression/amplification of HDM2 (Scheffner et al. 1990). These observations therefore demonstrate the importance of the TP53 gene in the suppression of HNSCC tumour formation and progression. Given that PTTG has been reported to be upregulated in HNSCC tumours, we hypothesise that the interacting partners PTTG and PBF are overexpressed in HNSCC and that high tumoural PTTG and PBF expression is associated with poor prognosis. Furthermore, as PTTG and PBF have been implicated in the regulation of p53 activity in other tumour types, we hypothesise that PTTG and PBF bind to p53 in the setting of head and neck cancer. We further hypothesise that PTTG and PBF overexpression in HNSCC cells leads to decreased p53 stability and hence inactivation of its tumour suppressor function, which may serve to promote HNSCC tumourigenesis and progression.

The aims of this thesis therefore were:

*Analysis of PTTG and PBF expression in matched HNSCC tumour specimens.* Quantitative real-time PCR and immunohistochemistry techniques were employed to determine PTTG/PBF mRNA expression in matched fresh-frozen HNSCC normal and tumour tissue specimens and PTTG/PBF protein expression in formalin-fixed paraffin-embedded tissue microarray sections. Expression data were then evaluated alongside the available clinical follow-up data to determine whether PTTG and PBF expression correlated with any clinicopathological features.

*Assessment of PTTG:p53 and PBF:p53 interactions in HNSCC cells.* Co-immunoprecipitation assays were performed to examine the potential interactions between PTTG/PBF and p53 in HPV-positive and HPV-negative HNSCC cell lines. Further co-immunoprecipitation assays were performed in the presence of reduced PTTG or PBF expression to determine the relative influence of PTTG and PBF on p53 binding.

*Assessment of the effects of PTTG:p53 and PBF:p53 interactions on p53 stability and function.* Anisomycin half-life studies were used to determine the relative contributions of PTTG and PBF to p53 protein stability in HNSCC cells. Additional real-time quantitative PCR analyses were performed to determine the consequences of PTTG and PBF expression on p53 transcriptional activity in the presence and absence of irradiation-induced DNA damage.

*Assessment of the effects of PTTG and PBF expression on the invasiveness of HNSCC cells.* 2D Boyden chamber invasion assays and classical wound healing assays were used to examine the effects of PTTG and PBF expression on the invasiveness of HNSCC cells. Colony formation assays were also performed to determine whether manipulation of PTTG and PBF expression could alter the transforming capacities of HNSCC cells.

# Chapter 2

# Materials and Methods

## 2.1 Cell lines

The human head and neck squamous cell carcinoma (HNSCC) cell lines, 92-VU-040T and 93-VU-147T were kindly provided by Professor Hisham Mehanna (The Institute of Head and Neck Studies and Education, School of Cancer Sciences, University of Birmingham). The clinical features of the HNSCC cell lines and the personal characteristics of the patients associated with the cell lines are summarised in Table 2.1. The 92-VU-040T cell line is a moderately differentiated HPV-negative HNSCC line. It was derived from biopsies of a primary squamous cell carcinoma of the oral cavity (tongue) of a 65 year-old female patient and expresses wild-type p53 (Hermsen et al. 1996, White et al. 2006). The 93-VU-147T cell line is also a moderately differentiated HNSCC line, which was derived from biopsies of a primary squamous cell carcinoma of the oral cavity (floor of mouth) of a 58 year-old male patient (White et al. 2006, Hermsen et al. 1996). The cells contain a heterozygous mutation in the TP53 gene (c.770T>G, p.L257R) predicted to render the translated p53 protein non-functional (Kimple et al. 2013). The cells also contain integrated HPV-16 DNA (Hermsen et al. 1996, White et al. 2006). All HNSCC lines were routinely cultured as a monolayer in 75 $cm^2$ vented-cap flasks in complete Dulbecco's Modified Eagle's Medium [Sigma-Aldrich, St. Louis, MO, USA] supplemented with L-glutamine [Life Technologies Ltd, Thermo Fisher Scientific, Paisley, UK], Penicillin ($10^5$ U/L) [Life Technologies Ltd], Streptomycin (100 mg/L) [Life Technologies Ltd] and 10 % heat-inactivated foetal bovine serum (FBS) [Life Technologies Ltd]. Cells were passaged twice weekly and split at 12.5-20 %. Human HNSCC cell lines were authenticated by short tandem repeat (STR) DNA profiling.

HeLa cells were obtained from the European Collection of Cell Cultures, UK. These epithelial cells, derived from a human epidermoid carcinoma of the cervix (Scherer et al. 1953), were used due to their well-characterised phenotype and their ability to be easily

transfected. Cells were cultured in complete DMEM containing L-glutamine, penicillin ($10^5$ U/L), streptomycin (100 mg/L) and 10 % FBS. Cells were passaged twice weekly and split at 17 %.

| | Patient details | | | | Clinical features | | | |
|---|---|---|---|---|---|---|---|---|
| **Cell line** | **Age** | **Gender[a]** | **Smoking** | **Alcohol** | **Origin[b]** | **Site** | **Pathological stage** | **TP53 codon** |
| **92-VU-040T** | 65 | F | - | - | NP | Tongue | T3N0 | WT |
| **93-VU-147T** | 58 | M | + | + | NP | Floor of mouth | T4N2 | c.770T>G |

[a] Abbreviations: F, female; M, male.
[b]Abbreviations: NP, new primary.

*Table 2.1 Clinical features and personal characteristics of the patients associated with the HNSCC cell lines.*

## 2.2 Transfection

### 2.2.1 Vectors

Transient over-expression was achieved by transfecting cells with the expression vectors, pCDNA3.1+ [Invitrogen™, Thermo Fisher Scientific, Paisley, UK] or pCI-NEO [Promega, Madison, WI, USA], containing the full coding sequence of the gene of interest. Both expression vectors contained the human cytomegalovirus (CMV) immediate-early promoter and sites for antibiotic resistance (Figure 2.1).

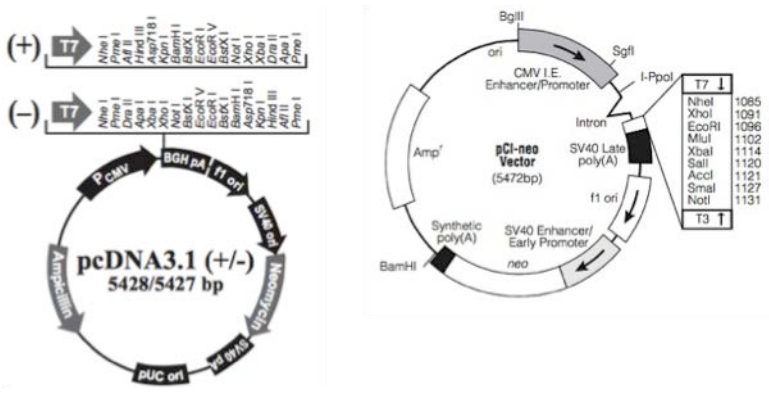

*Figure 2.1 pcDNA3.1+ and pCI-NEO vector maps, showing the origin of replication (ori), ampicillin resistance gene (Amp$^r$/Ampicillin) and restriction endonuclease sites.*

*2.2.1.1 Bacterial transformation*

Subcloning Efficiency™ DH5$\alpha$™ chemically competent E. coli cells were used, according to the manufacturer's instructions [Invitrogen™]. Once thawed on ice, 50 µl of bacterial cells were transferred to 1.5ml microcentrifuge tubes and 10 µg of plasmid DNA added. Following a 30-minute incubation on ice, the cells were heat-shocked at 42 °C for 20 seconds and placed on ice for a further 2 minutes. Lysogeny broth (LB) was added (950 µl per tube) and the cells incubated at 37 °C for 1 hour at 225 rpm. Bacterial cells were pelleted by centrifugation at 13,000 rpm for 3 minutes in a bench-top centrifuge and re-suspended in 50-100 µl of LB. The bacterial cells were then spread onto pre-warmed LB-agar plates containing the appropriate antibiotics and incubated at 37 °C without shaking for 16 hours. A single colony was selected from each LB-agar plate and incubated at 37 °C for a further 16 hours at 225 rpm in 5 ml of LB containing antibiotics.

*2.2.1.2 DNA purification and sequencing*

All steps were performed at room temperature. Plasmid DNA was purified using the Wizard® Plus SV Minipreps DNA Purification System [Promega]. 4.5 ml of the bacterial starter culture was centrifuged at 10,000 x *g* in a table-top centrifuge for 5 minutes and the supernatant discarded. The bacterial pellets were then re-suspended in 250 µl of cell lysis solution and incubated for 5 minutes, or until the solution had cleared. 10 µl of alkaline protease was added to inhibit endonucleases and other proteins released during lysis and the solution incubated for 5 minutes. Following this, 350 µl of neutralisation solution was added and the bacterial lysate centrifuged at 14,000 x *g* for 10 minutes. The cleared lysate was then transferred to a spin column, centrifuged at 14,000 x *g* for 1 minute and the flow-through

discarded. Plasmid DNA was then washed twice with column wash solution, centrifuged at 14,000 x *g* for 2 minutes and the spin column transferred to a new 1.5 ml microcentrifuge tube. Plasmid DNA was finally eluted in 100 µl of nuclease-free water and the DNA concentration quantified using the NanoDrop 1000 Spectrophotometer [NanoDrop, Wilmington, DE, USA].

For sequencing, 250 ng of plasmid DNA was mixed with 3.2 pmol of forward or reverse primers in a total volume of 10 µl. T7 short forward and BGH reverse primers were used for sequencing pcDNA3.1+ plasmids and T7 short forward and T3 reverse primers were used for sequencing pCI-NEO plasmids (Table 2.2).

| Sequence Name | Sequence |
|---|---|
| **T7 short forward** | 5' TAATACGACTCACTATAGGG 3' |
| **T3 reverse** | 5' ATTAACCCTCACTAAAG 3' |
| **BGH reverse** | 5' TAGAAGGCACAGTCGAGG 3' |

*Table 2.2 Table of forward and reverse primer sequences for sequencing pcDNA3.1+ and pCI-NEO vectors.*

*2.2.1.3 DNA amplification*

Plasmid DNA, with the correct sequence, was amplified using the GenElute™ High Performance (HP) Plasmid Maxiprep Kit [Sigma]. 300 µl of the bacterial starter culture was transferred to 150 ml of LB containing antibiotics and incubated overnight at 37 °C in an orbital shaker set to 225 rpm. All steps were performed at room temperature. The overnight culture was centrifuged at 5,000 x *g* for 10 minutes and the bacterial pellets re-suspended in 12 ml of resuspension/RNase A solution. The bacterial cells were then lysed upon addition of 12 ml of lysis solution, immediately followed by 6-8 inversions. After a 5-minute incubation, 12 ml of chilled neutralisation solution was added to terminate lysis and the solution inverted 4-6 times. 9 ml of binding solution was then added and the bacterial lysate inverted twice

before being transferred to the barrel of a filter syringe, where it was left to stand for 5 minutes. During this incubation period, the binding column was prepared by adding 12 ml of column preparation solution followed by centrifugation at 3,000 x *g* for 2 minutes. The cleared bacterial lysate was then filtered through the syringe into the binding column and centrifuged at 3,000 x *g* for 2 minutes. The bound DNA was then washed by centrifuging with 12 ml of wash solution 1 at 3,000 x *g* for 2 minutes. This was followed by a second wash-step with 12 ml of wash solution 2 and centrifugation at 3,000 x *g* for 5 minutes. DNA was finally eluted in 3 ml of nuclease-free deionised water (NF-$dH_2O$) by centrifuging at 3,000 x *g* for 5 minutes. Plasmid DNA concentration was determined using the NanoDrop 1000 Spectrophotometer [NanoDrop].

### 2.2.2 Transfection of Bacterial Plasmids

Plasmid transfection was performed 24 hours after seeding cells using *Trans*IT®-LT1 or *Trans*IT®-2020 transfection reagents [Mirus Bio LLC, Madison, WI, USA] at a 3:1 ratio with plasmid DNA (6 µl of transfection reagent : 2 µg plasmid DNA per well of a 6-well plate). Transfections were carried out according to the manufacturer's instructions. Plasmid DNA was diluted in pre-warmed Opti-MEM® I reduced serum medium [Life Technologies Ltd] before addition of the transfection reagent, which was warmed to room temperature and briefly vortexed beforehand. The mixture was then left to stand for 30 minutes to enable DNA-lipid/polymer complexes to form. After this incubation period, 200 µl of the transfection mixture was added per well. For T25 $cm^2$ flasks, 5 µg of plasmid DNA was required and 500 µl of the transfection mixture was added per flask. Total protein and RNA was harvested 24 or 48 hours post-transfection.

### 2.2.3 siRNA transfection

Small double-stranded RNA molecules, known as short interfering RNA (siRNA), were used to initiate the RNA interference pathway (RNAi) in order to silence expression of specific messenger RNAs (mRNA). siRNA transfection was carried out using either Lipofectamine™ 2000 [Invitrogen™] or siPORT™ *NeoFX*™ [Invitrogen™] transfection reagents according to the manufacturer's instructions. Briefly, target gene-specific siRNA or non-targeting scrambled control siRNA were delivered to cells, seeded 24-hours prior to transfection, in pre-warmed Opti-MEM® I reduced serum medium [Life Technologies Ltd] at a final concentration of 100 nM. The transfection reagent and siRNA were diluted in separate aliquots of Opti-MEM® and incubated for 5 minutes at room temperature. The aliquots were then combined and left to stand for an additional 15 minutes. The media was then removed from the cells and replaced with 1 ml per well (6-well plate) of the transfection mixture. Total protein or RNA was then harvested 48-72 hours post-transfection.

## 2.3 RNA extraction and quantification

Total RNA was extracted from matched human HNSCC tumour and normal tissue specimens using the RNeasy® Micro Kit [Qiagen] according to the manufacturer's instructions. Total RNA was quantified using the NanoDrop 1000 Spectrophotometer at the λ260 nm wavelength [NanoDrop].

RNA extraction from cells was carried out using a guanidine thiocyanate and phenol monophasic solution (TRI reagent [Sigma-Aldrich]). All quantities refer to RNA extraction from cells seeded in a 6-well plate. Media was removed and the cells washed once with phosphate buffered saline (PBS). 500 µl per well of TRI reagent was then added and the samples transferred to 1.5 ml microcentrifuge tubes and subjected to a freeze/thaw cycle at -

80 °C. Once thawed, 100 µl of chloroform (≥ 99.5 %) [Sigma-Aldrich] was added and the samples shaken vigorously for 15 seconds before being left to stand for 15 minutes at room temperature. Samples were then subjected to centrifugation at 12,000 *x* g for 15 minutes at 4 °C and the uppermost aqueous layer containing the RNA transferred to a clean 1.5 ml microcentrifuge tube, to which, 250 µl of isopropanol [Sigma-Aldrich] was added. Following this, the samples were incubated for a further 10 minutes at room temperature, centrifuged at 12,000 *x* g for 10 minutes at 4 °C and the supernatant discarded. The pelleted RNA was washed once in 500 µl of 75 % ethanol [VWR International Ltd, Lutterworth, UK] and then centrifuged at 9,000 *x* g for 5 minutes at 4 °C. The ethanol was removed and the pellet left to air-dry for approximately 10 minutes before being resuspended in 20-30 µl of NF-$dH_2O$. Total RNA concentrations were quantified using the NanoDrop 1000 Spectrophotometer at the λ260 nm wavelength [NanoDrop].

## 2.4 Reverse transcription

Total RNA was reverse transcribed using the Reverse Transcription System [Promega]. 500 ng of RNA was reverse transcribed in a total reaction volume of 10 µl with the avian myeloblastosis virus (AMV) reverse transcriptase. The reaction mix consisted of 2 µl of 25 mM magnesium chloride ($MgCl_2$), 1 µl of 10X reverse transcription buffer, 1 µl of 10 mM deoxynucleotide triphosphate (dNTP) mix, 0.25 µl of recombinant RNasin® ribonuclease inhibitor, 7.5 units of AMV reverse transcriptase, 0.5 µl of random hexamer primers and 4.9 µl of RNA. The reactions were as follows; room temperature for 10 minutes, 42 °C for 60 minutes, 95 °C for 5 minutes and 4 °C for 5 minutes. The samples were then briefly centrifuged and diluted to 10 ng/µl in 40 µl of NF-$dH_2O$.

## 2.5 Quantitative real-time PCR (qPCR)

The relative expression levels of mRNAs encoding different proteins were determined by quantitative, real-time PCR. Experiments were performed using the ABI 7500 Sequence Detection System [Applied Biosystems™, Thermo Fisher Scientific, Paisley, UK] in conjunction with pre-designed and pre-optimised Taqman® gene expression assays [Applied Biosystems™] or with custom-designed primers [Sigma-Aldrich].

Taqman® gene expression assays consist of a pair of unlabelled sequence-specific forward and reverse primers and a Taqman® probe. Covalently linked to the 3' end of the probe is a fluorescent reporter dye, either VIC® (full name patent protected) or FAM™ (6-carboxy-fluorescien), and at the 3' end the quencher dye, TAMRA™ (tetramethylrhodamine). Whilst the probe is intact, the quencher dye is in close proximity to and suppresses fluorescence emission by the reporter dye via a mechanism known as fluorescence resonance energy transfer (FRET). During this process, the reporter dye, in its electronic excited state, acts as a donor and transfers energy to the low energy quencher dye. The probe anneals downstream of the primers and, as Taq DNA polymerase extends the primers, is degraded by the 5' to 3' endonuclease activity of the polymerase. Degradation of the probe releases the reporter dye, which is no longer in close proximity with the quencher dye and therefore enables fluorescence emission and detection of this excitation by the real-time PCR thermal cycler. As the reporter dyes are cleaved from their respective probe during each PCR cycle, the fluorescence detected by the real-timer PCR thermal cycler is directly proportional to the level of DNA template in the sample.

Real-time PCR reactions were carried out in duplicate in MicroAmp optical 96-well PCR reaction plates [Applied Biosystems™] in a total volume of 20 µl. Each reaction consisted of 2 µl of cDNA (10 ng/µl), 1 µl of the appropriate Taqman® gene expression assay [Applied

Biosystems™], 10 µl of 2X qPCR Master Mix Plus QGS (HotGoldStar DNA polymerase, dNTP, dUTP, $MgCl_2$, Uracil-N-glycosylase (UNG), stabilisers and ROX™ passive reference) [Eurogentec, Southampton, UK], and 8 µl of NF-$dH_2O$. Where, custom-designed primers and probes were being used, the reaction buffer consisted of the following: 2 µl of cDNA, 1 µl of forward PCR primer, 1 µl of reverse PCR primer, 1 µl of probe, 10 µl of 2X qPCR Master Mix Plus QGS and 5 µl of NF-$dH_2O$. All target gene probes were labelled with FAM™. 18S and PPIA were used as internal references to account for variations in reverse transcription and real-time PCR amplification efficiencies between samples and were labelled with VIC® and FAM™, respectively. PCR reactions were performed under the following conditions: 50 °C for 2 minutes to enable activation of UNG, which minimises carry-over of PCR products (Longo et al. 1990), 95 °C for 10 minutes, for activation of HotGoldStar DNA polymerase and to inactivate UNG, followed by 45 cycles of 95 °C for 15 seconds (to denature the DNA template) and 60 °C for 1 minute (to enable primers and probe annealing and primer extension).

The threshold line for each PCR reaction was positioned within the exponential phase of the amplification curve. The threshold cycle ($C_t$) value was then calculated as the PCR cycle number at which each logarithmic PCR plot on the amplification curve intersected the set threshold line. The $\Delta C_t$ value was then calculated by subtracting the $C_t$ value of the internal reference from the $C_t$ value of the target gene for each sample. Fold changes in mRNA expression levels between the control and experimental groups were then assessed by use of the formula $2^{-\Delta\Delta Ct}$, where $\Delta\Delta C_t$ was the $\Delta C_t$ value of the experimental group subtracted by the $\Delta C_t$ value of the control group.

## 2.6 Western blotting

### 2.6.1 Protein extraction and quantification

24-48 hours post-transfection, cells were washed with phosphate buffered saline (PBS) and lysed with radioimmunoprecipitation assay (RIPA) lysis buffer (150 mM sodium chloride, 50 mM Tris pH 7.4, 6 mM sodium deoxycholate, 1 % v/v Igepal CA-630 and 1 mM ethylenediaminetetraacetic acid (EDTA)), containing 60 µl/ml of Protease Inhibitor Cocktail (104 mM 4-(2-aminoethyl)benzenesulfonyl fluoride (AEBSF), 80 µM Aprotinin, 4 mM Bestatin, 1.4 mM E-64, 2 mM Leupeptin and 1.5 mM Pepstatin A in dimethyl sulfoxide (DMSO)) [Sigma-Aldrich], which inhibits serine, cysteine and aspartic proteases, as well as, aminopeptidases. For the specific detection of phosphorylated proteins, phosphatase inhibitor cocktails [Sigma-Aldrich] (Cocktail 2 (for Tyrosine phosphatase inhibition): sodium orthovanadate, sodium molybdate, sodium tartrate, imidazole; Cocktail 3 (for Serine/Threonine Phosphatase inhibition): Cantharidin, (−)-p-Bromolevamisole oxalate and Calyculin A) were also added at 10 µl/ml. Cells were then subjected to a single freeze-thaw cycle at -20 °C for a minimum of 20 minutes to aid cellular lysis, scraped and then transferred to clean microcentrifuge tubes following centrifugation at 12,000 *x* g for 20 minutes at 4 °C.

Protein concentrations were assessed by Pierce™ bicinchoninic acid (BCA) colorimetric assay [Thermo Scientific™, Thermo Fisher Scientific, Paisley, UK]. Bovine serum albumin (BSA) protein standards were prepared at concentrations 0, 0.125, 0.25, 0.5, 0.75, 1.0, 1.5, 2.0, 2.5 and 5.0 µg/ml in RIPA buffer to compare with the cell lysates. Protein standards and cell lysates were measured in duplicate in a 96-well plate, with 78.4 µl of Reagent A and 1.6 µl of reagent B added to each sample. The plate was then incubated for 30 minutes at 37 °C and absorbance measured at 560 nM using the Victor$^3$ 1420 Multilabel Counter [PerkinElmer,

Waltham, MA, USA]. Protein concentrations were then determined using the standard curve generated from the BSA protein standards.

### 2.6.2 Western blotting

Protein samples were prepared at 25-30 µg with 20 % v/v 5X protein loading buffer (250 mM Tris pH 6.8, 10 % sodium dodecyl sulphate (SDS), 0.02 % bromophenol blue, 50 % glycerol and 12.5 % β-mercaptoethanol) and incubated at 95ºC for 5 minutes before pulse centrifuging at 13,000 rpm in a bench-top centrifuge. The resolving gel (375 mM Tris pH 8.8, 12 % acrylamide (from 30 % (w/v) acrylamide:0.8 % (w/v) bis-acrylamide stock) [Geneflow, Lichfield, UK], 3.5 mM SDS, 0.1 % (v/v) tetramethylethylenediamine (TEMED) [Sigma-Aldrich] and 4.4 mM ammonium persulphate (APS) [Sigma-Aldrich] was prepared, followed by the stacking gel (375 mM Tris pH 6.8, 5 % acrylamide, 7 mM SDS, 0.2 % TEMED and 8.8 mM APS), and the protein samples separated by SDS-polyacrylamide gel electrophoresis (SDS-PAGE) in running buffer (24.8 mM Tris, 192 mM glycine and 3.5 mM SDS). Protein samples were run alongside 5 µl of BLUeye pre-stained protein ladder (10-245 kDa) molecular weight marker [Geneflow].

The separated proteins were subsequently transferred onto polyvinylidene difluoride (PVDF) membranes [Fisher Scientific™], previously activated by immersion in 100 % methanol for a minimum of 30 seconds, in transfer buffer (25 mM Tris, 192 mM glycine and 20 % methanol) at 360 mA for 1 hour and 20 minutes. Membranes were then blocked with 5 % w/v skimmed milk powder [Marvel; Premier Foods Group Ltd, London, UK] or 5 % w/v IgG-free BSA [Stratech, Scientific Ltd, Suffolk, UK] in Tris-buffered saline containing tween (TBS-T; 20 mM Tris pH 7.6, 137 mM sodium chloride, 0.00025 % v/v tween-80®) for 1 hour 30 minutes at room temperature. Primary antibodies were prepared in 5 % skimmed milk or 5

% IgG-free BSA in TBS-T at the following v/v ratios: polyclonal rabbit anti-human PBF 1: 500 (made for our laboratory using the full length PBF protein as the epitope (Smith et al. 2009) [Eurogentec, Seraing, Germany], monoclonal mouse anti-human PTTG 1:1000 [Abcam, Cambridge, UK], monoclonal rabbit anti-human T60-phosphorylated PTTG 1:200 [CovalAb, Villeurbanne, France], monoclonal mouse anti-human HA 1:1000 [Biolegend, San Diego, CA, USA] and monoclonal mouse anti-human p53 1:500 [Santa Cruz Biotechnology, Dallas, TX, USA]. The membranes were incubated with 5 ml of primary antibody overnight at 4ºC with gentle rocking. Excess antibody was removed by washing 3 times for 10 minutes at room temperature with TBS-T before incubating with the secondary antibody (horseradish peroxidase (HRP)-conjugated polyclonal goat anti-rabbit or rabbit anti-mouse immunoglobulins) prepared in 5 ml of 5 % skimmed milk in TBS-T for 1 hour at room temperature with rocking. Following 3 10-minute washes with TBS-T, membranes were incubated with Pierce™ ECL chemiluminescent substrate [Thermo Scientific™] in order to detect antigen-antibody complexes.

## 2.7 Co-immunoprecipitation

Cells seeded in 25 $cm^2$ tissue culture flasks were harvested in 500 µl of modified RIPA buffer (150 mM sodium chloride, 50 mM Tris pH 7.4, 6 mM sodium deoxycholate, 1 % v/v Igepal CA-630 and 1 mM ethylene glycol tetraacetic acid (EGTA)) containing 60 µl/ml of PI cocktail. Samples were sonicated twice for 30 seconds on the medium setting of the Diagenode Bioruptor® [Diagenode, Seraing, Belgium] before centrifuging at 4 °C for 30 minutes at 13,000 rpm. The cell lysate was then transferred to a clean microcentrifuge tube and 50 µl removed and stored at -20 °C. Primary antibody at the appropriate concentration was then added to the remaining cell lysate and incubated overnight at 4 °C with end-over-

end mixing. Protein G sepharose beads [GE Healthcare Life Sciences, Little Chalfont, Buckinghamshire, UK] were pulse centrifuged and resuspended in modified RIPA buffer. 50 µl of the protein G sepharose bead slurry was then added and the samples incubated at 4 °C with end-over-end mixing for a further 2 hours. The samples were pulse centrifuges to pellet the beads and the supernatant discarded. Unbound protein was eliminated by washing the beads in 500 µl of modified RIPA buffer followed by pulse centrifugation. Bound protein was subsequently eluted in 2x loading buffer (1:20 β-mercaptoethanol and 1 % SDS in Laemmli buffer [Bio-rad Laboratories Ltd, Hemel Hempstead, Hertfordshire, UK]) and incubated at 37 °C for 30 minutes. Loading buffer was also added at a 1:1 ratio (v:v) to the retained whole cell lysates and both these and the immunoprecipitated samples loaded onto 12 % acrylamide gels for subsequent analysis via Western blotting (as described above).

## 2.8 p53 half-life assay

Half-life assays to determine the effect of PBF and PTTF on p53 stability were performed 24 hours post-transfection. Media was removed from the cells and replaced with 1 ml per well of Anisomycin [Sigma-Aldrich] diluted in pre-warmed Opti-MEM® I reduced serum medium at a final concentration of 100 mM at the following time points: 0, 60, 90 and 120 minutes. Following the 2-hour time-course, total cellular protein was harvested in RIPA buffer containing 60 µl/ml of PI cocktail and the samples prepared for Western blotting.

## 2.9 BrdU cell proliferation assay

The rate of cellular proliferation was assessed by labelling cellular DNA with the pyrimidine analog, BrdU (5-bromo-2’deoxyuridine) [Cell proliferation ELISA, BrdU (colorimetric), Roche, Burgess Hill, UK]. BrdU becomes incorporated into newly synthesised

DNA during cell proliferation, substituting for thymidine. Detection of incorporated BrdU using antibodies specific for BrdU allows labelling of actively replicating cells in the S phase of the cell cycle.

Cells were seeded into 96-well tissue culture plates in 100 µl of complete medium and incubated overnight at 37 °C, 5 % $CO_2$ to allow cells to adhere. After 20 hours, the cells were incubated for a further 4 hours at 37 °C, 5 % $CO_2$ with 100 µM BrdU labelling reagent. The BrdU labelling reagent was then aspirated and the cells fixed and DNA denatured upon addition of 200 µl per well of FixDenat with subsequent incubation at room temperature for 30 minutes. After removal of the FixDenat solution, the cells were incubated for 90 minutes at room temperature with 100 µl per well of anti-BrdU-peroxidase antibody. The anti-BrdU-peroxidase antibody binds to the BrdU incorporated into newly synthesised DNA. Immune complexes were then detected by addition of 100 µl per well TMB (3,3',5,5'-Tetramethylbenzidine) substrate solution for 15 minutes. Absorbance was measured at 405 nm using the Victor$^3$ 1420 Multilabel Counter [PerkinElmer].

## 2.10 Immunuhistochemistry

Paraffin embedded formalin fixed tissue sections were immunostained using the Novocastra™ Novolink™ Max Polymer Detection System [Leica Biosystems, Wetzlar, Germany], according to the manufacturer's instructions. Sections were dewaxed in Xylene [Fisher Scientific™] and rehydrated using a propan-2-ol [Fisher Scientific™] concentration gradient. The slides were then rinsed with $dH_2O$ and antigen retrieval performed using Target Retrieval Solution, Sodium Citrate pH 6.0 [Dako] at a 1:10 dilution in $dH_2O$. Slides in diluted Target Retrieval Solution were then placed in a bench-top antigen retrieval chamber [2100-Retriever, Electron Microscopy Sciences, Hatfield, PA, USA] for 30 minutes and allowed to

cool for a further 20 minutes. The slides were then washed with 50mM Tris/150mM sodium chloride (pH 7.6) (TBS) and incubated with 100µl of 3 % (v/v) hydrogen peroxide for 10 minutes to block endogenous peroxidase activity. Following 3 5-minute washes in TBS, the slides were blocked with 100µl of 0.4 % casein in phosphate-buffered saline (PBS), with stabilisers, surfactant, and 0.2 % Bronidox L as a preservative [Leica Biosystems] for 10 minutes. After blocking, the slides were incubated with 100µl of the relevant primary antibody diluted in PBS containing 1 % IgG-free Bovine Serum Albumin (BSA) [Jackson ImmunoResearch Laboratories, Pennsylvania, USA], 0.1 % Tween-20, and 10 % normal serum for 16 hours at 4 °C in a humidity chamber. The specificity of each antibody was confirmed by addition of control tissue sections, in which the, the primary antibody was replaced with non-immune serum. Following 3 5-minute washes in TBS, the slides were incubated with 100µl of Post Primary Block solution (rabbit anti-mouse IgG (<10µg/ml) in 10 % (v/v) animal serum in TBS/0/09 % ProClin™ 950) [Leica Biosystems] for 30 minutes, followed by 3 5-minutes washes with TBS, and then incubated with 100µl of Novolink™ Polymer solution (anti-rabbit-Poly-HRP-IgG (<25µg/ml) in 10 % (v/v) animal serum in TBS/0.09 % ProClin™ 950) [Leica Biosystems] for 30 minutes. Excess polymer solution was removed with 5 minute washes in TBS, after which, the peroxidase activity was developed by addition of 100µl of DAB Working solution (DAB chromogen (1.74 % w/v 3,3' -diaminobenzidine) diluted 1:20 in Novolink™ DAB Substrate Buffer (solution containing ≤0.1 % hydrogen peroxide) [Leica Biosystems]. Nuclei were then counterstained using Meyer's Haematoxylin [Sigma-Aldrich] for 10 seconds and the slides subsequently dehydrated using graded propan-2-ol concentrations. Lastly, sections were cleared in Xylene and mounted with coverslips using VectaMount™ permanent mounting medium [Vector Laboratories, Burlingame, CA, USA]. Slides were stored at room temperature.

## 2.11 List of antibodies

| Antibody | Clone | Supplier |
|---|---|---|
| Anti-PBF-8 | Rabbit polyclonal | Eurogentec |
| Anti-Y174-phosphorylated PBF | Rabbit monoclonal | CovalAb |
| Anti-PTTG1 | Mouse monoclonal $IgG2_a$ [DCS-280] [ab3305] | Abcam |
| Anti-T60-phosphorylated PTTG1 | Rabbit monoclonal | CovalAb |
| Anti-p53 | Mouse monoclonal $IgG2_a$ [DO-1] [sc-126] | Santa Cruz Biotechnology |
| Anti-HA11 | Mouse monoclonal IgG1 [16B12] | Biolegend |
| Anti-CDKN2A/$p16^{INK4a}$ | Rabbit monoclonal IgG [EPR1473] [ab108349] | Abcam |
| Anti-Rb | Mouse monoclonal IgG1 [IF8] [sc-102] | Santa Cruz Biotechnology |
| Anti-phospho-p53 (Ser-15) | Rabbit polyclonal [9284] | Cell Signaling |
| Anti-phospho-Histone H2A.X (S139) | Mouse monoclonal [JBW301] [16-193] | Millipore |
| Anti-β-actin | Mouse monoclonal [AC-15] | Sigma-Aldrich |

## 2.12 Statistical analysis

Data were analysed using GraphPad Prism version 5.0. The Normal Quantile Plot test was used to determine whether data followed normal distribution. If the data was found to follow normal distribution, statistical analysis was performed using a two-sample student's *t* test. On the other hand, for non-parametric data, the Mann-Whitney *U* test was utilised when comparing two groups of data. Analysis of variance (ANOVA) and Kruskal-Wallis tests were used for between-group comparisons of multiple groups of parametric and non-parametric data, respectively. Significance was taken as $p < 0.05$.

# Chapter 3

# PTTG expression in head and neck tumour tissue

## 3.1 General Introduction

Head and neck squamous cell carcinomas (HNSCC) are a highly diverse group of malignancies that arise in the mucosal lining of various sites within the head and neck region. These include the oral cavity, nasal cavity, paranasal sinuses, nasopharynx, oropharynx, hypopharynx and larynx. As a result of such heterogeneity, the epidemiological, histological and biological characteristics, as well as the clinical outcomes of this disease, vary considerably (Gillison 2004, Cancer Genome Atlas Network 2015).

HNSCC has been historically associated with heavy tobacco and alcohol consumption (Blot et al. 1988, Franceschi et al. 1990). The malignancy predominantly affects older individuals and is almost three times more common in males than females (Jemal et al. 2011). Locally advanced HNSCC is generally aggressive and can be difficult to treat. At present, a multimodal approach is used and involves surgical resection of the tumour mass followed by radiotherapy, with or without chemotherapy (Homer 2016, Nutting 2016). Unfortunately such indiscriminate therapy is often associated with severe long-term side-effects and functional deformities and despite treatment, the majority of patients carry a poor prognosis, with extremely low survival rates, particularly compared to other cancers, such as breast, cervix and colon (Jemal et al. 2011).

In recent years high-risk human papilloma viruses (HPV), in particular HPV-16, have been established as important drivers of OPSCC (Gillison et al. 2000, Chaturvedi et al. 2008). Interestingly, HPV-related OPSCC tends to occur in younger individuals and is associated with lower tobacco and alcohol consumption (Gillison et al. 2008, van Monsjou et al. 2013). Furthermore, evidence from global genomic screening efforts have demonstrated significant differences in chromosomal and gene expression profiles between HPV-negative and HPV-positive OPSCC and it is now widely accepted that both represent entirely distinct disease

subtypes (Dahlgren et al. 2003, Pyeon et al. 2007, Lohavanichbutr et al. 2009, Cancer Genome Atlas Network 2015). Importantly, although initial therapeutic strategies do not differ between HPV-negative and HPV-positive OPSCC, patients with HPV-positive OPSCC consistently have a more favourable prognosis (Fakhry et al. 2008) and often undergo treatment de-intensification to reduce toxicity associated with therapy (Mirghani et al. 2015). However, there remains a small subpopulation of HPV-positive OPSCC patients who demonstrate a worse outcome (Ang et al. 2010), thus making de-intensification problematic. Due to the aetiological, biological and clinical heterogeneity associated with HNSCC, particularly OPSCC, novel prognostic and predictive biomarkers are urgently required to help facilitate better patient selection, which will invariably prevent unnecessary treatment and related toxicity. With the exception of HPV status, risk stratification is currently based on the anatomical site, histological grade and TNM stage (Patel, Shah 2005). Additional biological markers will enable identification and further stratification of patients who are more likely to benefit from targeted molecular therapies, hopefully improving patient outcome.

Since its discovery, the pituitary tumor transforming gene (PTTG) has been shown to be involved in a diverse array of cellular processes including DNA repair (Kim et al. 2007b), growth factor expression (Boelaert et al. 2003a) and angiogenesis (Kim et al. 2007a). Known as the human securin, PTTG also plays a crucial role in mitotic regulation during the metaphase to anaphase transition by mediating sister chromatid separation (Zou et al. 1999). Furthermore, overexpression of PTTG has been documented in a wide range of tumour types, including oesophageal cancer and squamous cell carcinomas of the head and neck, where elevated expression is independently associated with advanced tumour stage, lymph node metastasis and poor survival rates (Shibata et al. 2002, Zhou et al. 2005, Solbach et al. 2006, Ito et al. 2008, Zhang et al. 2013, Zhang et al. 2014), thereby suggesting PTTG

overexpression may be of prognostic significance in the setting of HNSCC. However, the precise mechanisms underlying the involvement of PTTG in tumourigenesis remain elusive.

Phosphorylation of PTTG may be of particular importance as mis-regulation of this process may contribute to PTTG's oncogenic action. Systematic mutation of all 32 potential phosphorylatable serine, threonine and tyrosine residues in the human PTTG protein to alanine or glycine has recently led to the discovery of a putative phosphorylation site, threonine-60 (T60), near the destruction box motif (D-box) (Mora-Santos et al. 2013). Abrogation of PTTG-T60 phosphorylation by mutation (T60A) resulted in greater expression as a consequence of a prolonged half-life (30 minutes compared to 18 minutes for wild type PTTG) (Mora-Santos et al. 2013). Moreover, stable transfection of the T60A mutant in HCT116 cells devoid of PTTG ($HCT116^{sec-/-}$) induced tetraploidy, a form of chromosomal instability, as ascertained through fluorescent in-situ hybridisation (FISH). The T60A mutant also augmented the invasiveness of $HCT116^{sec-/-}$ cells when assessed using Matrigel invasion assays, possibly as a result of altered expression of numerous invasion-related genes, including matrix metalloproteases (MMP7, MMP9 and MMP13), cell adhesion molecules (CDH1, NCAM, CTNND2, LAMA3 and LAMB3) and integrins (ITGB5, ITGB2 and ITGA7) (Mora-Santos et al. 2013). The discovery of a point mutation (T60N) at this residue in human breast cancer provides further support that PTTG-T60 phosphorylation may be of biological and clinical importance, particularly, in the early detection and treatment of cancer (Stephens et al. 2012).

The purpose of this chapter was firstly to validate previously published data suggesting PTTG is overexpressed in HNSCC and may serve as a prognostic biomarker. We next wanted to assess whether PTTG is phosphorylated at residue T60 in human HNSCC and whether this is also associated with various clinicopathological parameters, such as tumour stage and nodal

status. Finally, as HPV-positive and HPV-negative OPSCCs represent biologically distinct disease subtypes, we also wished to elucidate any potential differences in PTTG expression and/or subcellular localisation between these two groups. To this end, total RNA was extracted from fresh-frozen tissue sections and PTTG mRNA expression assessed by real-time quantitative PCR. In addition, total and T60-phosphorylated PTTG protein expression was determined in formalin-fixed, paraffin-embedded microarray tissue sections by immunohistochemistry.

## 3.2 Methods

### 3.2.1 Cell Lines

HeLa cells were maintained in complete culture medium as described in section 2.1.

### 3.2.2 Human tissue specimens

#### *3.2.2.1 Fresh-frozen tissue*

Matched tumour and normal tissue specimens were a kind gift from Professor Hisham Mehanna (Institute of Head and Neck Studies and Education (inHANSE), University of Birmingham, Birmingham, UK). HNSCC tissue specimens were available from 24 patients who underwent surgery at the University Hospital Birmingham NHS Trust, UK. The samples provided were from 4 representative anatomical locations; oral cavity (14), oropharynx (5), larynx (3) and hypopharynx (2). Matched normal tissue was taken at least 3 cm from the tumour margin and was histologically examined to confirm the tissue was non-cancerous. Tissue samples were immediately snap-frozen in liquid nitrogen and then stored at -80 °C. Clinical follow-up data, including tumour type, tumour sub-site, TNM staging, smoking/alcohol history and p16 status were also available.

*3.2.2.2 Tissue microarrays*

Formalin-fixed, paraffin-embedded tissue sections were a kind gift from Professor Hisham Mehanna (Institute of Head and Neck Studies and Education (inHANSE), University of Birmingham, Birmingham, UK). HNSCC tumour specimens were arranged on tissue microarrays (TMA), with 2-4 sections per patient. Each section had a diameter of 1 mm and a thickness of 4 mm and was taken from morphologically representative areas of the whole tumour. A total of 53 cases were available from patients who underwent surgery at the University Hospitals Coventry and Warwickshire NHS Trust, UK or the Royal Liverpool and Broadgreen University Hospitals NHS Trust, UK. All samples provided were from the oropharynx. Demographic and clinical follow-up data, including tumour type, tumour sub-site, TNM staging, smoking/alcohol history and HPV status were also available.

*3.2.2.3 Ethics*

All specimens at the time of surgery were obtained following appropriate ethical approval and informed patient consent. Ethical approval was granted by the Yorkshire & the Humber-Leeds East National Research Ethics Service (NRES) committee (REC no. 14/YH/1101, secondary objective 10).

### 3.2.3 RNA extraction, reverse transcription and quantitative real-time PCR

Total RNA was extracted from fresh-frozen tissue specimens using the RNeasy® Micro Kit [Qiagen] according to the manufacturer's instructions. Total RNA was quantified using the NanoDrop 1000 Spectrophotometer at the λ260 nm wavelength [NanoDrop].

Total RNA was then reverse transcribed using the Tetro cDNA synthesis kit [Bioline] as per the manufacturer's guidelines. Briefly, 1 µg of RNA was reverse transcribed in a total volume of 20 µl with moloney murine leukemia virus (MMLV) reverse transcriptase. The

reaction mix consisted of 1 µl of random hexamer primers, 1 µl of 10 mM dNTP mix, 1 µl of 5X reverse transcription buffer, 1 µl of RiboSafe RNase inhibitor (10 U/µl), 1 µl of MMLV reverse transcriptase (200 U/µl), 1 µg of total RNA and diethylpyrocarbonate (DEPC)-treated water up to 20 µl total volume. The reactions were then incubated at 25 °C for 10 minutes, followed by 45 °C for 1 hour and 85 °C for 5 minutes. The samples were then briefly centrifuged and stored at -20 °C.

Quantitative real-time PCR was performed as previously described in section 2.5. Taqman gene-specific expression assays for PPIA (Hs04194521_s1) and PTTG (Hs00851754_u1) were purchased from Applied Biosystems.

### 3.2.4 Protein extraction, quantification and Western blotting

Protein was extracted from cell lysates and quantified as described in section 2.6.1. Western blotting was performed as described in section 2.6.2 using anti-PTTG 1:750, anti-T60-phosphorylated PTTG 1:200 and anti-β actin 1:15,000 antibodies. The T60 phospho-specific PTTG antibody was produced by CovalAb using three different peptides; CUK-1323A long phospho-peptide: $NH_2$ – C – FDAPPALPKATpRKAL –co$NH_2$, CUK-1323B short phospho-peptide: $NH_2$ – C –LPKATpRKA – co$NH_2$, and CUK-1323C control peptide: $NH_2$ – C – FDAPPALPKATRKAL – co$NH_2$. Both CUK-1232A and B were used for the immunisations to obtain antibodies specific to the modification. The serum was then purified against the control peptide to remove non-specific antibodies and against CUK-1323B to retain only specific antibodies. The antibody was then immunopurified from the serum and stored at -20°C for long-term use. A small aliquot was also stored in 1 % BSA (w/v) to help stabilise the antibody solution. For peptide blocking experiments, the phospho-specific PTTG-T60 antibody was incubated with a two-fold excess of neutralising peptide (supplied

by CovalAb) for 2 hours at room temperature with gentle shaking before incubation with the appropriate Western blot membrane. Detected bands were then analysed and quantified by densitometry using Image J (public domain software, available at http://rsb.info.nih.gov/ij/).

### 3.2.5 Immunohistochemistry

Paraffin-embedded, formalin-fixed tissue sections were immunostained using the Novocastra™ Novolink™ Max Polymer Detection System [Leica Biosystems], as outlined in section 2.10. Antibodies used were anti-PTTG 1:700 and anti-T60-phosphorylated PTTG 1:50. Evaluation of the stained slides was performed independently and in a blinded manner by Dr Rasoul Amel-Kashipaz (Clinical Laboratory Services, Cellular Pathology, University Hospitals Birmingham NHS Foundation Trust, Queen Elizabeth Hospital Birmingham, Birmingham, UK) and I. Each individual section was analysed by light microscopy and visually scored according to staining intensity (Figure 3.1; 0= negative, +1= weak intensity, +2= moderate intensity and +3= strong intensity (for total PTTG only)) and percentage of staining observed in each of the three intensity categories. Conflicting results were reviewed until a final agreement was reached. Sections which were damaged or contained < 25 % tumourous tissue were excluded from further analyses. As the total number of patient samples was relatively low, cases where only one representative section was available were still included. For each tumour tissue section, an H-score was then calculated using a scoring method previously described by Hsueh et al. (Hsueh et al. 2013). The H-score was calculated by adding the percentage of cells stained at each intensity multiplied by the intensity of staining category as outlined in the following formula: **H-score = [(1 x (% cells 1+)) + (2 x (% cells 2+)) + (3 x (% cells 3+))].**

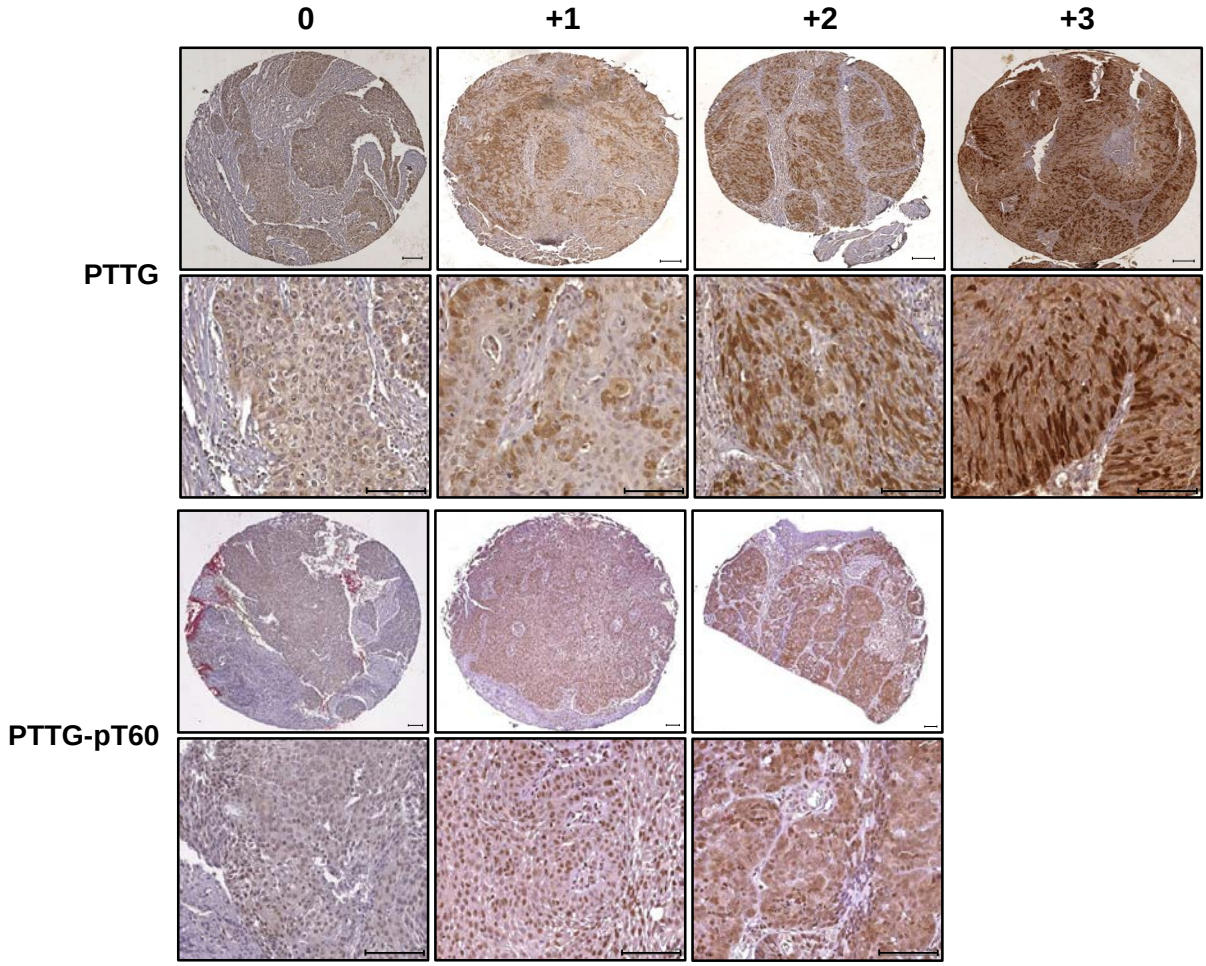


*Figure 3.1 Representative immunohistochemical staining of total PTTG (top panel) and T60-phosphorylated PTTG (bottom panel) protein expression in head and neck tumour tissue microarray (TMA) sections. Columns 1-4 are representative of the different staining intensity scores (0= negative, +1= weak intensity, +2= moderate intensity, +3= strong intensity). Top row of images were taken at 4x magnification. Bottom row of images were taken at 20x magnification. Scale bars 100 µm.*

### 3.2.6 Statistical analysis

Statistical analyses were performed using GraphPad Prism version 5.0. The non-parametric Wilcoxon matched pairs signed-rank test was used to assess PTTG mRNA expression in matched the head and neck tissue specimens. The non-parametric Mann-Whitney *U* test was used to assess correlations between clinical follow-up data and PTTG mRNA expression. Correlations between PTTG/PTTG-T60 H-scores and clinical follow-up data were assessed by Mann-Whitney *U* test and Fisher's exact test. Statistical analyses could

not be performed for PTTG-pT60 H-score and alcohol status by Mann-Whitney *U* test as the majority of patients had a history of alcohol consumption, thus making the numbers in one category too small to analyse. The significance of the association between gene expression datasets was assessed by use of the Spearman's rank-based correlation coefficient. Statistical significance was taken as $p < 0.05$.

## 3.3 Results

### 3.3.1 PTTG mRNA expression in head and neck squamous cell carcinoma

*3.3.1.1 PTTG mRNA is overexpressed in squamous cell carcinomas of the head and neck*

To determine whether PTTG was upregulated in head and neck squamous cell carcinoma (HNSCC), PTTG mRNA expression levels were initially assessed in a series of 24 matched tumour and normal head and neck tissue specimens by quantitative real-time PCR. Complete demographic and clinical follow-up data were collected for all patient samples and are summarised in Table 3.1. The study population consisted of 16 males and 8 females and the majority had a history of previous or current tobacco and/or alcohol consumption. Nodal disease was present in almost 55 % of subjects and a further 21 % went on to develop recurrent disease.

| Case | Gender[a] | Smoking status | Alcohol status[b] | Type | Site | Sub-site[c] | T[d] | N[e] | M[f] | R[g] | P16[h] |
|---|---|---|---|---|---|---|---|---|---|---|---|
| 1 | M | Previous | X | Primary | Hypopharynx | Pyriform fossa | 3 | 2b | 0 | Y | - |
| 2 | M | Current | Current | Primary | Oral | Floor of mouth | 2 | 2c | 0 | N | - |
| 3 | F | Current | Current | Primary | Larynx | N/A | 3 | 0 | 0 | N | N/A |
| 4 | M | Previous | Current | Primary | Oropharynx | Tonsil | 3 | 2b | 0 | N | + |
| 5 | F | Never | Current | Primary | Hypopharynx | X | 3 | 1 | 1 | N | N/A |
| 6 | M | Never | Never | Primary | Oral | Tongue | 4 | 2a | 0 | N | N/A |
| 7 | M | Previous | Current | Primary | Oral | Tongue | 1 | 1 | 0 | Y | N/A |
| 8 | M | Current | Current | Primary | Oral | Floor of mouth | 2 | 2b | 0 | N | N/A |
| 9 | F | Previous | Never | Primary | Oral | Floor of mouth | 2 | 2c | 0 | N | N/A |
| 10 | M | Current | Current | Primary | Oral | Tongue | 3 | 0 | 0 | N | N/A |
| 11 | M | Current | Current | Primary | Oral | Tongue | 1 | 0 | 0 | N | N/A |
| 12 | F | Never | Current | Primary | Oral | Mandible | 4a | 0 | 0 | Y | N/A |
| 13 | F | Current | Current | Primary | Oral | Mandible | 1 | 0 | 0 | N | N/A |
| 14 | F | Current | Current | Primary | Oral | Tongue | 4 | 0 | 0 | N | + |
| 15 | M | Previous | Previous | Primary | Oral | Mandible | 4a | 2b | 0 | N | - |
| 16 | M | Previous | Previous | Primary | Larynx | X | 4a | 0 | 0 | N | N/A |
| 17 | M | Current | Previous | Recurrent | Oropharynx | Tonsil | 2 | 0 | 0 | Y | - |
| 18 | M | Never | Previous | Primary | Larynx | X | 4a | 1 | 0 | N | N/A |
| 19 | F | Never | Current | Primary | Oral | Tongue | 2 | 0 | 0 | Y | X |
| 20 | M | Current | Current | Primary | Oral | Tongue | 4a | 2b | 0 | N | - |
| 21 | M | Current | Current | Primary | Oral | Floor of mouth | 2 | 2c | 0 | N | X |
| 22 | M | Current | Current | Primary | Oropharynx | Tonsil | X | X | X | N | X |
| 23 | F | Current | Current | Primary | Oropharynx | Tongue base | 4a | 0 | 0 | N | - |
| 24 | M | Never | Current | Primary | Oropharynx | Tonsil | 2 | 2c | 0 | N | + |

[a] Abbreviations: F, female; M, male
[b] Abbreviations: X, no data available
[c] Abbreviations: X, no data available, N/A, not applicable
[d] T stage. Abbreviations: X, no data available; 1, tumour ≤ 2 cm; 2, tumour > 2 cm; 3, tumour > 4 cm; 4a, moderately advanced local disease; 4b, very advanced local disease
[e] N stage. Abbreviations: X, no data available; 0, No regional lymph node metastasis; 1, Metastasis in a single ipsilateral lymph node ≤ 3 cm in greatest dimension; 2a, Metastasis in a single ipsilateral lymph node > 3 cm but not more than 6 cm in greatest dimension; 2b, Metastasis in a multiple ipsilateral lymph nodes - none > 6 cm in greatest dimension; 2c, Metastasis in bilateral or contralateral lymph nodes - none > 6 cm in greatest dimension; 3, Metastasis in a lymph node > 6 cm in greatest dimension
[f] M stage. Abbreviations: X, no data available; 0, no distant metastasis; 1, distant metastasis
[g] Tumour recurrence. Abbreviations: 0, no; 1, yes
[h] p16 status determined by immunohistochemistry. Abbreviations: X, no data available; N/A, not applicable; -, negative; +, positive

*Table 3.1 Table of patient characteristics for fresh-frozen tissue specimens.*

As shown in Figure 3.2, PTTG mRNA expression was significantly upregulated in the HNSCC tumours when compared to corresponding matched normal head and neck tissue specimens (1.9-fold, p=0.047).

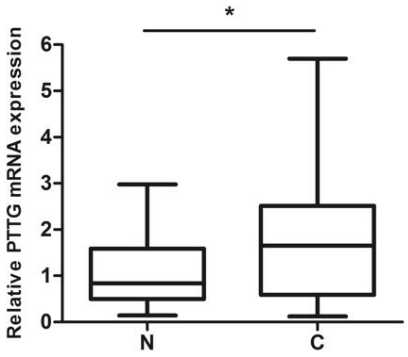


*Figure 3.2 PTTG mRNA expression is upregulated in head and neck squamous cell carcinoma. Quantification of PTTG mRNA expression in head and neck squamous cell carcinoma (HNSCC) tumours (C) relative to matched normal (N) head and neck tissue specimens (n=24). Data presented as a box-whisker plot. The centre line represents the median fold change in mRNA expression, the box indicates the 25$^{th}$ and 75$^{th}$ percentiles and the whiskers represent the minimum and maximum values. * p ≤0.05.*

As expected when using clinical specimens, there was a high degree of variability in PTTG mRNA expression between individual tumour specimens, as shown in Figure 3.3. Relative PTTG mRNA expression ranged from a 0.08-fold reduction to a 5.9-fold increase across the group of HNSCC tumours. Tumour specimens were obtained from four different anatomical sites; larynx, oral cavity, hypopharynx and oropharynx. Again, for each tumour site, the level of PTTG mRNA expression varied but was found to be significantly elevated in tumours originating in the oropharynx when compared with tumours originating in the oral cavity (Figure 3.4; 2.1-fold, p=0.047). No significant difference in PTTG mRNA expression was observed in any of the remaining demographic or clinical follow-up categories (data not shown).

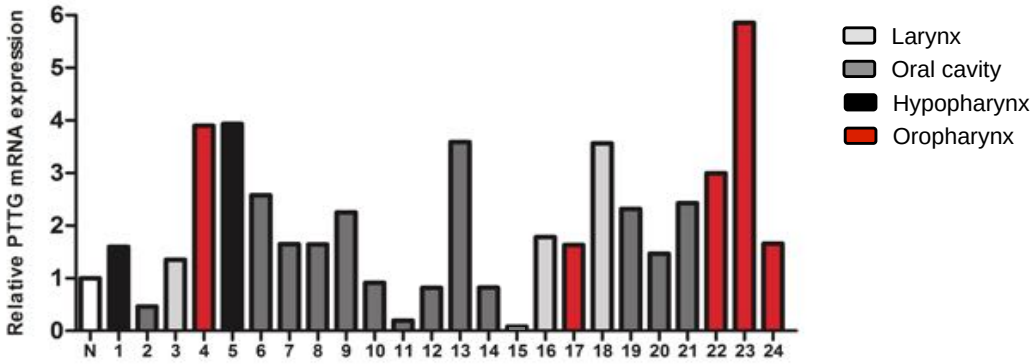


*Figure 3.3 PTTG mRNA expression across the panel of head and neck squamous cell carcinomas. PTTG mRNA expression in head and neck squamous cell carcinoma (HNSCC) samples (1-24) compared to matched normal tissue (N). Data presented as fold change in mRNA expression.*

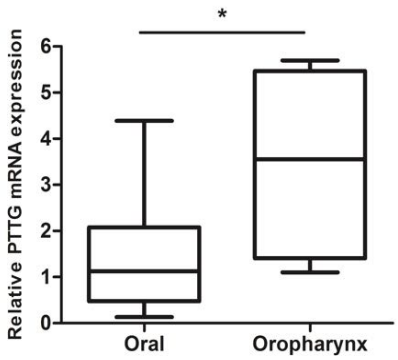


*Figure 3.4 PTTG mRNA expression varies according to the anatomical site of the tumour. Relative PTTG mRNA expression levels in tumours of the oral cavity (n=14) and oropharynx (n=5). Data presented as a box-whisker plot. The centre line represents the median fold change in mRNA expression, the box indicates the 25$^{th}$ and 75$^{th}$ percentiles and the whiskers represent the minimum and maximum values. * p ≤0.05.*

### 3.3.2 PTTG protein expression in head and neck squamous cell carcinoma

#### *3.3.2.1 PTTG-pT60 antibody validation*

The recent discovery that abrogation of the phosphorylatable residue, T60, results in altered PTTG half life, in addition to inducing genetic instability and cell invasion prompted us to investigate PTTG-pT60 phosphorylation, as well as assessment of total PTTG protein expression in head and neck cancers. To this end, we generated a rabbit antibody against

PTTG phosphorylated at residue T60 and conducted a series of experiments to validate use of the antibody for Western blotting and immunohistochemistry purposes.

Initial experiments sought to determine antibody specificity. HeLa cells transfected with wild-type PTTG, a T60A mutant or vector only (VO) were harvested and the protein lysates analysed by Western blotting. Transfection of PTTG plasmids was clearly evident upon detection of total PTTG protein at the expected molecular weight, as demonstrated in Figure 3.5A. Subsequent probing with our PTTG-pT60 antibody confirmed detection of a specific product at ~35 kDa, which was almost undetectable in T60A mutant-transfected cell lysates when compared with wild-type and VO-transfected cells. Densitometry analysis of the Western blots revealed that this decrease in T60-phosphorylated PTTG protein expression was statistically significant (Figure 3.5B). Furthermore, parallel peptide-blocking experiments using a neutralising peptide completely blocked antibody detection of the specific protein product (Figure 3.5C). Immunohistochemical staining of PTTG in head and neck whole tumour serial sections revealed predominantly nuclear expression for both total PTTG and T60-phosphorylated PTTG protein (Figure 3.6A and B). Importantly, addition of the neutralising peptide led to a complete loss of staining (Figure 3.6C).

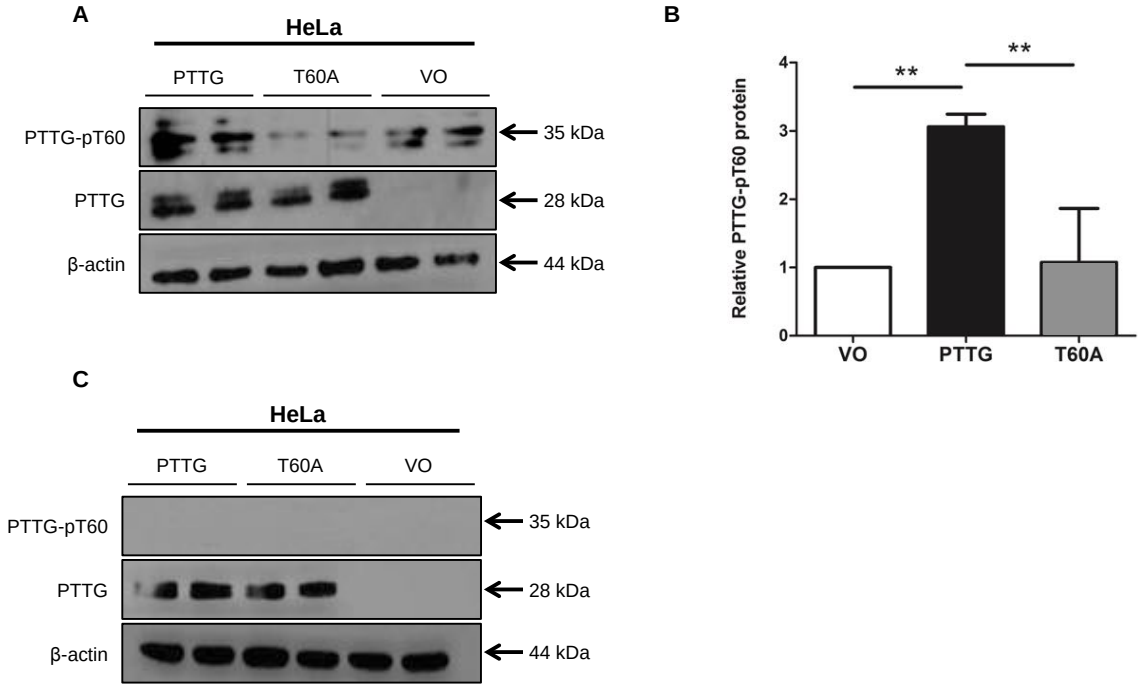


*Figure 3.5 Western blot analysis of total PTTG and pT60-phosphorylated PTTG in lysates from HeLa cells following transfection with wild-type PTTG, T60A or vector only (VO).* ***A*** *– Representative Western blot probed with pT60 antibody.* ***B*** *– Scanning densitometry results showing PTTG-pT60 protein expression levels in wild type PTTG and T60A-transfected cells relative to VO (n=3).* ***C*** *– Representative Western blot probed with pT60 antibody pre-incubated with 2x concentration of neutralising peptide. Data shown as mean ± SEM. ** p ≤0.01.*

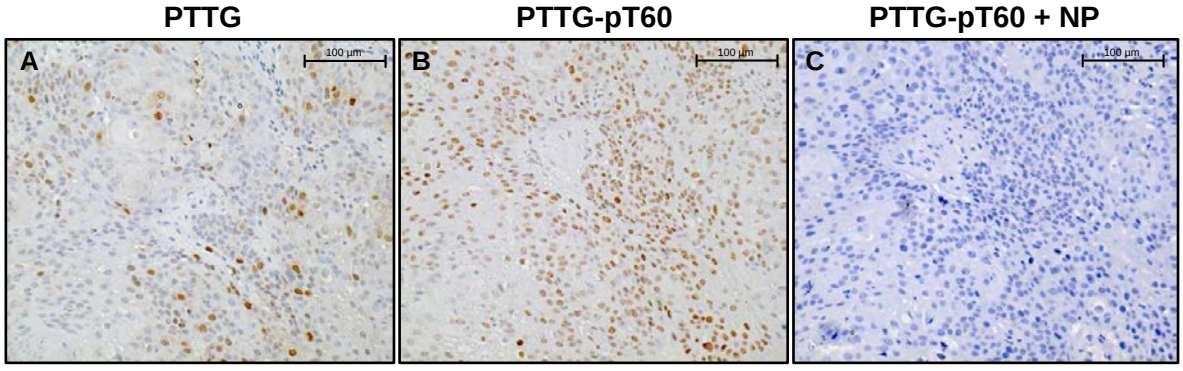


*Figure 3.6 Representative images of formalin-fixed paraffin-embedded whole oropharyngeal tumour sections stained for PTTG. Sections were stained for* ***A*** *– PTTG,* ***B*** *– PTTG-pT60 or* ***C*** *– PTTG-pT60 pre-incubated with the 2x concentration of neutralising peptide (NP). Sections were counterstained with Haematoxylin. All images were taken at 10x magnification. Scale bars 100 µm.*

Phospho-specific detection of PTTG-pT60 was further appraised through siRNA knockdown and co-immunoprecipitation experiments. PTTG siRNA knockdown led to a clear reduction in total and T60-phosphorylated PTTG protein expression, to levels undetectable by Western blotting (Figure 3.7). Furthermore, immunoprecipitation of total PTTG protein and subsequent probing with the PTTG-pT60 antibody demonstrated detection of the 35 kDa band in HeLa cells (Figure 3.8). However, the T60A mutant was barely detected by the PTTG-pT60 phospho-specific antibody. Taken together, these series of experiments demonstrated phospho-specific detection of PTTG-pT60 through use of our PTTG-pT60 antibody in a variety of assays, including Western blotting, immunohistochemistry and co-immunoprecipitation.

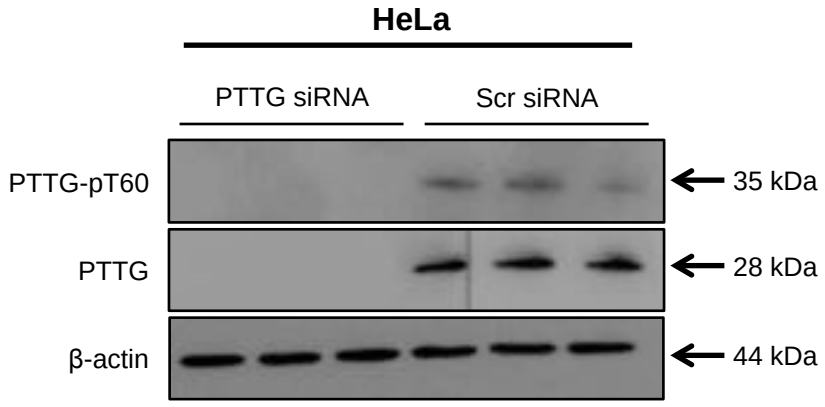


*Figure 3.7 Western blot analysis of total PTTG and pT60-phosphorylated PTTG expression. Total PTTG and T60-phosphorylated PTTG protein expression in lysates from HeLa cells following transfection with PTTG siRNA or scrambled siRNA (Scr siRNA) (n=2).*

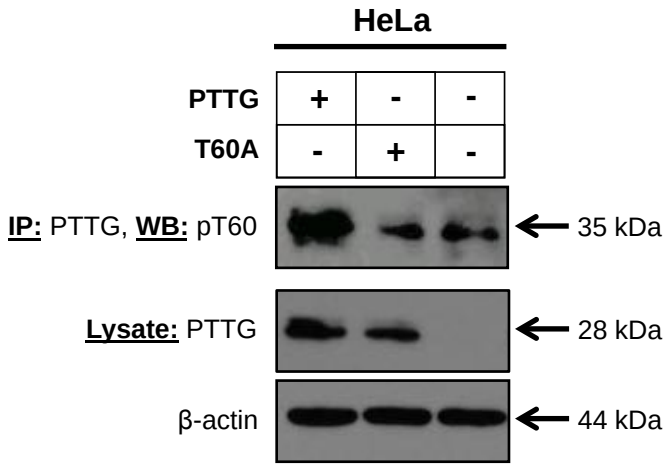


*Figure 3.8 Immunoprecipitation of PTTG and subsequent probing with a phospho-specific T60 antibody in HeLa cells transfected with wild-type PTTG, T60A or vector only (VO). Analysis of total protein lysate shown below demonstrates the presence of PTTG in each sample.*

*3.3.2.2 PTTG protein is expressed and phosphorylated at residue T60 in head and neck squamous cell carcinoma*

With a validated PTTG-pT60 antibody, the expression of total and T60-phosphorylated PTTG protein was next investigated in HNSCC. To determine whether protein expression varied in HNSCC, tumour TMA samples (two samples of normal tonsil, kidney and liver tissue were incorporated as reference or control samples) were analysed for total and T60-phosphorylatd PTTG protein expression. Due to poor tissue quality, only 51 out of the 53 tumour TMA samples were analysed for total PTTG protein expression and 24 out of the 53 for T60-phosphorylated PTTG protein expression. Full patient demographic, clinical and pathological data were available and are outlined in Table 3.2. The study population consisted of 39 males and 14 females and the median age at diagnosis was 54 years. The majority of subjects had a history of prior or current tobacco and/or alcohol consumption. Nodal disease was present in approximately 60 % of the study population and nearly 30 % went on to develop recurrent disease. Of the 53 patients with known tumour HPV-status, 13 were HPV-positive.

| Case | Age at Diagnosis (yr) | Gender[a] | Smoking status[b] | Alcohol status[c] | Site | Sub-site[d] | T[e] | N[f] | M[g] | R[h] | HPV status[i] |
|---|---|---|---|---|---|---|---|---|---|---|---|
| **1** | 62 | F | Previous | Previous | Oropharynx | Tonsil | 2 | 0 | 0 | N | - |
| **2** | 57 | F | N/A | N/A | Oropharynx | Tonsil | 2 | 2a | 0 | N | + |
| **3** | 50 | F | Current | Current | Oropharynx | Base of tongue | 4 | 2a | 0 | N | - |
| **4** | 56 | M | Previous | N/A | Oropharynx | X | 1 | 1 | 0 | Y | - |
| **5** | 57 | M | Current | Previous | Oropharynx | Tonsil | 3 | 2a | 0 | X | - |
| **6** | 49 | F | Never | Previous | Oropharynx | Tonsil | 2 | 1 | 0 | Y | + |
| **7** | 57 | M | Never | Previous | Oropharynx | Base of tongue | 4 | 0 | 0 | N | + |
| **8** | 42 | M | Never | Previous | Oropharynx | Tonsil | 2 | 2b | 0 | N | + |
| **9** | 48 | M | Current | Current | Oropharynx | Base of tongue | 4 | 2b | 0 | N | - |
| **10** | 72 | M | Current | Never | Oropharynx | Soft palate | 2 | 0 | 0 | N | - |
| **11** | 51 | F | Previous | Previous | Oropharynx | X | 4 | 0 | 0 | N | - |
| **12** | 51 | M | Current | Current | Oropharynx | Soft palate | 4 | 0 | 0 | Y | - |
| **13** | 52 | M | Never | Current | Oropharynx | Tonsil | 4 | 0 | 0 | N | + |
| **14** | 54 | M | Never | Previous | Oropharynx | Tonsil | 2 | 0 | 0 | Y | + |
| **15** | 47 | F | Current | Previous | Oropharynx | Tonsil | 1 | 0 | 0 | Y | - |
| **16** | 51 | M | Previous | Previous | Oropharynx | X | 4 | 0 | 0 | N | - |
| **17** | 51 | M | Never | Previous | Oropharynx | Tonsil | 2 | 2c | 0 | N | + |
| **18** | 70 | M | Previous | Previous | Oropharynx | Base of tongue | 4 | 2a | 0 | N | - |
| **19** | 45 | M | Current | Current | Oropharynx | Soft palate | 2 | 2c | 0 | N | - |
| **20** | 67 | F | Current | Previous | Oropharynx | Tonsil | 2 | 2b | 0 | N | - |
| **21** | 46 | F | Never | Previous | Oropharynx | Tonsil | 2 | 1 | 0 | N | - |
| **22** | 56 | F | Current | Previous | Oropharynx | Base of tongue | 4 | 0 | 0 | N | - |
| **23** | 59 | M | Previous | Previous | Oropharynx | Tonsil | 2 | 0 | 0 | N | + |
| **24** | 51 | M | Never | Previous | Oropharynx | Base of tongue | 2 | 2a | 0 | N | + |
| **25** | 48 | M | Never | Previous | Oropharynx | Tonsil | 1 | 2a | 0 | N | - |
| **26** | 40 | M | Previous | Never | Oropharynx | Base of tongue | 2 | 2b | 0 | N | - |
| **27** | 66 | M | Previous | Current | Oropharynx | Base of tongue | 2 | 2b | 0 | Y | + |
| **28** | 66 | M | Previous | Previous | Oropharynx | Base of tongue | 3 | 0 | 0 | N | - |
| **29** | 45 | M | Never | Previous | Oropharynx | Tonsil | X | 3 | 0 | N | + |
| **30** | 57 | F | Current | Previous | Oropharynx | Tonsil | 1 | 1 | 0 | N | + |
| **31** | 62 | M | Current | Previous | Oropharynx | Base of tongue | 4 | 2 | X | N | - |
| **32** | 58 | M | Current | N/A | Oropharynx | Tonsil | 3 | 0 | X | N | - |
| **33** | 57 | F | Never | Previous | Oropharynx | Base of tongue | 3 | 2b | 0 | N | - |
| **34** | 46 | M | Previous | Previous | Oropharynx | Tonsil | 2 | 2a | X | N | + |
| **35** | 41 | M | Previous | Previous | Oropharynx | Tonsil | 3 | 2 | 0 | N | - |
| **36** | 75 | F | Previous | Previous | Oropharynx | Soft palate | 2 | 0 | 0 | Y | - |
| **37** | 67 | M | Current | Previous | Oropharynx | Tonsil | 3 | 1 | 0 | N | - |
| **38** | 72 | M | N/A | Previous | Oropharynx | Base of tongue | 2 | 3 | X | Y | - |
| **39** | 56 | M | Previous | Previous | Oropharynx | Tonsil | 2 | 3 | X | Y | - |
| **40** | 55 | M | Never | Previous | Oropharynx | Base of tongue | 2 | 2 | 0 | Y | - |
| **41** | 50 | M | Never | Previous | Oropharynx | Tonsil | 3 | 2b | 0 | N | - |
| **42** | 51 | M | Current | Current | Oropharynx | Tonsil | 3 | 2b | X | N | - |
| **43** | 53 | M | Current | Previous | Oropharynx | Base of tongue | 3 | 1 | X | Y | - |
| **44** | 45 | F | Current | Current | Oropharynx | Soft palate | 3 | 2c | X | N | - |
| **45** | 51 | M | Current | Current | Oropharynx | Soft palate | 1 | 0 | 0 | Y | - |
| **46** | 66 | M | Never | Current | Oropharynx | Base of tongue | 1 | 3 | X | Y | - |
| **47** | 56 | M | Current | Previous | Oropharynx | Tonsil | 2 | 0 | 0 | N | NA |
| **48** | 58 | F | Previous | Previous | Oropharynx | Tonsil | 1 | 0 | 0 | N | NA |
| **49** | 62 | M | Current | Previous | Oropharynx | Soft palate | 2 | 0 | 0 | N | - |
| **50** | 53 | M | Current | Previous | Oropharynx | Piriform | 2 | 1 | X | N | - |
| **51** | 74 | M | Current | Never | Oropharynx | Tonsil | 3 | 2c | X | N | - |
| **52** | 64 | M | Current | Previous | Oropharynx | Tonsil | X | X | X | N | - |
| **53** | 46 | M | Previous | X | Oropharynx | Base of tongue | X | X | X | Y | - |

[a] Abbreviations: F, female; M, male
[b] Abbreviations: N/A, not applicable
[c] Abbreviations: X, no data available, N/A, not applicable
[d] Abbreviations: X, no data available
[e] T stage. Abbreviations: X, no data available; 1, tumour ≤ 2 cm; 2, tumour > 2 cm; 3, tumour > 4 cm; 4a, moderately advanced local disease; 4b, very advanced local disease
[f] N stage. Abbreviations: X, no data available; 0, No regional lymph node metastasis; 1, Metastasis in a single ipsilateral lymph node ≤ 3 cm in greatest dimension; 2a, Metastasis in a single ipsilateral lymph node > 3 cm but not more than 6 cm in greatest dimension; 2b, Metastasis in a multiple ipsilateral lymph nodes - none > 6 cm in greatest dimension; 2c, Metastasis in bilateral or contralateral lymph nodes - none > 6 cm in greatest dimension; 3, Metastasis in a lymph node > 6 cm in greatest dimension
[g] M stage. Abbreviations: X, no data available; 0, no distant metastasis; 1, distant metastasis
[h] Tumour recurrence. Abbreviations: N, no; Y, yes
[i] HPV status determined by in-situ hybridisation histochemistry. Abbreviations: X, no data available; N/A, not applicable; -, negative; +, positive

*Table 3.2 Table of patient characteristics for head and neck tissue microarray specimens.*

Low to moderate levels of PTTG and, more specifically, PTTG-pT60 protein expression were observed in normal head and neck tissue, whereas abundant PTTG expression was evident in oropharyngeal tumours of all tumour stages (Figure 3.9). However, the extent of staining did vary between tumour cores, particularly with regard to total PTTG protein expression. Interestingly, total PTTG protein appeared to be expressed both in the nucleus and cytoplasm, with stronger nuclear staining in the majority of cases. In contrast, expression of T60-phosphorylated PTTG was predominantly nuclear.

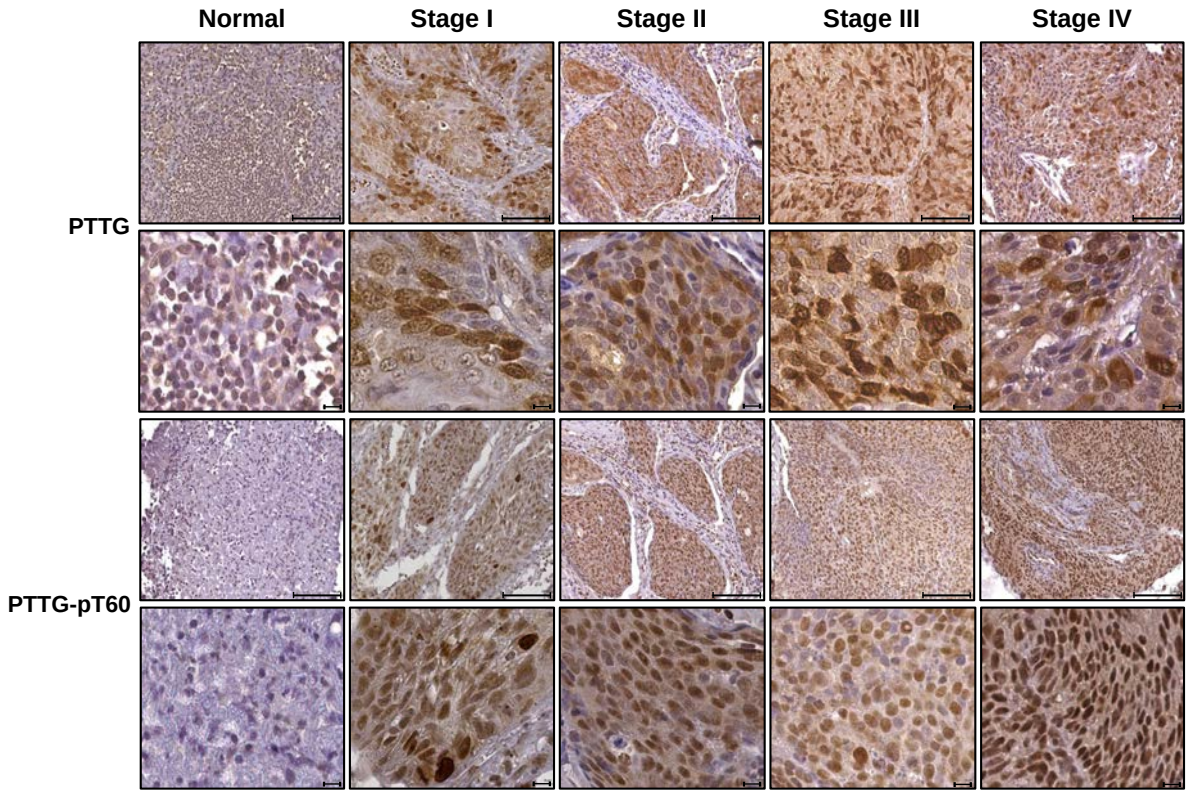


*Figure 3.9 Representative images of formalin-fixed, paraffin-embedded head and neck tumour tissue microarray (TMA) sections of various tumour stages stained for total PTTG (top panel) and T60-phosphorylated PTTG (bottom panel) protein. Sections were counterstained for Haematoxylin. Top row of images were taken at 20x magnification – scale bars 100 µm. Bottom row of images were taken at 80x magnification – scale bars 10 µm.*

### *3.3.2.3 Total PTTG protein expression correlates with HPV status*

Intensity scores and the percentage of cells staining at each intensity were determined for each tumour tissue section and subsequently converted to a 'histo' score, or H-score, as

outlined in section 3.2.5 above. When the H-scores for total PTTG protein expression were correlated with the available demographic and clinicopathological characteristics for each patient, it was found that HPV status positively correlated with PTTG expression (Table 3.3; p=0.046). The H-scores of the tumour tissues ranged from 1-300 for total PTTG protein expression, with a median of 50. An H-score of 50 was therefore used to divide patients into low PTTG expression and high PTTG expression groups. Subdivision based on low (H-score ≤50) and high (H-score >50) PTTG expression and subsequent re-analysis of the data by Fisher's exact test confirmed a significant association between high PTTG expression and HPV-positive status (Table 3.3; p=0.045). Approximately 38 % of HPV-positive patients had low levels of PTTG expression. In contrast, high levels of PTTG expression were observed in 62 % of HPV-positive patients. None of the remaining categories, including tumour sub-site, TNM stage or recurrence status, were found to be associated with PTTG expression using either method of analysis.

| Clinical and pathological features | | PTTG | | | |
|---|---|---|---|---|---|
| | | Mann-Whitney *U* test | | | Fisher's exact test |
| | | No. of patients | H-score (mean±SEM) | p-value | p-value |
| **Age (yr)** | <50 | 13 | 37.9±11.0 | 0.21 | 1.00 |
| | >50 | 38 | 61.0±9.4 | | |
| **Gender**[a] | F | 14 | 34.9±7.7 | 0.23 | 0.20 |
| | M | 37 | 62.7±9.9 | | |
| **Smoking status** | Never | 14 | 76.8±14.8 | 0.07 | 0.12 |
| | Previous/Current | 35 | 47.0±9.1 | | |
| **Alcohol status** | Never | 3 | 76.7±43.2 | 0.49 | 0.55 |
| | Previous/Current | 44 | 52.9±7.9 | | |
| **Sub-site** | Tonsil | 25 | 59.3±10.2 | 0.67 | 0.75 |
| | Base of tongue | 15 | 59.7±17.2 | | |
| **T stage** | pT1-2 | 29 | 54.4±8.7 | 0.99 | 0.37 |
| | pT3-4 | 19 | 62.7±15.3 | | |
| **N stage** | pN0-1 | 23 | 70.0±14.2 | 0.39 | 0.78 |
| | pN2-3 | 26 | 46.1±7.2 | | |
| **Recurrence** | No | 36 | 57.8±8.0 | 0.34 | 0.76 |
| | Yes | 14 | 51.7±18.9 | | |
| **HPV status**[b] | - | 36 | 44.2±8.7 | **0.05** | **0.05** |
| | + | 13 | 82.0±15.8 | | |

[a] Abbreviations: F, female; M, male
[b] Abbreviations: -, negative; +, positive

*Table 3.3 Table of PTTG H-scores and their association with the clinical and pathological features of HNSCC patients. H-score values were assessed by Mann-Whitney U test and Fisher's exact test.*

### *3.3.2.4 Expression of T60-phosphorylated PTTG correlates with tumour sub-site*

When the H-scores for PTTG-pT60 protein expression were evaluated alongside the demographic and clinicopathological characteristics of each patient, expression of T60-phosphorylated PTTG did not significantly correlate with any of the categories, including TNM stage, recurrence status and HPV status (Table 3.4). The H-scores of the tumour tissues

ranged from 1-150 for PTTG-pT60 protein expression, with a median of 50. An H-score of 50 was therefore used to divide patients into low PTTG-pT60 expression and high PTTG-pT60 protein expression groups. Subdivision based on low (H-score ≤50) and high (H-score >50) PTTG-pT60 expression and subsequent re-analysis of the data by Fisher's exact test demonstrated a significant correlation between PTTG-pT60 protein expression and tumour sub-site (Table 3.4; p=0.044). Tumours originating in the tonsils demonstrated both low and high levels of PTTG-pT60 protein expression. In contrast, only low levels of PTTG-pT60 protein expression were observed in carcinomas originating from the base of the tongue.

| Clinical and pathological features | | PTTG-pT60 | | | |
|---|---|---|---|---|---|
| | | Mann-Whitney *U* test | | | Fisher's exact test |
| | | No. of patients | H-score (mean±SEM) | p-value | p-value |
| **Age (yr)** | <50 | 5 | 60.5±24.5 | 0.77 | 1.00 |
| | >50 | 19 | 54.6±13.4 | | |
| **Gender**[a] | F | 5 | 65.0±27.2 | 0.94 | 0.33 |
| | M | 19 | 53.5±13.1 | | |
| **Smoking status** | Never | 5 | 20.7±9.7 | 0.15 | 0.12 |
| | Previous/Current | 18 | 68.8±13.9 | | |
| **Alcohol status** | Never | - | - | - | 1.00 |
| | Previous/Current | | | | |
| **Sub-site** | Tonsil | 13 | 70.8±17.7 | 0.19 | **0.04** |
| | Base of tongue | 6 | 25.0±11.2 | | |
| **T stage** | pT1-2 | 12 | 43.3±14.8 | 0.13 | 0.40 |
| | pT3-4 | 9 | 83.4±21.0 | | |
| **N stage** | pN0-1 | 9 | 82.2±20.1 | 0.09 | 0.40 |
| | pN2-3 | 13 | 42.3±14.5 | | |
| **Recurrence** | No | 16 | 61.9±16.3 | 0.78 | 0.66 |
| | Yes | 8 | 43.8±12.1 | | |
| **HPV status**[b] | - | 19 | 56.4±12.7 | 0.13 | 0.52 |
| | + | 3 | 6.7±6.7 | | |

[a] Abbreviations: F, female; M, male
[b] Abbreviations: -, negative; +, positive

*Table 3.4 Table of PTTG-pT60 H-scores and their association with the clinical and pathological features of HNSCC patients. PTTG-pT60 H-score values were assessed by Mann-Whitney U test and Fisher's exact test.*

## 3.4 Discussion

HNSCCs are increasingly being recognised as a heterogeneous group of disease entities, displaying vastly different aetiological, biological and clinical characteristics. Current work is therefore focused on identifying novel biomarkers to stratify patients based on molecular criteria and to distinguish patient groups who are more likely to benefit from specific

treatment strategies. In the present chapter, we have demonstrated that PTTG is overexpressed and phosphorylated at residue T60 in human HNSCC tumours. Furthermore, we revealed significant correlations between PTTG expression and a small selection of patient clinicopathological characteristics.

Given that high PTTG expression levels have been observed in several malignancies (Saez et al. 1999, Shibata et al. 2002, Solbach et al. 2004, Stratford et al. 2005), we examined PTTG mRNA expression in 24 matched human HNSCC tumour and normal tissue specimens by quantitative real-time PCR. PTTG mRNA expression was significantly elevated in HNSCC tumours, thus validating previous findings. Furthermore, expression was correlated with tumour site, with the highest degree of PTTG expression evident in tumours originating from the oropharynx. Although an entirely novel finding, it is worth noting that the majority of publications reporting overexpression of PTTG in HNSCC have focused specifically on oesophageal squamous cell carcinomas. Solbach et al. are the only group so far to have assessed PTTG expression in HNSCC tumours enriched for OPSCC (66 out of a total of 89 patients). However, they did not perform statistical analyses of PTTG expression based upon tumour site (Solbach et al. 2006).

Further immunohistochemical assessment of PTTG protein expression was performed using oropharyngeal TMA specimens. To determine whether protein expression varied, the staining intensity and percentage of cells staining at each intensity category were established for each patient and converted into a single H-score (Hsueh et al. 2013). Similar to PTTG mRNA expression in HNSCC tumours, PTTG protein expression was evident in a relatively large number of samples (46 out of a total of 51 patients). Closer histological examination revealed strong nuclear staining, as well as frequent cytoplasmic staining. The subcellular localisation of PTTG has been extensively debated. Several reports have suggested mainly

cytoplasmic expression, with little nuclear staining (Dominguez et al. 1998, Stratford et al. 2005), whereas other studies have argued that PTTG is predominantly a nuclear protein (Yu et al. 2000b). A previous publication assessing PTTG protein expression in the oesophageal squamous carcinoma cell lines HAS/c, KYSE140 and KYSE410 concluded that PTTG staining was mainly observed in the cytoplasm, with occasional nuclear staining (Ito et al. 2008). Furthermore, cytoplasmic but not nuclear PTTG staining was associated with patient clinicopathological features (Ito et al. 2008). The reported discrepancies in localisation may be a result of cell type and tissue specific expression of PTTG or may be dependent on the methods used. For example, PTTG was demonstrated to be localised mainly in the nucleus in cervical cancer HeLa cells, monkey kidney Cos-7 cells and prostate cancer DU154 cells, whilst in the same study, in lung cancer A549 cells, colorectal adenocarcinoma DLD-1 cells and mouse NIH3T3 fibroblasts PTTG protein was expressed diffusely throughout the nucleus and cytoplasm (Mu et al. 2003).

Additional analyses highlighted a significant correlation between PTTG protein expression and HPV status, as illustrated by higher PTTG protein expression scores in HPV-positive tumours compared to HPV-negative tumours. An association between PTTG protein expression and HPV status has not been reported before and the functional significance of such a correlation warrants further exploration. The HPV life cycle is tightly linked with the differentiation state of the host cell and requires the host cell to remain actively proliferating (Kajitani et al. 2012). It is also well established that PTTG plays a crucial role in cell cycle regulation and genetic instability, and its expression usually peaks in mitotically active cells (Ramos-Morales et al. 2000, Yu et al. 2000b, Yu et al. 2003). It is therefore perceivable that PTTG could serve to ‘prime’ HPV-infected basal cells, thus making them more vulnerable to further neoplastic changes. Indeed, PTTG has been shown to cooperate with other viruses to

promote cellular transformation. Human T-cell leukemia virus type 1 (HTLV-1) is a retrovirus that primarily infects $CD4^+$ T lymphoctyes and has been implicated in the pathogenesis of adult T-cell leukemia (Sheleg et al. 2007). Sheleg et al. demonstrated cooperation between PTTG and the HTLV-1 oncoprotein, Tax, with co-expression inducing chromosomal instability, cell proliferation and transformation (Sheleg et al. 2007). Similarly, PTTG might cooperate with HPV oncoproteins E5, E6 or E7 to promote neoplastic transformation in HNSCC.

The precise mechanisms regulating PTTG involvement in tumourigenesis remain largely unknown. A recent publication demonstrated that inhibition of phosphorylation at residue threonine-T60 results in prolonged PTTG half-life, chromosomal instability and enhanced cellular invasion *in vitro* (Mora-Santos et al. 2013). In addition, a point mutation has recently been identified at this particular residue (T60N) in a breast cancer sample (Stephens et al. 2012). We therefore generated a phospho-specific PTTG antibody to residue T60 to investigate PTTG T60 phosphorylation in head and neck cancer. Here we showed that mutation of the T60 residue results in a significant reduction in expression of T60-phosphorylated PTTG protein in HeLa cells as detected using our optimised phospho-specific antibody by Western blot. This is consistent with the idea that PTTG is phosphorylated at residue T60, as suggested by Mora-Santos et al. (Mora-Santos et al. 2013).

Interestingly, the T60 residue is directly adjacent to the D-box motif (amino acids 61-68). In budding yeast cells, phosphorylation sites located in this region are critical for regulation of the yeast securin homologue, Pds1, by APC/C (Holt 2008). CDK1-mediated phosphorylation of Pds1 near its D-box motif led to a marked reduction in ubiquitination by APC/C (Holt et al. 2008). Conversely, removal of CDK1-dependent phosphates from Pds1 by CDC14 promoted Pds1 ubiquitination and its subsequent degradation (Holt et al. 2008). In humans the sole

CDK1 consensus motif is located at serine residue 165, far from the D-box motif. Loss of phosphorylation at this site triggers cell transformation and proliferation *in vitro* (Boelaert et al. 2004). Although no CDK1 consensus sequence can be found near residue T60, CDK1 has been shown to phosphorylate other mitotic proteins both at consensus and non-consensus sites, for example cyclin B1/CDK1-phosphorylation of Poly (A) Polymerase (Colgan et al. 1998) and CDK1-phosphorylation of Ribosomal S6 Kinase 1 (Shah et al. 2003).

Alternatively, T60 phosphorylation may be regulated by Glycogen Synthase Kinase (GSK)-3β, another kinase known to phosphorylate PTTG (Mora-Santos et al. 2011). GSK-3β is a serine/threonine kinase implicated in the phosphorylation of numerous protein substrates, many of which regulate cell proliferation, differentiation and apoptosis (Frame, Cohen 2001, Xu et al. 2009). GSK-3β-mediated phosphorylation of PTTG induced its ubiquitination and degradation by the SKP1-CUL1-F-box protein complex (SCF), a key E3 ubiquitin ligase responsible for the ubiquitination of certain phosphorylated forms of PTTG (Gil-Bernabe et al. 2006). Phosphorylation at residue T60 may therefore represent an important modification regulating both APC/C- and SCF-mediated degradation of PTTG.

With a validated PTTG-pT60 antibody, we investigated expression of T60-phosphorylated PTTG protein in oropharyngeal tumour TMA specimens. We found that T60-phosphorylated PTTG protein appeared to be expressed in the vast majority of nuclei, which is interesting considering nuclear translocation of PTTG is required for all its functional activities (Chien, Pei 2000). Further immunohistochemical examination revealed a significant association with tumour sub-site. Specifically, ~60 % of tumours originating in the tonsils were associated with high PTTG-pT60 expression compared to low PTTG-pT60 expression in all tumours originating from the base of the tongue. Many studies have noted a higher prevalence of HPV infection in tonsillar carcinomas, with an overall detection rate of approximately 50-60 %

(Klussmann et al. 2001, Sethi et al. 2012). This preference of HPV for the tonsils is not fully understood but may be linked to their specialised structural features. These secondary lymphoid organs are lined with stratified squamous epithelium, which forms numerous tonsillar crypts, greatly increasing the surface area and thus enabling more efficient capture of antigens (Perry 1994). Importantly, the invaginations have a discontinuous basement membrane and basal cell layer to allow for passage of antigens, lymphocytes and antigen-presenting cells (Perry 1994) but this is also thought to leave the basal cell layer more vulnerable to viral deposition and infection. As OPSCCs, including those arising in the lingual and palatine tonsils, have a higher prevalence of HPV infection, the observed increase in PTTG mRNA expression in oropharyngeal tumours and the potential correlation between T60-phosphorylated PTTG and tumours of the tonsil may in fact be a result of the described positive association between total PTTG protein expression and HPV-positive HNSCC.

PTTG serves as a prognostic marker for many cancers, including breast (Solbach et al. 2004), thyroid (Boelaert et al. 2003a) and oesophageal cancers (Shibata et al. 2002). However, the prognostic significance of PTTG expression in OPSCC remains to be fully elucidated. Surprisingly, in our panel of HNSCC and oropharyngeal tumour specimens, PTTG expression did not correlate with any of the prognostic factors, including TNM stage or tumour recurrence. Our analyses were performed on a relatively small number of patient samples, as we did not have many tissue specimens at our disposal. In addition analysis of protein expression was conducted by immunohistochemistry, which can be criticised as a relatively semi-quantitative assessment. These factors may have impacted upon our statistical power. Furthermore, due to the loss of tissue sections during the construction of the TMA slides and subsequent immunohistochemical procedures, in some cases only one representative section was available for analysis. Given the high morphological and molecular

heterogeneity associated with head and neck cancers, this may also have impacted upon our statistical power and may pose a significant problem with regards to whether accurate representation of the whole tissue specimen was achieved. However, some studies have concluded that even a single 0.6 mm tissue section can provide results that are similar to those achieved when scoring 3 tissue sections per patient (Kamp et al. 2000, Rosen et al. 2004, Khouja et al. 2010).

A common assumption when analysing mRNA expression is that it is predictive of protein expression. However, many studies exploring mRNA-protein correlations have yielded relatively inconsistent results, thus suggesting that mRNA expression may not always reflect the level of protein expression (Greenbaum et al. 2003, Guo et al. 2008, Lahtvee et al. 2017). This is likely due to a number of factors, including differences in the stability of mRNAs and proteins and variations in the rate of transcription versus translation. Additional paired fresh-frozen OPSCC tissue specimens for both mRNA and protein data would have allowed for a better powered and more detailed assessment of PTTG expression and the association between PTTG and clinical outcome, through quantitative real-time PCR and Western blotting. Further TMA specimens from the same patient group would have minimised the differences associated with analysing different patient cohorts.

### 3.4.1 Concluding statements

The data presented in this chapter demonstrate that PTTG is frequently overexpressed in HNSCC tumours, particularly those originating in the oropharynx. Moreover, expression was found to be associated with tumour site and HPV status but did not correlate with any clinicopathological parameters. In addition, PTTG appears to be phosphorylated at residue T60 in these tumours, which may alter its well described mitotic regulatory function.

# Chapter 4

# PBF expression in head and neck tumour tissue

## 4.1 Introduction

The central functions ascribed to PTTG require its nuclear localisation and a yeast-2 hybrid screening system initially identified PBF as a functional interacting partner of PTTG (Chien, Pei 2000). As PBF contains a bipartite nuclear localisation signal (NLS) sequence, it soon became an obligate model of subcellular shuttling for PTTG, facilitating its nuclear transport and subsequent tumourigenic and transforming abilities (Chien, Pei 2000). Since this discovery however, PBF has demonstrated transforming abilities independent of its interaction with PTTG (Stratford et al. 2005) and PBF overexpression has been identified in several tumour types, including breast (Watkins et al. 2010, Xiang et al. 2012), thyroid (Hsueh et al. 2013) and colon (Read et al. 2016b). Importantly, high levels of PBF expression and promoter activity have been associated with poorer clinical outcome. In papillary thyroid cancer, PBF expression was independently correlated with distant metastases at diagnosis, locoregional recurrence and reduced disease-specific survival (Hsueh et al. 2013). Furthermore, in colorectal and breast cancers, PBF overexpression has been linked with tumour invasion and metastasis, with high PBF-expressing tumours demonstrating greater vascular invasion (Watkins et al. 2010, Xiang et al. 2012, Read et al. 2016b). Not surprisingly, PBF has since been identified as a central driver gene in human cancer, as ascertained by DOTS-finder bioinformatic analysis performed across 34 different tumour types (Melloni et al. 2014).

The molecular events governing PBF function are yet to be fully delineated. However, phosphorylation of PBF at residue Y174 has been demonstrated to be of biological and clinical relevance. Extensive evidence has shown that PBF is capable of post-translationally modulating sodium iodide symporter (NIS) localisation at the plasma membrane in breast, colorectal and thyroid cancer cell lines, and as such, impairing radioiodide uptake (Smith et

al. 2013, Read et al. 2011, Boelaert et al. 2007, Smith et al. 2009). PBF phosphorylation by the proto-oncogene tyrosine kinase, Src, at residue Y174 is essential for regulation of PBF endocytosis and abrogation of this residue results in significant retention of NIS at the plasma membrane, ultimately restoring iodide uptake in primary human thyroid cells (Smith et al. 2013). More recently, PBF-Y174 phosphorylation has been implicated in the regulation of cell migration and invasion (Watkins et al. 2016). In a panel of breast, thyroid and colon cancer cell lines, PBF was able to induce potent cell migration and invasion when assessed using an array of different assays, including classical wound healing assays, 2D Boyden chamber assays and 3D organotypic assays (Watkins et al. 2016). This highly invasive signature was contingent upon a direct interaction between PBF and the F-actin binding protein, cortactin (Watkins et al. 2016). Importantly, phosphorylation of PBF at residue Y174 was found to be critical to the functional interaction between these two proteins and abrogation of Y174 led to diminished wound healing capacities and completely abolished cellular invasion in all cell lines tested (Watkins et al. 2016). Similarly, PBF phosphorylation may have a significant impact on other cellular processes involving PBF function and may represent a novel therapeutic target. However, whilst total PBF expression is prognostic in thyroid and breast cancers (Xiang et al. 2012, Hsueh et al. 2013), it is not known whether PBF phosphorylation status may have potential use as a prognostic marker.

PBF expression and function has not previously been examined in head and neck squamous cell carcinoma (HNSCC), although a recent unpublished GEO profile cDNA array analysis of matched tumour and normal HNSCC samples demonstrated PBF overexpression in 15 of 22 tumours compared to normal tissue (1.25-fold induction, $p=0.02$). Furthermore, recent investigations by our group, outlined above, have established phosphorylation of PBF at residue Y174 to be important for its biological function. We therefore wished to examine

total and Y174-phosphorylated PBF expression and localisation in HNSCC. To this end, total RNA was extracted from fresh-frozen tissue sections and PBF mRNA expression assessed by real-time quantitative PCR. In addition, total and Y174-phosphorylated PBF protein expression was determined in formalin-fixed, paraffin-embedded microarray tissue sections by immunohistochemistry.

## 4.2 Methods

### 4.2.1 Human tissue specimens

#### *4.2.1.1 Fresh-frozen tissue*

Details of the matched tumour and normal tissue specimens are outlined in the previous chapter (section 3.2.2.1).

#### *4.2.1.2 Tissue microarrays*

Details regarding the formalin-fixed, paraffin-embedded tissue sections are also described in the previous chapter (section 3.2.2.2).

#### *4.2.1.3 Ethics*

Details regarding ethical approval are described in the previous chapter (section 3.2.2.3).

### 4.2.2 RNA extraction, reverse transcription and quantitative real-time PCR

Total RNA was extracted from fresh-frozen tissue specimens and reverse transcribed as described in 3.2.3. Quantitative real-time PCR was performed as previously described in section 2.5. Taqman gene-specific expression assays for PPIA (Hs04194521_s1) were purchased from Applied Biosystems. Custom designed primers and probes, which have been previously validated (Stratford et al. 2005), were used for assessment of PBF expression. Their sequences are given in Table 4.1.

| Primer | Sequence |
|---|---|
| **Forward** | 5'- GCAGAGATGAAGACAAGACATGA -3' |
| **Reverse** | 5'- GCGTGCACCTCACAGGAAG -3' |
| **Probe** | 5'- FAM-TCCAGCACATCAGTCCCGACG-TAMRA -3' |

*Table 4.1 Table of PBF primer and probe sequences. FAM=6-carboxy-fluorescien, TAMRA= tetramethylrhodamine.*

### 4.2.3 Immunohistochemistry

Paraffin-embedded, formalin-fixed tissue sections were immunostained using the Novocastra™ Novolink™ Max Polymer Detection System [Leica Biosystems], as outlined in section 2.10. Antibodies used were anti-PBF 1:175 [Santa Cruz Biotechnology, Dallas, Texas, USA] and anti-Y174-phosphorylated PBF 1:50 (Smith et al. 2013). Evaluation of the stained slides was performed independently and in a blinded manner by Dr Rasoul Amel-Kashipaz (Clinical Laboratory Services, Cellular Pathology, University Hospitals Birmingham NHS Foundation Trust, Queen Elizabeth Hospital Birmingham, Birmingham, UK) and I. Each individual section was analysed by light microscopy and visually scored according to staining intensity (Figure 4.1; 0= negative, +1= weak intensity, +2= moderate intensity and +3= strong intensity) and percentage of staining observed in each of the three intensity categories. Sections which were damaged or contained < 25 % tumourous tissue were excluded from further analyses. As the total number of patient samples was relatively low, cases where only one representative section was available were still included. For each tumour tissue section, an H-score was then calculated as described in 3.2.5.

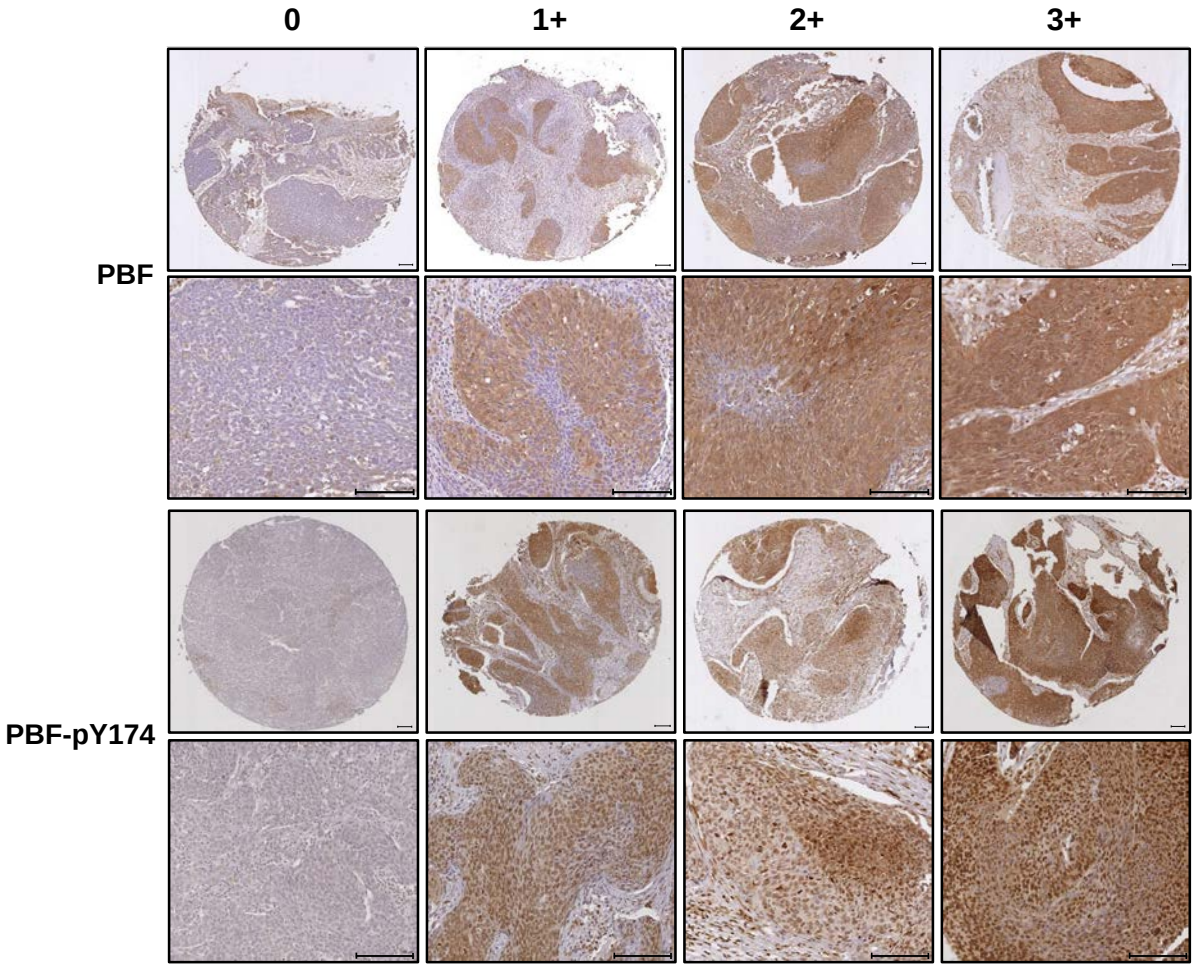


*Figure 4.1 Representative immunohistochemical staining of total PBF (top panel) and Y174-phosphorylated PBF (bottom panel) protein expression in head and neck tumour tissue microarray (TMA) sections. Columns 1-4 are representative of the different staining intensity scores (0= negative, +1= weak intensity, +2= moderate intensity, +3= strong intensity). Top row of images were taken at 4x magnification. Bottom row of images were taken at 20x magnification. Scale bars 100 µm.*

### 4.2.4 Statistical analysis

Statistical analyses were performed using GraphPad Prism version 5.0. The non-parametric Wilcoxon matched pairs signed-rank test was used to assess PBF mRNA expression in the matched head and neck tissue specimens. The non-parametric Mann-Whitney *U* test was used to assess correlations between clinical follow-up data and PBF mRNA expression. Correlations between PBF/PBF-Y174 H-scores and clinical follow-up data were assessed by Mann-Whitney *U* test and Fisher's exact test. Statistical analyses could

not be performed for PBF or PBF-Y174 H-scores and alcohol status by Mann-Whitney *U* test as the majority of patients had a history of alcohol consumption, thus making the numbers in one category too small to analyse. Statistical analyses could not be performed for PBF-Y174 and HPV status by Mann-Whitney *U* test for the same reasons. The significance of the association between gene expression datasets was assessed by use of the Spearman's rank-based correlation coefficient. Statistical significance was taken as $p < 0.05$.

## 4.3 Results

### 4.3.1 PBF mRNA expression in head and neck squamous cell carcinoma

#### *4.3.1.1 PBF mRNA is overexpressed in squamous cell carcinomas of the head and neck*

PBF mRNA expression levels were initially assessed in matched tumour and normal head and neck tissue specimens by quantitative real-time PCR. The same set of 24 paired samples used to assess PTTG mRNA expression in the previous chapter were used for the assessment of PBF mRNA expression. Full demographic and clinical data were available for all patients and are summarised in chapter 3, section 3.3.1. As shown in Figure 4.2, PBF mRNA expression levels were significantly higher in the tumour tissues when compared to expression in the matched normal specimens (1.6-fold, p=0.008).

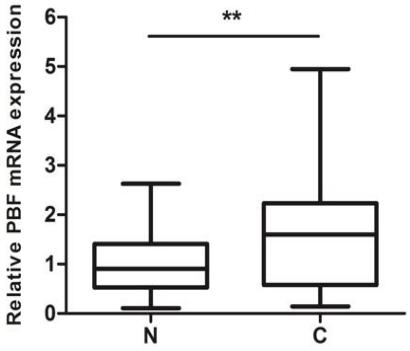


*Figure 4.2 PBF mRNA expression is upregulated in head and neck squamous cell carcinoma. Quantification of PBF mRNA expression in head and neck squamous cell carcinoma (HNSCC) tumours (C) relative to matched normal (N) head and neck tissue specimens (n=24). Data presented as a box-whisker plot. The centre line represents the median fold change in mRNA expression, the box indicates the 25$^{th}$ and 75$^{th}$ percentiles and the whiskers represent the minimum and maximum values. ** p ≤0.01.*

As demonstrated with PTTG mRNA expression (section 3.3.1), PBF mRNA expression varied considerably between the tumour specimens (Figure 4.3). Relative levels of PBF mRNA expression ranged from a 0.3-fold decrease to a 5-fold increase across the panel of tumours. Specimens were obtained from four anatomical sites; larynx, oral cavity, hypopharynx and oropharynx. Some variability in PBF mRNA expression was observed between these different tumour sites, although these differences were not found to be statistically significant. Further statistical analysis revealed no significant differences in PBF mRNA expression when compared with any of the remaining demographic or clinicopathological features (data not shown).

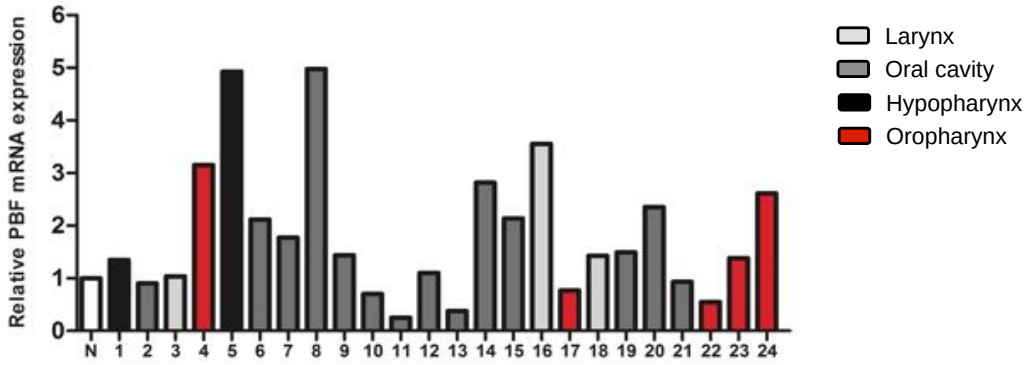


*Figure 4.3 PBF mRNA expression across the panel of head and neck squamous cell carcinomas. PBF mRNA expression in head and neck squamous cell carcinoma (HNSCC) samples (1-24) compared to matched normal tissue (N). Data presented fold change in mRNA expression.*

*4.3.1.2 PBF mRNA expression correlates with PTTG mRNA expression in head and neck squamous cell carcinoma*

Interestingly, comparison of the mRNA expression of both PBF and PTTG in the same set of paired tumour specimens revealed a positive and significant correlation (Figure 4.4; n=24, p=0.0007). This also became apparent when comparing Figure 3.3 and Figure 4.3, where many of the tumour specimens demonstrated a similar fold change in mRNA expression for PBF and PTTG.

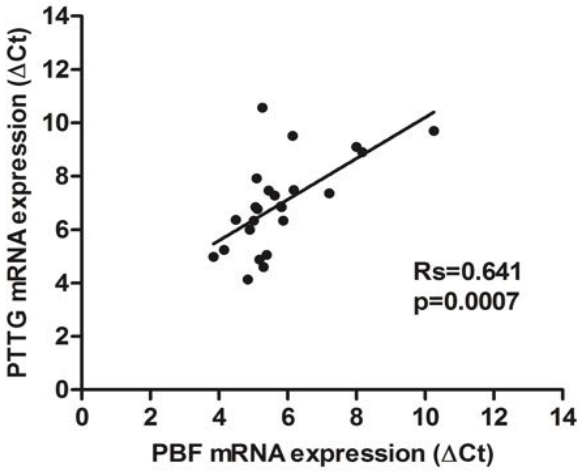


*Figure 4.4 PBF mRNA expression correlates with PTTG mRNA expression in head and neck squamous cell carcinoma. Scatterplot showing a significant correlation between PBF and PTTG mRNA expression in squamous cell carcinomas of the head and neck (HNSCC) (n=24). Data presented as ΔCt values. * p =0.0007, $R_s$=0.641.*

### 4.3.2 PBF protein expression in head and neck squamous cell carcinoma

#### *4.3.2.1 PBF antibody optimisation*

Immunohistochemical detection of PBF protein was optimised using a panel of PBF-specific antibodies, including an in-house rabbit anti-human PBF-8 polyclonal antibody [Eurogentec] (Read et al. 2011), another recently purified in-house rabbit anti-human PBF-4 polyclonal antibody (manufactured for the McCabe group by Eurogentec), two commercially available rabbit anti-human PBF polyclonal antibodies [S-15 and C-19, Santa Cruz Biotechnology, Dallas, Texas, USA] and a rabbit anti-human PBF monoclonal antibody [LS-B6285, LifeSpan BioSciences, Seattle, WA, USA], specifically designed for use in immunohistochemistry applications. As a negative control, primary antibodies were replaced by 10% normal serum [Vector Laboratories]. Representative images of formalin-fixed, paraffin-embedded oropharyngeal whole tissue sections stained with each of the antibodies are shown in Figure 4.5.

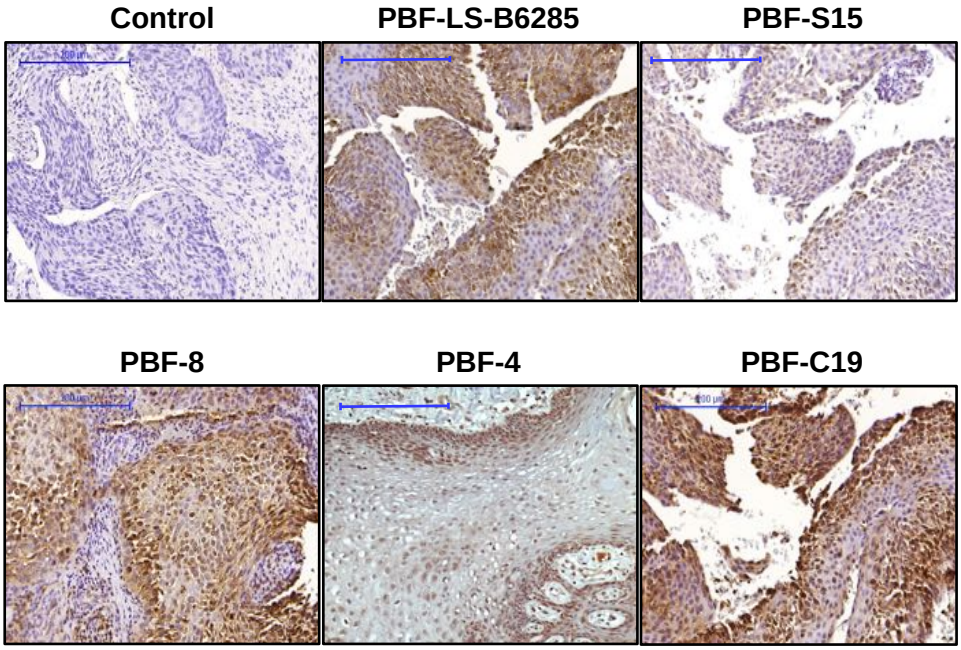


*Figure 4.5 Representative images of formalin-fixed paraffin-embedded whole head and neck tumour tissue sections stained for PBF using a panel of PBF-specific antibodies. Control – secondary antibody only; PBF-LS-B6285 – LifeSpan Biosciences rabbit polyclonal IgG 1:250; PBF-S15 – Santa Cruz Biotechnology rabbit polyclonal IgG 1:250; PBF-8 – in-house rabbit polyclonal IgG 1:500; PBF-4 – in-house rabbit polyclonal IgG 1:250; PBF-C19 - Santa Cruz Biotechnology rabbit polyclonal IgG 1:175. Sections were counterstained with Haematoxylin. All images were taken at 10x magnification. Scale bars 200 µm.*

Abundant total PBF protein expression was evident in the oropharyngeal tissue whole sections and appeared to be nuclear and cytoplasmic, similar to that shown previously in the thyroid (Stratford et al. 2005) and breast (Watkins et al. 2010). Both PBF-4 and PBF-S15 antibodies demonstrated very weak PBF staining at high concentrations (1:250) and were therefore disregarded. On the other hand, antibodies PBF-8, PBF-C19 and PBF-LS-B6285 all demonstrated moderate to strong staining for PBF. As antibody PBF-C19 demonstrated clear and strong staining, with little background signal, this antibody was chosen for subsequent immunohistochemical analysis of total PBF protein expression in head and neck tumour tissue microarrays (TMA).

*4.3.2.2 PBF protein is expressed and phosphorylated at residue Y174 in head and neck squamous cell carcinoma*

With an optimised PBF antibody, total and Y174-phosphorylated PBF protein expression was investigated in the same series of formalin-fixed, paraffin-embedded HNSCC tumour TMA sections described in section 3.2.2.2. Due to poor tissue quality, only 24 out of the 53 tumour TMA samples were analysed for total PBF protein expression and 23 for analysis of Y174-phosphorylated PBF protein expression.

Detailed examination of the TMA sections revealed moderate expression of total PBF protein and low to moderate expression of PBF-pY174 protein in normal head and neck tissue (Figure 4.6). Expression of total PBF and PBF-pY174 in the tumour cores however was generally higher and was present in oropharyngeal tumours of all tumour grades (Figure 4.6). As mentioned previously, total PBF expression was distributed throughout the cytoplasm and occasionally in the nucleus but appeared to be more concentrated in the cytoplasm. PBF-pY174 protein expression was also found in the nucleus and cytoplasm but with no clear pattern of distribution between the two subcellular compartments.

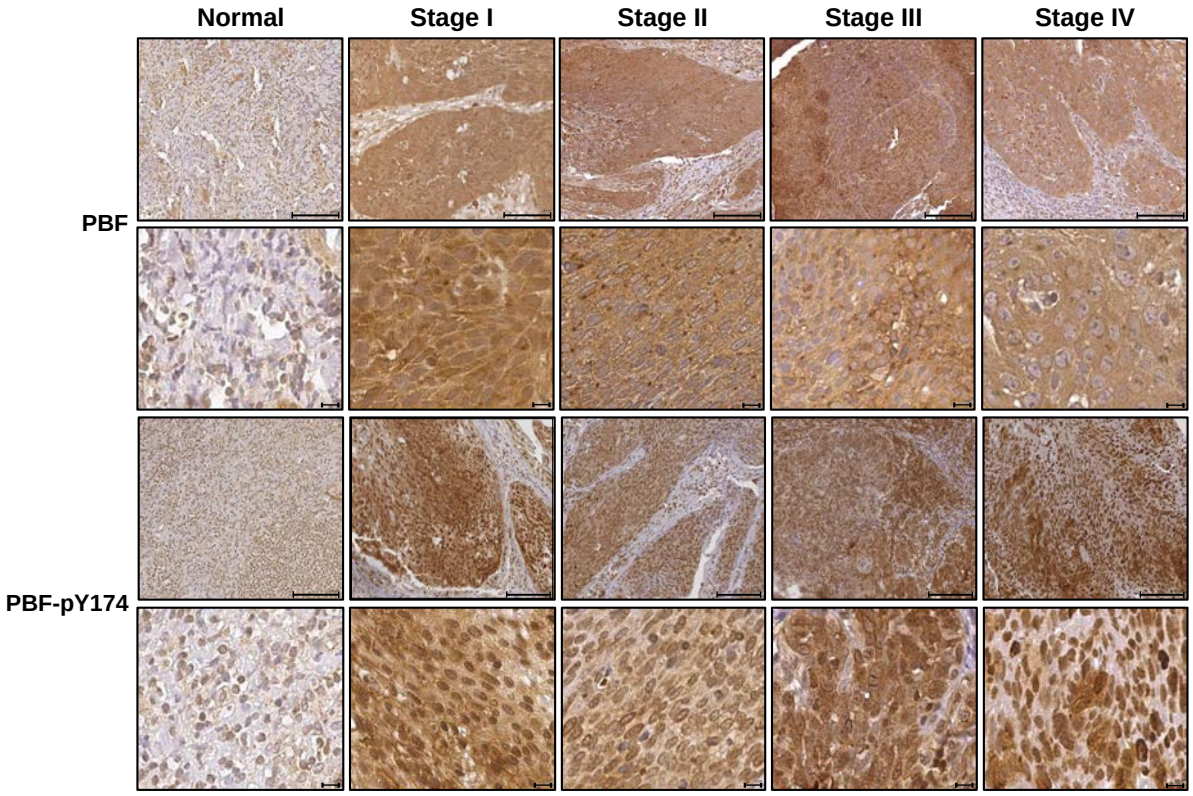


*Figure 4.6 Representative images of formalin-fixed, paraffin-embedded head and neck tumour tissue microarray (TMA) sections of various tumour stages stained for total PBF (top panel) and Y174-phosphorylated PBF (bottom panel) protein. Sections were counterstained for Haematoxylin. Top row of images were taken at 20x magnification – scale bars 100 µm. Bottom row of images were taken at 80x magnification – scale bars 10 µm.*

#### *4.3.2.3 Total PBF protein expression correlates with gender and tumour sub-site*

The intensity scores and percentage of cells staining at each intensity score were determined and then converted into an H-score as outlined in section 4.2.3 above. When the H-scores for total PBF protein expression were categorically analysed alongside the available demographic and clinical follow-up data for each individual patient, PBF protein expression was shown to correlate with tumour sub-site (Table 4.2). Tumours originating in the tonsils expressed significantly lower levels of PBF protein when compared with tumours originating from the base of the tongue (82.8±15.4 vs. 139.3±19.2, p=0.016). The H-scores of the tumour tissues ranged from 1-300 for total PBF protein expression, with a median of 100. An H-score of 100 was therefore used to divide patients into low PBF expression and high PBF

expression groups. Subdivision of the H-scores into low PBF expression (H-score ≤100) and high PBF expression (H-score >100) and subsequent re-analysis of the data by Fisher's exact test confirmed an association between PBF protein expression and tumour sub-site and revealed an additional correlation between high PBF protein expression and gender (Table 4.2; p=0.047). High levels of PBF expression were evident in only 26 % of the male study population compared to 80 % in the female study population. None of the remaining categories were found to be associated with PBF protein expression using either method of analysis.

| Clinical and pathological features | | PBF | | | |
|---|---|---|---|---|---|
| | | Mann-Whitney *U* test | | | Fisher's exact test |
| | | No. of patients | H-score (mean±SEM) | p-value | p-value |
| **Age (yr)** | <50 | 5 | 84.4±24.9 | 0.61 | 1.00 |
| | >50 | 19 | 110.8±11.8 | | |
| **Gender**[a] | F | 5 | 143.0±28.3 | 0.09 | **0.05** |
| | M | 19 | 95.4±10.5 | | |
| **Smoking status** | Never | 5 | 126.8±39.0 | 0.24 | 0.15 |
| | Previous/Current | 18 | 99.4±9.9 | | |
| **Alcohol status** | Never | - | - | - | 0.53 |
| | Previous/Current | | | | |
| **Sub-site** | Tonsil | 12 | 82.8±15.4 | **0.02** | **0.04** |
| | Base of tongue | 7 | 139.3±19.2 | | |
| **T stage** | pT1-2 | 12 | 114.8±13.4 | 1.00 | 0.67 |
| | pT3-4 | 9 | 116.0±14.4 | | |
| **N stage** | pN0-1 | 8 | 111.0±13.2 | 0.75 | 0.40 |
| | pN2-3 | 14 | 109.6±15.1 | | |
| **Recurrence** | No | 16 | 99.2±14.4 | 0.16 | 0.41 |
| | Yes | 8 | 117.5±14.3 | | |
| **HPV status**[b] | - | 19 | 109.3±10.8 | 0.08 | 0.27 |
| | + | 3 | 50.0±28.8 | | |

[a] Abbreviations: F, female; M, male
[b] Abbreviations: -, negative; +, positive

*Table 4.2 Table of PBF H-scores and their association with the clinical and pathological features of HNSCC patients. H-score values were assessed by Mann-Whitney U test and Fisher's exact test.*

#### *4.3.2.4 Expression of Y174-phosphorylated PBF does not correlate with demographic or clinicopathological characteristics*

For PBF-pY174, H-scores for both nuclear and cytoplasmic protein expression were determined and correlated with the demographic and clinical follow-up data. When analysed by the Mann-Whitney U test, PBF-pY174 expression did not correlate with any of the categories (Table 4.3). The H-scores of the tumour tissues ranged from 1-250 for cytoplasmic and nuclear PBF-pY174 protein expression, with a median of 50. An H-score of 50 was

therefore used to divide patients into low PBF-pY174 expression and high PBF-pY174 expression groups. When analysed based on low PBF-pY174 protein expression (H-score ≤50) vs. high PBF-pY174 protein expression (H-score >50), no significant differences in PBF-pY174 protein expression were identified (Table 4.3).

| | | | **PBF-pY174 nuclear** | | | **PBF-pY174 cytoplasmic** | | |
|---|---|---|---|---|---|---|---|---|
| | | | **Mann-Whitney *U* test** | | **Fisher's exact test** | **Mann-Whitney *U* test** | | **Fisher's exact test** |
| Clinical and pathological features | | No. of patients | H-score (mean±SEM) | p-value | p-value | H-score (mean±SEM) | p-value | p-value |
| **Age (yr)** | <50 | 5 | 100.5±53.3 | 0.40 | 1.00 | 47.9±32.7 | 0.67 | 0.62 |
| | >50 | 18 | 53.4±17.6 | | | 30.7±10.5 | | |
| **Gender**[a] | F | 4 | 50.0±50.0 | 0.54 | 1.00 | 66.3±40.3 | 0.30 | 0.56 |
| | M | 19 | 66.6±19.4 | | | 27.8±9.7 | | |
| **Smoking status** | Never | 5 | 17.0±17.0 | 0.20 | 1.00 | 39.8±25.9 | 0.45 | 0.62 |
| | Previous/Current | 17 | 72.3±22.3 | | | 34.3±12.5 | | |
| **Alcohol status** | Never | | | | | | | |
| | Previous/Current | - | - | - | 1.00 | - | - | 1.00 |
| **Sub-site** | Tonsil | 12 | 46.6±23.4 | 0.28 | 0.34 | 30.8±13.3 | 0.58 | 0.25 |
| | Base of tongue | 6 | 85.0±41.6 | | | 10.8±8.0 | | |
| **T stage** | pT1-2 | 11 | 48.2±17.5 | 0.57 | 0.67 | 30.7±12.8 | 0.43 | 0.64 |
| | pT3-4 | 9 | 75.5±32.9 | | | 49.7±21.4 | | |
| **N stage** | pN0-1 | 8 | 61.7±23.7 | 0.56 | 0.65 | 25.1±15.1 | 0.33 | 0.66 |
| | pN2-3 | 13 | 55.1±23.6 | | | 45.5±15.8 | | |
| **Recurrence** | No | 15 | 58.3±21.9 | 0.43 | 0.67 | 30.3±14.1 | 0.43 | 0.66 |
| | Yes | 8 | 73.8±32.2 | | | 42.3±15.9 | | |
| **HPV status**[b] | - | 19 | 109.3±10.8 | 0.08 | 0.50 | - | - | 0.53 |
| | + | 3 | 50.0±28.8 | | | | | |

[a] Abbreviations: F, female; M, male
[b] Abbreviations: -, negative; +, positive

*Table 4.3 Table of PBF-pY174 H-scores and their association with the clinical and pathological features of HNSCC patients. PBF-pY174 H-score values were assessed by Mann-Whitney U test and Fisher's exact test.*

## 4.4 Discussion

Given that PTTG expression levels were elevated in our series of HNSCC tumour specimens, as described in Chapter 3, we next sought to determine expression of its interacting partner, PBF, in the same patient cohort. In this current chapter, we have demonstrated that like PTTG, PBF is also abundantly and frequently expressed in HNSCC. In addition we identified significant correlations between total PBF protein expression and various patient demographic and clinicopathological parameters. Although PBF was phosphorylated at residue Y174 in these tumours, it was not associated with patient demographics or clinical outcome in our patient cohort.

PBF is both a transforming and tumourigenic gene and its overexpression has been demonstrated in a number of cancers, such as pituitary (McCabe et al. 2003), thyroid (Stratford et al. 2005) and breast (Watkins et al. 2010). However expression has not been systematically examined in HNSCC. A recent unpublished GEO profile cDNA array analysis hinted at a potential upregulation of PBF in HNSCC tumours and prompted us to further investigate PBF mRNA expression in our series of 24 paired human HNSCC tumour and normal tissue specimens by quantitative real-time PCR. Upon comparison of normal and tumourous HNSCC tissue specimens, PBF mRNA expression was found to be significantly upregulated in the tumours. Furthermore, we reported a parallel increase in PBF and PTTG mRNA expression in these tumour samples.

Co-ordinated expression has been demonstrated before in pituitary and thyroid tumours (McCabe et al. 2003, Stratford et al. 2005). As many of the oncogenic actions of PTTG are dependent on PBF-mediated shuttling of PTTG into the nucleus and PTTG is capable of upregulating PBF mRNA expression in the thyroid (Stratford et al. 2005), the observed increase in PBF mRNA expression in our cohort of HNSCC tumours may be, in part, a

secondary effect of elevated PTTG mRNA expression. Alternatively, correlated PTTG and PBF mRNA expression may be a result of a common mechanism by which expression of both genes are regulated. Indeed, oestrogen induction of PTTG and PBF has been described before (Heaney et al. 1999, Watkins et al. 2010, Xiang et al. 2012).

Additional immunohistochemical analysis of PBF protein expression was conducted using a panel of OPSCC TMA specimens. Abundant PBF protein expression was observed in ~92 % (22 out of a total of 24 patients) of OPSCC tissue specimens. Closer inspection revealed mainly cytoplasmic staining with occasional nuclear staining in some of the tumour cores. This observation of both cytoplasmic and nuclear PBF expression is similar to previous observations in normal thyroid tissues and well-differentiated thyroid tumours (Stratford et al. 2005, Hsueh et al. 2013). High PBF expression was also detected in tissue microarrays of breast tumours, where expression was mostly confined to the cytoplasm, with some nuclear staining visible (Watkins et al. 2010). Furthermore, overexpression studies in COS-7 (Chien, Pei 2000) and HCT116 (Stratford et al. 2005) cells using heamagglutinin- or EGFP-tagged PBF have again demonstrated significant cytoplasmic and nuclear staining. However PBF expression has also been detected within intracellular vesicles and at the plasma membrane (Smith et al. 2009). Such inconsistencies are possibly due to methodological differences. Stratford et al., Hsueh et al. and Watkins et al. had all analysed PBF subcellular localisation by immunohistochemical staining of normal and tumorous human thyroid and breast tissue sections, respectively. On the other hand, Chien & Pei and Smith et al. had used immunofluorescence techniques to detect and analyse PBF protein expression in a number of cell lines. Importantly, these assays were performed in various cell types derived from different species and are likely to have differing levels of sensitivity.

As full patient demographic and clinical follow-up details were available for the TMA samples, further statistical analyses were performed against PBF protein expression. PBF protein expression correlated with tumour sub-site, demonstrating increased expression in tumours originating at the base of the tongue. Interestingly, total PBF protein was also significantly associated with gender, with higher PBF protein expression scores noted in females when compared with male individuals. This gender bias is pertinent given the reported association between PBF and oestrogen receptor-α (ER-α) in differentiated thyroid cancer and the knowledge that PBF expression is regulated in an oestrogen-dependent manner in breast tumours (Watkins et al. 2010, Xiang et al. 2012) and suggests that oestrogen signalling may be partly responsible for the enhanced PBF expression observed in HNSCC patients. Preliminary studies have demonstrated ER-α expression in squamous cell carcinomas of the oral cavity, larynx and hypopharynx (Lukits et al. 2007) and high nuclear ER-α expression has been further linked with poor disease-free survival in HNSCC patients (Egloff et al. 2009). Perturbed ER expression and oestrogen metabolism have also subsequently been demonstrated in numerous cell lines derived from premalignant and malignant HNSCC lesions (Colella et al. 2011, Shatalova et al. 2011). However, the exact role of ER-signalling in HNSCC remains to be distinguished. Initial reports have proposed a role for ER-signalling in oral cancer cell survival and invasion (Ishida et al. 2007).

It has recently come to light that phosphorylation of PBF at residue Y174 by the tyrosine kinase Src is important in regulating PBF binding and cycling of NIS from intracellular vesicles to the membrane (Smith et al. 2013). As PBF is involved in a diverse array of cellular processes, phosphorylation may have important implications with regard to its other biological functions. We therefore assessed expression of Y174-phosphorylated PBF protein in the same set of oropharyngeal tumour TMA specimens. Expression of PBF-pY174 was

evident in both the nucleus and cytoplasm. Rare occasions of membranous staining were also noted. However, further examination of the expression scores did not reveal any striking associations with patient demographic and clinical follow-up data, suggesting that although PBF phosphorylation may of biological importance it may not represent a suitable prognostic or predictive marker in HNSCC. Given that the staining for PBF-pY174 appeared to be very intense and the fact that the human eye cannot discriminate between subtle differences in staining colour or intensity very well, it is possible that the current study lacked the sensitivity to be able to distinguish potential differences between PBF-pY174 expression and clinicopathological features. Computer-aided scoring and analysis of these TMAs may have overcome some of these limitations, enabling rapid and reliable scoring.

A lack of correlation between total PBF protein expression and standard clinicopathological parameters was surprising considering PBF has been recognised as an independent prognostic factor in papillary thyroid carcinoma (Hsueh et al. 2013) and colorectal cancer (Read et al. 2016b). As our patient cohort contained mainly OPSCC patients, it could be that PBF expression represents a significant predictor of recurrence in HNSCCs collectively but not specifically in oropharyngeal cancer patients. Alternatively, as overexpression of PBF is clearly evident in the majority of OPSCCs it is likely to be required for tumour initiation and progression but may cease to be important once the tumour has become invasive. Our current study was limited by the relatively small size of our patient cohort, with only 24 paired HNSCC tumour and normal tissue specimens for PCR analysis and 23-24 TMA individual patient cores for histological examination of total and Y174-phohsphorylated PBF protein expression. Whether or not PBF may serve as a potential biomarker will undoubtedly require further evaluation on a much larger scale. As recommended for future analysis of PTTG expression in section 3.4, fresh-frozen tissue

specimens and TMAs from the same patient cohort would be ideal as this will help to minimise any potential variation that is often associated with analysing mRNA and protein expression in separate groups of patients.

### 4.4.1 Concluding statements

In the present chapter we have provided evidence that PBF expression is significantly upregulated in HNSCC tumours. Furthermore, PBF displayed a significant gender bias, with higher expression levels observed in female patients. In addition, PBF is phosphorylated at residue Y174 in these tumours but does not correlate with patient demographic or clinical follow-up data.

# Chapter 5

# Stable gene silencing in head and neck cancer cells by lentiviral vectors

## 5.1 Introduction

The proto-oncogenes PTTG and PBF are frequently overexpressed in a wide variety of tumours, including those occurring in the thyroid (McCabe, Gittoes 1999, Stratford et al. 2005), colon (Heaney et al. 2000, Read et al. 2016b) and breast (Solbach et al. 2004, Watkins et al. 2010), and have been independently associated with tumour metastasis and recurrence (Stratford et al. 2005, Watkins et al. 2010, Read et al. 2014). Recent studies have also elucidated a role for PTTG in head and neck cancer, with overexpression again being linked to poorer prognosis (Solbach et al. 2006, Ito et al. 2008). In previous chapters we confirmed that PTTG expression is elevated in head and neck cancer, particularly those occurring in the oropharynx. In addition, we identified its binding partner, PBF, to be upregulated and significantly correlated with PTTG expression in these tumours. However, despite an abundance of evidence implicating PTTG, and now PBF, in head and neck cancers, the precise roles of these two proto-oncogenes in head and neck tumourigenesis have not been fully explored.

The RNA interference (RNAi) pathway is an evolutionarily conserved process that is initiated by eukaryotic cells in response to endogenous double-stranded RNA molecules (dsRNA) or exogenous pathogenic nucleic acids. Activation of the pathways results in the sequence-specific silencing of eukaryotic gene expression via degradation of specific messenger RNA transcripts (mRNA). Other endogenous non-coding RNA molecules are also capable of triggering the RNAi pathway, including microRNA (miRNA). Short hairpin RNAs (shRNA) are synthetic molecules designed to interact with components of the RNAi pathway to induce potent and specific inhibition of target gene expression. Recently developed retrovirus-/lentivirus-based vectors have become increasingly powerful tools for the delivery of these target-specific shRNAs into cells to facilitate permanent target gene knockdown

(Brummelkamp et al. 2002, McManus et al. 2002). The process by which lentiviral vectors transduce and deliver the shRNA into the cell are detailed in Figure 5.1.

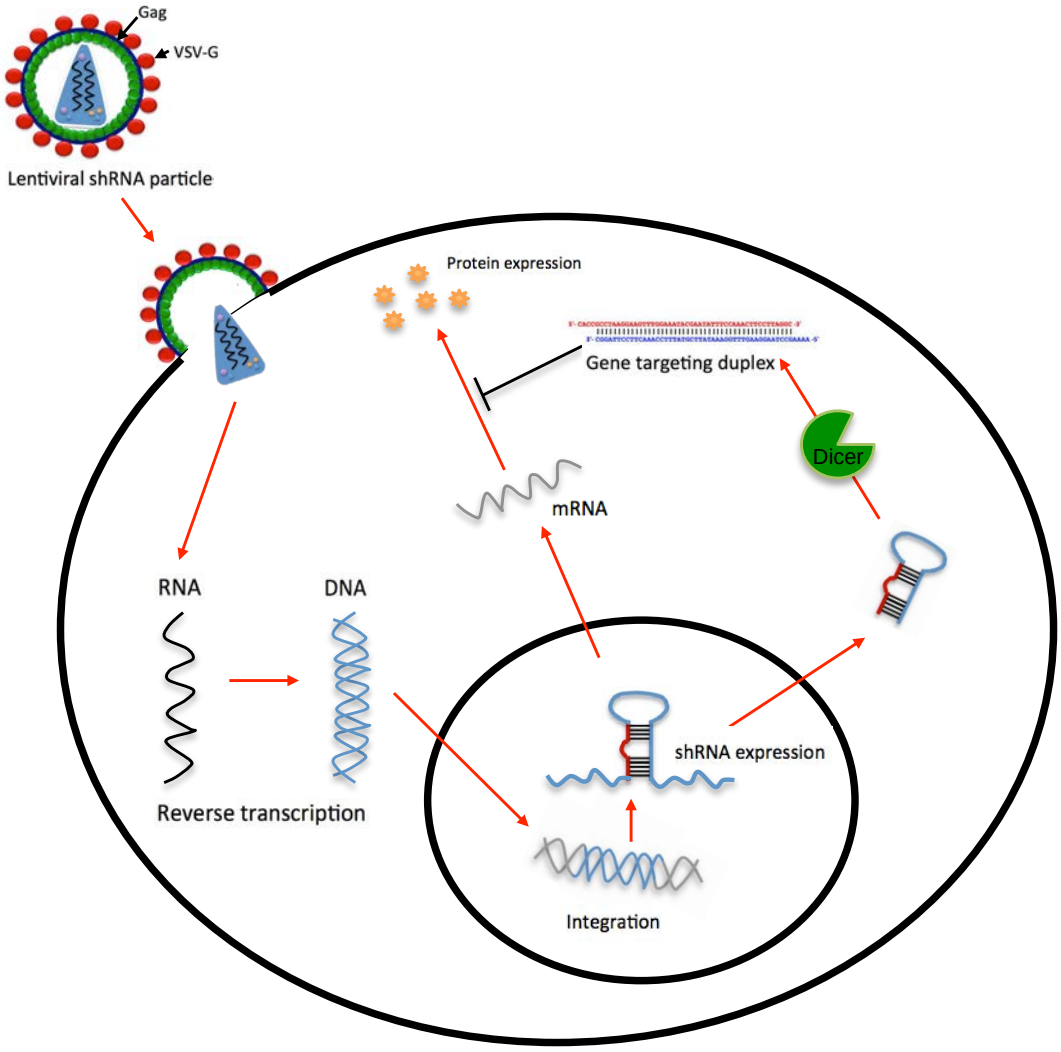


*Figure 5.1 Lentiviral delivery of shRNAs capable of triggering the RNAi pathway in mammalian cells. Binding of the lentiviral particle envelope protein (VSV-G) with receptors in the host cell membrane results in release of the viral core and delivery of the viral genome into the cytoplasm. Here, the viral RNA is reverse transcribed to generate DNA. The DNA is then transported into the nucleus where it becomes stably integrated in to the host cell genome. The viral DNA (encoding the silencing construct) is then constitutively expressed by the host cell and processed into shRNAs, which then enter the RNAi pathway to affect target gene expression.*

Upon binding to the host cell surface, the viral core is released into the cytoplasm. Here, the viral genome, encoding the shRNA target sequence, is reverse transcribed to generate

DNA using the host replication machinery. The viral DNA is subsequently transported in to the nucleus where it becomes stably incorporated in the host cell genome, resulting in constitutive expression of the shRNA. The expressed shRNA is processed by the RNA-specific endonuclease, DICER, to generate 21-23 nucleotide short interfering RNA duplexes (siRNA) (Bernstein et al. 2001). These siRNA duplexes are then separated into single strands of RNA (ssRNA) and used, as a template, by the RNA-induced silencing complex (RISC) to recognize and cleave the target mRNA transcript, thereby preventing further translation of the target mRNA (Hammond et al. 2000).

To further assess PTTG and PBF function in the setting of HPV-negative and HPV-positive head and neck cancer we constructed a lentivirus encoding gene-specific shRNAs to silence expression of PTTG and PBF. The purpose of this chapter was therefore to establish and characterise stable PTTG and PBF shRNA-expressing HNSCC cell lines for use in downstream applications.

## 5.2 Methods

### 5.2.1 Cell lines

92-VU-040T and 93-VU-147T cells were maintained as described in section 2.1.

### 5.2.2 BLOCK-iT™ Lentiviral RNAi Expression System

The Invitrogen™ BLOCK-iT lentiviral RNAi expression system was used to facilitate lentiviral-based delivery of shRNA into the HNSCC cell lines. The main steps involved in generating the lentiviral particles are outlined in the flow chart below (Figure 5.2). All reagents described were purchased from Invitrogen™ unless stated otherwise.

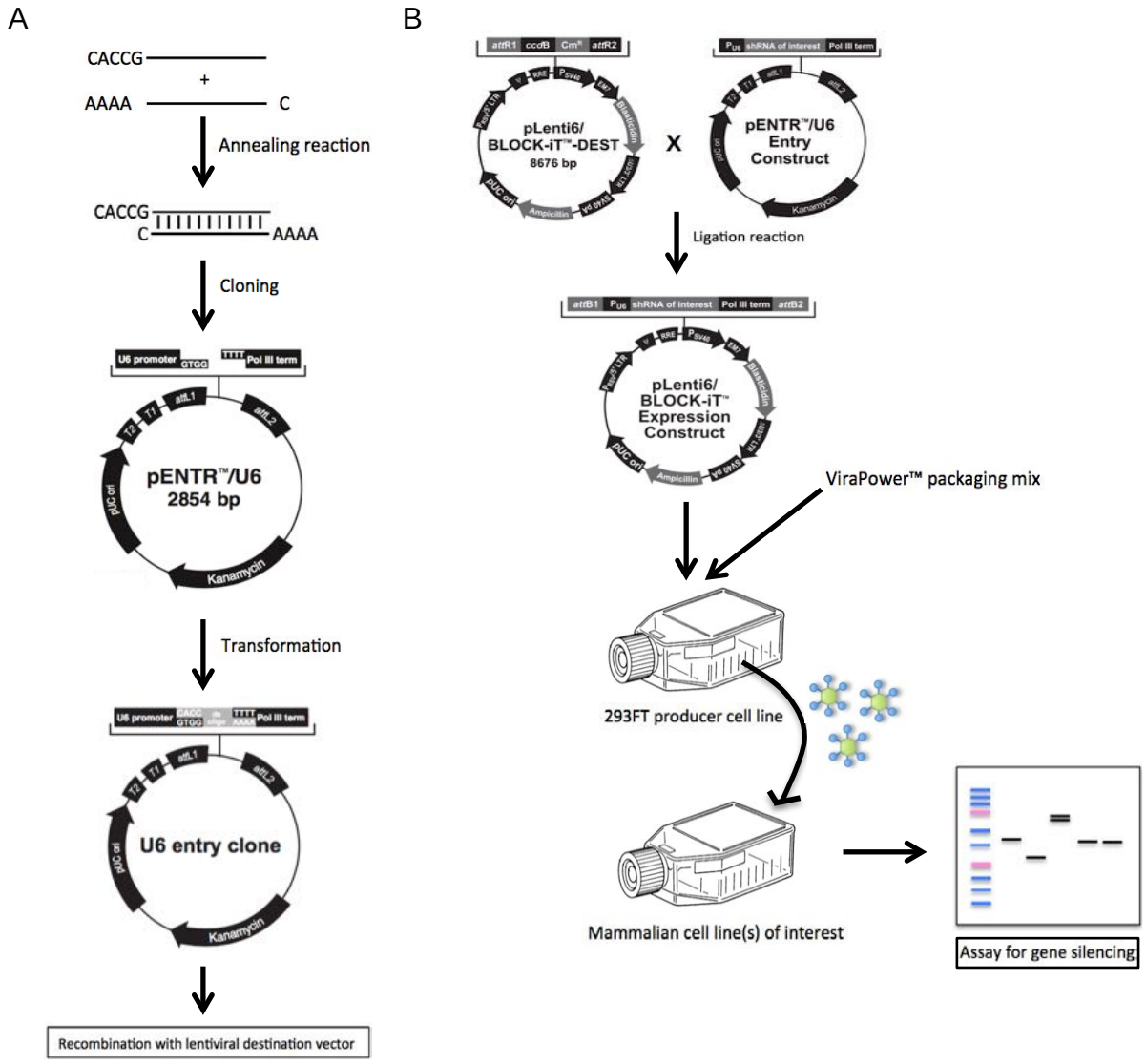


*Figure 5.2 Flow charts demonstrating the process by which stable shRNA-expressing cell lines were generated using the BLOCK-iT™ lentiviral RNAi expression system.* ***A*** *– Complementary single-stranded oligonucleotides encoding the shRNA target sequence were synthesised and annealed to generate a double-stranded oligonucleotide. This was then cloned in to the pENTR™/U6 vector to create an U6 entry clone.* ***B*** *– To generate the lentiviral expression construct, an LR recombination reaction was performed using the U6 entry clone and the pLenti6/BLOCK-iT™ -DEST vector. The HEK 293FT producer cell line was then co-transfected with the pLenti6/BLOCK-iT™ -DEST expression construct and viral packaging mix. The viral supernatant was subsequently harvested and added to the cell line(s) of interest. Cells were assayed for knockdown of the target gene and selected for stable transduction using Blasticidin.*

*5.2.2.1 Cell lines*

293FT cells were used for lentiviral particle production. The 293FT line is a variant of the well-established HEK 293 line, which is established from human primary embryonal kidney cells transformed with sheared human adenovirus type 5 DNA (Graham et al. 1977). The 293FT line is a fast-growing variant and stably expresses the SV40 large T antigen from the pCMVSPORT6Tag.neo.plasmid. Cells were routinely cultured as a monolayer in vented 75 $cm^2$ flasks in filter-sterilised high-glucose DMEM supplemented with 10 % heat-inactivated FBS, $10^5$ U/I penicillin, 100 mg/L streptomycin, 6 mM L-Glutamine, 0.1 mM non-essential amino acids, 1 mM MEM sodium pyruvate and 500 µg/ml Geneticin®. Cells were passaged twice weekly and incubated in a humidified atmosphere at 37 °C and 5 % $CO_2$. The medium was replaced with fresh complete medium containing Geneticin® every three days.

*5.2.2.2 Vectors*

Down-regulation of PTTG and PBF gene expression was achieved by transduction with Gateway®-adapted lentiviral expression vectors. Double-stranded oligonucleotides encoding the shRNA target sequence were initially cloned in to the pENTR™/U6 entry vector. This vector contains an RNA Pol III-dependent expression cassette (U6 RNAi cassette) for transient RNAi analysis (Figure 5.3A). The U6 RNAi cassette was then transferred from the entry vector into the pLenti6/BLOCK-iT™-DEST lentiviral vector by LR recombination for use in downstream RNAi applications (Figure 5.3B).

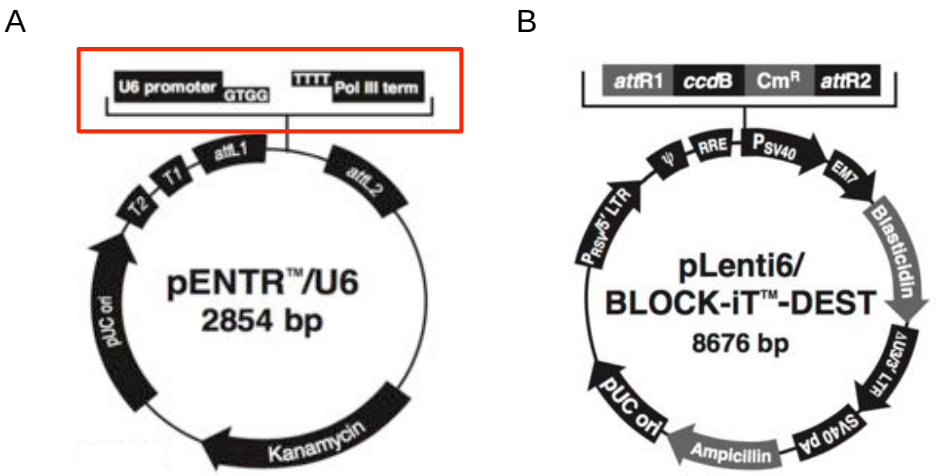


*Figure 5.3 BLOCK-iT™ RNAi Vector Maps.* ***A*** *– The pENTR™/U6 entry vector map. Highlighted (red box) is the U6 RNAi cassette, which contains all the elements required for expression of the shRNA from the pLenti6/BLOCK-iT™ -DEST expression.* ***B*** *– The pLenti6/BLOCK-iT™-DEST vector map. The U6 RNAi cassette from the pENTR™/U6 entry clone replaces the region between bases 1,875 and 4,111.*

*5.2.2.3 Design of shRNA sequences*

Two single-stranded complementary DNA oligonucleotides, encoding shRNA target sequences predicted to result in silencing of PTTG and PBF gene expression, were designed with the help of the Invitrogen™ BLOCK-iT RNAi design algorithm (rnadesigner.lifetechnologies.com). In addition, two complementary single-stranded DNA oligonucleotides encoding a scrambled sequence, with no known homology to human sequences, were also designed for use as a negative control (Scr shRNA). The structural features of each single-stranded DNA oligonucleotide and the predicted shRNA structure are presented in Figure 5.4.

Each single-stranded DNA oligonucleotide contained a four base-pair overhang sequence to enable directional cloning into the entry vector. This was followed by a short 21-nucleotide sequence derived from the target gene, the loop sequence, 5’-CGAA-3’, and the reverse complement of the target sequence. Single-stranded oligonucleotides were synthesised at

standard scale [Sigma-Aldrich]. Two sets of single-stranded oligonucleotides were generated to target PTTG and four sets to target PBF, all containing different shRNA target sequences (see Appendix A for more details).

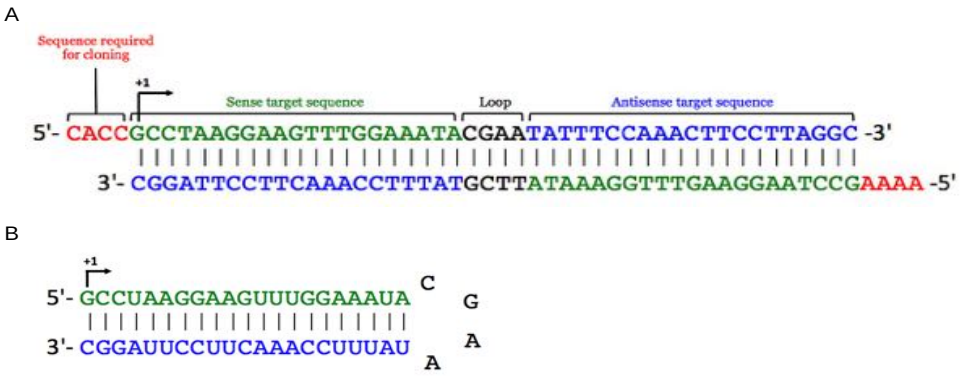


*Figure 5.4 Schematic representation of the required features of the double-stranded oligonucleotide encoding the target shRNA and it's predicted structure.* ***A*** *– Example of a double-stranded DNA oligonucleotide design.* ***B*** *– Predicted structure of the shRNA. Upon transcription, the sense target sequence (green) base pairs with the reverse complement sequence (blue) to form an intermolecular stem-loop structure.*

#### *5.2.2.4 Annealing and ligation reactions*

Annealing reactions were performed using each single-stranded DNA oligonucleotide diluted in 10X oligo annealing buffer at a concentration of 50 µM. Samples were incubated at 95 °C for 4 minutes and allowed to cool to room temperature for 10 minutes. Following a brief centrifugation step, 1 µl of the annealed mixture was removed and diluted 10,000-fold in NF-$dH_2O$. Ligation of the annealed double-stranded DNA oligonucleotide into the entry vector was performed using T4 DNA ligase and a 10:1 molar ratio of the double-stranded DNA oligonucleotide and pENTR/U6 vector. The samples were incubated at room temperature for 2 hours, briefly centrifuged and then placed on ice.

#### *5.2.2.5 Bacterial transformation*

Bacterial transformation was conducted using OneShot® TOP10 chemically competent *E. coli* according to the manufacturer's guidelines. To each 50 µl vial of TOP10 cells was added

2 µl of the ligation reaction. The mixture was incubated on ice for 30 minutes and heat shocked for 30 seconds at 42 °C before being placed back on ice for a further 2 minutes. Pre-warmed super optimal broth with Catabolite repression (S.O.C.) medium was added and the cells shaken at 225 rpm and 37 °C for 1 hour. The transformed cells were then spread onto pre-warmed LB-agar plates containing 50 µg/ml Kanamycin and incubated for 12-16 hours at 37 °C. After incubating overnight, 3 colonies were selected from each LB-agar plate and incubated at 37 °C for a further 16 hours at 225 rpm in 5 ml of LB containing antibiotics.

*5.2.2.6 DNA purification, sequencing and amplification*

DNA purification was performed using the Wizard® Plus SV Minipreps DNA Purification System [Promega], as described in section 2.2.1.2. For sequencing, 250 ng of plasmid DNA was mixed with 3.2 pmol of forward or reverse primers (Table 5.1) in a total volume of 10 µl. Due to low plasmid yields using TOP10 *E. coli*, plasmid DNA was then transformed into DH5α chemically competent *E. coli* and amplified using the GenElute™ High Performance (HP) Plasmid Maxiprep Kit [Sigma], as outlined in section 2.2.1.3. Purified plasmid DNA was sequenced again to ensure the insert sequence was still correct.

| Primer Direction | Sequence |
|---|---|
| Forward | 5'- AAGGTCGGGCAGGAAGAG -3' |
| Reverse | 5'- GCAACGAACAGGTCACTATCAG -3' |

*Table 5.1 Table of forward and reverse primers sequences for sequencing the pENTR™/U6 vector.*

*5.2.2.7 Subcloning the U6 RNAi cassette into the pLenti6/BLOCK-iT™-DEST vector*

The U6 RNAi cassette containing the U6 promoter sequence, the double-stranded DNA oligonucleotide encoding the shRNA target sequence and Pol III terminator sequence was transferred from the pENTR™/U6 entry clone to the pLenti6/BLOCK-iT™-DEST lentiviral vector by LR recombination according to the manufacturer's protocol. Briefly, 150 ng/µl of

entry clone was diluted in TE buffer pH 8.0 and incubated at 25 °C for 1 hour with 150 ng/µl of the lentiviral vector and 2 µl of Gateway® LR Clonase® II enzyme mix. Following this, 1 µl of Proteinase K (2 µg/µl) was added and the reaction mixture incubated at 37°C for a further 10 minutes. The LR recombination reaction was then transformed into OneShot Stbl3 chemically competent *E. coli*.

*5.2.2.8 Bacterial transformation of lentiviral vectors*

OneShot® Stbl3™ chemically competent *E. coli* cells were used according to the manufacturer's instructions. One vial was thawed on ice for each transformation reaction. Once thawed, 3 µl of the LR recombination reaction was added and the reaction mixture incubated on ice for 30 minutes. The cells were subsequently heat-shocked at 42 °C for 45 seconds and placed back on ice. After 2 minutes on ice, 250 µl of pre-warmed S.O.C. medium was added and the vials incubated for 1 hour at 37 °C with shaking. The transformation reaction was then spread onto pre-warmed LB agar plates containing 100 µg/ml ampicillin and incubated overnight at 37 °C without shaking. Colonies were selected from each LB-agar plate the following day and incubated at 37 °C for a further 16 hours at 225 rpm in 5 ml of LB containing antibiotics. Plasmid DNA was then purified using the GenElute™ High Performance (HP) Plasmid Maxiprep Kit [Sigma-Aldrich], as outlined in section 2.2.1.3.

*5.2.2.9 Producing lentivirus in 293FT packaging cells*

Lentiviral plasmid transfection was performed 24 hours after seeding the 293FT packaging cell line at 6 x $10^6$ cells per well in 100 mm tissue culture dishes. The ViraPower™ packaging mix was co-transfected with the lentiviral plasmid DNA to facilitate viral packaging. The ViraPower™ packaging mix was diluted in Opti-MEM® I reduced serum medium along with the lentiviral plasmid at a 3:1 ratio. In a separate vial, Lipofectamine® 2000 transfection reagent was diluted in Opti-MEM® I reduced serum medium. After a 5-minute incubation at

room temperature, the diluted DNA was combined with the Lipofectamine® 2000 and incubated for a further 20 minutes to enable DNA-lipid complex formation. The transfection mix was then added to the tissue culture plate containing complete culture medium. After 24 hours, the medium was removed and replaced with complete culture medium. The virus-containing supernatant was then harvested 72 hours post-transfection, briefly centrifuged at 3000 rpm to pellet cell debris and then concentrated using Spin-X ultrafiltration concentrators [Sigma-Aldrich]. Viral supernatants were subsequently aliquoted and stored at -80 °C.

*5.2.2.10 Transduction of cells with BLOCK-iT™ Lentiviral Particles*

HNSCC cells were seeded in 35 mm tissue culture dishes and incubated at 37 °C and 5 % $CO_2$ 24 hours prior to transduction with lentiviral particles. 92-VU-040T and 93-VU-147T cells were seeded at $2.0x10^5$ and $2.5x10^5$ cells per well, respectively. On the day of transduction, the lentiviral particles were thawed on ice. The medium was then removed from the cells and replaced with 1 ml of viral particles, along with Polybrene. The plates were covered with foil to reduce the amount of evaporation and returned to the incubator. After incubating for 24 hours, the medium was replaced with complete medium containing serum and Blasticidin to select for stably transduced cells. Transduced cells were then analysed for levels of PTTG and PBF mRNA knockdown and also re-seeded for selection of Blasticidin-resistant colonies.

### 5.2.3 SMARTvector 2.0 lentiviral particles

Transduction-ready lentiviral particles were purchased from Dharmacon [GE Healthcare, Little Chalfont, UK]. A set of three pre-designed SMARTvector 2.0 human lentiviral shRNAs targeting the PBF gene were chosen. Details of the shRNA target sequences are presented in Appendix A.

*5.2.3.1 Vectors*

The lentiviral particles contained a SMARTvector 2.0 human lentiviral shRNA vector. This vector has several features, including a TurboGFP (tGFP) reporter gene to facilitate optimisation of transduction conditions and visualisation of shRNA expression within the cell, one of three pre-designed microRNA-adapted PBF shRNA target sequences under the control of the human CMV promoter and a puromycin resistance gene to enable selection of stably-transduced cells (Figure 5.5). Lentivral particles containing a SMARTvector 2.0 human lentiviral negative control shRNA vector were also purchased as a control (herein known as scrambled shRNA (Scr shRNA)).

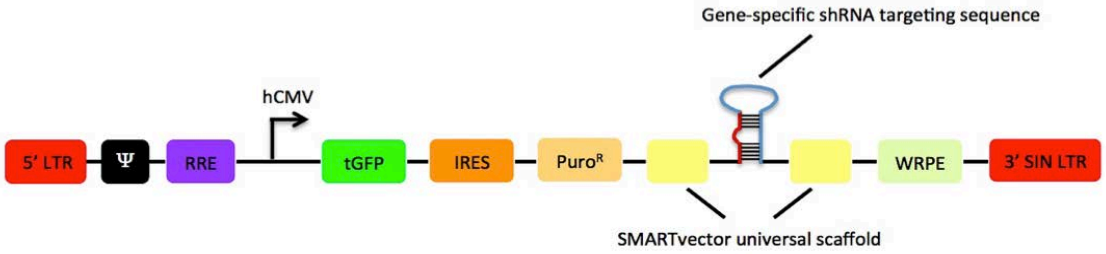


*Figure 5.5 The SMARTvector 2.0 lentiviral shRNA vector features. LTR = long terminal repeat, Ψ = Psi packaging signal, IRES = internal ribosome entry site, Puro$^R$ = Puromycin. resistance gene, WRPE = Woodchuck Hepatitis Virus posttranscriptional response element, SIN LTR = self-inactivating long terminal repeat.*

*5.2.3.2 SMARTchoice shRNA promoter selection plate*

SMARTvector 2.0 non-targeting control vector lentiviral particles expressing TurboGFP were arranged in two-fold dilutions across the SMARTchoice shRNA promoter selection plate to enable identification of the optimal promoter for both 92-VU-040T and 93-VU-147T cell lines. Cells were seeded 10.5 x $10^3$ cells per well in 96-well plate format, 24 hours before transduction. Lentiviral transduction was then performed according to the manufacturer's instructions. Cells were visually inspected for TurboGFP expression 48 and 72 hours post-

transduction. Expression was considered to be a semi-qualitative assessment of relative promoter activity.

*5.2.3.3 Transduction of cells with SMARTvector 2.0 lentiviral shRNA*

SMARTvector lentiviral PBF shRNAs, with the optimal vector configuration, were provided as lentiviral particles. To determine the volume of viral particles required per well, the total number of transducing units per ml (TU/ml), determined for each lentiviral shRNA, was divided by the desired Multiplicity of Infection (MOI) multiplied by the number of cells seeded per well. The MOI refers to the number of viral particles added per number of cells, for example, MOI = 1 means that 1 million viral particles have been added to 1 million cells:

**Volume of viral stock per well = (MOI x cells seeded) / TU/ml**

Once thawed on ice, the appropriate volumes of viral particles were diluted in complete medium containing Polybrene, but lacking serum. Following a 20-minute incubation at room temperature, medium was removed from the cells and replaced with 50 µl per well of the diluted viral particles. The plates were returned to the incubator and, 24 hours later, the viral particles removed and replaced with complete medium containing serum and 2 µg/ml Puromycin. Cells were visually inspected for TurboGFP expression 48-72 hours post-transduction and the medium replaced every 3 days to select for stably transduced cells. Transduced cells were then analysed for the levels of PBF mRNA knockdown and sorted by fluorescence activated cell sorting (FACS) to isolate single-cell transfectants.

*5.2.3.4 Fluorescence-Activated Cell Sorting (FACS)*

92-VU-040T and 93-VU-147T cells transduced with SMARTvector 2.0 lentiviral particles were trypsinised with 0.25% trypsin solution [Invitrogen], resuspended in complete medium and then centrifuged at 1500 rpm for 5 minutes. The pelleted cells were resuspended in sterile

phosphate buffered saline (PBS) and transferred to test tubes. Samples were then analysed by the FACSAria II 4-colour cytometer. Single-cell transfectants were isolated and re-plated into a 96-well plate with complete medium already aliquoted into each well. The plate was returned to the incubator and the medium containing Puromycin replaced every 3 days. Once confluent, the cells were transferred to a 24-well plate and then grown up into T75 flasks.

### 5.2.4 RNA extraction, quantification and quantitative real-time PCR

Total RNA was extracted from 92-VU-040T and 93-VU-147T cells as described in section 2.3 for downstream Taqman®-based expression assays. Reverse transcription and real-time quantitative PCR (qPCR) techniques were as described above (see sections 2.4 and 2.5) and Taqman gene expression assays for PBF (Hs01036322_m1), PTTG (Hs00851754_u1), TP53 (Hs01034249_m1), Rb (Hs01078066_m1), CDKN1A (Hs00355782_m1), CDKN2A (Hs99999189_m1), BAX (Hs00180269_m1) and BCL-2 (Hs00248075_m1) were purchased from Applied Biosystems™.

### 5.2.5 Western Blotting

Protein extraction, quantification and Western blotting techniques were performed as previously described in section 2.6. Antibodies used were anti-PBF-8 1:500, anti-PTTG 1:750, anti-Y174-phosphorylated PBF 1:1000 and anti-β actin 1:15,000.

### 5.2.6 BrdU cell proliferaton assay

The rate of cell proliferation in stably transduced 92-VU-040T and 93-VU-147T cells was assessed as outlined in section 2.9. Cells were seeded at 4 x$10^3$ cells per well in 96-well plates

and incubated for 24 hours before conducting the assay. The absorbance at 405 nm was measured using the Victor$^3$ 1420 Multilabel Counter [PerkinElmer].

### 5.2.7 Statistical analysis

Statistical analysis was performed as outlined in section 2.12. Following expert statistical advice suggesting the ΔΔCt transformation skews the standard error, qPCR data was presented as the mean fold change in mRNA expression and the mean ΔCt and SEM values provided in a table below each graph.

## 5.3 Results

In order to investigate the roles of PTTG and PBF in the context of head and neck tumourigenesis, RNAi was utilised to knockdown expression of each proto-oncogene in the HPV-negative and HPV-positive HNSCC cell lines, 92-VU-040T and 93-VU-147T, respectively. Stable knockdown clones were then generated and PTTG and PBF function assessed in downstream functional assays. To this end, multiple shRNA target sequences, designed to different nucleotide sequences within the cDNA sequence of PTTG and PBF, were screened to ensure optimal levels of target gene knockdown. A scrambled sequence with no homology to any known human sequence was designed for use as a negative control to demonstrate that the effects observed were solely due to depletion of PTTG and PBF and not a result of lentiviral-mediated delivery of the shRNA into the cell.

### 5.3.1 BLOCK-iT™ lentiviral RNAi expression system

*5.3.1.1 Evaluation of PTTG mRNA expression in stably transduced head and neck cancer cell lines*

Following transduction with lentiviral particles and antibiotic selection of stably transduced cells, PTTG mRNA expression was assessed by qPCR. Preliminary screening of PTTG mRNA expression in both cell lines, demonstrated successful PTTG mRNA knockdown upon transduction with both PTTG shRNA constructs (PTTG shRNA #1-2), when compared to the scrambled control (Scr shRNA) (Figure 5.6). The degree of PTTG gene silencing varied for each construct, with PTTG shRNA #1 providing approximately 90 % knockdown in 92-VU-040T and 93-VU-147T cells, and PTTG shRNA #2 providing approximately 77 % knockdown in 92-VU-040T cells and around 60 % in 93-VU-147T cells.

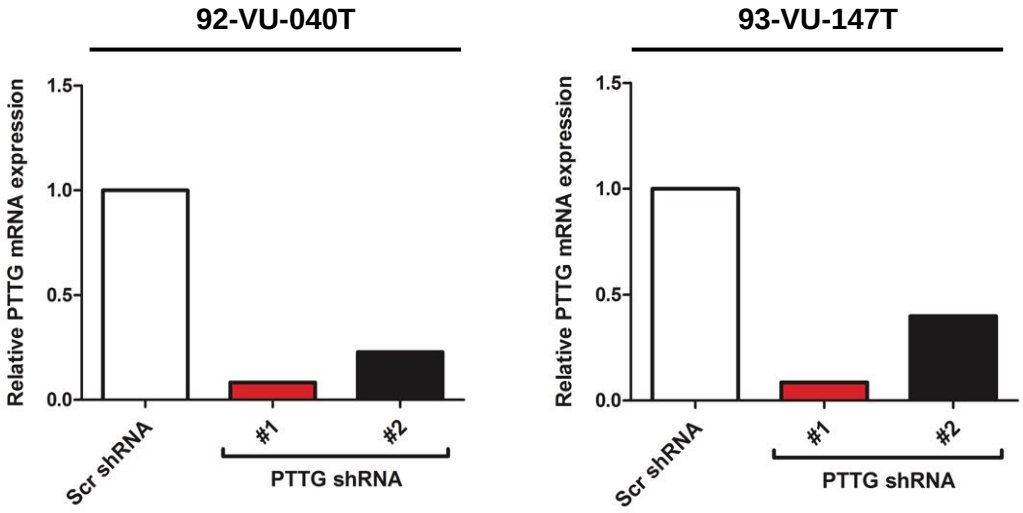


*Figure 5.6 Real-time PCR analysis of PTTG mRNA expression in head and neck cancer cells transduced with PTTG-specific shRNA. PTTG mRNA expression in 92-VU-040T and 93-VU-147T cells stably transduced with BLOCK-iT™ lentivirus expressing a scrambled control shRNA construct (Scr shRNA) or one of two PTTG shRNA constructs (PTTG shRNA #1 and PTTG shRNA #2). The PTTG shRNA constructs highlighted in red were selected for the generation of clonal cell lines. Data presented as fold change in mRNA expression (n=1).*

Based on the above results, cells transduced with PTTG shRNA #1 were expanded and four antibiotic-resistant colonies selected to provide a genetically homogeneous and clonal

cell population. The clonal cell lines underwent further gene expression analysis to identify the clonal cell population with the greatest reduction in PTTG mRNA expression. In 92-VU-040T cells, all four colonies selected demonstrated reduced PTTG mRNA expression in comparison to Scr shRNA-transduced cells (Figure 5.7). Colony 2 (C2) provided the greatest degree of knockdown and was therefore selected for further characterisation and for use in downstream functional assays. Unfortunately, for 93-VU-147T cells, the majority of colonies did not survive and thus could not be analysed for gene expression or used in subsequent experiments. The one surviving colony (C1) displayed a reasonable level of PTTG mRNA knockdown (~85 % reduction) and so was carried forward for further characterisation (Figure 5.7).

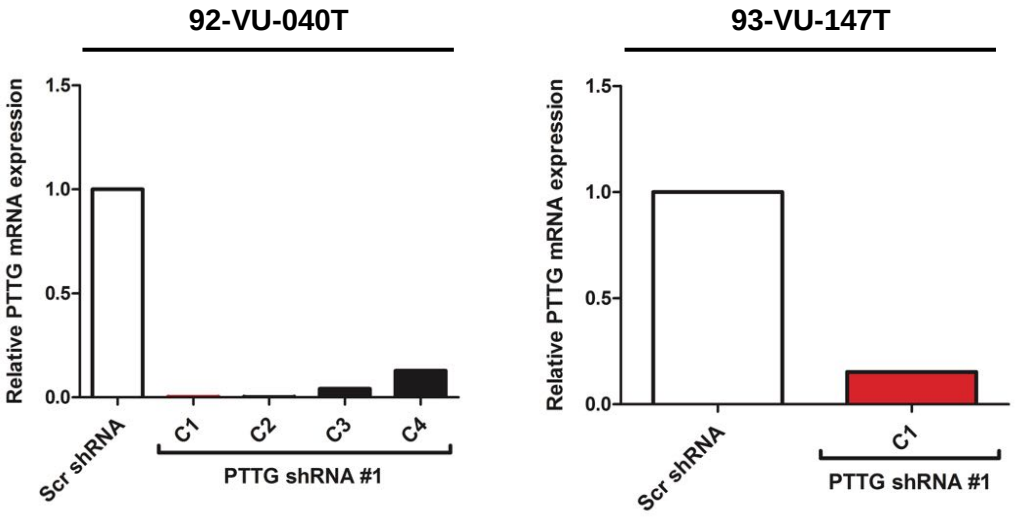


*Figure 5.7 Real-time PCR analysis of PTTG mRNA expression in clonal head and neck cancer cell lines stably transduced with PTTG shRNA #1. PTTG mRNA expression in 92-VU-040T and 93-VU-147T cells stably transduced with BLOCK-iT™ lentivirus expressing PTTG shRNA construct #1 (PTTG shRNA #1) or a scrambled shRNA construct (Scr shRNA). The PTTG shRNA-expressing clones highlighted in red were selected for further analysis and future experiments. Data presented as fold change in mRNA expression (n=1).*

*5.3.1.2 Evaluation of PBF mRNA expression in stably transduced head and neck cancer cell lines*

HNSCC cell lines were also subjected to RNAi-mediated PBF gene silencing using four different PBF shRNA constructs (PBF shRNA #1-4). PBF mRNA expression was measured by quantitative real-time PCR following transduction with the lentiviral particles and subsequent antibiotic selection. As shown in Figure 5.8, PBF mRNA expression, on average, was only reduced by around 30 % in both cell lines. Such low levels of gene knockdown were suggestive of either weak shRNA activity or low transduction efficiency and were unlikely to result in a change of phenotype. To address this issue, pre-designed, transduction-ready SMARTvector 2.0 lentiviral particles expressing three different PBF-specific shRNA sequences were purchased.

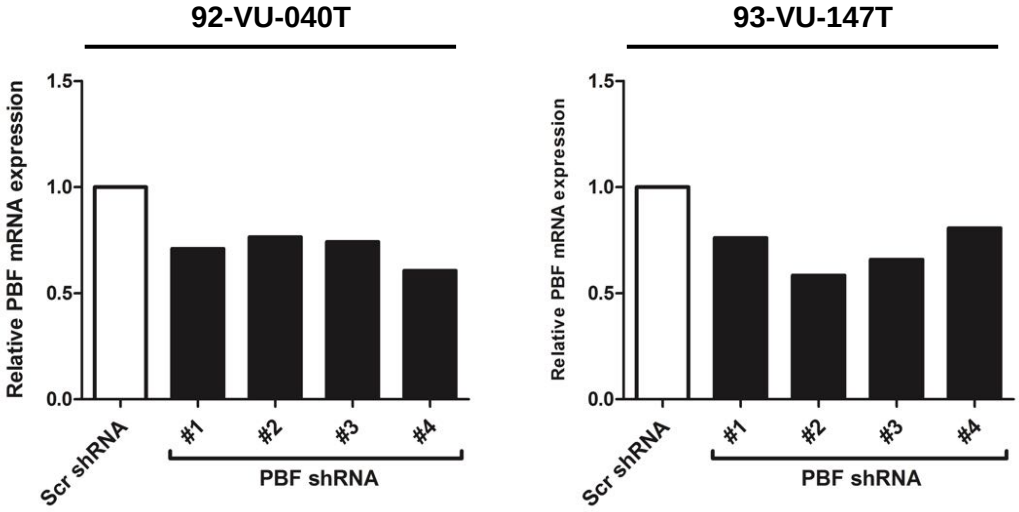


*Figure 5.8 Real-time PCR analysis of PBF mRNA expression in head and neck cancer cells. PBF mRNA expression in 92-VU-040T and 93-VU-147T cells stably transduced with BLOCK-iT™ lentivirus expressing a scrambled control shRNA construct (Scr shRNA) or one of four PBF shRNA constructs (PBF shRNA #1, PBF shRNA #2, PBF shRNA #3 and PBF shRNA #4). No constructs were selected for further analysis or future experiments, as the levels of PBF gene knockdown were low. Data presented as fold change in mRNA expression (n=1).*

### 5.3.2 SMARTvector 2.0 lentiviral particles

#### *5.3.2.1 Identifying the most active promoter*

Promoter activity varies considerably across different cell types and species. This can have a significant impact on shRNA expression and consequently the potency of gene silencing. Few studies have systematically compared promoter performance in HNSCC cell lines. We therefore opted for the SMARTchoice platform of lentiviral vectors as these could be tailored to contain the most active transcriptional promoter for any given cell type. The SMARTchoice promoter selection plate was used to evaluate the strength of the available seven constitutive promoters in our cell lines, prior to purchasing the lentiviral particles.

Viral particles co-expressing a non-targeting control shRNA and TurboGFP (tGFP) under the control of each of the seven transcriptional promoters were arrayed in two-fold dilutions, ranging from 4.0 x $10^5$ transducing units (TU) to 0.125 x $10^5$ TU, across the 96-well promoter selection plate. These arrayed viral particles were used to transduce both 92-VU-040T and 93-VU-147T cells. Promoter activity was then assessed 72 hours post-transduction by means of tGFP fluorescence intensity. As shown in Figure 5.9 and Figure 5.10, the human immediate early cytomegalovirus (hCMV) promoter was the most active promoter in 92-VU-040T and 93-VU-147T cells. The mouse-derived CMV promoter was aslo able to induce expression of tGFP in the two cell lines, albeit, to a lesser degree. In addition, low-level activity was observed with both human and mouse elongation factor-1-alpha (EF1α) promoters, but only when cells were transduced with the highest number of viral particles (4.0 x $10^5$ TU and 2.0 x $10^5$ TU). Based on this data, PBF shRNA lentiviral constructs were designed to contain the hCMV promoter.

From these preliminary transduction experiments, we were also able to estimate the number of viral particles that would be required to transduce our cell lines (MOI), again, on

the basis of tGFP expression. The MOI is defined as the number of viral particles added per cell during transduction. As the MOI increases, so does the number of integration events and therefore shRNA expression levels too. However, with high MOIs also comes the risk of greater cellular toxicity. In both our cell lines, tGFP expression was clearly evident when cells were transduced with lentiviral particles at 4.0, 2.0, 1.0 and 0.5 x $10^5$ TU (Figure 5.9 and Figure 5.10, hCMV row). As 10.5 x $10^3$ cells were seeded per well and transduced with 25 µl of lentiviral particles, the results from the selection plate suggested that transduction with a range of MOIs between 10 and 30 would provide similar transduction results for the PBF shRNA-expressing lentiviral particles.

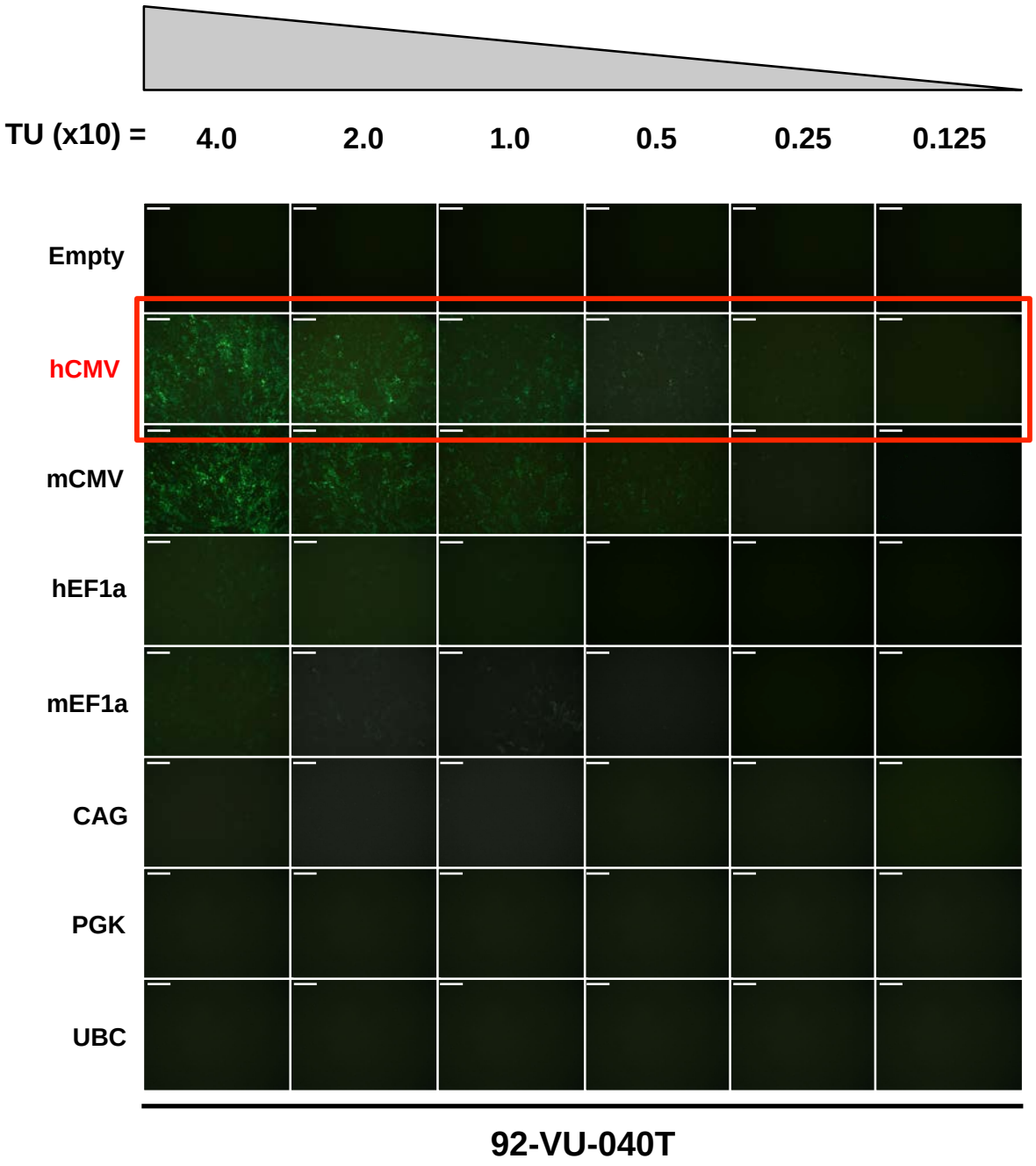


*Figure 5.9 Fluorescence microscopy images demonstrating promoter-selective tGFP expression in 92-VU-040T cells. Cells were transduced with SMARTvector 2.0 lentiviral particles expressing a non-targeting control shRNA and the TurboGFP reporter under one of seven different promoters. Scale bars = 500 µm. Empty = DMEM only, hCMV = human cytomegalovirus immediate early promoter, mCMV = mouse cytomegalovirus immediate early promoter, hEF1α = human elongation factor 1 alpha promoter, mEF1α = mouse elongation factor 1 alpha promoter, CAG = chicken beta actin hybrid promoter, PGK = mouse phosphoglycerate kinase promoter, UBC = human ubiquitin C promoter.*

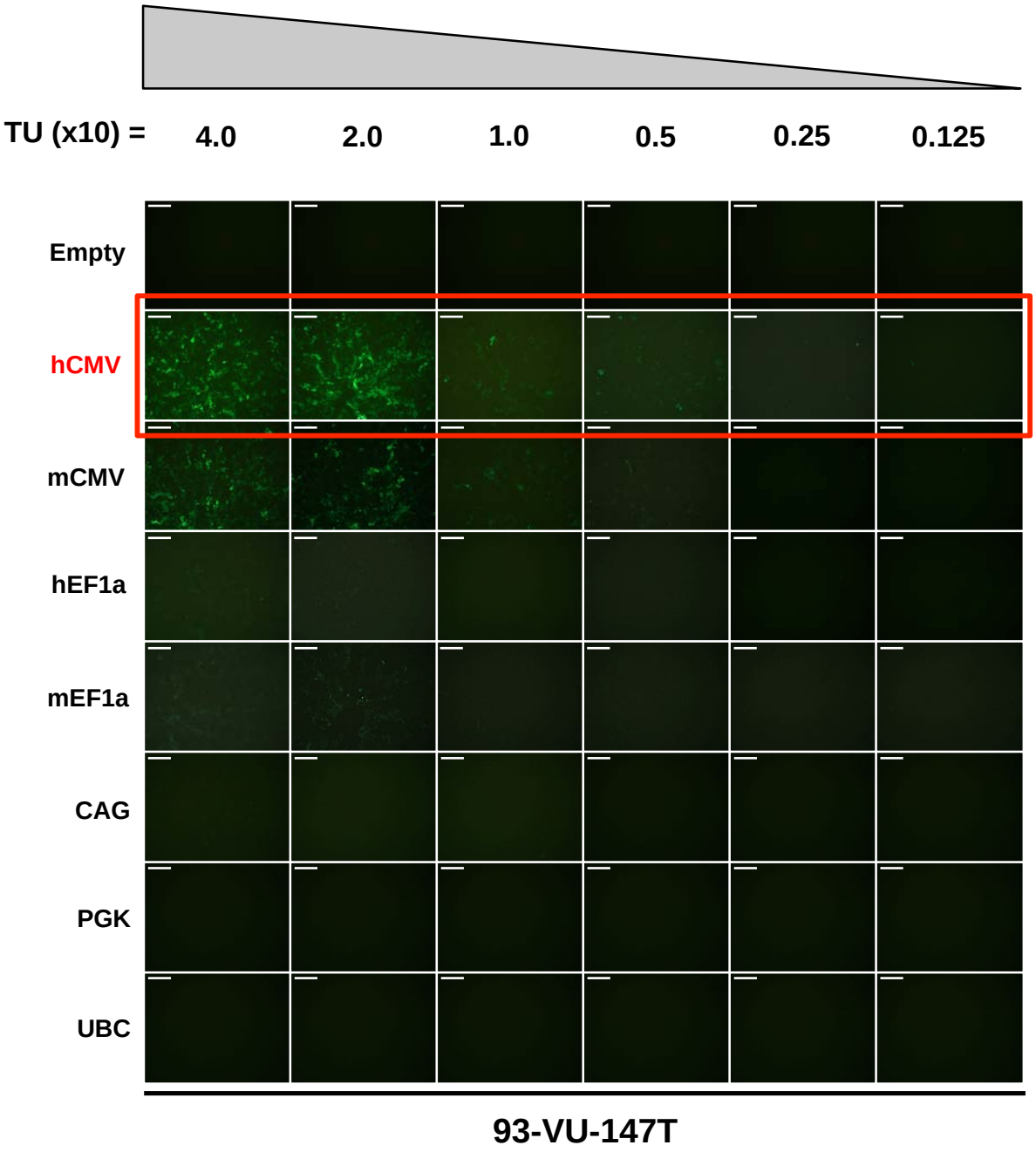


*Figure 5.10 Fluorescence microscopy images demonstrating promoter-selective tGFP expression in 93-VU-147T cells. Cells were transduced with SMARTvector 2.0 lentiviral particles expressing a non-targeting control shRNA and the TurboGFP reporter under one of seven different promoters. Scale bars = 500 µm. Empty = DMEM only, hCMV = human cytomegalovirus immediate early promoter, mCMV = mouse cytomegalovirus immediate early promoter, hEF1α = human elongation factor 1 alpha promoter, mEF1α = mouse elongation factor 1 alpha promoter, CAG = chicken beta actin hybrid promoter, PGK = mouse phosphoglycerate kinase promoter, UBC = human ubiquitin C promoter.*

*5.3.2.2 Determining the optimal MOI*

Having deduced the most suitable vector configuration, we next tested a range of MOIs, similar to those mentioned above, using lentiviral particles targeting three separate regions of the PBF gene (PBF shRNA #1-3). Cells were transduced with lentiviral particles at MOIs of 5, 10 and 20. Upon inspection 72 hours later, MOI of 20 was shown to provide the most effective transduction, as demonstrated by tGFP fluorescence intensity in 92-VU-040T and 93-VU-147T cells (Figure 5.11). This observation was consistent across all three constructs. Furthermore, visual inspection of the cells in brightfield suggested there was minimal cellular toxicity associated with transduction at all MOIs tested (data not shown).

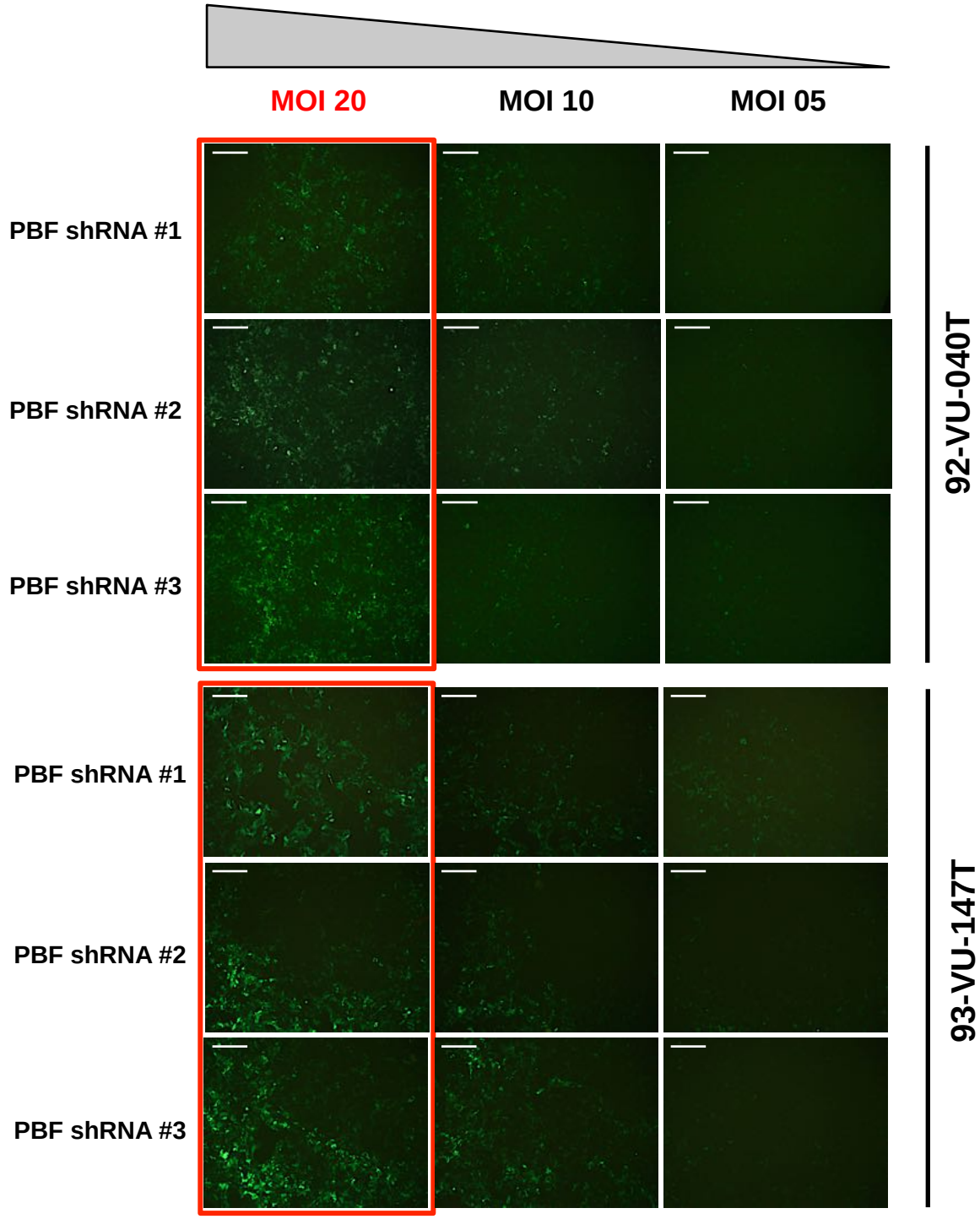


*Figure 5.11 Fluorescence microscopy images demonstrating the optimal Multiplicity of Infection (MOI) in 92-VU-040T and 93-VU-147T head and neck cancer cell lines. TurboGFP (green) fluorescence intensity was assessed 72 hours post-transduction. Scale bars = 200 µm.*

*5.3.2.3 Evaluation of PBF mRNA expression in stably transduced head and neck cancer cell lines*

92-VU-040T and 93-VU-147T cells transduced at MOI 20 were analysed for PBF mRNA expression. Transduction with each of the three PBF shRNA constructs resulted in a modest down-regulation of PBF mRNA expression, as shown in Figure 5.12. In 92-VU-040T cells, expression was knocked down, on average, by around 60 %. PBF shRNA #1 demonstrated the greatest level of knockdown, at approximately 80 %, and was therefore selected for generating a PBF shRNA-expressing clonal cell population. In 93-VU-147T cells, the extent of knockdown was not as high, demonstrating an average reduction in expression of around 40 %. However, this was slightly better than the knockdown observed with the lentiviral particles generated in-house (see Figure 5.8 above). Once again, transduction of PBF shRNA #1 resulted in the most effective knockdown in 93-VU-147T cells and was thus selected for further analysis.

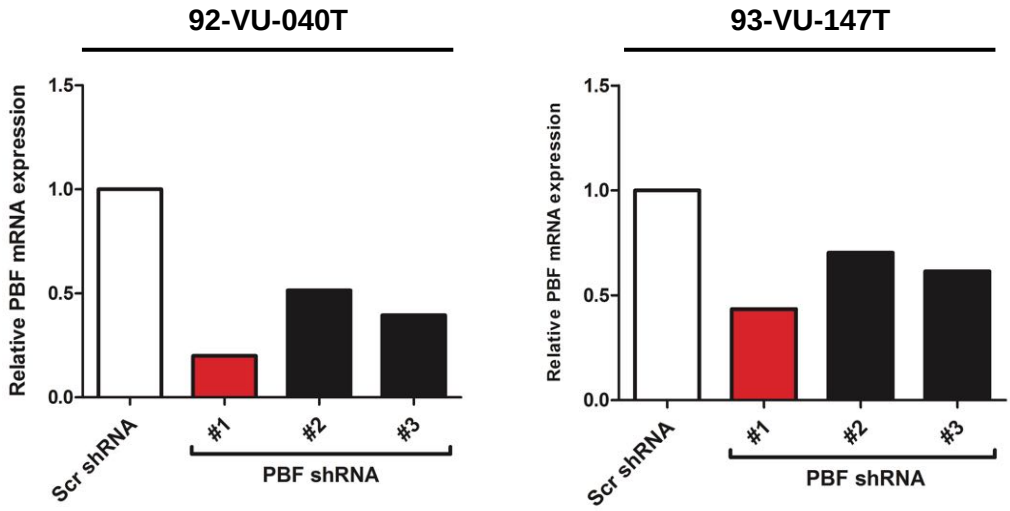


*Figure 5.12 Real-time PCR analysis of PBF mRNA expression in head and neck cancer cells transduced with SMARTvector 2.0 lentivirus. PBF mRNA expression in 92-VU-040T and 93-VU-147T cells stably transduced with SMARTvector 2.0 lentivirus expressing a scrambled control shRNA construct (Scr shRNA) or one of three PBF shRNA constructs (PBF shRNA #1-3). The PBF shRNA constructs highlighted in red were selected for the generation of clonal cell lines. Data presented as fold change in mRNA expression (n=1).*

*5.3.2.4 Generating PBF shRNA-expressing clonal cell lines*

92-VU-040T and 93-VU-147T single cell transfectants, expressing PBF shRNA construct #1, were isolated based upon tGFP fluorescence by FACS. Following trypsinisation, cells were re-suspended in sterile PBS. Non-transduced cells were initially used to gate for viable, single cell events on the basis of forward scatter (FSC) and side scatter (SSC) ('P1' gate) (Figure 5.13A). As can be seen in the univariate histogram, these cells demonstrated very little baseline autofluorescence and, as such, were also used to guide gating for tGFP fluorescence in the stable cell lines. Additional gating was implemented at this stage to select and isolate only cells displaying relatively high levels of tGFP ('P2' gate). When transduced cells were analysed under these conditions, a higher proportion of cells fell within the P2 gate, as expected, and were classed as 'tGFP-positive' (Figure 5.13B). Individual transduced, P1- and P2-gated cells were then isolated and transferred to individual wells containing complete medium. Following clonal expansion, four FACS-sorted colonies were selected per cell line and per transduction condition for analysis of PBF mRNA expression.

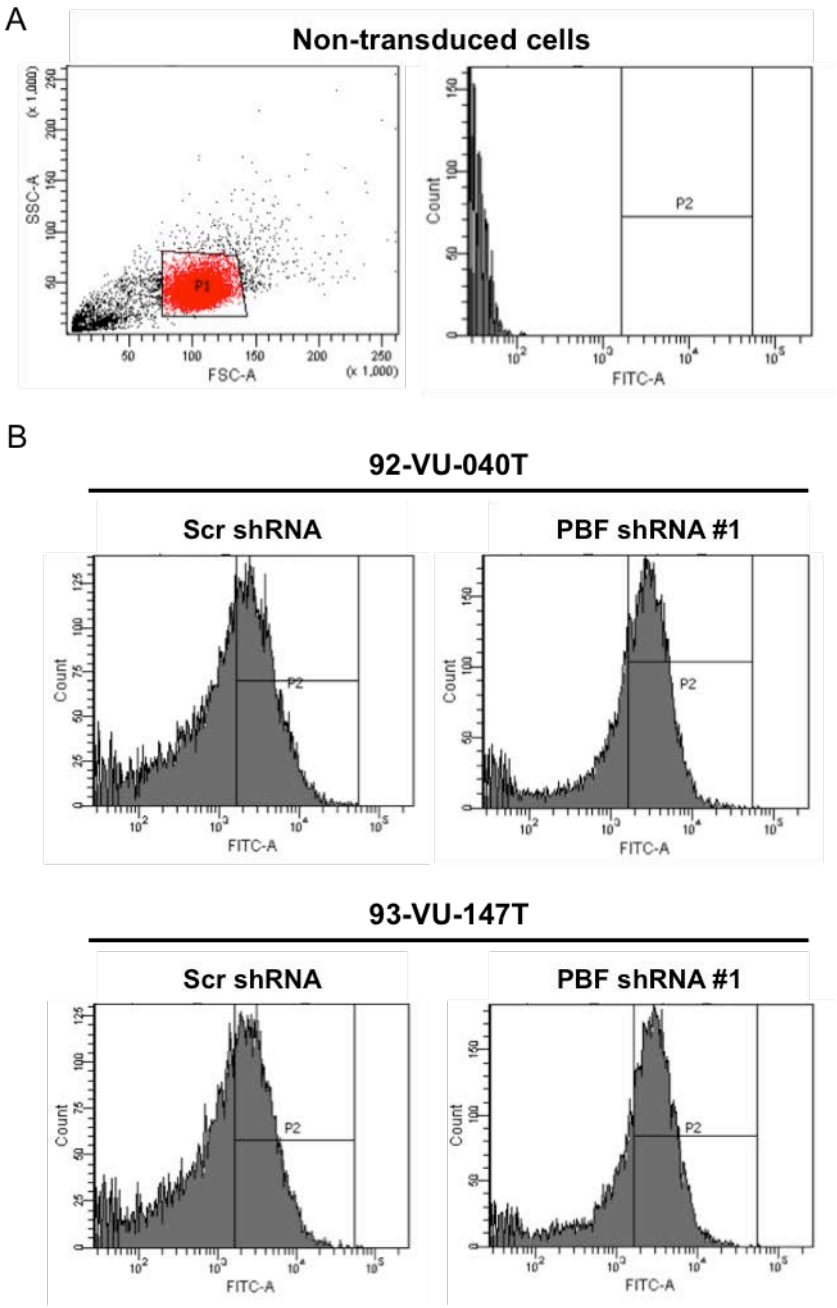


*Figure 5.13 Selection of PBF shRNA clones based on TurboGFP reporter expression. Fluorescence Activated Cell Sorting (FACS) was used to isolate and re-plate single cells stably transduced with the SMARTvector 2.0 lentivirus expressing either scrambled control shRNA (Scr shRNA) or PBF shRNA (PBF shRNA #1).* ***A*** *– Non-transduced cells were used to gate for viable, single cell events (red dots within black box labelled 'P1') based upon their forward (FSC-A) and side (SSC-A) scatter. These cells did not express TurboGFP (FITC-A), as demonstrated in the univariate histogram.* ***B*** *– Univariate histograms showing TurboGFP expression in Scr-shRNA and PBF shRNA #1- expressing head and neck cancer cell lines. Additional gating was used to select and isolate transduced cells expressing mid-high levels of TurboGFP (region outlined and labelled 'P2').*

PBF gene expression was assessed by qPCR and was successfully depleted in all three 92-VU-040T colonies and all four 93-VU-147T colonies (Figure 5.14). Furthermore, expression was reduced to a greater extent in all colonies, when compared with PBF expression in the polyclonal lines (see Figure 5.12). The most effective knockdown was observed with 92-VU-040T colony 1 (~85 % reduction) and 93-VU-147T colony 3 (C3; 87 % reduction). Both colonies were further expanded and used in downstream applications.

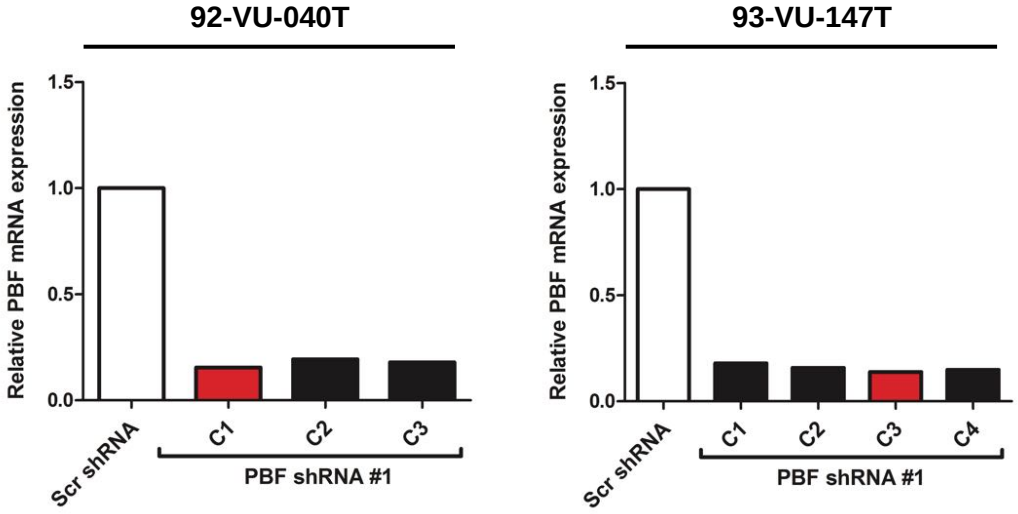


*Figure 5.14 Real-time PCR analysis of PBF mRNA expression in head and neck cancer cell clones following FACS sorting. PBF mRNA expression in clones from 92-VU-040T and 93-VU-147T cells stably transduced with SMARTvector 2.0 lentivirus expressing a scrambled control shRNA construct (Scr shRNA) or PBF shRNA construct #1 (PBF shRNA #1). The PBF shRNA-expressing clones highlighted in red were selected for further analysis and future experiments. Data presented as fold change in mRNA expression (n=1).*

### 5.3.3 Confirmation of RNAi-mediated PTTG and PBF depletion *in vitro*

Having identified resistant colonies demonstrating knockdown of PTTG and PBF at the transcriptional level, we next wished to confirm knockdown both at the mRNA and protein levels. Figure 5.15 shows a significant decrease in PTTG mRNA expression levels in both 92-VU-040T (~95 % reduction, p=0.000003, n=4) and 93-VU-147T (90 % reduction, p=0.007, n=4) cells, when comparing PTTG shRNA with scrambled control shRNA. Furthermore,

analysis of PTTG protein expression in these samples revealed a marked reduction in protein levels following transduction with PTTG shRNA.

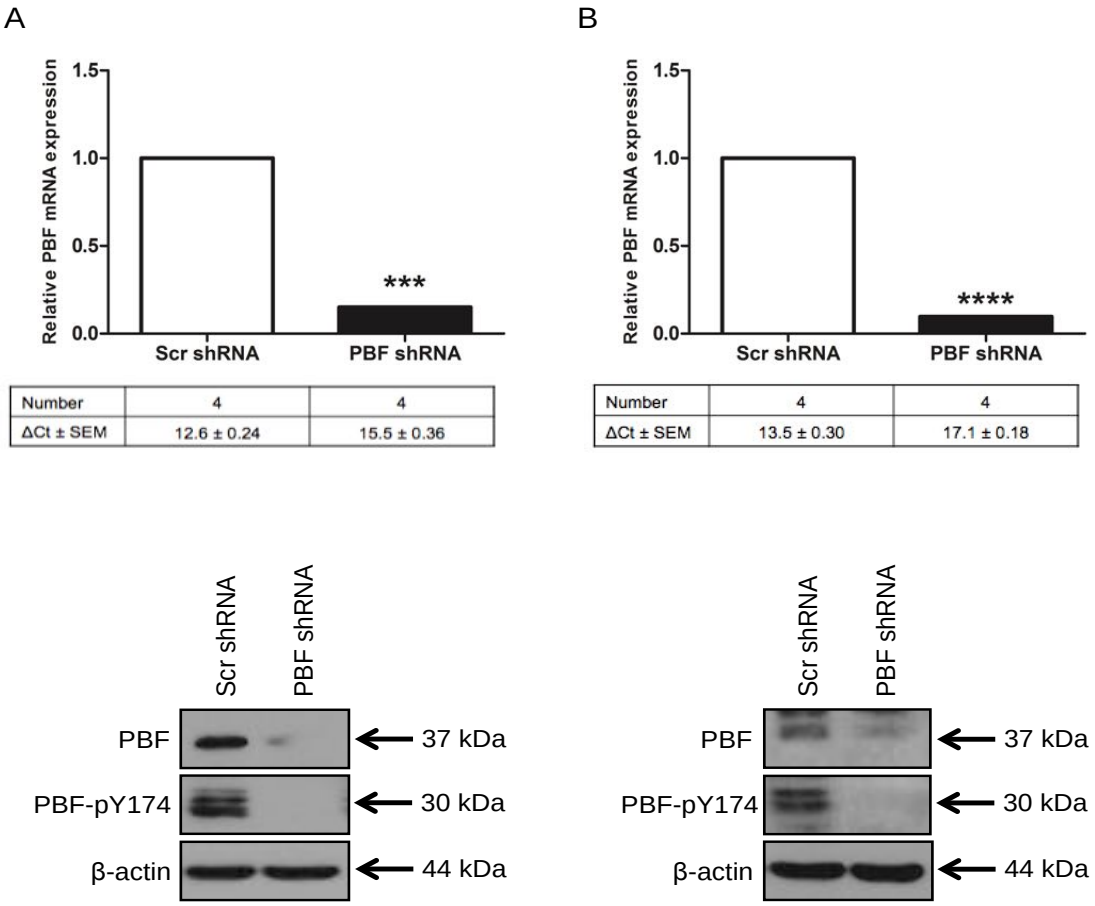


*Figure 5.15 Knockdown of PTTG expression in selected colonies.* ***A*** *– PTTG mRNA and protein expression in 92-VU-040T cells stably transduced with scrambled shRNA or PTTG shRNA assessed by real-time PCR and western blotting, respectively.* ***B*** *– PTTG mRNA and protein expression in 93-VU-147T cells stably transduced with scrambled shRNA or PTTG shRNA assessed by real-time PCR and western blotting, respectively. Data presented as mean fold change in mRNA expression (n=4). The number of samples used and the mean ΔCt values ± SEM for each group are given in the corresponding columns in the table below each graph. * p ≤0.05, ** p ≤0.01, *** p ≤0.001, **** p ≤0.0001.*

Analysis of the PBF shRNA clones also demonstrated significant depletion of PBF mRNA expression in 92-VU-040T (85 % reduction, p=0.0006, n=4) and 93-VU-147T (90 % reduction, p=0.00005, n=4) cells compared to the scrambled control shRNA (Figure 5.16). Similarly, PBF protein expression was reduced following PBF knockdown in both cell lines.

Phosphorylation of PBF at position Y174 has been shown by our group to be critical for PBF function (Smith et al. 2013, Watkins et al. 2016). Importantly, expression of Y174-phosphorylated PBF was also downregulated in cells transduced with PBF shRNA. No significant differences in cellular morphology were observed in any of the lentivirus-transduced cell lines when compared with their non-transduced counterparts (Figure 5.17).

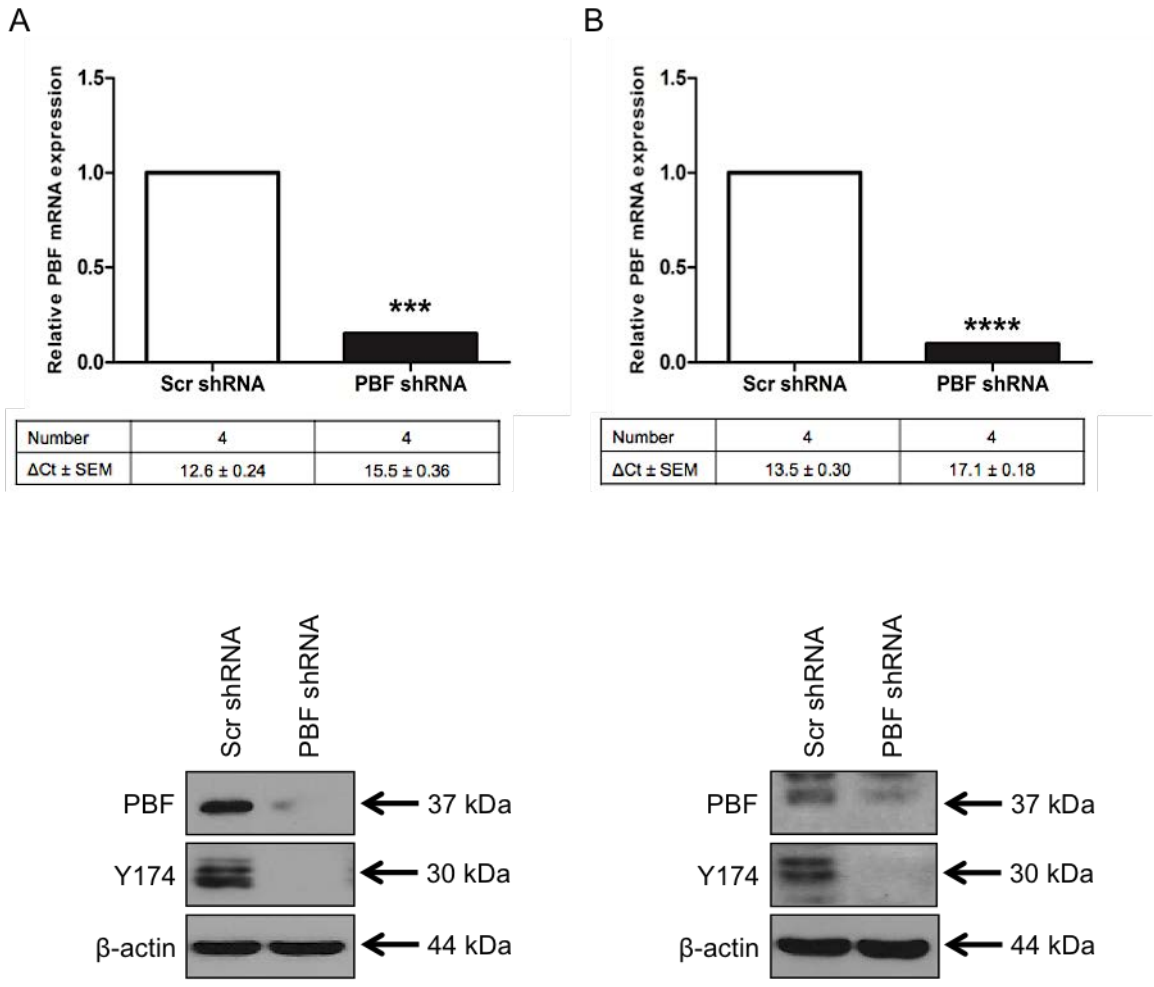


*Figure 5.16 Knockdown of PBF expression in selected colonies.* ***A*** *– PBF mRNA and protein expression in 92-VU-040T cells stably transduced with scrambled shRNA or PBF shRNA assessed by real-time PCR and western blotting, respectively.* ***B*** *– PBF mRNA and protein expression in 93-VU-147T cells stably transduced with scrambled shRNA or PBF shRNA assessed by real-time PCR and western blotting, respectively. Data presented as mean fold change in mRNA expression (n=4). The number of samples used and the mean ΔCt values ± SEM for each group are given in the corresponding columns in the table below each graph. * p ≤0.05, ** p ≤0.01, *** p ≤0.001, **** p ≤0.0001.*

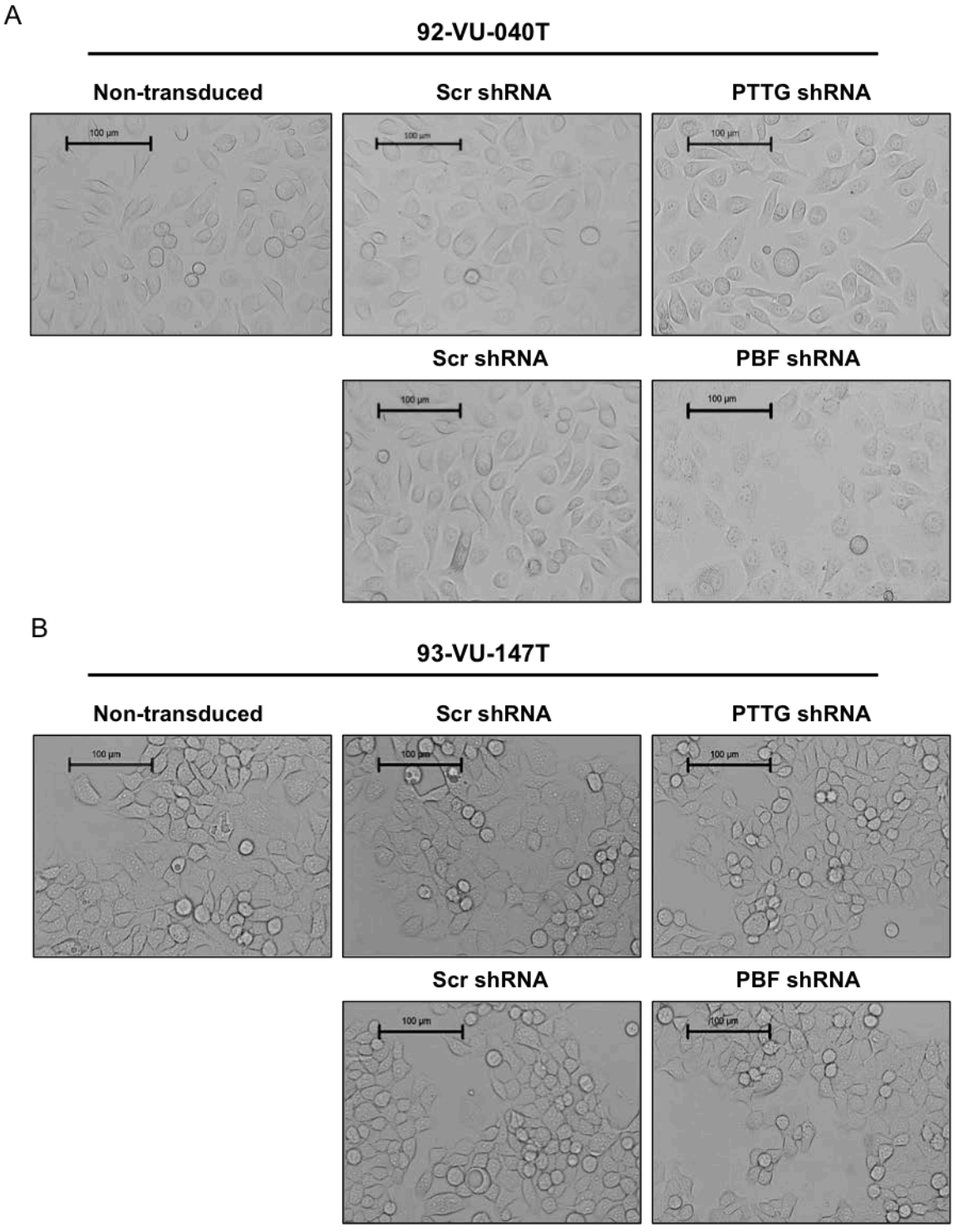


*Figure 5.17 No alteration in cell morphology following lentiviral transduction. Representative brightfield images of 92-VU-040T (**A**) and 93-VU-147T (**B**) cells showing no obvious change in cellular morphology following lentiviral transduction with the indicated shRNA constructs. Scale bars = 100 µm.*

### 5.3.4 Profiling of lentiviral stably transduced cell lines

#### *5.3.4.1 Effect of PTTG and PBF gene silencing on cell proliferation*

In light of PTTG's crucial role as a securin in regulating mitosis, and PBF's reported pro-proliferative effect in the thyroid, we examined the influence of PTTG and PBF depletion on HNSCC cell proliferation. BrdU assays were used to examine the rate of cellular proliferation. Non-transduced cells did not display any observable difference in cell proliferation when compared to Scr shRNA-transduced cells (Figure 5.18). In contrast, depletion of PTTG led to a significant increase in both 92-VU-040T and 93-VU-147T cell proliferation when compared to Scr shRNA-transduced cells (Figure 5.18 – top panel). On the other hand, knockdown of PBF led to a marginal yet significant decrease in 92-VU040T and 93-VU-147T cell proliferation compared to Scr shRNA-transduced and non-transduced cells (Figure 5.18 – bottom panel).

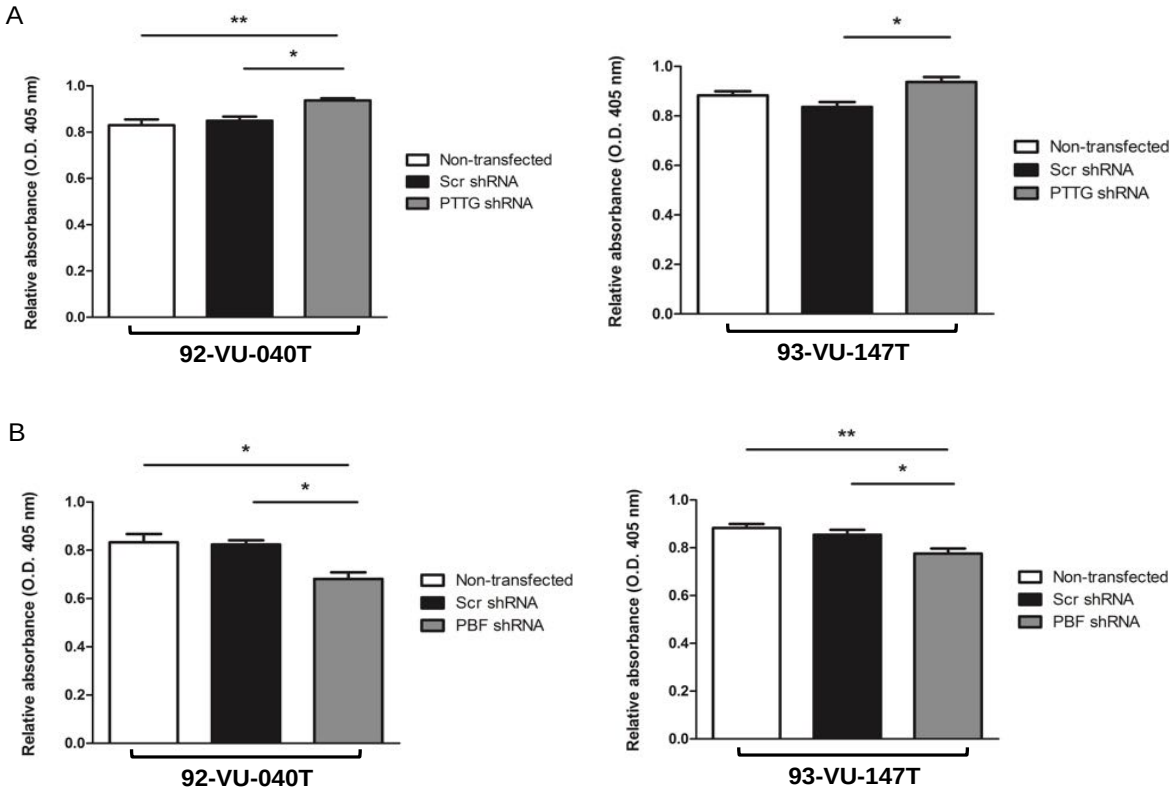


*Figure 5.18 The effect of PTTG and PBF gene silencing on cellular proliferation in 92-VU-040T and 93-VU-147T cells as assessed by BrdU assay. Non-transduced 92-VU-040T and 93-VU-147T cells were seeded alongside cells stably transduced with either scrambled shRNA and PTTG shRNA (**A**), or scrambled shRNA and PBF shRNA (**B**) (n=4 with 8 replicates). * p ≤0.05, ** p ≤0.01.*

### *5.3.4.2 The effect of PTTG and PBF gene silencing on their reciprocal expression*

We have previously demonstrated that PTTG is capable of inducing PBF mRNA expression in vitro and have reported parallel increases in PTTG and PBF mRNA expression in pituitary tumours (Stratford et al. 2005). In chapter 4, we found that PTTG and PBF mRNA expression levels were significantly and positively correlated in HNSCC tumours. We therefore examined PTTG and PBF mRNA expression levels following PBF and PTTG gene silencing in our head and neck tumour cell lines, respectively. Interestingly, in both 92-VU-040T and 93-VU-147T cells PTTG gene silencing had no effect on PBF mRNA expression (Figure 5.19A). Conversely, PBF knockdown resulted in a significant increase in PTTG

mRNA expression in 92-VU-040T cells only but had no effect on PTTG mRNA expression in 93-VU-147T cells (Figure 5.19B; p=0.015, n=4).

A

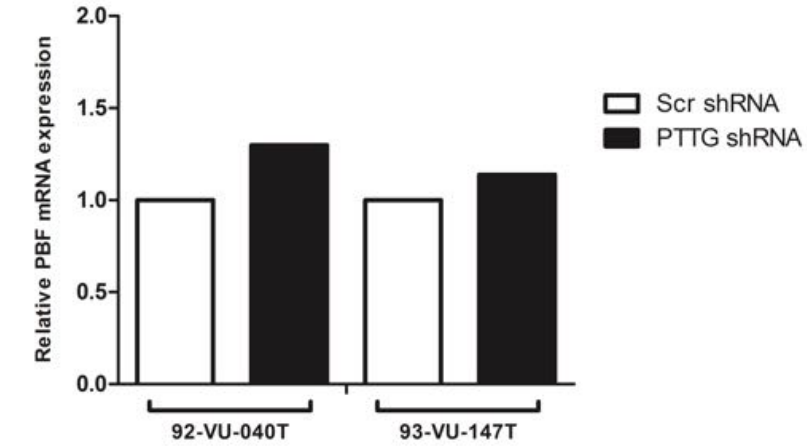


| Number | 4 | 4 | 4 | 4 |
|---|---|---|---|---|
| ΔCt ± SEM | 13.1±0.50 | 12.8±0.71 | 12.3±0.57 | 12.2±0.90 |

B

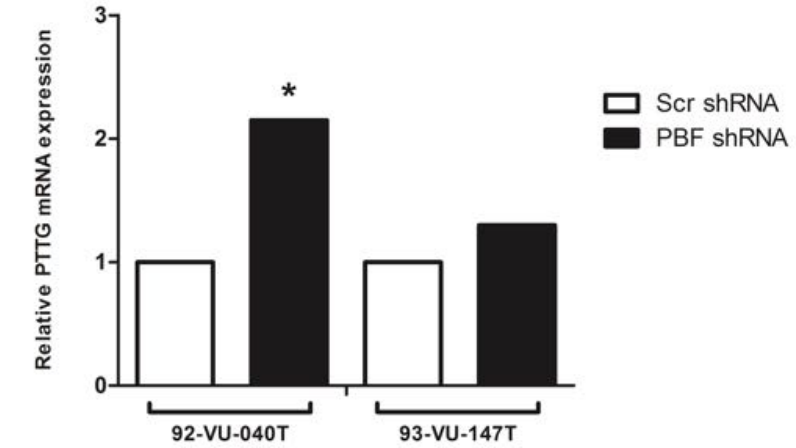


| Number | 4 | 4 | 4 | 4 |
|---|---|---|---|---|
| ΔCt ± SEM | 13.7 ± 0.59 | 12.7 ± 0.21 | 11.7 ± 0.60 | 11.5 ± 0.64 |

*Figure 5.19 PBF and PTTG mRNA expression in 92-VU-040T and 93-VU-147T cells as assessed by real-time PCR.* ***A*** *– PBF mRNA expression in 92-VU-040T and 93-VU-147T cells stably transduced with scrambled shRNA or PTTG shRNA.* ***B*** *- PTTG mRNA expression in 92-VU-040T and 93-VU-147T cells stably transduced with scrambled shRNA or PBF shRNA Data presented as mean fold change in mRNA expression (n=4). The number of samples used and the mean ΔCt values ± SEM for each group are given in the corresponding columns in the table below each graph. * p ≤0.05.*

*5.3.4.3 The effect of PTTG and PBF gene silencing on expression of cell cycle regulatory genes*

Given the observed changes in cellular proliferation following knockdown of PTTG and PBF, we next assessed mRNA expressions of TP53 and Rb cell cycle-related signalling pathways. In 92-VU-040T cells mRNA levels of TP53, CDKN1A and Rb were unaltered following PTTG or PBF knockdown and CDKN2A mRNA was undetectable (Figure 5.20A and Figure 5.21A). Similarly, in 93-VU-147T cells, TP53, CDKN1A and Rb mRNA expression levels were unaltered following PTTG or PBF knockdown (Figure 5.20B and Figure 5.21B) CDKN2A mRNA was however detected in these cells but again was unaffected by PTTG or PBF knockdown.

A

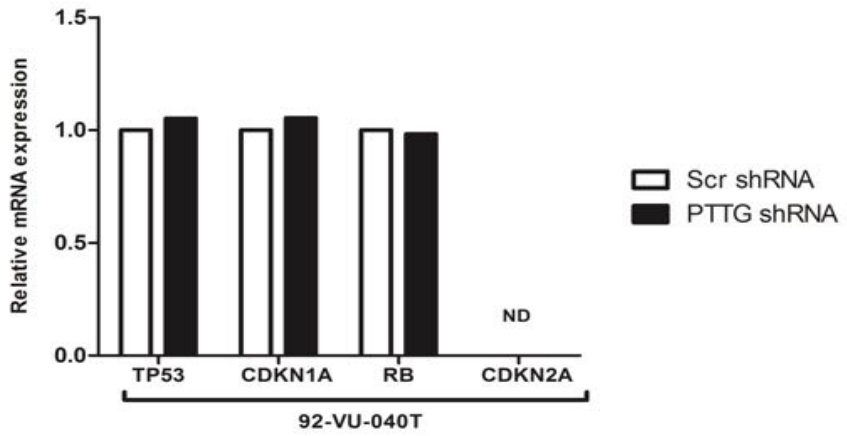


| Number | 4 | 4 | 4 | 4 | 4 | 4 | 4 | 4 |
|---|---|---|---|---|---|---|---|---|
| ΔCt ± SEM | 12.0±0.11 | 12.2±0.26 | 11.6±0.22 | 11.5±0.22 | 15.0±0.28 | 14.8±0.31 | - | - |

B

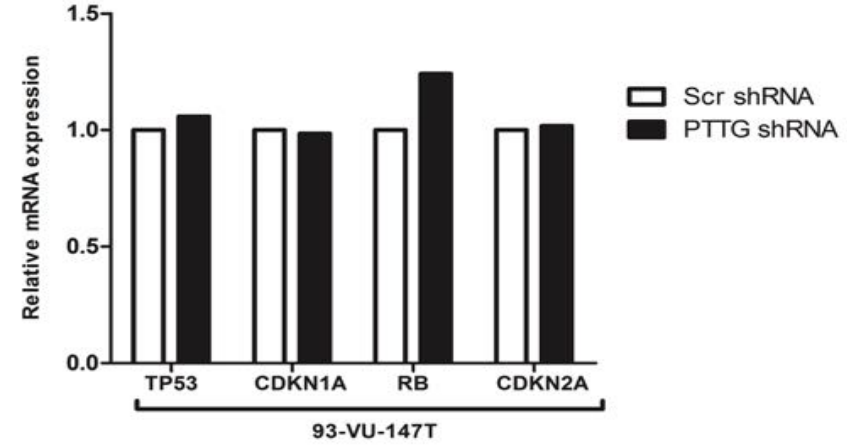


| Number | 4 | 4 | 4 | 4 | 4 | 4 | 4 | 4 |
|---|---|---|---|---|---|---|---|---|
| ΔCt ± SEM | 9.7±0.51 | 9.8±0.38 | 12.5±0.52 | 12.6±0.27 | 13.0±0.52 | 12.8±0.59 | 9.9±0.30 | 10.1±0.48 |

*Figure 5.20 The effect of PTTG gene silencing on the mRNA expression of several key cell cycle regulatory genes. TP53, CDKN1A, Rb and CDKN2A mRNA expression was assessed by quantitative real-time PCR in 92-VU-040T (**A**) and 93-VU-147T (**B**) cells following PTTG gene silencing. Data presented as mean fold change in mRNA expression (n=4). The number of samples used and the mean ΔCt values ± SEM for each group are given in the corresponding columns in the table below each graph. ND = not detected.*

A

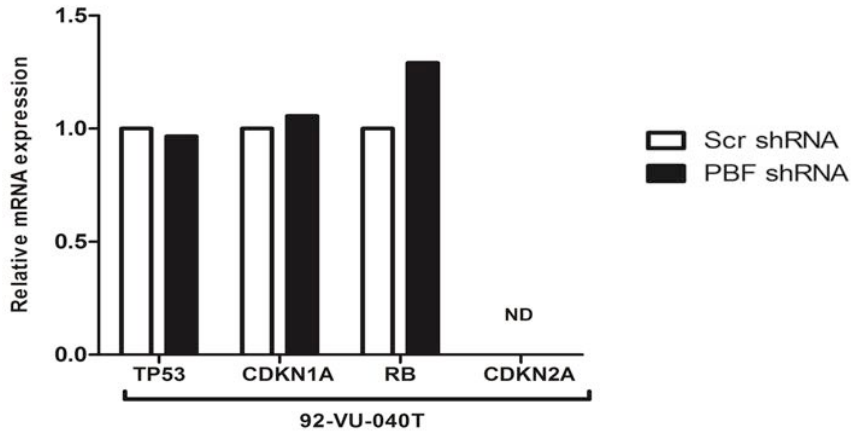


| Number | 4 | 4 | 4 | 4 | 4 | 4 | 4 | 4 |
|---|---|---|---|---|---|---|---|---|
| ΔCt ± SEM | 12.3±0.26 | 12.4±0.61 | 10.8±0.31 | 11.0±0.74 | 13.8±0.28 | 13.8±0.32 | - | - |

B

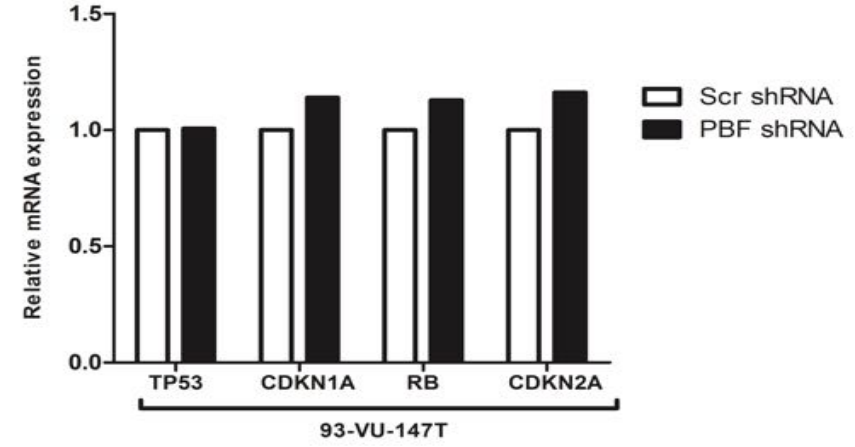


| Number | 4 | 4 | 4 | 4 | 4 | 4 | 4 | 4 |
|---|---|---|---|---|---|---|---|---|
| ΔCt ± SEM | 10.0±0.31 | 10.1±0.17 | 13.1±0.19 | 13.0±0.25 | 13.9±0.20 | 13.8±0.28 | 10.4±0.20 | 10.2±0.07 |

*Figure 5.21 The effect of PBF gene silencing on the mRNA expression of several key cell cycle regulatory genes. TP53, CDKN1A, Rb and CDKN2A mRNA expression was assessed by quantitative real-time PCR in 92-VU-040T (**A**) and 93-VU-147T (**B**) cells following PBF gene silencing. Data presented as mean fold change in mRNA expression (n=4). The number of samples used and the mean ΔCt values ± SEM for each group are given in the corresponding columns in the table below each graph. ND = not detected.*

*5.3.4.4 The effect of PTTG and PBF gene silencing on expression of markers of apoptosis*

Given the potential proliferative advantage conferred by PTTG knockdown and the opposing effect of PBF knockdown, we aimed to determine the effects of PTTG and PBF gene silencing on the gene expression of two important apoptotic factors, B-cell lymphoma 2 (BCL-2) and BCL-2-associated X protein (BAX). BAX is a pro-apoptotic gene whose protein product forms heterodimers with the anti-apoptotic BCL-2. The BCL-2:BAX ratio within the cell is therefore thought to play a crucial role in the cells response to apoptotic stimuli (Basu, Haldar 1998). When BCL-2 levels are high, BCL-2:BCL-2 homodimers create an anti-apoptotic environment within the cell. Once activated, BAX can displace BCL-2, resulting in the formation of BCL-2:BAX heterodimers. This results in inhibition of BCL-2 function and invariably leads to the induction of cell apoptosis (Basu, Haldar 1998).

BAX gene expression was not significantly affected by PTTG or PBF gene silencing in either cell line (Figure 5.22). However, PTTG gene silencing in 92-VU-040T (Figure 5.22A; 2.7-fold, $p=0.033$, $n=4$) and 93-VU-147T (Figure 5.22B; 3.4-fold, $p=0.05$) cells led to a significant induction in BCL-2 expression. In contrast, PBF gene silencing in 92-VU-040T (Figure 5.22A; 0.5-fold, $p=0.038$, $n=4$) and 93-VU-147T (Figure 5.22B; 0.5-fold, $p=0.009$, $n=4$) cells resulted in a significant reduction in BCL-2 gene expression.

A

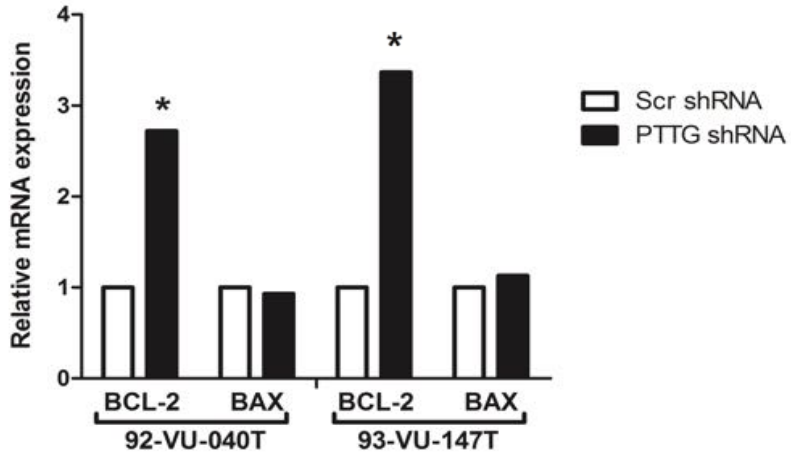


| Number | 4 | 4 | 4 | 4 | 4 | 4 | 4 | 4 |
|---|---|---|---|---|---|---|---|---|
| ΔCt ± SEM | 16.7±0.36 | 15.3±0.36 | 11.3±0.22 | 11.4±0.27 | 15.6±0.43 | 13.9±0.53 | 10.4±0.36 | 10.3±0.40 |

B

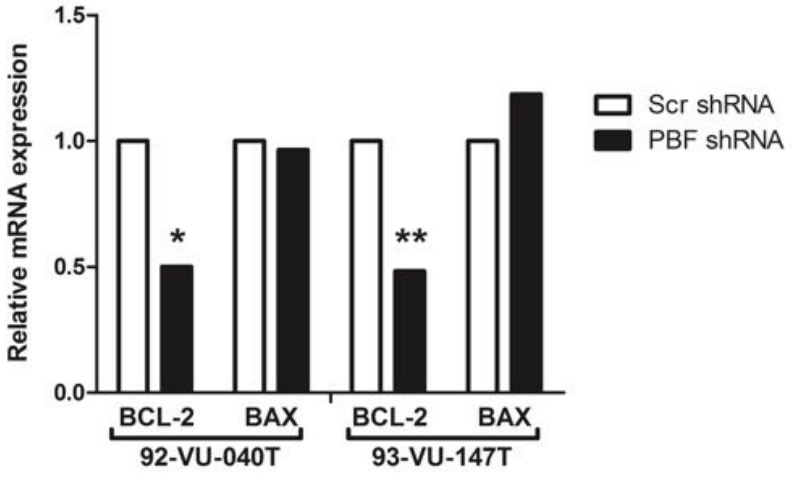


| Number | 4 | 4 | 4 | 4 | 4 | 4 | 4 | 4 |
|---|---|---|---|---|---|---|---|---|
| ΔCt ± SEM | 14.8±0.15 | 16.2±0.51 | 12.2±0.16 | 12.3±0.32 | 16.1±0.19 | 17.3±0.23 | 11.5±0.06 | 11.3±0.09 |

*Figure 5.22 The effect of PTTG and PBF gene silencing on mRNA expression of the apoptotic factors BCL-2 and BAX in 92-VU-040T and 93-VU-147T cells.* ***A*** *– BCL-2 and BAX mRNA expression in 92-VU-040T and 93-VU-147T cells stably transduced with PTTG shRNA.* ***B*** *– BCL-2 and BAX mRNA expression in 92-VU-040T and 93-VU-147T cells stably transduced with PBF shRNA. Data presented as mean fold change in mRNA expression (n=4). The number of samples used and the mean ΔCt values ± SEM for each group are given in the corresponding columns in the table below each graph. * $p \leq 0.05$.*

## 5.4 Discussion

### 5.4.1 Generation of lentiviral stably transduced cell lines

Overexpression of the proto-oncogenes PTTG and PBF has been reported in numerous cancers and both are believed to play a crucial role in tumour progression (Boelaert et al. 2003a, Stratford et al. 2005). Recent studies have also implicated PTTG expression in the tumourigenesis of head and neck cancer, where overexpression has been shown to promote migration, invasion and epithelial-to-mesenchymal transition (EMT), primarily through induction of ECM-degrading matrix metalloproteinases (MMP) (Ito et al. 2008). In previous chapters we confirmed overexpression of PTTG in a series of paired HNSCC tumour and normal tissue specimens. Furthermore, we identified PBF expression to also be elevated in these tumour specimens. However, despite a wealth of data implicating PTTG and now PBF in head and neck cancers, the precise roles of both genes in head and neck tumour progression have not been delineated.

The majority of HNSCC cell lines are extremely difficult to transfect using conventional methods. Lentivirus-based RNAi expression systems have become a powerful tool for the delivery of gene-specific shRNAs into primary, non-dividing or hard-to-transfect cell lines. These vectors, unlike adenoviral and adeno-associated viral (AAV) vectors, provide long-term, stable gene knockdown through efficient integration into the host genome (Naldini 1998). In addition, lentiviral vectors appear to have a different integration pattern than retroviruses, showing a preference for integration at sites far from transcriptional start sites, thus rendering them less genotoxic (Montini et al. 2006, Dropulić 2011). To date, the application of lentivirus to the transduction of HNSCC cells has been relatively successful (Lo et al. 2011, Que et al. 2015, Khan et al. 2016), providing a robust platform for modulating gene expression and function in hard-to-transfect cell lines. In order to further our

understanding of the roles PTTG and PBF play in head and neck tumourigenesis we therefore developed lentivirus-based vectors to effectively knockdown PTTG and PBF gene expression and activity in HPV-negative 92-VU-040T and HPV-positive 93-VU-147T HNSCC cell lines.

We initially utilised the Invitrogen™ lentiviral BLOCK-iT RNAi expression system to facilitate lentivirus-based shRNA delivery into our HNSCC cells. Proper target sequence selection is imperative for successful target gene knockdown. We therefore used an online algorithm to design multiple shRNA sequences against different sites within the PTTG and PBF genes in order to increase the possibility of at least one target sequence providing sufficient target gene knockdown. Quantitative real-time PCR analysis of PTTG and PBF gene expression in both HNSCC cell lines following transduction with our lentiviral particles revealed some variation in the extent of gene knockdown observed with the various target sequences. This was to be expected and could be due to any number of reasons, although it is important to note that these preliminary screenings were only performed once due to constraints of time and, as such, may not provide a reliable estimation of the degree of gene knockdown achieved with each individual shRNA construct. Several factors are known to have a significant impact on the efficacy of these molecules. For example, a high GC content is a strong negative determinant of shRNA activity (Reynolds et al. 2004, Li et al. 2007). As a result, we selected target sequences with a low GC content of 30-55 %. However, there are reports of functionally active siRNAs containing a higher overall GC content (Bertrand et al. 2002). The location of the target sequence within the gene is equally important. Current guidelines suggest avoiding known RNA-binding sites. These sites are typically located within the 3’ UTR and 5’ UTR regions and may impair access for the processed siRNA molecules and/or RISC complex to the target sequence, thus reducing siRNA activity. As some of our target sequences for PTTG and PBF were targeted against the 3’ UTR and 5’

UTR, this may also explain some of the observed differences in shRNA efficacy. Even with these strict parameters, shRNA molecules may face difficulties in accessing the target sequence due to secondary structure formation. Furthermore, cell types will express the shRNAs to differing extents and will also differ in their ability to process them into smaller functional siRNAs. All of these factors will invariably have an impact on the extent of target gene knockdown.

Although PTTG gene expression was reduced sufficiently for use in downstream applications, knockdown of PBF gene expression by all shRNA target sequences and using the current RNAi expression system was poor. Super-infection of cells with more than one of the shRNA target sequences might have been a suitable solution. However, it would have also increased the number of integration events due to transduction of multiple viral vectors, thus increasing the likelihood of potential adverse and off-target effects. An alternative approach could have been to construct a single lentiviral expression vector containing multiple shRNA sequences targeting different sites within the target mRNA. This may have maximised the efficiency of gene silencing without the additional integration events and toxicity associated with super-infection. Indeed, several reports have successfully demonstrated that RNAi pooling has a synergistic effect in repressing target gene expression (Song et al. 2008, Mcintyre et al. 2011, Wang et al. 2013).

A novel genomic editing tool to have emerged in recent years is the clustered regularly interspaced palindromic repeat/Cas9 (CRISPR-Cas9) system, which provides bacteria with an intracellular defence mechanism against exogenous DNA (Makarova et al. 2006). In bacteria, a small fragment of the invading DNA is inserted into the CRISPR region of its own genome. These inserts are then transcribed and processed to generate target-specific RNA transcripts termed CRISPR RNA (crRNA). The crRNAs then hybridise with endogenous target-

independent transactivating RNA transcripts (tracrRNA) and together form a complex with the CRISPR-associated protein Cas9. Cas9, a DNA endonuclease, is then guided by the crRNA to the exogenous DNA target sequence, thereby allowing Cas9 to introduce a double strand break (Deltcheva et al. 2011, Jinek et al. 2012).

Researchers have exploited CRISPR-Cas9 technology to effectively edit the genomes of a wide range of cell types and organisms (Jinek et al. 2013, Mali et al. 2013). Using this approach, it would have been possible to introduce site-specific mutations to either induce or repress PTTG and PBF gene expression, simultaneously, in our HNSCC cell lines. Unfortunately, due to constraints of time, it was not possible to establish the CRISPR-Cas9 technique or to re-configure the existing lentiviral expression vectors to enable insertion of more than one shRNA target sequence. We decided instead to purchase SMARTchoice pre-designed, transduction-ready lentiviral particles expressing three validated PBF target sequences. As the SMARTchoice lentiviral vectors could be tailored to contain one of seven constitutively active gene promoters, we assessed the level of activity for each available promoter in our HNSCC cell lines.

Although there is no known tissue-specific promoter, certain promoters are thought to be highly active in HNSCC cells. Separate studies have identified promoters derived from the mouse mammary tumor virus (MMTV) (Gibson et al. 2000) and papilloma viruses (Chen et al. 1997) as strong promoters in oral cancer cells. However, few publications have systematically examined promoter performance in HNSCC cell lines. Shillitoe et al. compared reporter gene expression from a set of eight gene promoters, including the human cytomegalovirus (hCMV), Simian virus 40 (SV40), mouse mammary tumor virus (MMTV), HPV-16 and HPV-18 viruses in a panel of oral cancer cell lines (Shillitoe, Noonan 2000). Reporter gene expression was revealed to be greatest in cells transfected with the plasmid

containing the hCMV promoter (Shillitoe, Noonan 2000). When we evaluated tGFP reporter gene expression from the available gene promoters in our HNSCC cell lines, we found that there was significant variability in promoter activity; however, both cell lines displayed a similar preference for the hCMV promoter. Based on these data, and the previous findings by Shillitoe et al., we designed our PBF shRNA lentiviral constructs to contain the hCMV promoter and using these tailored lentiviral particles we achieved sufficient knockdown of PBF gene expression in our cell lines.

### 5.4.2 Profiling of lentiviral stably transduced cell lines

#### *5.4.2.1 Cell proliferation*

Having established clonal cell lines stably expressing PTTG and PBF shRNAs, we next sought to determine the impact of PTTG and PBF gene knockdown on HNSCC cell proliferation. Although PTTG expression has been implicated in the control of cellular proliferation, its exact role remains somewhat contradictory. Pei et al. initially discovered that overexpression of rat PTTG significantly repressed mouse fibroblast NIH3T3 cell proliferation (Pei, Melmed 1997). Furthermore, placental JEG-3 cells were shown to undergo cell cycle arrest and subsequent apoptosis as a result of overexpressed PTTG (Yu et al. 2000b). On the other hand, the pro-proliferative oncogene, c-myc, was identified as a downstream target of PTTG (Pei 2001). In cervical HeLa cells, overexpression of PTTG not only resulted in elevated expression of c-myc, but also induced rapid cell proliferation (Pei 2001). In addition, recent studies have shown that suppression of PTTG expression by siRNA inhibits proliferation of cutaneous squamous cell carcinoma, endometrial and ovarian cancer cell lines (Xia et al. 2013, Wang et al. 2015, Zhang et al. 2016). These discrepancies have been proposed to reflect variation between different cell types, differing levels of PTTG

overexpression and changes in its phosphorylation status (Boelaert et al. 2003b, Boelaert et al. 2004).

In our hands, transduction with the lentiviral particles alone did not appear to affect 92-VU-040T or 93-VU-147T cell proliferation, as demonstrated by comparison of cellular proliferation in the parental, non-transduced cell lines to those transduced with the Scr shRNA construct. However, silencing of PTTG expression resulted in a significant increase in the rate of 92-VU-040T and 93-VU-147T cell proliferation. PTTG's role in preventing premature sister chromatid separation by separase is well documented and both up-regulation and down-regulation of PTTG expression result in altered cell division and genetic instability (Yu et al. 2000a, Wang et al. 2001). PTTG depletion may therefore give way to increased separase activity, resulting in abnormal exchange of sister chromatids and chromosomal instability. This could in turn result in altered expression of genes involved in regulating cell proliferation and growth, such as c-myc and PTEN. Whilst these genetic alterations would not have occurred during the 48-hour duration of the assay, they could have accumulated in the months prior to performing the assay, when the cells were under selection.

Involvement of PBF in cellular proliferation has been less extensively investigated. We found that depletion of PBF gene expression led to a marked reduction in the rate of cell proliferation in both HNSCC cell lines. This is in accordance with previous findings, which have demonstrated PBF overexpression induces thyroid and breast cancer cell turnover (Watkins et al. 2010, Read et al. 2011). Altered PBF expression has also been implicated in liver cancer cell proliferation (Li et al. 2013). In a panel of three hepatocellular carcinoma cell lines, upregulation of PBF led to rapid cell proliferation, whereas, PBF knockdown was found to strongly inhibit proliferation (Li et al. 2013). Although the mechanisms by which PBF regulate cell turnover have not been fully defined, PBF-mediated thyroid cell proliferation is

thought to be associated with enhanced Akt signalling (Read et al. 2011). Although HNSCC is a genetically diverse malignancy, the PI3K-Akt pathway represents a key mitogenic signalling pathway, which is consistently dysregulated (Vander Broek et al. 2015). It has been proposed that up to one third of all HNSCC tumours harbour PI3K-Akt pathway mutations (Lui et al. 2013). It is therefore possible that PBF may be acting via Akt signalling in our HNSCC cell lines too. Furthermore, as depletion of PTTG caused an increase in HNSCC cell proliferation, the observed decrease in cell turnover upon knockdown of PBF gene expression is unlikely an indirect result of reduced nuclear shuttling of PTTG.

*5.4.2.2 Gene expression profiling*

Previous research conducted by our group has shown that PTTG is able to induce the expression of PBF mRNA in the thyroid (Stratford et al. 2005). This prompted us to investigate whether PTTG and PBF gene knockdown would have an effect on the mRNA expression of each other in our HNSCC cells. Interestingly, knockdown of PTTG mRNA expression had no significant effect on PBF mRNA expression in both cell lines. These disparate findings may be attributable to the different cell types employed. In addition, the effects of PTTG function on PBF mRNA expression may be dependent on the degree of PTTG expression within the cell. Further experiments in our HNSCC cell lines with varying levels of PTTG knockdown and overexpression will help to clarify this. On the other hand, knockdown of PBF led to a significant increase in PTTG mRNA levels in 92-VU-040T cells but not in 93-VU-147T cells. This was an unexpected finding considering Stratford et al. demonstrated no change in PTTG mRNA expression following stable overexpression of PBF in NIH3T3 cells (Stratford et al. 2005). However, as mentioned previously, this may be a result of the different cell types used.

Next we sought to determine expression of the cell cycle regulatory genes, TP53 and Rb, as well as their downstream targets, CDKN1A and CDKN2A. There were no obvious changes in expression of any of these genes in both HNSCC cell lines. This was perhaps to be expected, as it is usually the protein products of the TP53 and Rb genes that are targeted by posttranslational modification. However, due to constraints of time, I was unable to assess protein expression.

Given that cell proliferation was significantly altered following PTTG and PBF depletion, we also examined expression of the important apoptotic regulators BAX and BCL-2. Previous work performed by our group has demonstrated no observable difference in BAX mRNA/protein expression following overexpression of PBF in thyroid TPC-1 and colorectal HCT116 cells (Read et al. 2014, Read et al. 2016b). Accordingly, we observed no change in BAX mRNA expression in either of our cell lines following knockdown of PBF. One study has shown that BAX mRNA expression is induced by PTTG (Hamid, Kakar 2004). In contrast, we found that BAX mRNA expression remained unaltered after silencing of PTTG gene expression in both HNSCC cell lines. We have also shown previously that PBF expression has no impact on BCL-2 mRNA/protein expression in TPC-1 and HCT116 cells, whereas PTTG is reported to induce BCL-2 expression in the pituitary glands of *pttg*$^{-/-}$ mice (Chesnokova et al. 2007). In contrast, we observed a significant decrease in BCL-2 mRNA expression in PBF knockdown HNSCC cells. However, PTTG knockdown led to a significant increase in BCL-2 mRNA expression in both HNSCC cell lines. These significant differences in BCL-2 expression suggest the changes in cell turnover described above may be associated with altered apoptosis. However, further caspase 3/7 apoptosis assays would need to be performed to determine if this is the case. Although beyond the scope of this body of work, it will also be important to characterise the expression profiles of other oncogenes, as it is

entirely plausible that the shRNAs could be inducing PTTG/PBF gene silencing via off-target effects.

### 5.4.3 Concluding Statements

The data presented in this chapter demonstrate that gene-specific shRNAs delivered by lentiviral vector are capable of rapidly and efficiently silencing PTTG and PBF gene expression in hard-to-transfect HNSCC cell lines. The data also indicate that gene knockdown is maintained over an extended period of time, without any adverse or toxic effects on the cells. Further characterisation of our stable PTTG and PBF knockdown cell lines revealed significant alterations in cellular proliferation, which may be associated with changes in expression of the apoptotic factor BCL-2.

# Chapter 6

# Investigating the interaction between PTTG, PBF and p53 in head and neck cancer cells

## 6.1 Introduction

HNSCC poses a significant health burden, with the global number of new cases estimated to be in excess of 687,000 per annum and steadily rising (Torre et al. 2015, Ferlay et al. 2015). Although recent progress has been made with regards to improving the quality of life of patients with this disease, the high mortality rate has remained essentially unchanged (Leemans et al. 2011). A better understanding of the molecular mechanisms and key effectors involved in HNSCC tumour initiation and progression is therefore needed to enable development of more effective treatments to improve long-term patient survival.

Inactivation of the tumour suppressor p53 remains a crucial event in the initiation and progression of almost all human cancer types. The p53 protein is known to be involved in a diverse array of cellular processes and loss of function has been associated with genomic instability, desensitisation to apoptotic signals and enhanced cell migration and invasion (Zhou et al. 2016). A large body of next-generation genomic sequencing studies have demonstrated that mutations in the TP53 gene represents one of the most common genetic alterations in head and neck cancer, occurring in 50-80 % of all cases (Agrawal et al. 2011, Stransky et al. 2011). Typically, mutations in the gene occur early on and the frequency increases with progression of HNSCC (Boyle et al. 1993). Disruption of p53 function in the remaining HNSCC tumours harbouring wild-type p53 may be achieved by other mechanisms, such as HPV infection. In such cases, the p53 protein is targeted by the HPV oncogene, E6, which functionally inactivates p53 by triggering its ubiquitination and subsequent proteasomal degradation (Scheffner et al. 1990, Scheffner et al. 1993). Whilst the mechanisms responsible for viral oncogene-mediated disruption of p53 function are well characterised, far less is known about regulation of p53 expression and activity by cellular oncogenes frequently overexpressed in HNSCC.

A functional interaction between the proto-oncogene PTTG and p53 has previously been described, although the exact nature of their relationship remains unclear. Overexpression of PTTG in p53-deficient MG-63 osteosarcoma cells and p53 wild-type MCF-7 breast cancer cells led to cell cycle arrest and apoptosis, suggesting PTTG could induce apoptosis in a p53-dependent and p53-independent manner (Yu et al. 2000a). In addition, PTTG induced significant aneuploidy in MG-63 cells but not MCF-7 cells, further suggesting that PTTG-induced aneuploidy could be blocked by wild-type p53 (Yu et al. 2000a). Hamid et al. further demonstrated that PTTG could upregulate p53 expression, both at the transcriptional and translational levels via induction of c-myc expression (Hamid, Kakar 2004). Furthermore, p53 induction was associated with increased expression of the p53 target gene BAX, thus demonstrating that PTTG could induce the transactivation function of p53 (Hamid, Kakar 2004).

Subsequent studies demonstrated that PTTG could directly interact with p53 *in vitro* (Bernal et al. 2002). However, in contrast with the initial findings, this interaction was shown to inhibit p53 binding to DNA and, as such, repressed p53 transcriptional activity and p53-mediated apoptosis (Bernal et al. 2002). Similarly, PTTG expression has been reported to reduce p53-mediated transcription of PTTG-targeting microRNAs (miRNA) in pituitary tumours, primarily through a dose-dependent decrease in p53 protein levels (Liang et al. 2015). These data also indicated the existence of a regulatory feedback loop between PTTG and p53 via modulation of p53-mediated PTTG-targeting miRNA transcription (Liang et al. 2015). However, the intimate relationship between PTTG and p53 is further complicated by the fact that PTTG itself is a direct transcriptional target of p53 (Zhou et al. 2003a). Doxorubicin and bleomycin induction of DNA damage resulted in suppression of PTTG expression in HCT116 cells harbouring wild-type p53 but not in U2OS cells, which are

devoid of p53, thus suggesting that p53 can act upstream of PTTG and inhibit its expression following DNA damage (Zhou et al. 2003a).

Recent research has also suggested a functional interaction exists between PBF and p53 in thyroid and colorectal cancer (Read et al. 2014, Read et al. 2016a, Read et al. 2016b). Through a series of GST pull-down and co-immunoprecipitation assays, it was demonstrated that PBF could directly interact with p53 in colorectal cancer HCT116 and papillary thyroid cancer K1 and TPC-1 cell lines (Read et al. 2014, Read et al. 2016b). Interestingly, this interaction was further increased following irradiation treatment of K1 and TPC-1 cells (Read et al. 2014). Subsequent half-life assays using anisomycin, which blocks de-novo protein synthesis, showed that overexpression of PBF led to a significant increase in turnover of p53 protein levels in all three colorectal and thyroid cancer cell lines (Read et al. 2014, Read et al. 2016b). Additional assays performed in PBF-transfected cells following treatment with the proteasome inhibitor MG132 demonstrated the presence of several higher molecular weight p53 conjugates in HCT116 and TPC-1 cell lysates, thus suggesting accumulation of ubiquitinated p53 (Read et al. 2014, Read et al. 2016b). Further investigations into this interaction, through transient reporter assays using H1299 cells, which are devoid of p53, revealed that PBF was capable of repressing p53-mediated HDM2 and p21 promoter activity and was also able to alter the sensitivity of thyroid cells to irradiation in a p53-dependent manner (Read et al. 2014, Read et al. 2016b). Additional irradiation experiments using PBF transgenic (PBF-Tg) mouse primary thyroctyes revealed significant dysregulation of p53-responsive DNA repair gene expression, which was associated with a significant increase in genomic instability (Read et al. 2014).

Given that both PTTG and PBF are known to functionally interact with p53 and disrupt p53 protein stability and activity in a number of cancer types, we assessed their potential

interactions in the setting of head and neck cancer. Furthermore, given the close relationship between PTTG and PBF, we performed co-immunoprecipitation assays in the presence of reduced PTTG or PBF expression and half-life assays using mutant forms of PTTG and PBF, which are unable to interact with one another, to determine the relative influence of PTTG and PBF on p53 binding and protein stability. Additional studies were conducted to determine the consequences of these interactions on p53 transcriptional activity, both in the prescence and absence of ionising radiation by quantitative real-time PCR.

## 6.2 Methods

### 6.2.1 Cell lines and plasmid transfections

92-VU-040T and 93-VU-147T cells were maintained in complete DMEM as described in section 2.1. For experiments involving ionising radiation, 92-VU-040T and 93-VU-147T cells were seeded in 35 mm x 10 mm (diameter x height) tissue culture dishes at 2.0 x $10^5$ and 2.5 x $10^5$ cells per dish, respectively. Following a 24-hour incubation period, the cells were exposed to specific doses of γ-irradiation using a Caesium-137 γ-emitter. At the time this research was conducted the γ-emitter delivered 37 mGy of γ-irradiation per second of exposure. Following γ-irradiation treatment, the cells were returned to incubation and harvested 24 hours later. For experiments requiring transient overexpression of PTTG and/or PBF, 92-VU-040T and 93-VU-147T cells were seeded in 6-well tissue culture plates at 2.0 x $10^5$ and 2.5 x $10^5$ cells per well, respectively. After 24 hours, the cells were transfected with the relevant expression plasmids as described in section 2.2.

### 6.2.2 Co-immunoprecipitation

92-VU-040T and 93-VU-147T cells were seeded in 25 $cm^2$ tissue culture flasks at 3.5 x $10^5$ and 4.0 x $10^5$ cells per flask, respectively. Protein was extracted from cell lysates as described in section 2.6.1 and co-immunoprecipitation performed as described in section 2.7 using an anti-HA antibody (1:150), an anti-p53 antibody (1:100) or an anti-PTTG antibody (1:100). No antibody and an IgG isotype antibody were used as negative controls.

### 6.2.3 p53 half-life assay

92-VU-040T and 93-VU-147T cells were seeded in 6-well tissue culture plates at 2.0 x $10^5$ and 2.5 x $10^5$ cells per well, respectively. Cells were then co-transfected with full-length wild-type PTTG, full-length wild-type PBF, PTTG BD- (lacking amino acids 123-154 responsible for interaction with PBF (Chien, Pei 2000) and PBF M1 (lacking amino acids 149-180 responsible for interaction with PTTG) as described in section 2.2. Half-life assays were performed as described in section 2.8, 24 hours after transient transfection.

### 6.2.4 Protein extraction, quantification and Western blotting

Protein was extracted from cell lysates and quantified as described in section 2.6.1. Western blotting was performed as described in section 2.6.2. Antibodies used were anti-PTTG 1:750, anti-PBF-8 1:500, anti-HA 1:1000, anti-p53 1:500, anti-p16 1:2000, anti-Rb 1:200, anti-S15-phosphorylated p53 1:1000, anti-γH2AX 1:1000 and anti-β actin 1:15,000.

### 6.2.5 RNA extraction, quantification and quantitative real-time PCR

Total RNA was harvested, quantified and reverse transcribed as described in sections 2.3 and 2.4. Quantitative real-time PCR was conducted as previously described in section 2.5.

The following Taqman gene-specific expression assays were used: PBF (Hs01036322_m1), PTTG (Hs00851754_u1), TP53 (Hs01034249_m1), RB (Hs01078066_m1), CDKN1A (Hs00355782_m1), CDKN2A (Hs99999189_m1), BAX (Hs00180269_m1), BCL-2 (Hs00248075_m1), CHEK1 (Hs00967506_m1), RAD51 (Hs00947967_m1) and BRCA1 (Hs01556193_m1).

### 6.2.6 BrdU cell proliferaton assay

The rate of cell proliferation in stably transduced γ-irradiated 92-VU-040T and 93-VU-147T cells was assessed as outlined in section 2.9. Cells were seeded at 4 $x10^3$ cells per well in 96-well plates and incubated for 24 hours before conducting the assay. The absorbance at 405 nm was measured using the Victor$^3$ 1420 Multilabel Counter [PerkinElmer].

### 6.2.7 Statistical analysis

Statistical analysis was performed as outlined in section 2.12.

## 6.3 Results

### 6.3.1 PTTG interacts with p53 *in vitro*

To examine whether PTTG interacts with p53 *in vitro*, total cellular protein was extracted from 92-VU-040T and 93-VU-147T cells transiently transfected with PTTG-HA and the protein lysates subjected to co-immunoprecipitation assay. Co-immunoprecipitation of PTTG-HA with an anti-p53 antibody was observed in 92-VU-040T and 93-VU-147T cells (Figure 6.1). No interaction was observed in VO and no antibody control lanes, suggesting a specific interaction between PTTG and p53 *in vitro* (Figure 6.1). Reciprocal co-immunoprecipitation,

in which p53 protein was immunoprecipitated with an anti-HA antibody, also demonstrated an interaction in 92-VU-040T and 93-VU-147T cell lines (Figure 6.1B).

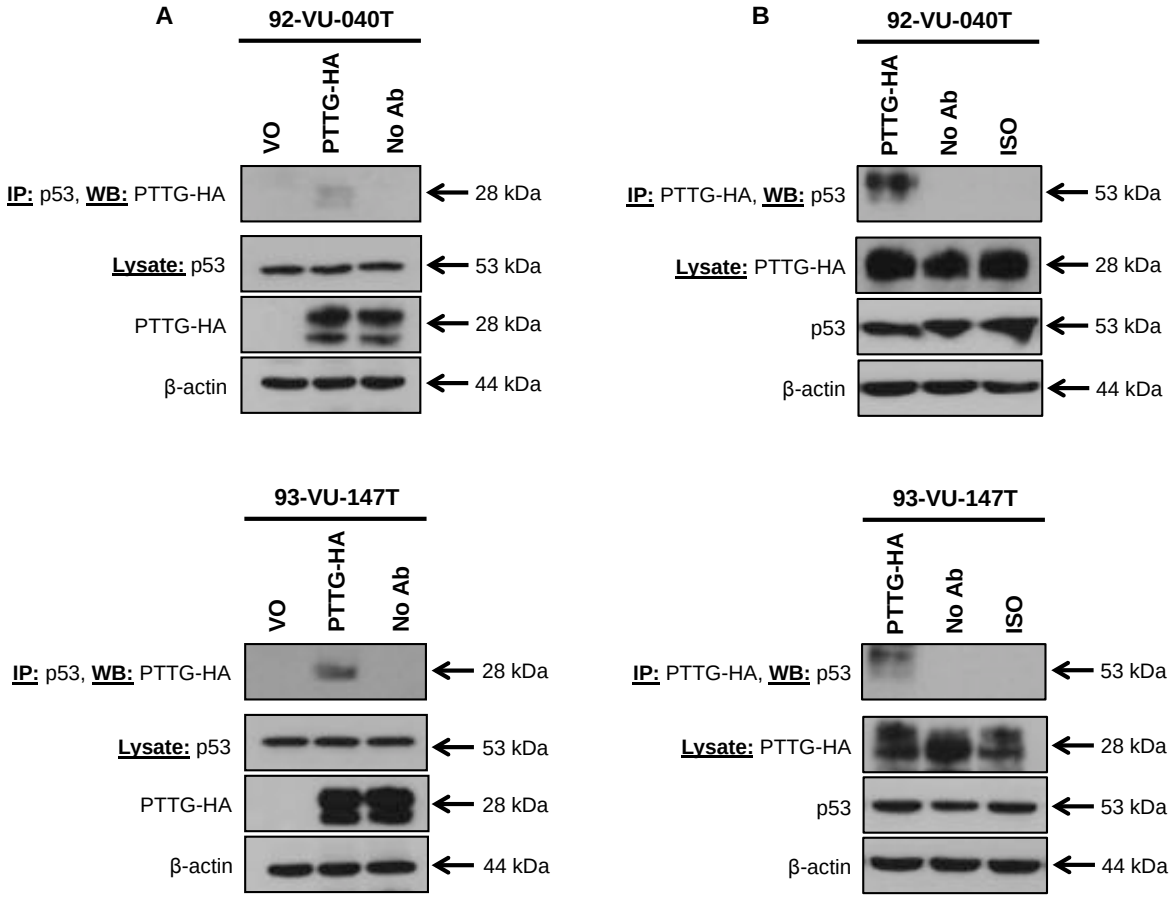


*Figure 6.1 PTTG binds p53 in vitro as demonstrated by co-immunoprecipitation assay.* ***A*** *– Western blot demonstrating co-immunoprecipitation of PTTG-HA in 92-VU-040T and 93-VU-147T cells following transfection with VO or PTTG-HA and immunoprecipitation with an anti-p53 antibody (n=3).* ***B*** *– Western blot demonstrating reciprocal co-immunoprecipitation of p53 in 92-VU-040T and 93-VU-147T cells following transfection with PTTG-HA and immunoprecipitation with an anti-HA antibody (n=3). Analysis of total protein lysates shows the presence of PTTG-HA and p53 protein in each sample. No Ab = no antibody control, ISO = IgG isotype control.*

### 6.3.2 PBF interacts with p53 *in vitro*

Having established that PTTG binds to p53 *in vitro*, co-immunoprecipitation assays were employed to determine whether PBF also interacts with p53 in our HNSCC cell lines. 92-VU-040T and 93-VU-147T cells were transiently transfected with PBF-HA and

immunoprecipitated with an anti-p53 antibody. Subsequent immunoblotting with an anti-HA antibody revealed an interaction between PBF-HA and p53 in both cell lines (Figure 6.2A, n=3). Co-immunoprecipitation using protein lysates extracted from cells transfected with VO demonstrated no protein band, as did the no antibody control samples, thus suggesting a specific interaction between PBF and p53 (Figure 6.2A). Reciprocal co-immunoprecipitation was performed using an anti-HA antibody for immunoprecipitation of transfected PBF-HA and subsequent immunoblotting for p53, which demonstrated co-immunoprecipitation of p53 with PBF-HA in both cell lines (Figure 6.2B, n=3). An interaction between PBF and p53 was not observed in the no antibody or isotype controls (Figure 6.2B).

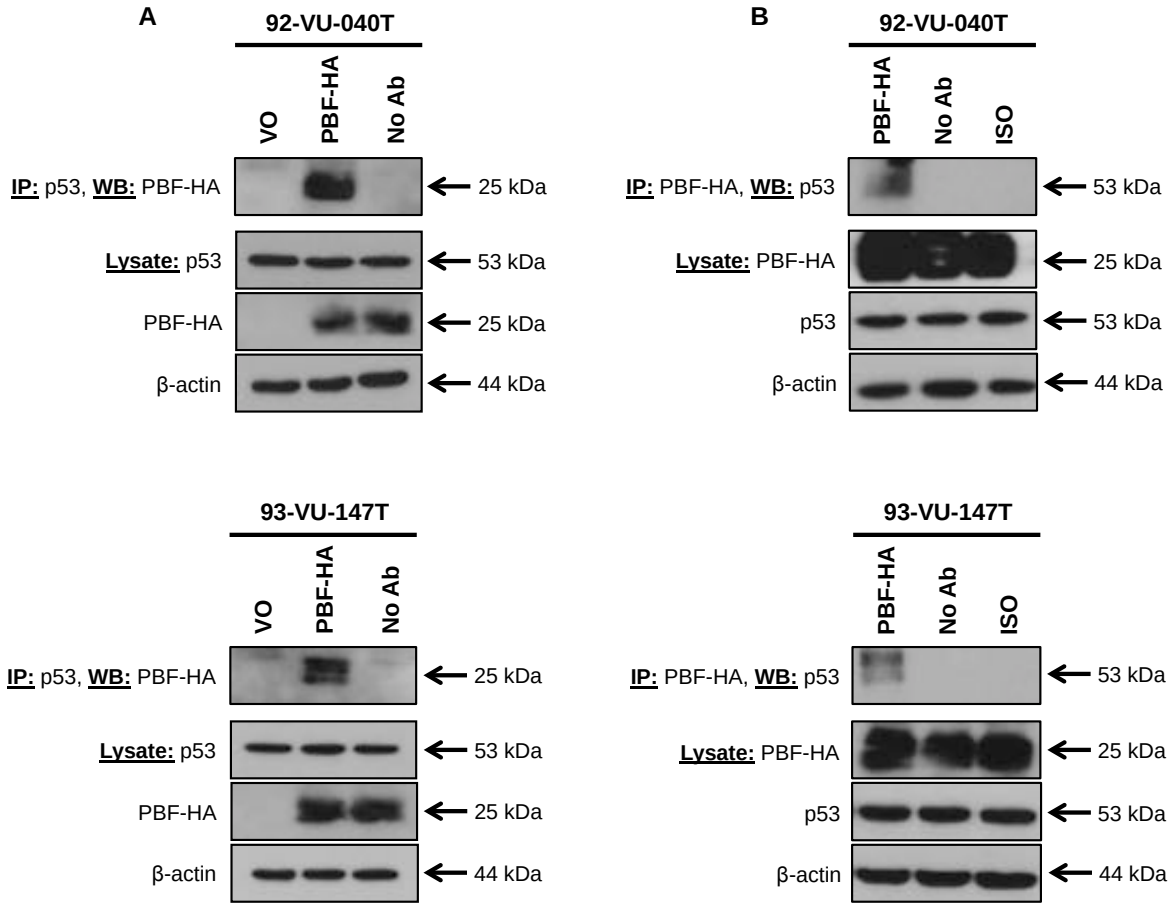


*Figure 6.2 PBF binds p53 in vitro as demonstrated by co-immunoprecipitation assay.* ***A*** *– Western blot demonstrating co-immunoprecipitation of PBF-HA in 92-VU-040T and 93-VU-147T cells following transfection with VO or PBF-HA and immunoprecipitation with an anti-p53 antibody (n=3).* ***B*** *– Western blot demonstrating reciprocal co-immunoprecipitation of p53 in 92-VU-040T and 93-VU-147T cells following transfection with PBF-HA and immunoprecipitation with an anti-HA antibody (n=3). Analysis of total protein lysates shows the presence of PBF-HA and p53 protein in each sample. No Ab = no antibody control, ISO = IgG isotype control.*

### 6.3.3 PTTG and PBF gene silencing alters the stringency of p53 binding

Given both PBF and PTTG independently bind p53 *in vitro*, we next investigated whether PBF can bind to p53 in the presence of significantly reduced PTTG expression in 92-VU-040T and 93-VU-147T cells, and whether PTTG can bind to p53 in the presence of reduced PBF expression. To this end, 92-VU-040T and 93-VU-147T cells stably transduced to express

gene-specific shRNAs targeting PTTG or PBF were transiently transfected with PBF-HA or PTTG, respectively and further co-immunoprecipitation assays conducted.

Following transfection of stable PTTG shRNA expressing 92-VU-040T and 93-VU-147T cells with PBF-HA, total protein lysates were harvested and immunoprecipitated with an anti-HA antibody. Subsequent immunoblotting with an anti-p53 antibody demonstrated that PBF was still capable of directly interacting with p53 in the near absence of PTTG in both cell lines (Figure 6.3). Furthermore, PBF appeared to bind to p53 which greater affinity, with PTTG-depleted 92-VU-040T cells displaying a 4-fold greater level of intensity than Scr shRNA-transduced cells when corrected for β-actin expression (Figure 6.3A; 4.0 ± 0.61-fold, p=0.005, n=3). PTTG-depleted 93-VU-147T cells displayed a similar 3.6-fold increase in p53 band intensity when compared with Scr shRNA control cells and corrected for β-actin expression (Figure 6.3B; 3.6 ± 0.25-fold, p=0.0007, n=3).

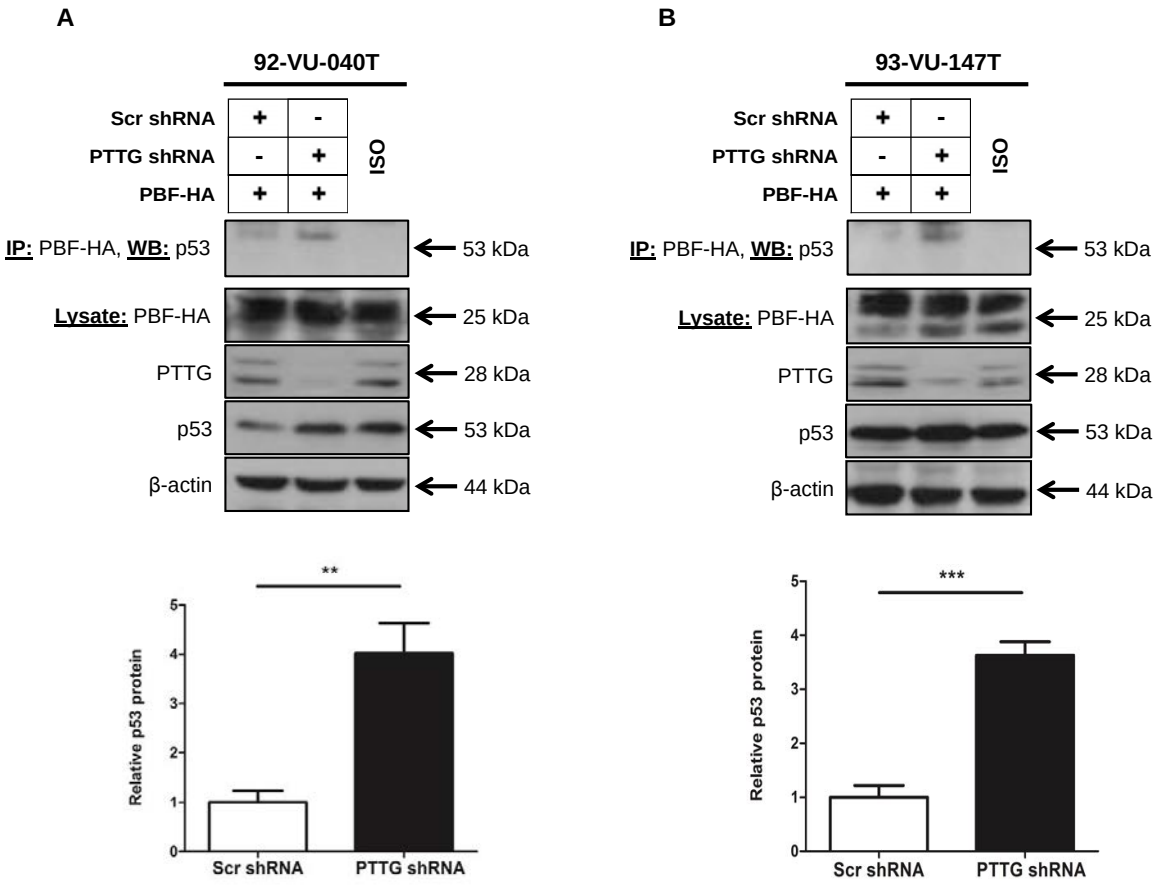


*Figure 6.3 Co-immunoprecipitation of p53 with PBF is enhanced in the absence of PTTG as demonstrated by co-immunoprecipitation assay.* ***A*** *– Western blot demonstrating co-immunoprecipitation of PBF-HA in stable Scr shRNA- or PTTG shRNA-expressing 92-VU-040T or 93-VU-147T cells co-transfected with PBF-HA and subsequently immunoprecipitated with an anti-p53 antibody (n=3).* ***B*** *– Scanning densitometry revealed that in the absence of PTTG, more p53 co-immunoprecipitated with PBF-HA (n=3). Data presented as mean ± SEM. ** p ≤0.01, *** p ≤0.001. ISO = IgG isotype control.*

Transient transfection of PBF shRNA expressing 92-VU-040T and 93-VU-147T cells with PTTG, followed by immunoprecipitation with an anti-PTTG antibody and immunoblotting with an anti-p53 antibody demonstrated that PTTG was still able to bind to p53 in the absence of PBF (Figure 6.4). However, the stringency of the interaction was significantly reduced in PBF-depleted 92-VU-040T (A; 0.25 ± 0.06-fold, p=0.0001, n=3) and 93-VU-147T (Figure 6.4B; 0.67 ± 0.13-fold, p=0.037, n=3) cells when compared to Scr shRNA-transduced cells and corrected for β-actin expression.

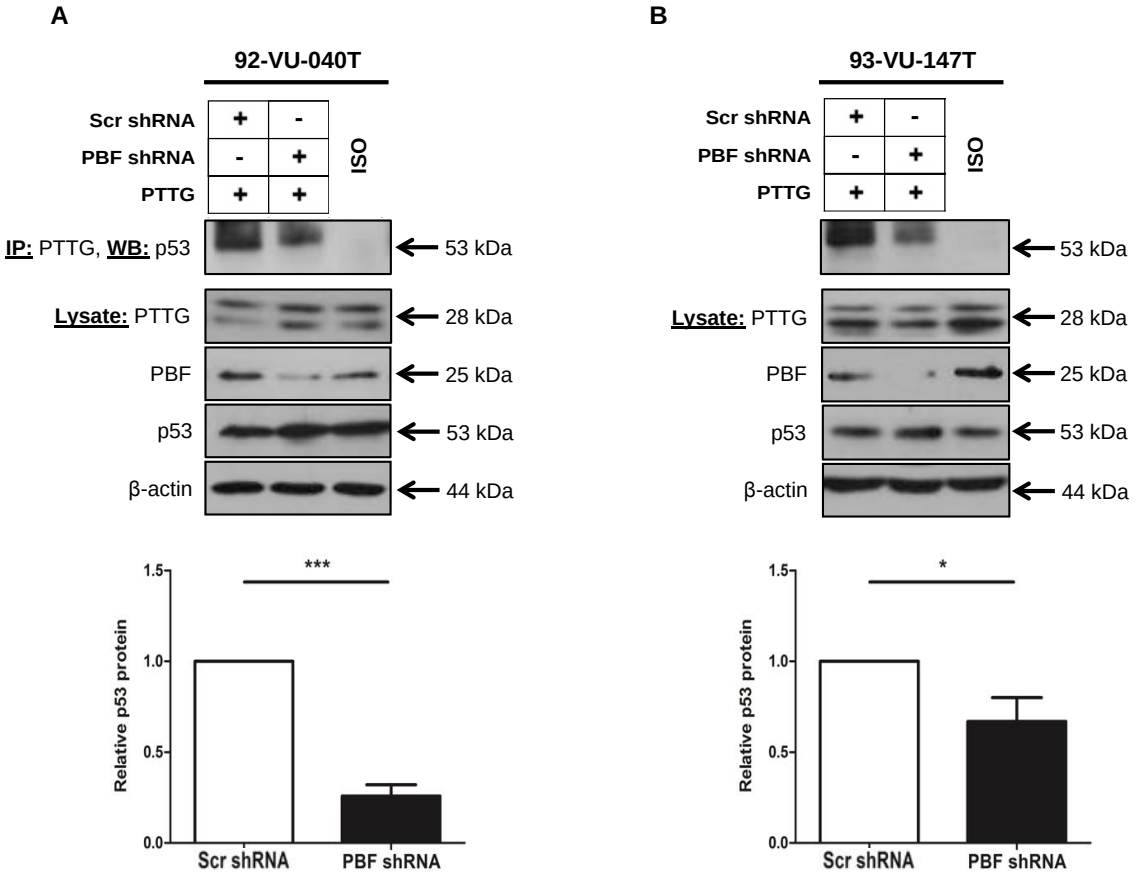


*Figure 6.4 Co-immunoprecipitation of p53 with PTTG is reduced in the absence of PBF as demonstrated by co-immunoprecipitation assay.* ***A*** *– Western blot demonstrating co-immunoprecipitation of PTTG in stable Scr shRNA- or PBF shRNA-expressing 92-VU-040T or 93-VU-147T cells co-transfected with PTTG and subsequently immunoprecipitated with an anti-p53 antibody (n=3).* ***B*** *– Scanning densitometry revealed that in the absence of PBF, less p53 co-immunoprecipitated with PTTG (n=3). Data presented as mean ± SEM. * p ≤0.05, *** p ≤0.001. ISO = IgG isotype control.*

### 6.3.4 PTTG and PBF cooperate to reduce p53 protein stability

To further investigate the relationship between PBF, PTTG and p53 in HNSCC cells, the impact of individual and combined overexpression of PBF and PTTG on intracellular p53 protein stability was ascertained through half-life studies using anisomycin to inhibit de novo protein synthesis. As shown in Figure 6.5 and Figure 6.6, p53 protein was detectable across the time-course in VO-transfected 92-VU-040T and 93-VU-147T cells and decreased at 60 minutes, but remained fairly stable at each of the remaining time points. However, PBF

overexpression significantly increased turnover of p53 protein in 92-VU-040T (Figure 6.5; 0.16 ± 0.04, p=0.001, n=3) and 93-VU-147T (Figure 6.6; 0.16 ± 0.03, p=0.005, n=3) cells by ~6-fold when compared with VO-transfected cells after 120 minutes. Likewise, PTTG overexpression resulted in a significant increase in turnover of p53 protein in 92-VU-040T cells (Figure 6.5; 0.18 ± 0.06, p=0.002, n=3), with a ~5.5-fold reduction in the levels of p53 protein at 120 minutes when compared with VO controls. A non-significant ~3-fold reduction in p53 protein levels was also observed in 93-VU-147T cells after 120 minutes following transfection with PTTG (Figure 6.6; 0.29 ± 0.04, p=ns, n=3). Interestingly, co-transfection of PBF and PTTG in 92-VU-040T and 93-VU-147T cells resulted in a more pronounced reduction in p53 protein stability than that observed in PBF- or PTTG-transfected cells alone. Co-expression led to a ~13-fold decrease in p53 protein levels in 92-VU-040T (Figure 6.5;0.08 ± 0.05, p=0.0008, n=3) cells and a ~12-fold decrease in p53 protein levels in 93-VU-040T (Figure 6.6; 0.04 ± 0.08, p=0.005, n=3) cells compared with VO controls after 120 minutes.

To determine the relative influence of PBF and PTTG on p53 stability, additional half-life studies were performed using mutant forms of PBF (PBF M1) and PTTG (PTTG BD-), which are unable to interact with one another. In 92-VU-040T (0.38 ± 0.11, p=ns, n=3) and 93-VU-147T (0.41 ± 0.15, p=ns, n=3) cells, co-transfection with PBF M1 and wild-type PTTG led to greater p53 protein stability after 120 minutes, when compared with cells overexpressing PBF, PTTG or PBF + PTTG. In contrast, a marked reduction in p53 protein stability was observed following co-transfection with wild-type PBF and PTTG BD- after 120 minutes in 92-VU-040T (Figure 6.5; ~4-fold, 0.23 ± 0.06, p=0.004, n=3) and 93-VU-147T (Figure 6.6; ~6-fold, 0.17 ± 0.01, p=0.005, n=3) cells. Interestingly, when 92-VU-040T (0.62 ± 0.14, p=ns, n=3) and 93-VU-147T (0.48 ± 0.09, p=ns, n=3) cells were transfected with both PBF

M1 and PTTG BD- mutants, p53 protein stability was restored to similar levels to those observed in VO-transfected cells after 120 minutes (Figure 6.5 and Figure 6.6). Taken together, these data suggest that PBF and PTTG cooperate together to disrupt p53 protein stability in 92-VU-040T and 93-VU-147T HNSCC cell lines.

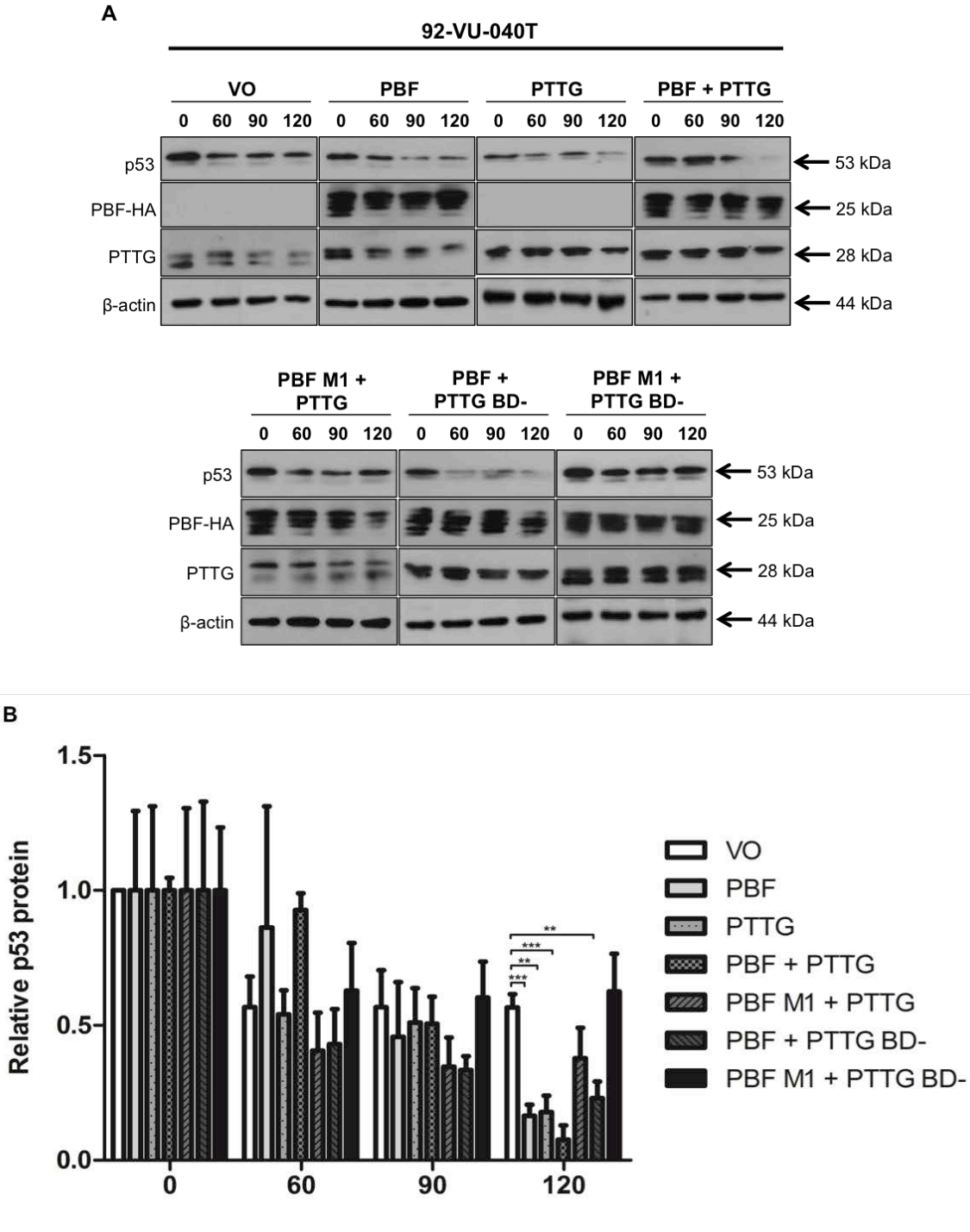


*Figure 6.5 PTTG and PBF cooperate together to disrupt p53 protein stability in 92-VU-040T cells.* ***A*** *– Representative Western blot analysis demonstrating the effects of PTTG and PBF expression on p53 protein stability in 92-VU-040T cells co-transfected with PBF, PTTG, PBF M1 and PTTG BD-. p53 protein turnover was assessed by anisomycin half-life assays across a 120-minute time-course (n=3). Exogenous PBF was detected using an anti-HA antibody.* ***B*** *– Scanning densitometry quantification of β-actin corrected p53 protein levels for each indicated time-point and transfection condition (n=3). Data presented as mean ± SEM. ** p ≤0.01, *** p ≤0.001.*

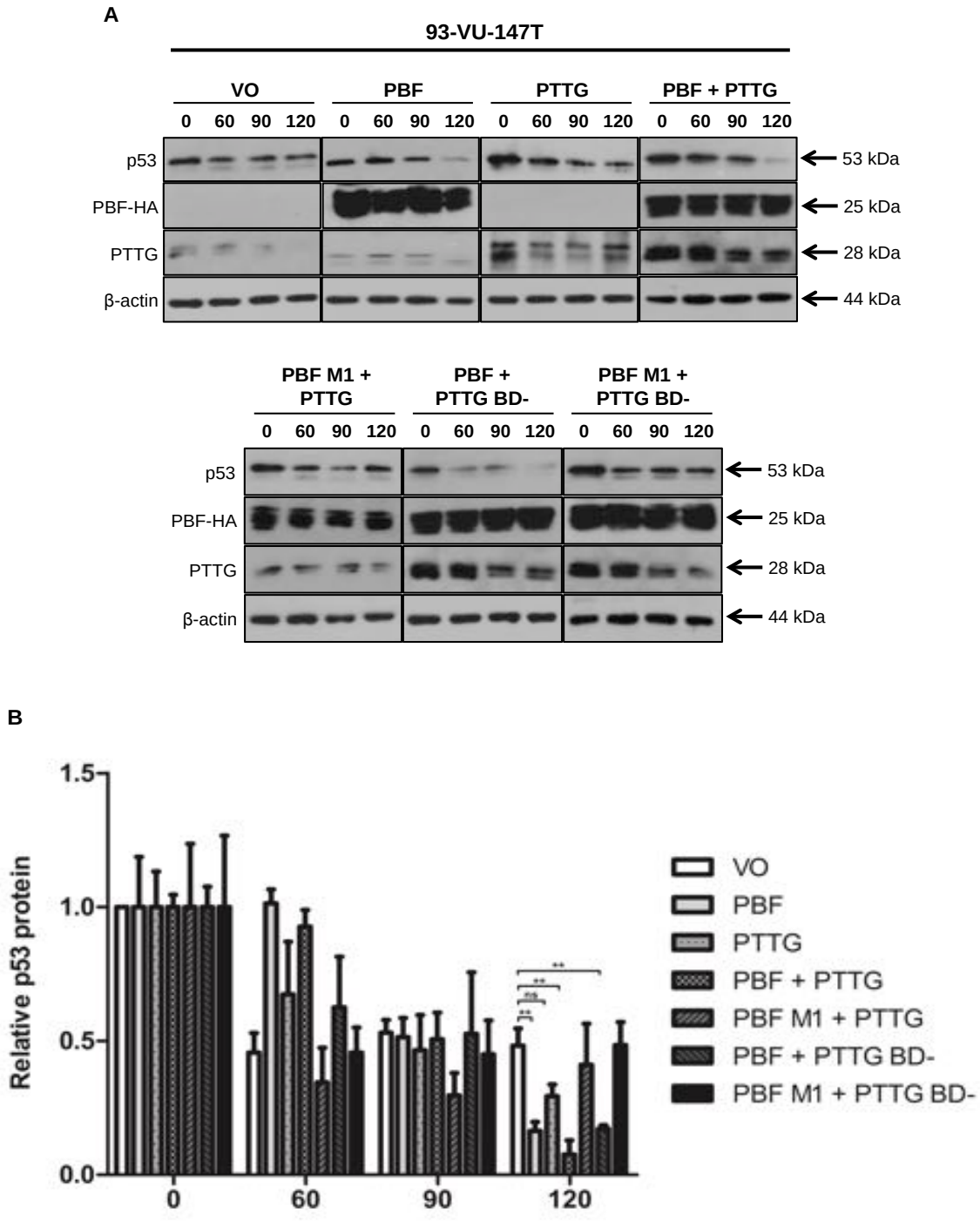


*Figure 6.6 PTTG and PBF cooperate together to disrupt p53 protein stability in 93-VU-147T cells.* ***A*** *– Representative Western blot analysis demonstrating the effects of PTTG and PBF expression on p53 protein stability in 93-VU-147T cells co-transfected with PBF, PTTG, PBF M1 and PTTG BD-. p53 protein turnover was assessed by anisomycin half-life assays across a 120-minute time-course (n=3). Exogenous PBF was detected using an anti-HA antibody.* ***B*** *– Scanning densitometry quantification of β-actin corrected p53 protein levels for each indicated time-point and transfection condition (n=3). Data presented as mean ± SEM. ns = non-significant, ** p ≤0.01.*

### 6.3.5 γ-irradiation: establishing an optimal dose

Intracellular p53 protein is normally maintained at low levels but becomes rapidly stabilised following irradiation-induced DNA damage, thus allowing p53 protein to accumulate within the cell (Kastan et al. 1991). In order to further examine whether PBF and PTTG depletion in HNSCC cells results in dysregulation of p53-responsive genes, non-transduced parental and stably transduced 92-VU-040T and 93-VU-147T cells expressing PBF shRNA or PTTG shRNA were exposed to a range (0-30 Gy) of doses of γ-irradiation and total protein harvested 24 hours post-treatment to assess the p53 response to irradiation-induced DNA damage.

Inherent p53 protein expression levels differed markedly between the various transduced 92-VU-040T and 93-VU-147T cell lines, making it difficult to decide on a suitable γ-irradiation dose based solely on total p53 protein levels. In parental and Scr shRNA or PTTG shRNA-transduced 92-VU-040T cell lines, total p53 protein levels remained fairly stable across the range of γ-irradiation doses (Figure 6.7A). In contrast, PBF shRNA-transduced cells demonstrated maximal p53 protein expression at a dose of 5 Gy, when compared to non-irradiated control cells (Figure 6.7A). At the highest dose of 30 Gy, p53 protein expression was visibly reduced compared to non-irradiated control cells (Figure 6.7A). However, it is important to note that treatment with 30 Gy of γ-irradiation was associated with significant cellular toxicity in all 92-VU-040T and 93-VU-147T cell lines analysed, which was not present at lower doses of γ-irradiation (data not shown). Specific phosphorylation of p53 at residue serine-15 (S15) is an important hallmark of p53 activity and its expression was also assessed in these cell lines. Significant induction of p53 S15-phosphorylation was observed following γ-irradiation in all cell lines, with maximal expression in parental, Scr shRNA- and

PTTG shRNA-transduced 92-VU-040T cells at a dose of 15 Gy. Conversely, PBF shRNA-transduced cells demonstrated maximal expression of p53-S15 at 5 Gy (Figure 6.7A).

When cells are subjected to ionising radiation, double-strand breaks (DSB) are generated, which result in rapid phosphorylation of the histone H2A molecule H2AX at residue serine-139 (γH2AX) (Sharma et al. 2012). This phosphorylation step forms the initial step of the DNA damage response and enables the recruitment of DNA repair proteins to sites of DNA damage (Sharma et al. 2012). γH2AX therefore represents an important marker of DNA damage and its expression was examined following γ-irradiation. 92-VU-040T cell lines demonstrated a dose-dependent increase in γH2AX protein expression following γ-irradiation, suggesting a robust γH2AX response to DNA damage (Figure 6.7A). Closer examination showed that levels of γH2AX peaked after treatment with doses of 15 and 30 Gy. Interestingly, PBF and PTTG protein expression levels were also elevated after treatment with γ-irradiation at the lower doses of 5 and 15 Gy in PBF shRNA-transduced cells and Scr shRNA- or PTTG shRNA-transduced cells, respectively (Figure 6.7A).

Similar results were also obtained following treatment of 93-VU-147T cells with the same range of doses of ionising radiation (Figure 6.7B). However, alterations in total p53 protein expression were more pronounced when compared with 92-VU-040T cells. Maximal p53 protein expression was observed following treatment with 15 Gy of γ-irradiation in all 93-VU-147T cell lines, with the exception of those transduced with PBF shRNA, in which, total p53 protein levels peaked after treatment at the lowest dose of 5 Gy (Figure 6.7B).

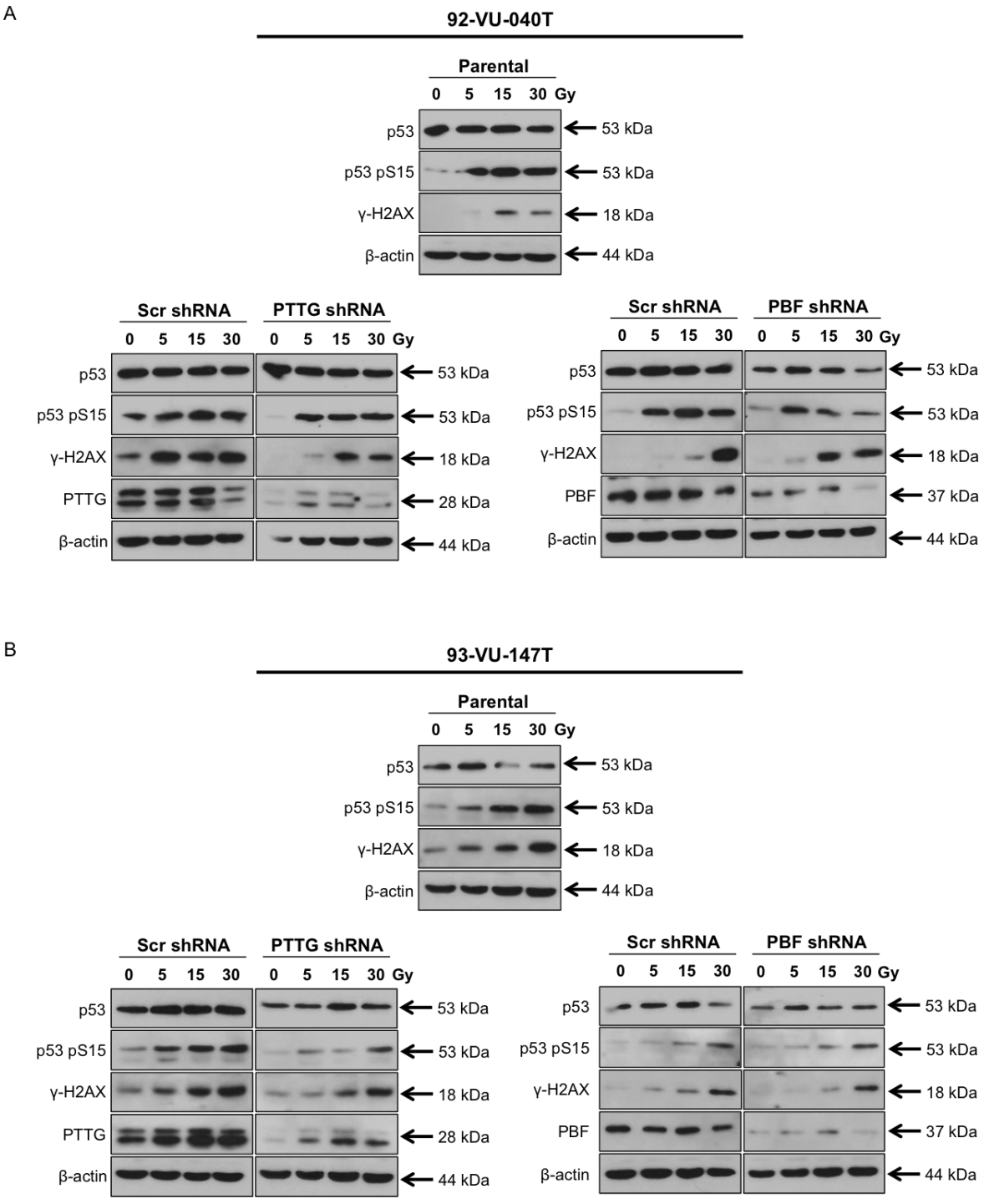


*Figure 6.7 Induction of DNA damage response pathways following treatment of 92-VU-040T and 93-VU-147T cell lines with a range of doses of ionising radiation.* ***A*** *– Western blot analysis of p53 and γ-H2AX protein expression following treatment with 0-30 Gy of γ-irradiation in non-transduced parental 92-VU-040T cells and those stably transduced to express Scr shRNA, PTTG shRNA or PBF shRNA (n=2).* ***B*** *- Western blot analysis of p53 and γ-H2AX protein expression following treatment with 0-30 Gy of γ-irradiation in non-transduced parental 93-VU-147T cells and those stably transduced to express Scr shRNA, PTTG shRNA or PBF shRNA (n=2).*

These initial experiments demonstrated that stably transduced 92-VU-040T and 93-VU-147T cells induce a robust DNA damage response to ionising radiation, which is similar to that observed in the non-transduced parental cell lines. The greatest responses, as measured by induction of expression and specific phosphorylation of p53 and γH2AX proteins, were observed in the majority of cell lines at a treatment dose of 15 Gy, with the exception of PBF shRNA-transduced 92-VU-040T and 93-VU-147T cell lines. 92-VU-040T cells expressing PBF shRNA showed peak expression of total and S15-phosphorylated p53 protein at 5 Gy, whereas maximal expression of γH2AX was observed at 30 Gy. In PBF shRNA expressing 93-VU-147T cells, total p53 protein expression levels also peaked at 5 Gy, whereas S15-phosphorylated p53 and γH2AX protein levels were at their highest following 30 Gy of γ-irradiation. As treatment with 30 Gy resulted in profound cytotoxicity and Scr shRNA control cell lines displayed an inadequate p53 and γH2AX response at 5 Gy, a dose of 15 Gy was chosen for all transduced 92-VU-040T and 93-VU-147T cell lines and was used in subsequent experiments requiring ionising radiation.

To ensure that the elevated expression and phosphorylation of p53 following treatment with 15 Gy of γ-irradiation correlated with increased p53 activity, 92-VU-040T and 93-VU-147T stable cell lines were treated with 15 Gy of γ-irradiation and total cellular RNA extracted 24 hours later. Quantitative real-time PCR was then performed and mRNA expression of the p53-responsive gene CDKN1A analysed. As shown in Figure 6.8, CDKN1A mRNA expression was upregulated by up to ~4-fold in 92-VU-040T stable cell lines and up to ~3-fold in 93-VU-147T stable cell lines after treatment with 15 Gy of γ-irradiation, when compared with untreated control cells.

A

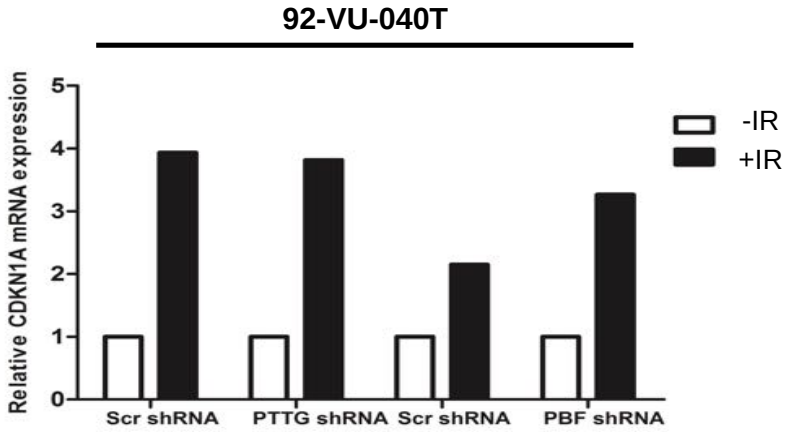


| Number | 2 | 2 | 2 | 2 | 2 | 2 | 2 | 2 |
|---|---|---|---|---|---|---|---|---|
| ΔCt ± SEM | 9.8±0.20 | 7.8±0.25 | 9.6±0.63 | 7.7±0.17 | 9.1±0.39 | 8.0±0.22 | 9.6±0.35 | 7.9±0.56 |

B

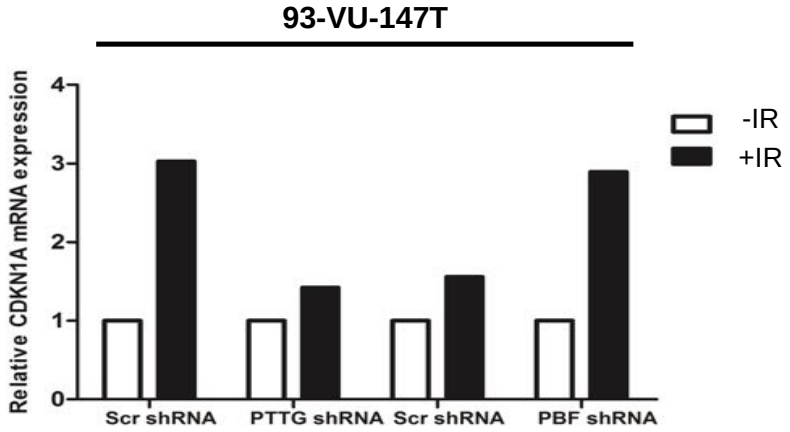


| Number | 2 | 2 | 2 | 2 | 2 | 2 | 2 | 2 |
|---|---|---|---|---|---|---|---|---|
| ΔCt ± SEM | 13.6±0.73 | 12.0±0.46 | 14.5±0.13 | 14.0±0.58 | 11.6±0.37 | 11.0±0.47 | 11.3±0.50 | 9.8±0.17 |

*Figure 6.8 Induction of CDKN1A mRNA expression following treatment of 92-VU-040T and 93-VU-147T stable cell lines with the optimal dose of 15 Gy of γ-irradiation.* ***A*** *– Induction of CDKN1A mRNA expression in 92-VU-040T stable cell lines 24 hours after treatment with 15 Gy of γ-irradiation (n=2).* ***B*** *– Induction of CDKN1A mRNA expression in 92-VU-040T stable cell lines 24 hours after treatment with 15 Gy of γ-irradiation (n=2). Data presented as mean fold change in mRNA expression. The number of samples used and the mean ΔCt values ± SEM for each group are given in the corresponding columns in the table below each graph. – IR = untreated, +IR = 15Gy of γ-irradiation.*

### 6.3.6 PTTG and PBF gene silencing does not alter the sensitivity of 92-VU-040T and 93-VU-147T cells to ionising radiation

Having determined the optimal p53 response to γ-irradiation in 92-VU-040T and 93-VU-147T cells stably transduced to express PTTG or PBF shRNA, the influence of PTTG and PBF expression on cell survival following treatment with ionising radiation was next examined. BrdU assays were performed 24 hours post-treatment. PTTG and PBF depletion did not appear to significantly alter the radiation sensitivity of 92-VU-040T and 93-VU-147T cells (Figure 6.9 and Figure 6.10). In 92-VU-040T cells expressing Scr shRNA, cell proliferation was reduced by approximately 15 % following exposure to γ-irradiation. In PTTG shRNA-expressing cells, cell proliferation was reduced by 24 % following treatment with γ-irradiation (Figure 6.9A). Similarly, in 93-VU-147T cells transduced with Scr shRNA, cell proliferation was reduced by 19 % after γ-irradiation treatment and in PTTG shRNA-transduced cells, cell proliferation was reduced by 26 % following treatment with γ-irradiation (Figure 6.9B). However, the number of proliferating cells was not significantly altered following ionising radiation when comparing Scr shRNA-expressing cells with PTTG shRNA-expressing cells (Figure 6.9; p=ns, n=3).

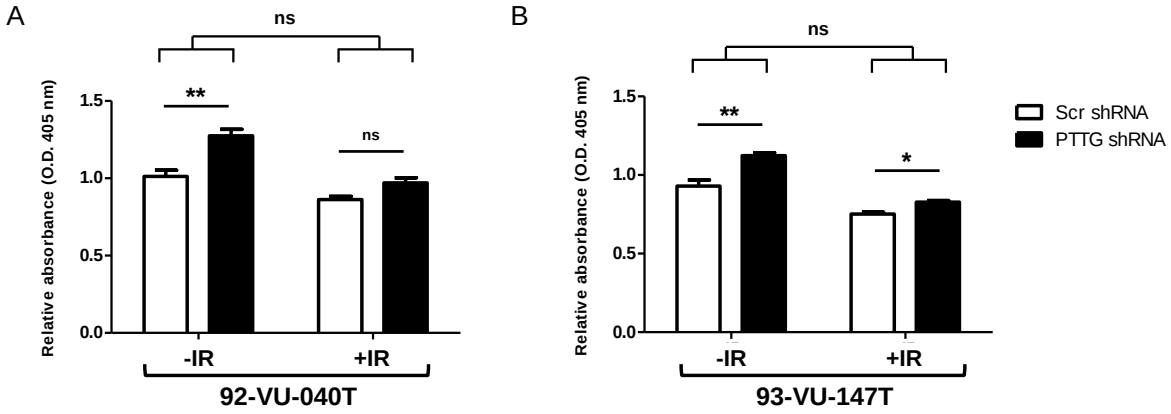


*Figure 6.9 PTTG depletion does not alter the sensitivity of 92-VU-040T and 93-VU-147T cells to ionising radiation.* ***A*** *– 92-VU-040T cells stably transduced with either Scr shRNA or PTTG shRNA were irradiated with a 15 Gy dose or untreated and cell survival measured 24 hours post-treatment by BrdU assay (n=3 with 8 replicates).* ***B*** *– 93-VU-147T cells stably transduced with either Scr shRNA or PTTG shRNA were irradiated with a 15 Gy dose or untreated and cell survival measured 24 hours post-treatment by BrdU assay (n=3 with 8 replicates). Data presented as mean ± SEM. ns = non-significant, * p ≤0.05, ** p ≤0.01.*

BrdU assays were repeated in PBF knockdown stable cell lines. In 92-VU-040T cells expressing Scr shRNA, cell proliferation was reduced by approximately 22 % in response to γ-irradiation and PBF depleted cells demonstrated a further reduction in cell proliferation of 21 % (Figure 6.10A). A similar result was observed in 93-VU-147T stable cell lines, where Scr shRNA-transduced cells displayed a 22 % reduction in cell proliferation and PBF shRNA-transduced cells demonstrated a further decrease in cell proliferation of around 10 % following treatment with γ-irradiation (Figure 6.10B). However, the number of proliferating cells was not significantly altered following ionising radiation when comparing Scr shRNA-expressing cells with PBF shRNA-expressing cells (Figure 6.10; p=ns, n=3).

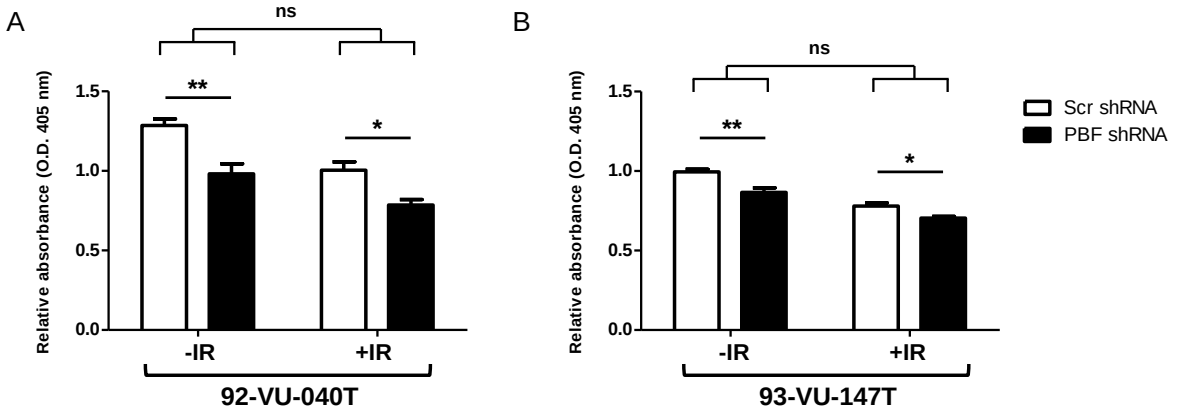


*Figure 6.10 PBF depletion does not alter the sensitivity of 92-VU-040T and 93-VU-147T cells to ionising radiation.* ***A*** *– 92-VU-040T cells stably transduced with either Scr shRNA or PBF shRNA were irradiated with a 15 Gy dose or untreated and cell survival measured 24 hours post-treatment by BrdU assay (n=3 with 8 replicates).* ***B*** *– 93-VU-147T cells stably transduced with either Scr shRNA or PBF shRNA were irradiated with a 15 Gy dose or untreated and cell survival measured 24 hours post-treatment by BrdU assay (n=3 with 8 replicates). Data presented as mean ± SEM. * p ≤0.05, ** p ≤0.01.*

### 6.3.7 PTTG gene silencing alters the expression of p53-related genes in 92-VU-040T and 93-VU-147T cells

As PTTG was revealed to interact with and alter p53 protein stability, the functional consequences of such an interaction were next investigated. Using the optimal irradiation dose established in section 6.3.5 above, stable 92-VU-040T and 93-VU-147T PTTG knockdown cells were subjected to γ-irradiation and total cellular proteins harvested 24 hours later. Western blotting was then performed to assess the p53 and γH2AX responses to ionising radiation. As shown in Figure 6.11, phosphorylation or p53 at residue S15 and H2AX at residue S139 (γH2AX) was readily detectable following genotoxic insult in all four cell lines.

Further expression profiling revealed irradiation-induced upregulation of PBF protein expression in all 92-VU-040T and 93-VU-14T stable cell lines (Figure 6.11). Exposure of these cell lines to γ-irradiation also resulted in an increase in the expression of PTTG in all four cell lines (Figure 6.11). No changes in total p53 protein expression were observed in 92-VU-040T Scr shRNA- and PTTG shRNA-transduced cell lines in the presence or absence of

ionising radiation and p16 protein remained undetectable (Figure 6.11). Total p53 and p16 protein expression levels were unchanged in 93-VU-147T stably transduced cell lines (Figure 6.11). However, Rb protein expression was elevated in response to γ-irradiation in both Scr shRNA- and PBF shRNA-transduced 93-VU-147T cell lines (Figure 6.11).

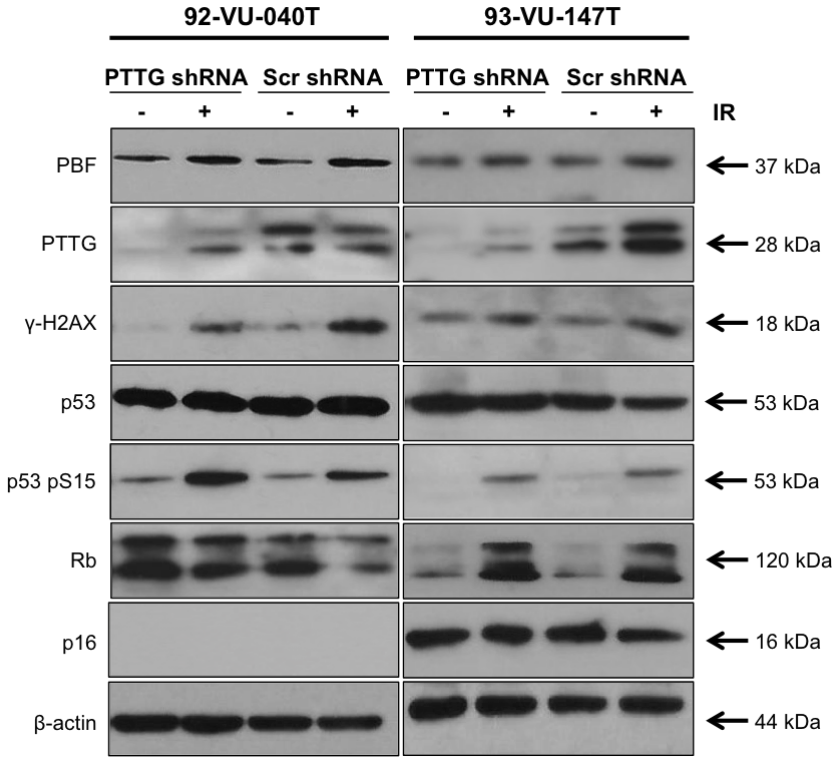


*Figure 6.11 Western blot analysis of PTTG depleted 92-VU-040T and 93-VU-147T cells following treatment with ionising radiation. Representative Western blots showing protein expression levels of PBF, PTTG, γ-H2AX, p53, Rb and p16 following treatment with 15 Gy of γ-irradiation in 92-VU-040T (left panel) and 93-VU-147T (right panel) cells stably transduced to express Scr shRNA and PTTG shRNA (n=3).*

Real-time PCR quantification of PTTG gene expression in the stably transduced 92-VU-040T and 93-VU-147T cell lines confirmed knockdown of PTTG mRNA expression in PTTG shRNA-transduced cell lines when compared with Scr shRNA control cells, both before (92-VU-040T: 0.06 ± 0.02-fold, p=0.0008; 93-VU-147T: 0.10 ± 0.03-fold, p=0.002; n=3) and after treatment (92-VU-040T: 0.13 ± 0.007-fold, p=0.001; 93-VU-147T: 0.19 ± 0.002-fold, p=0.002; n=3) with ionising radiation (Figure 6.12A). However, PTTG mRNA expression

was significantly induced following exposure of both Scr shRNA- (92-VU-040T: 1.57-fold, p=0.020; 93-VU-147T: 1.59-fold, p=0.034; n=3) and PTTG shRNA- (92-VU-040T: 2.10-fold, p=0.043; 93-VU-147T: 1.84-fold, p=0.019; n=3) expressing cell lines to γ-irradiation (Figure 6.12A). In addition, PBF mRNA expression was significantly induced after treatment of 92-VU-040T Scr shRNA control (2.07-fold, p=0.028, n=3) and PTTG knockdown cell lines (1.46-fold, p=0.003, n=3), as well as 93-VU-147T Scr shRNA control cells (2.02-fold, p=0.045, n=3) (Figure 6.12B). Elevated PBF mRNA expression was also noted in 93-VU-147T PTTG knockdown cells, however this did not reach statistical significance (Figure 6.12B; 1.61-fold, p=ns, n=3). Taken together, these data show that PTTG and PBF are responsive to γ-irradiation in 92-VU-040T and 93-VU-147T HNSCC cell lines and their expression can be induced both at the transcriptional and translational level following irradiation-induced DNA damage.

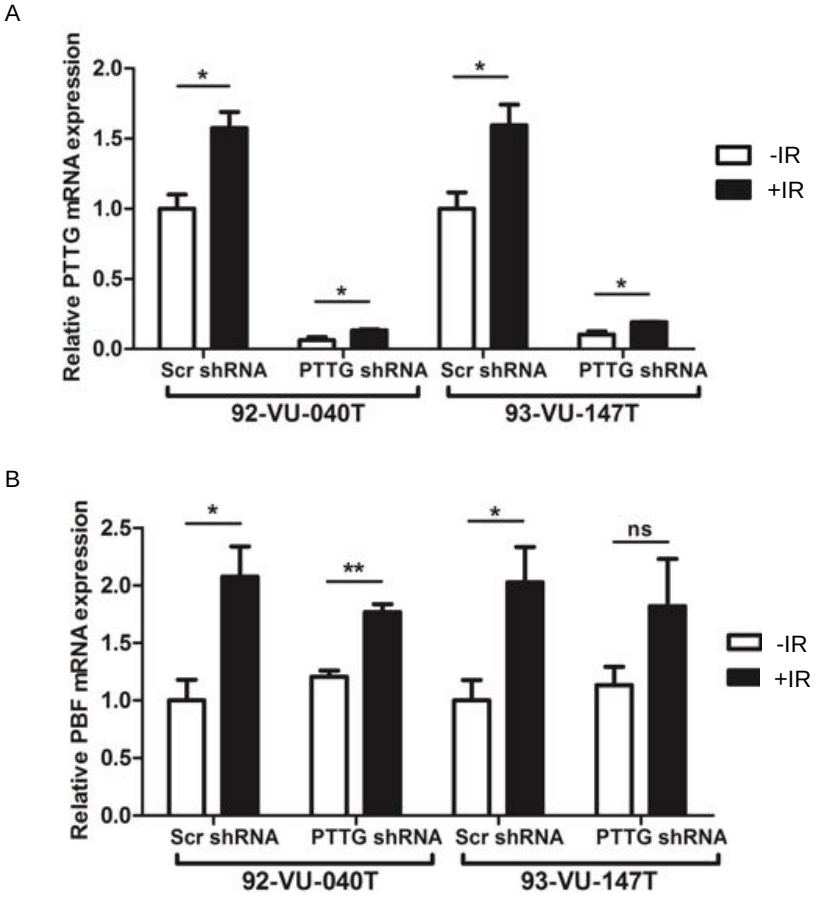


*Figure 6.12 Altered PTTG and PBF mRNA expression following irradiation of 92-VU-040T and 93-VU-147T cells stably transduced to express PTTG shRNA.* ***A*** *– Relative PTTG mRNA expression levels in 92-VU-040T and 93-VU-147T cells transduced with Scr shRNA or PTTG shRNA and then irradiated with a 15 Gy dose (n=3).* ***B*** *– Relative PBF mRNA expression levels in 92-VU-040T and 93-VU-147T cells transduced with Scr shRNA or PTTG shRNA and then irradiated with a 15 Gy dose (n=3). Data presented as mean ± SEM. –IR = untreated, +IR = irradiated, ns = non-significant, * p ≤0.05.*

Additional quantitative real-time PCR reactions were performed to examine whether PTTG depletion resulted in dysregulation of p53-related genes. A total of 8 p53-related genes were analysed for potential changes in mRNA expression following PTTG knockdown, including those involved in cell cycle regulation, apoptosis and DNA repair. As shown in Figure 6.13, and in support of the gene profiling data described in Chapter 5, mRNA expression of the anti-apoptotic gene BCL-2 was significantly upregulated in response to PTTG knockdown in 92-VU-040T (2.91 ± 0.11-fold, p=0.002, n=3) and 93-VU-147T (3.19 ±

0.50-fold, p=0.014, n=3) cells (Figure 6.13). Furthermore, genes known to play an important role in the maintenance of genomic integrity were also altered, including expression of RAD51, which was significantly increased in PTTG shRNA-expressing 93-VU-147T cells (2.31 ± 0.29-fold, p=0.016, n=3) but not in PTTG shRNA-expressing 92-VU-040T cells, and BRCA1, which was significantly upregulated in response to PTTG depletion in 92-VU-040T cells (1.85 ± 0.17-fold, p=0.038, n=3), but not in PTTG shRNA-transduced 93-VU-147T cells (1.47 ± 0.26-fold, p=ns, n=3) (Figure 6.13). Expression of the remaining genes (RB, CDKN1A, CDKN2A, BAX, CHEK1) remained unaltered following PTTG knockdown in 92-VU-040T and 93-VU-147T cells (Figure 6.13). Furthermore, PTTG knockdown did not cause any transcriptional changes in TP53 (Figure 6.13).

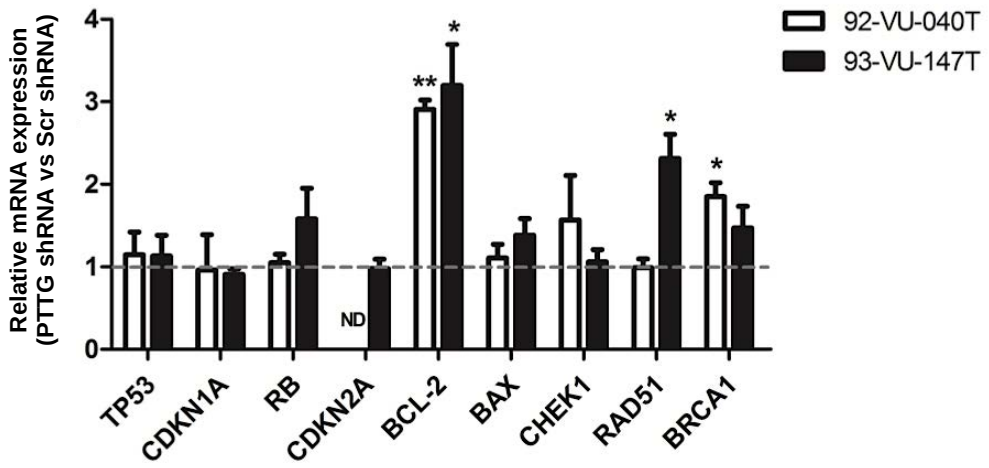


*Figure 6.13 Altered expression of p53-related genes following PTTG depletion in 92-VU-040T and 93-VU-147T cells. Relative mRNA expression of indicated genes in 92-VU-040T and 93-VU-147T cells transduced with PTTG shRNA compared with 92-VU-040T and 93-VU-147T Scr shRNA-transduced cells, respectively (n=3). Data presented as mean ± SEM. ND = not detected, * p ≤0.05, ** p ≤0.01.*

Finally, to further examine the influence of PTTG, quantitative real-time PCR analyses were repeated following γ-irradiation of PTTG shRNA depleted and Scr shRNA control 92-VU-040T and 93-VU-147T cell lines. Two genes were found to be significantly dysregulated following irradiation of PTTG shRNA-transduced 92-VU-040T cells (Figure 6.14A).

Expression of BCL-2 (1.7 ± 0.06, p=0.025, n=3) was significantly induced compared to Scr shRNA-transduced control cells following ionising radiation. In contrast, irradiation-induced expression of the DNA repair gene BRCA1 was significantly repressed in PTTG shRNA-transduced 92-VU-040T cells when compared with irradiated Scr shRNA-transduced cells (Figure 6.14A; 0.37-fold, p=0.0006, n=3). A non-significant reduction in CDKN1A mRNA expression was also observed following depletion of PTTG and subsequent induction of DNA damage (Figure 6.14A; 0.79-fold, p=ns, n=3). Exposure of PTTG depleted 93-VU-147T cells to γ-irradiation also resulted in significantly altered expression of a number of p53-related genes, including BCL-2 (2.57-fold, p=0.002, n=3) and RAD51 (1.21-fold, p=0.048, n=3), which were both significantly induced following treatment with γ-irradiation, when compared with untreated controls (Figure 6.14B). In addition, CDKN1A (0.63-fold, p=0.038, n=3) mRNA expression was significantly repressed, whilst BRCA1 mRNA expression was non-significantly repressed in these cells after treatment with ionising radiation (Figure 6.14; p=0.066, n=3). Taken together, these data imply an ability of PTTG to modulate expression of a small number of p53-responsive genes *in vitro* both in the presence and absence of genotoxic stress.

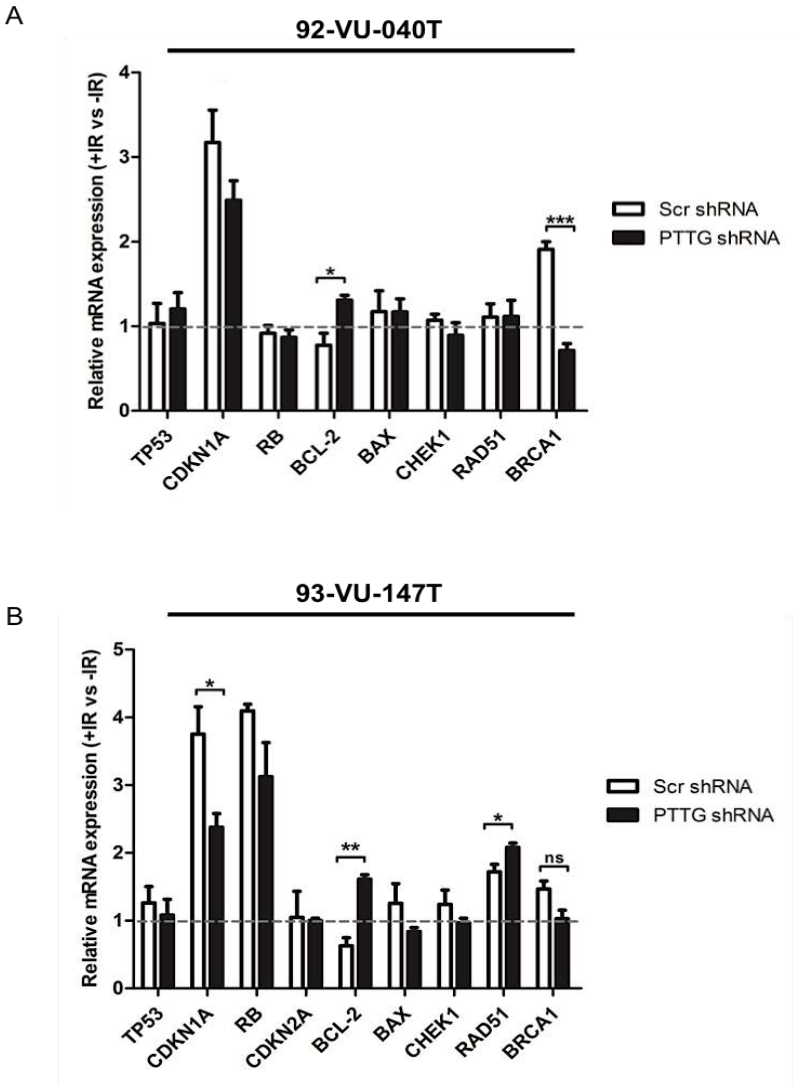


*Figure 6.14 Altered expression of p53-related genes in PTTG depleted 92-VU-040T and 93-VU-147T cells, following treatment with ionising radiation.* ***A*** *– Relative mRNA expression of indicated genes in PTTG shRNA-transduced 92-VU-040T cells compared with non-irradiated controls following irradiation with a 15 Gy dose (n=3).* ***B*** *– Relative mRNA expression of indicated genes in PTTG shRNA-transduced 93-VU-147T cells compared with non-irradiated controls following irradiation with a 15 Gy dose (n=3). Data presented as mean ± SEM. ns = non-significant, * p ≤0.05, ** p ≤0.01, *** p ≤0.001.*

### 6.3.8 PBF gene silencing alters the expression of p53-related genes in 92-VU-040T and 93-VU-147T cells

Having also identified that a direct interaction exists between PBF and p53 *in vitro* and the ability of PBF to induce p53 protein turnover, we next sought to characterise the impact of PBF depletion on the expression of p53-related genes in the presence and absence of ionising

radiation. Importantly, initial Western blot analysis confirmed induction of S15 phosphorylated p53 protein and γH2AX protein expression after irradiation treatment, thus demonstrating a robust DNA damage response in all 92-VU-040T and 93-VU-147T stably transduced cell lines (Figure 6.15). Expression of total p53 and total Rb protein remained unaltered and p16 protein expression remained undetectable in 92-VU-040T stable cell lines (Figure 6.15). In contrast, total Rb expression was upregulated following irradiation treatment in both 93-VU-147T Scr shRNA control and PBF knockdown stable cell lines but total p53 and p16 protein expression remained unaltered (Figure 6.15). Exposure of Scr control and PBF depleted 92-VU-040T and 93-VU-147T cell lines to γ-irradiation resulted in induction of PBF protein levels (Figure 6.15). Western blotting also revealed significant upregulation of PTTG protein levels in irradiated 92-VU-040T stably transduced Scr shRNA and PBF shRNA cell lines and also in irradiated 93-VU-147T Scr shRNA-transduced cell lines (Figure 6.15). However, there was no change in PTTG protein expression following irradiation of 93-VU-147T PBF shRNA-transduced cells (Figure 6.15).

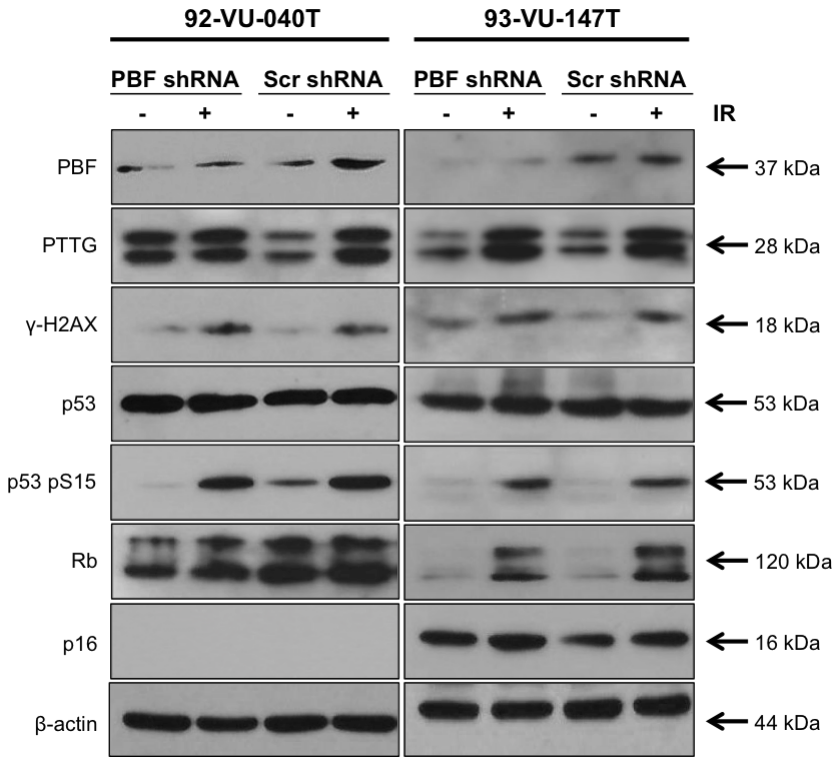


*Figure 6.15 Western blot analysis of PBF depleted 92-VU-040T and 93-VU-147T cells following treatment with ionising radiation. Representative Western blots showing protein expression levels of PBF, PTTG, γ-H2AX, p53, Rb and p16 following treatment with 15 Gy of γ-irradiation in 92-VU-040T (left panel) and 93-VU-147T (right panel) cells stably transduced to express Scr shRNA and PBF shRNA (n=3).*

Further quantification of PBF gene expression confirmed significant knockdown of PBF mRNA levels in PBF shRNA-transduced cell lines compared to Scr shRNA-transduced cells, both before (92-VU-040T: 0.13 ± 0.03-fold, p=0.0004; 93-VU-147T: 0.10 ± 0.02-fold, p <0.0001; n=3) and after treatment (92-VU-040T: 0.19 ± 0.01-fold, p=0.0004; 93-VU-147T: 0.13 ± 0.04-fold, p=0.0001; n=3) with ionising radiation (Figure 6.16A). Furthermore, significant upregulation of PBF mRNA expression was observed in irradiated 92-VU-040T (1.54-fold, p=0.044, n=3) and 93-VU-147T (1.49-fold, p=0.037, n=3) cells transduced with Scr shRNA when compared with non-irradiated cells (Figure 6.16A). A non-significant increase in PBF mRNA expression was also noted in irradiated 92-VU-040T (1.50-fold, p=ns, n=3) and 93-VU-147T (1.36-fold, p=ns, n=3) cells transduced with PBF shRNA (Figure

6.16A). PTTG mRNA expression levels were also elevated following irradiation in Scr shRNA-transduced 92-VU-040T (1.66-fold, p=ns, n=3) and 93-VU-147T (1.97-fold, p=0.014, n=3) cells when compared to non-irradiated controls (Figure 6.16B). However, the observed increase in PTTG mRNA expression in 92-VU-040T Scr shRNA cells did not reach statistical significance. In accord with the protein data, PTTG mRNA expression did not differ in PBF depleted 92-VU-040T cells following treatment with γ-irradiation, although a non-significant increase was noted in irradiated 93-VU-147T PBF knockdown cells (Figure 6.16B; 1.39-fold, p=ns, n=3).

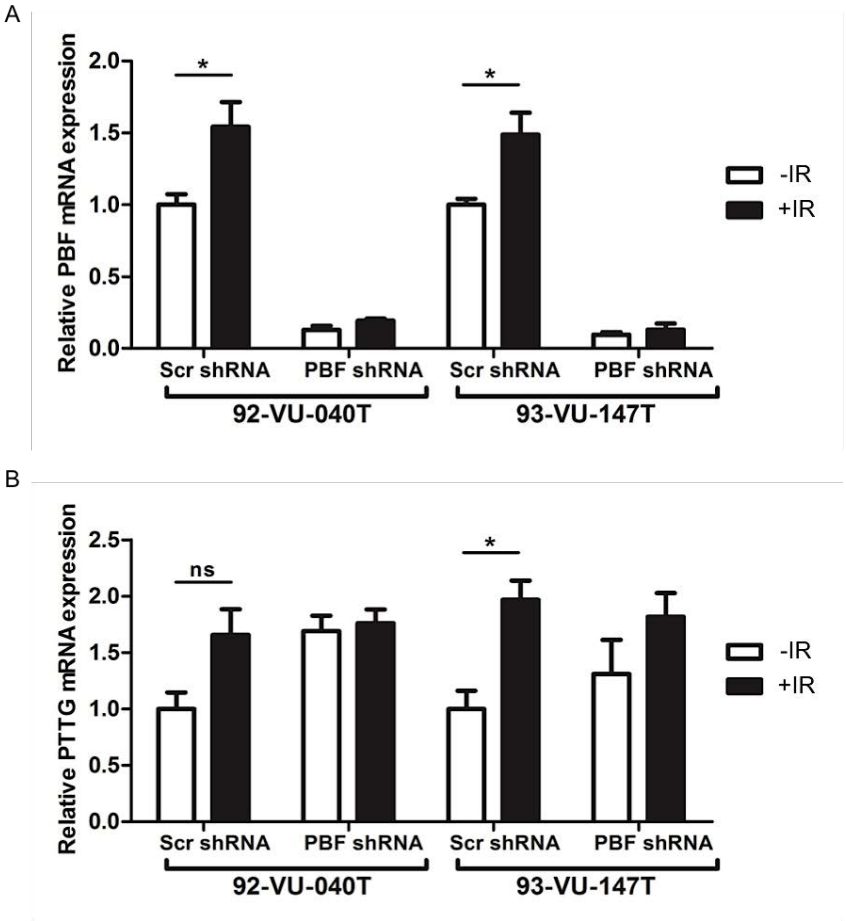


*Figure 6.16 Altered PBF and PTTG mRNA expression following irradiation of 92-VU-040T and 93-VU-147T cells stably transduced to express PBF shRNA.* ***A*** *– Relative PBF mRNA expression levels in 92-VU-040T and 93-VU-147T cells transduced with Scr shRNA or PBF shRNA (n=3).* ***B*** *– Relative PTTG mRNA expression levels in 92-VU-040T and 93-VU-147T cells transduced with Scr shRNA or PBF shRNA (n=3). Data presented as mean ± SEM. ns = non-significant, * p ≤0.05.*

Further examination of PBF shRNA-transduced 92-VU-040T and 93-VU-147T cell lines revealed that PBF depletion had very minimal impact on the expression of a selection of p53-related genes involved in cell cycle regulation, apoptosis and DNA repair (Figure 6.17). Considerably fewer p53-related genes were altered following PBF knockdown when compared with PTTG depleted cells, with only BCL-2 demonstrated significant gene expression changes following PBF gene silencing (Figure 6.13 vs. Figure 6.17). As shown in Figure 6.17, BCL-2 mRNA expression was significantly repressed in PBF depleted 92-VU-040T (0.42 ± 0.13, p=0.046, n=3) and 93-VU-147T (0.43 ± 0.06, p=0.025, n=3) cells when compared with Scr shRNA-transduced control cell lines. Expression of the remaining genes remained unaltered (Figure 6.17). In addition, PBF knockdown did not cause any transcriptional changes in TP53 (Figure 6.17).

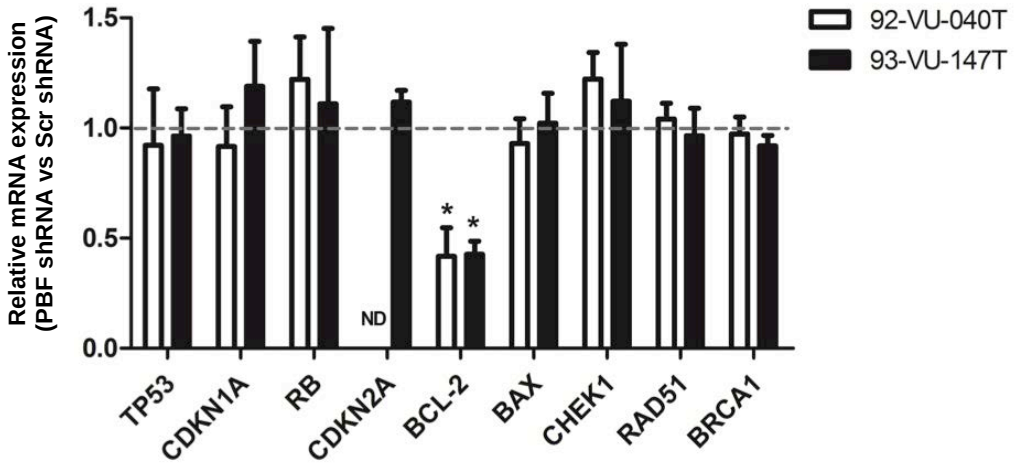


*Figure 6.17 Altered expression of p53-related genes following PBF depletion in 92-VU-040T and 93-VU-147T cells. Relative mRNA expression of indicated genes in 92-VU-040T and 93-VU-147T cells transduced with PBF shRNA compared with 92-VU-040T and 93-VU-147T Scr shRNA-transduced cells, respectively (n=3). Data presented as mean ± SEM. ND = not detected, * p ≤0.05, ** p ≤0.01.*

To identify additional changes in expression of p53-related genes, quantitative real-time PCR reactions were repeated in PBF depleted 92-VU-040T and 93-VU-147T cell lines following treatment with ionising radiation. Interestingly, irradiation-induced expression of

CDKN1A was significantly upregulated in PBF shRNA-transduced 92-VU-040T (2.40-fold, p=0.013, n=3) and 93-VU-147T (1.64-fold, p=0.031, n=3) cell lines when compared with irradiated Scr shRNA-transduced cells (Figure 6.18). Exposure of PBF depleted 92-VU-040T (1.26-fold, p=ns, n=3) and 93-VU-147T (2.04-fold, p=0.017, n=3) cells to γ-irradiation also resulted in further induction of BRCA1 mRNA expression, although statistical significance was not reached for 92-VU-040T cells (Figure 6.18). Additional non-significant alterations in BCL-2 mRNA expression were noted in both 92-VU-040T (0.68-fold, p=ns, n=3) and 93-VU-147T (0.79-fold, p=ns, n=3) PBF shRNA-expressing cell lines, with PBF knockdown repressing BCL-2 expression after treatment with γ-irradiation (Figure 6.18). Overall, these data suggest that whilst PBF is capable of binding to and altering p53 protein stability in 92-VU-040T and 93-VU-147T HNSCC cell lines, this interaction may have very little impact on p53 transcriptional activity, as evidenced by a lack of alterations in the expression of a panel of 8 p53-responsive genes following depletion of PBF *in vitro*.

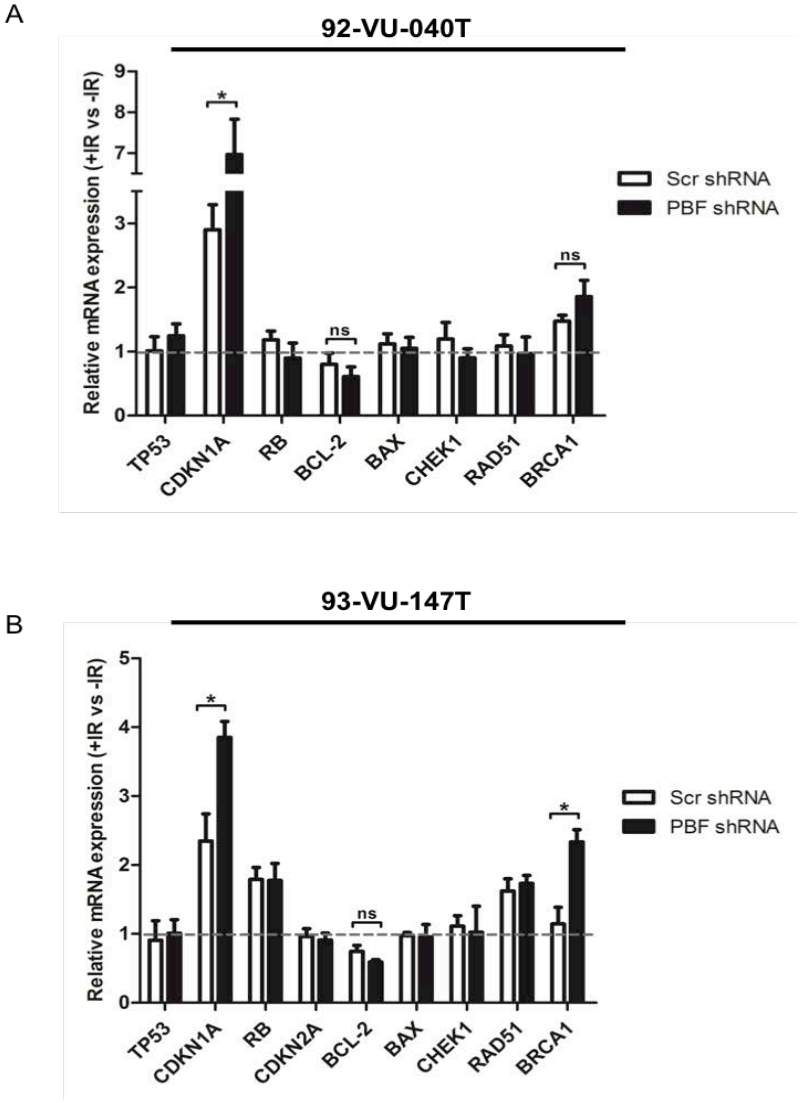


*Figure 6.18 Altered expression of p53-related genes in PBF depleted 92-VU-040T and 93-VU-147T cells, following treatment with ionising radiation.* ***A*** *– Relative mRNA expression of indicated genes in PBF shRNA-transduced 92-VU-040T cells compared with non-irradiated controls following irradiation with a 15 Gy dose (n=3).* ***B*** *– Relative mRNA expression of indicated genes in PBF shRNA-transduced 93-VU-147T cells compared with non-irradiated controls following irradiation with a 15 Gy dose (n=3). Data presented as mean ± SEM. ns = non-significant, * p ≤0.05.*

## 6.4 Discussion

### 6.4.1 PTTG and PBF bind p53 *in vitro*

The well-characterised proto-oncogene PTTG has been shown to specifically interact with p53 *in vitro* and *in vivo* (Bernal et al. 2002). This interaction was found to impair DNA

binding of p53 and led to significant repression of p53 transcriptional activity in human non-small cell lung cancer cells (Bernal et al. 2002). In addition, our group has recently demonstrated that its binding partner PBF also functionally interacts with p53 in thyroid and colorectal cancer cells (Read et al. 2014, Read et al. 2016b). In previous chapters, we revealed that PTTG and PBF are both frequently overexpressed in HNSCC tumours. Given that both proto-oncogenes are also known to interact with and impair p53 function in a variety of cancers, we performed co-immunoprecipitation assays to explore their potential interactions in HNSCC cell lines.

Transfected PTTG-HA and PBF-HA were successfully immunoprecipitated by an anti-p53 antibody in both HPV-negative 92-VU-040T and HPV-positive 93-VU-147T HNSCC cells. Further reciprocal assays, in which an anti-HA antibody was used for immunoprecipitation of PBF-HA or PTTG-HA, also demonstrated successful co-immunoprecipitation of p53 in both cell lines, thus providing evidence of a direct and specific interaction *in vitro*. Interestingly, the relative level of p53:PBF co-immunoprecipitates was significantly altered following depletion of PTTG, as was the level of p53:PTTG co-immunoprecipitates following PBF depletion. These data therefore suggest that the relative levels of PTTG and PBF within the cell strongly influence their interaction with p53 and are unlikely to reflect changes in p53 protein expression or stability following transfection, as differences in the levels of p53 protein in each sample were negligible.

Surprisingly, the interaction between exogenous PBF and p53 was enhanced following PTTG knockdown in 92-VU-040T and 93-VU-147T cells. As the binding sites for PTTG and PBF appear to be located within overlapping regions of the p53 protein (PTTG: amino acids 300-374 (Bernal et al. 2002); PBF: amino acids 318-393 (Read et al. 2014)), these results may be indicative of competitive binding between PTTG and PBF for p53, with PTTG displaying

greater affinity for p53 than PBF. Assessing whether PTTG and PBF competitively bind to p53 was beyond the scope of this body of work and would require further investigation, possibly through the use of GST pull-down assays. In contrast, the interaction between PTTG and p53 was significantly repressed following PBF knockdown in 92-VU-040T and 93-VU-147T cells, thus implying that PBF somehow facilitates PTTG:p53 binding. Indeed, PBF is known to facilitate the nuclear transport of PTTG (Chien, Pei 2000). It is therefore perceivable that PBF-driven nuclear translocation of PTTG might further augment its interaction with p53 in the nucleus. Alternatively, PBF may act as a co-factor, which binds to p53, redistributing it from the cytoplasm in to the nucleus, where it is then able to functionally interact with PTTG. However, further co-immunoprecipitation experiments using nuclear and cytoplasmic protein subfractions and proximity ligation assays (PLA) would be required. Future studies could also make use of specific mutants of PBF, which result in its retention in the cytoplasm, in order to further characterise the effects of PBF on the subcellular localisation of p53 and its interaction with PTTG.

### 6.4.2 PTTG and PBF co-operate to reduce p53 protein stability

As PTTG and PBF were both revealed to directly interact with p53, we next considered the individual and combined effects of PTTG and PBF expression on intracellular p53 protein stability through use of anisomycin half-life studies. Treatment of 92-VU-040T and 93-VU-147T cells with anisomycin resulted in a slight reduction in the levels of p53 protein over the 120-minute time-course. However, when these cells were transfected with PTTG or PBF, p53 protein levels were significantly reduced by 120 minutes. A significant finding was the synergistic effect of simultaneous induction of both proto-oncogenes. Indeed, combined

expression resulted in a more profound reduction in p53 protein stability than that observed following expression of either PTTG or PBF alone.

PTTG has previously been demonstrated to alter p53 stability (Bernal, Hernandez 2007). In colorectal cancer HCT116 cells, PTTG depletion resulted in stabilisation of p53 protein levels, as evidenced by cycloheximide chase experiments (Bernal, Hernandez 2007). Interestingly, stabilisation was achieved through PTTG-modulation of calpain activity on p53 degradation, rather than via modulation of the more typical ubiquitin-dependent degradation pathway (Bernal, Hernandez 2007). In addition, PTTG has been shown to directly bind to Ku70/Ku80, which forms the regulatory subunit of DNA-PK (Romero et al. 2001). Phosphorylation of p53 at residue S15 by DNA-PK is well characterised and disrupts its interaction with the crucial negative regulator and E3-ubiquitin ligase MDM2, thus stabilising p53 protein and causing it to accumulate within the cell (Shieh et al. 1997). PBF has also been shown to modulate p53 turnover in thyroid and colorectal cancer cells (Read et al. 2014). In these tumour settings, p53 degradation was induced by elevated PBF and could be blocked by the MDM2 antagonist, nutlin-3 (Read et al. 2014). Further research conducted by our group has also hinted at a potential interaction between PBF and the E2 ubiquitin-conjugating enzyme, Rad6, which forms a ternary complex with MDM2 and p53 and contributes to MDM2-mediated degradation of p53 in cervical carcinoma HeLa cells (Lyakhovich, Shekhar 2003). However, the precise mechanisms underlying the synergistic effects of PTTG and PBF remain to be clarified. It is possible that binding of PTTG with PBF may facilitate their interactions with proteins known to modulate p53 degradation, such as MDM2, Rad6 and calpain. Alternatively, they may function independently of one another, resulting in an additive effect when co-expressed.

To further characterise the impact of the interaction between PTTG and PBF on p53 stability, half-life studies were repeated following dual-transfection with wild-type PTTG or PBF and the existing mutants, PTTG BD- and PBF M1, which are unable to interact with one another. Transfection of 92-VU-040T and 93-VU-147T cells with wild-type PTTG and PBF M1 resulted in stabilisation of p53 protein, whereas transfection with wild-type PBF and PTTG BD- led to an increase in p53 protein degradation by 120 minutes, which was similar to that observed in PTTG or PBF transfected cells. Interestingly, transfection with PTTG BD- and PBF M1 reduced p53 protein turnover, thereby restoring p53 protein stability to similar levels observed in VO-transfected cells.

Given that both mutants disrupt PTTG:PBF interaction, if PTTG and PBF modulation of p53 was contingent upon this interaction, stabilisation of p53 protein would have been expected in all three transfection conditions. However, this was not the case and suggests that additional factors must be involved. p53 protein was consistently stabilised in 92-VU-040T and 93-VU-147T cells following transfection with PBF M1, whilst transfection with wild-type PBF typically led to a reduction in p53 stability. As described previously, the PBF M1 deletion mutant lacks the C-terminal 30 amino acids (Δ149-180), which mediate its binding to PTTG. Also within this region lies a critical tyrosine phosphorylation site, Y174, which plays an important role in PBF endocytosis, as well as in the binding and trafficking of NIS from intracellular vesicles to the plasma membrane (Smith et al. 2013). Furthermore, a functional interaction between PBF and the cytoskeletal remodelling protein cortactin has been shown to be contingent upon Src-mediated phosphorylation of PBF at residue Y174 (Watkins et al. 2016). Y174-phosphorylation of PBF may therefore represent an important post-translational modification, the loss of which may preclude PBF's ability to interact with or induce the degradation of p53. A lack of PBF-Y174 phosphorylation may also have important

connotations with regard to PTTG subcellular localisation and/or function and might explain the observed reduction in p53 stability following transfection with wild-type PTTG with wild-type PBF and wild-type PBF with PTTG BD-. Given the abundance of endogenous PBF in both cell lines, this might also explain the reduced p53 stability noted in cells transfected with PTTG alone. Together, these data support a central role for PTTG and PBF in the modulation of p53 protein stability in HNSCC.

### 6.4.3 PTTG and PBF gene silencing does not alter the sensitivity of 92-VU-040T and 93-VU-147T cells to ionising radiation

In light of the observed effects of PTTG and PBF expression on p53 protein interaction and stability, the impact of their depletion on 92-VU-040T and 93-VU-147T cell survival was assessed following treatment with ionising radiation. Cell survival was indirectly assessed by BrdU cell proliferation assay. In the absence of γ-irradiation, PTTG knockdown led to a significant increase in 92-VU-040T and 93-VU-147T cell proliferation compared to Scr shRNA-transduced control cells. Following γ-irradiation, Scr shRNA-transduced 92-VU-040T and 93-VU-147T cell proliferation was reduced by around 15 % compared to around 24 % in PTTG-depleted 92-VU-040T and 93-VU-147T cells. However, no difference was observed when comparing the relative change in proliferation of Scr shRNA- or PTTG shRNA-expressing cells treated with or without ionising radiation, thus suggesting that PTTG depletion has no impact on irradiation-induced mechanisms of growth arrest. In contrast, PBF knockdown led to a significant decrease in 92-VU-040T and 93-VU-147T cell proliferation in the absence of ionising radiation and this was further augmented following treatment with ionising radiation, with irradiated PBF shRNA-transduced 92-VU-040T and 93-VU-147T cells demonstrating a further reduction in cell proliferation of approximately 10-20 % when

compared with irradiated Scr shRNA control cells. However, no significant difference in relative proliferation rates was observed when comparing Scr shRNA-expressing cells vs. PBF shRNA-expressing cells in the presence or absence of ionising radiation, thus suggesting that PBF depletion has no impact on irradiation-induced mechanisms of growth arrest.

The data obtained from these BrdU assays cannot be directly linked to alterations in p53 stability and activity caused by depletion of PTTG or PBF. The lack of difference in sensitivity to ionising radiation observed in both 92-VU-040T and 93-VU-147T cells following PTTG and PBF depletion may therefore be a result of p53-independent mechanisms. In addition, BrdU assays effectively measure DNA synthesis, which does not necessarily correlate with cell viability. It will therefore be important to confirm these findings using more suitable methods and following siRNA-mediated knockdown of p53.

No observable differences in cell survival were noted between 92-VU-040T and 93-VU-147T cell lines after treatment with γ-irradiation. This was a surprising finding, as HPV-positive HNSCC cells are proposed to be more radiosensitive (Kimple et al. 2013, Rieckmann et al. 2013, Dok et al. 2014, Arenz et al. 2014). A possible reason for this discrepancy could be the method and cell models used to determine cell survival. Many of the cited studies used clonogenic survival assays to produce sensitive and accurate measures of cell survival following γ-irradiation, whereas BrdU assays can only provide an indirect measure of cell survival. It has also been suggested that the observed cellular radiosensitivity is likely due to induction of p53-mediated apoptosis (Kimple et al. 2013). Kimple et al. demonstrated upregulation of a number of p53-related genes following irradiation of HPV-positive cell lines when compared to HPV-negative cells and proposed that, despite downregulation of p53 by HPV E6, the remaining functional wild-type p53 could be activated in response to DNA damage, thereby inducing apoptosis (Kimple et al. 2013). The 93-VU-147T cell line has

recently been found to harbour a heterozygous mutation in TP53 (c.770T>G, p.L257R) and, when analysed alongside a panel of HPV-positive cell lines harbouring only wild-type p53, displayed the lowest radiation sensitivity and caspase 3/7 activity following γ-irradiation (Kimple et al. 2013). These factors combined may explain why no difference was observed in our hands.

### 6.4.4 PTTG and PBF gene silencing alters the expression of several p53-related genes in 92-VU-040T and 93-VU-147T cells

To further explore the functional significance of the interaction between PTTG, PBF and p53, expression of a panel of 8 p53-related genes was analysed in stable PTTG or PBF knockdown 92-VU-040T and 93-VU-147T cell lines in the presence and absence of ionising radiation. One of the most common and well-characterised p53-responsive genes is CDKN1A. The CDKN1A gene encodes the potent cyclin-dependent kinase inhibitor, p21, whose expression is induced by p53 in response to DNA damage and leads to p53-mediated G1 cell cycle arrest (Waldman et al. 1995). Surprisingly, PTTG depletion in 92-VU-040T and 93-VU147T cells led to significant repression of CDKN1A mRNA expression following γ-irradiation. Considering the direct interaction between PTTG and p53 and the fact that PTTG overexpression resulted in rapid degradation of p53 protein, knockdown of PTTG would have been expected to cause an increase in irradiation-induced expression of CDKN1A. However, it is possible that the observed reduction in CDKN1A mRNA expression is an indirect effect mediated by endogenous PBF, which is abundantly expressed in both cell lines. Indeed, depletion of PBF in 92-VU-040T and 93-VU-147T cells following exposure to γ-irradiation significantly increased expression of CDKN1A, thus providing support for the above hypothesis and further emphasizing a role for PBF in the negative regulation of p53.

Extensive characterisation of the apoptotic mediators BAX (pro-apoptotic factor) and BCL-2 (anti-apoptotic factor) has established the importance of apoptosis in cellular transformation and tumour development (Frenzel et al. 2009). In HNSCC p53 has been reported to initiate programmed cell death in response to DNA damage by inhibiting expression of BCL-2, thus suggesting a dependence on BCL-2 and not BAX for induction of p53 apoptotic responses following genotoxic insult in HNSCC cells. In accordance with this data, no changes in BAX mRNA expression were observed in 92-VU-040T and 93-VU-147T cells transduced with Scr shRNA, whereas BCL-2 mRNA expression was non-significantly downregulated following treatment of cells with γ-irradiation. Interestingly, PTTG knockdown resulted in significant induction of BCL-2 mRNA expression in 92-VU-040T and 93-VU-147T cells, both in the presence and absence of ionising radiation, although BAX mRNA expression remained unaltered. In contrast, PBF silencing led to a significant reduction in BCL-2 mRNA expression, which was further reduced upon treatment with γ-irradiation.

The observed increase in BCL-2 mRNA expression in PTTG knockdown cells is in accordance with a previous report, where PTTG depletion in murine pituitary glands was associated with elevated levels of BCL-2 protein (Chesnokova et al. 2007). However, as PTTG overexpression resulted in a significant decrease in p53 protein stability in 92-VU-040T and 93-VU-147T cell lines, it was expected that knockdown of PTTG would result in stabilisation of p53 protein levels and subsequent activation following DNA damage. As p53 negatively regulates transactivation of the BCL-2 gene (Basu, Haldar 1998), BCL-2 mRNA levels would have been expected to be reduced in PTTG depleted cells in the presence of ionising radiation. Therefore, the induction of BCL-2 following treatment with γ-irradiation is unlikely to be a result of activation of p53-dependent apoptotic pathways.

The association between PTTG and DNA damage repair (DDR) pathways has been extensively studied (Salehi et al. 2008) and recent research performed by our group revealed that co-expression of PTTG and PBF repressed expression of a significant number of DDR genes in murine thyroctyes, as well as human differentiated thyroid tumours (Read et al. 2016a). Analysis of DDR gene expression in our PTTG and PBF-depleted HNSCC cell lines revealed significant dysregulation of the DDR genes RAD51 and BRCA1. RAD51 is an essential component of the homologous recombination (HR) DNA repair pathway (Baumann, West 1998), while BRCA1 is implicated in the alternative non-homologous end-joining (NHEJ) DNA repair pathway (Bau et al. 2006). Analysis of 93-VU-147T cells with reduced PTTG expression revealed significant induction of RAD51 mRNA expression, whereas expression appeared to be unaltered by PTTG depletion or irradiation in 92-VU-040T cells. RAD51 mRNA expression was also unaffected by PBF depletion or irradiation in 92-VU-040T and 93-VU-147T cells transduced with PBF shRNA. We have previously demonstrated suppression of RAD51 mRNA expression in a transgenic mouse model of thyroid-specific PTTG overexpression (Read et al. 2016a). In addition, Park et al. have revealed dysregulated expression of RAD51 and RAD51 foci formation in HPV-positive cell lines and HPV E6-expressing cells, which was associated with impaired sub-lethal DNA damage repair (Park et al. 2014). It is therefore possible that the observed induction of RAD51 mRNA expression in PTTG depleted 93-VU-147T cells was due to the combined expression of HPV E7 and the loss of PTTG.

When taken together, this set of gene expression data demonstrate that PTTG and PBF depletion leads to dysregulated expression of several important p53-responsive genes. However, as only a small number of genes were affected, it may be that the interactions between PTTG, PBF and p53 have little impact on overall p53 transcriptional activity in 92-

VU-040T and 93-VU-147T HNSCC cell lines. It will be important to assess the effects of PTTG and PBF depletion across a much larger panel of p53-responsive genes, as this will provide a more accurate account of the relative contributions of PTTG and PBF to p53 transcriptional activity. It will also be important to determine whether the observed alterations in gene expression are p53-dependent, as expression of many of the genes analysed can also be regulated in a p53-independent manner.

### 6.4.5 Concluding statements

In the current chapter, we have demonstrated that the proto-oncogenes PTTG and PBF physically interact with p53 and co-operate to alter its protein stability in HPV-positive and HPV-negative HNSCC cell lines. We further defined a potential role for PTTG and PBF in the dysregulation of p53-related gene expression in the presence and absence of genotoxic insult.

# Chapter 7

# Effect of PTTG and PBF gene silencing on the invasiveness of head and neck cancer cells

## 7.1 Introduction

Despite recent advances in the management of recurrent and metastatic HNSCC, the overall survival rate remains less than one year (Price, Cohen 2012). A crucial step in the metastatic process is cellular invasion, which involves the loss of cell-to-cell adhesion, followed by degradation of the basement membrane and subsequent migration of cancerous cells into the surrounding connective tissue or nearby blood or lymphatic vessels (Chambers et al. 2002). DNA microarray expression profiles have highlighted a number of key genetic signatures associated with high-risk metastatic HNSCC, including gene alterations in cell adhesion molecules, intracellular signalling molecules and factors involved in epithelial-to-mesenchymal transition (EMT) (Chung et al. 2006). Among these commonly altered genes is the potent tumour suppressor, p53. As outlined in detail in chapter 6, p53 is activated in response to oncogenic stress and elicits a variety of critical cellular functions, including induction of cell cycle arrest, DNA repair, apoptosis and cell senescence (Levine, Oren 2009). Aside from these well-established roles, p53 has been implicated in the regulation of cell migration, invasion and EMT (Muller et al. 2009, Wang et al. 2009, Mukhopadhyay et al. 2010).

In previous chapters we demonstrated that PTTG and PBF are both overexpressed in human HNSCC. Furthermore, we provided evidence suggesting PTTG and PBF directly interact with, and potentially co-regulate, p53 *in vitro*. A role for PTTG in cell migration and invasion is also well documented. PTTG expression is a strong indicator of tumour invasiveness (Shibata et al. 2002, Boelaert et al. 2003a) and was recognised as a key signature gene in tumour metastasis (Ramaswamy et al. 2003, Carvalho et al. 2011). Many high profile studies have demonstrated that PTTG is an important regulator of cell motility in oesophageal cancer (ESCC) (Ito et al. 2008, Yan et al. 2009), and more recently, oral squamous cell

carcinoma (Zhang et al. 2014). In ESCC cells, PTTG depletion was significantly associated with reduced cell migration *in vitro* and was accompanied by reduced lymph node metastasis *in vivo* (Ito et al. 2008, Yan et al. 2009). Similarly, in oral squamous cell carcinoma, PTTG knockdown resulted in impaired cell motility and invasion (Zhang et al. 2014).

Subsequent studies have revealed upregulated PTTG expression to drive proliferation and migration in cancer cells derived from a variety of tumour types, including prostate (Lin et al. 2015b), colorectal (Zheng et al. 2015), cervical (Chen et al. 2015), and breast (Yoon et al. 2012). This observed pro-invasive behaviour has mainly been attributed to PTTG-mediated activation and secretion of the ECM-degrading matrix metalloproteases (MMP) (Malik, Kakar 2006, Xia et al. 2013, Lin et al. 2015b). However, PTTG has also been shown to orchestrate expression of EMT transcription factors (Shah, Kakar 2011a, Yoon et al. 2012), as well as focal adhesion molecules and integrins (Shah et al. 2012), thereby promoting acquisition of a more migratory phenotype.

Recent *in vitro* evidence has now linked PBF with tumour invasion and metastasis. We previously demonstrated that overexpression of PBF resulted in enhanced breast cancer cell invasion *in vitro* and that this could be abolished by siRNA-mediated silencing or specific mutation of the PBF gene (Watkins et al. 2010). High PBF expression was subsequently associated with high-grade papillary thyroid tumours (Hsueh et al. 2013) and increased PBF promoter activity correlated with poorer prognosis and an increased risk of metastasis in tumours of the breast (Xiang et al. 2012). In addition, higher PBF expression has been identified in colorectal tumours displaying greater extramural vascular invasion (Read et al. 2016b). Li et al. were also able to recapitulate these findings in hepatocellular carcinoma (HCC). PBF expression not only drove HCC cell proliferation, but also induced potent cellular invasion, as assessed by 3D matrigel assay (Li et al. 2013). Furthermore,

simultaneous expression of the microRNA, miR-122, for which PBF is a known target, abrogated these growth-promoting effects (Li et al. 2013). Recent research performed by our group has also sought to challenge our prior findings. In a panel of thyroid, breast and colon cancer cell lines, PBF consistently induced *in vitro* migration and invasion. Importantly, this pro-invasive phenotype was noted across all *in vitro* assays and was contingent upon direct interaction between PBF and the cytoskeletal protein cortactin (Watkins et al. 2016).

Given the apparent roles of PTTG and PBF in cell motility and invasion, we wanted to investigate whether manipulation of PTTG and PBF expression could result in an alteration in the invasive and transforming capacities of HNSCC cells. 3D Boyden chamber invasion assays, classical wound healing assays and colony formation assays were used to this effect.

## 7.2 Methods

### 7.2.1 Cell lines

92-VU-040T and 93-VU-147T cells stably transduced with shRNAs targeting PTTG and PBF were maintained in complete culture medium containing the appropriate antibiotic (Blasticidin® or Puromycin) as described in section 2.1.

### 7.2.2 2D Boyden Chamber Invasion Assay

Growth factor reduced Matrigel®-coated invasion chambers (8 µM pore size) [BD Bioscience, Oxford, UK] were rehydrated by addition of 500 µl of pre-warmed culture medium to the interior of each insert and incubation in a humidified atmosphere at 37 °C and 5 % $CO_2$ for 2 hours. Following rehydration, the medium was removed from the interior of the insert and 0.75 x $10^5$ 92-VU-040T cells or 4 x $10^5$ 93-VU-147T cells seeded into this upper compartment in a total volume of 500 µl of DMEM medium supplemented with either 2

% FBS (92-VU-040T cells) or 10 % FBS (93-VU-147T cells). Immediately after, 750 µl of pre-warmed complete DMEM supplemented with either 10 % FBS (for 92-VU-040T cells) or 20 % FBS (for 93-VU-147T cells) was added to the well below each cell culture insert and the chambers incubated in a humidified atmosphere at 37 °C and 5 % $CO_2$ for 24 or 48 hours. Subsequently, non-invading cells were removed from the upper surface of the insert and the invading cells fixed and stained using Mayer's Haematoxylin [Sigma-Aldrich] and eosin [Sigma-Aldrich]. Invading cells were then analysed by light microscopy at 10X magnification and counted using Image J software.

### 7.2.3 Wound healing Assay

Cells were seeded at 6 x $10^5$ (92-VU-040T) and 7 x $10^5$ (93-VU-147T) cells per well, in triplicate, in 6-well tissue culture plates and incubated overnight at 37 °C and 5 % $CO_2$ to allow cells to adhere. Once suitably confluent, wounds were created using a 10 µl pipette tip to scratch through the centre of each well. The cells were immediately washed with PBS and 2 ml of pre-warmed complete DMEM medium added to each well. The wounds were then imaged using a light microscope at 4X magnification at 4, 8 and 24 hours. Images were then analysed to calculate the area of wound healing using image J software.

### 7.2.4 Colony Formation Assay

Cells were seeded at 1 x $10^4$ cells per well, in duplicate, in 100 mm tissue culture dishes and incubated in a humidified atmosphere at 37 °C and 5 % $CO_2$. After approximately 18-21 days of incubation, colonies were fixed with 100 % methanol [VWR International] for 15 minutes at room temperature and stained with 0.05 % crystal violet [Sigma-Aldrich] for 30

minutes. Excess crystal violet was removed by washing with PBS and the dishes allowed to air-dry.

### 7.2.5 RNA extractions, quantification and quantitative real-time PCR

Stable 92-VU-040T and 93-VU-147T cell lines were seeded at $2.0x10^5$ and $2.5x10^5$ cells per well, respectively. Total RNA was harvested 24 hours later, reverse transcribed to cDNA and analysed by real-time quantitative PCR as described in sections 2.3, 2.4 and 2.5.

### 7.2.6 Protein extraction, quantification and Western blotting

Stable 92-VU-040T and 93-VU-147T cell lines were seeded at $2.0x10^5$ and $2.5x10^5$ cells per well, respectively. Protein was then harvested 24 hours later. Protein extraction, quantification and Western blotting techniques were performed as outlined in section 2.6. Antibodies used were anti-PBF-8 1:500, anti-PTTG 1:750, anti-Y174-phosphorylated PBF 1:1000 and anti-β actin 1:15,000.

### 7.2.7 BrdU cell proliferation assay

Stably transduced 92-VU-040T and 93-VU-147T cells were seeded in parallel with 2D Boyden chamber invasion assays and scratch-wound assays to assess the rate of cell proliferation. Cells were seeded at $4 x10^3$ cells per well in 96-well plates and incubated for 24 hours before conducting the assay as outlined in section 2.9. The absorbance at 405 nm was measured using the Victor$^3$ 1420 Multilabel Counter [PerkinElmer].

### 7.2.8 Statistical analysis

Statistical analysis was performed as described in section 2.12.

## 7.3 Results

### 7.3.1 PTTG gene silencing reduces the invasiveness of 92-VU-040T and 93-VU-147T cells

Overexpression of PTTG is associated with increased tumour invasiveness in multiple settings (Yan et al. 2009, Yoon et al. 2012, Lin et al. 2015b, Read et al. 2016b) and it has been identified as a key metastatic signature gene (Ramaswamy et al. 2003, Carvalho et al. 2011). However, the role of PTTG in the progression of squamous cell carcinomas of the head and neck remains to be distinguished. The impact of PTTG knockdown on head and neck tumour cell invasion was therefore assessed by 2D Boyden chamber invasion assay in 92-VU-040T and 93-VU-147T cells stably transduced to express PTTG shRNA or a scrambled control shRNA.

Cells were seeded onto growth factor-reduced matrigel-coated chambers and incubated for 24-48 hours. Western blot analysis demonstrated a clear reduction in the expression of endogenous PTTG protein (Figure 7.1A). Furthermore, a potent anti-invasive effect of PTTG knockdown was observed in both cell lines (Figure 7.1B). 92-VU-040T cells transduced with PTTG shRNA demonstrated a ~90 % reduction in the mean number of invading cells when compared with scrambled control cells (Figure 7.1B – left panel; 169 ± 3.24 vs. 17 ± 8.21, p=0.003, n=3). Similarly, 93-VU-147T cells transduced with PTTG shRNA displayed an ~85 % decrease in the mean number of invading cells when compared with scrambled shRNA control cells (Figure 7.1B – right panel; 180 ± 23.20 vs. 27 ± 6.23, p=0.0001, n=3).

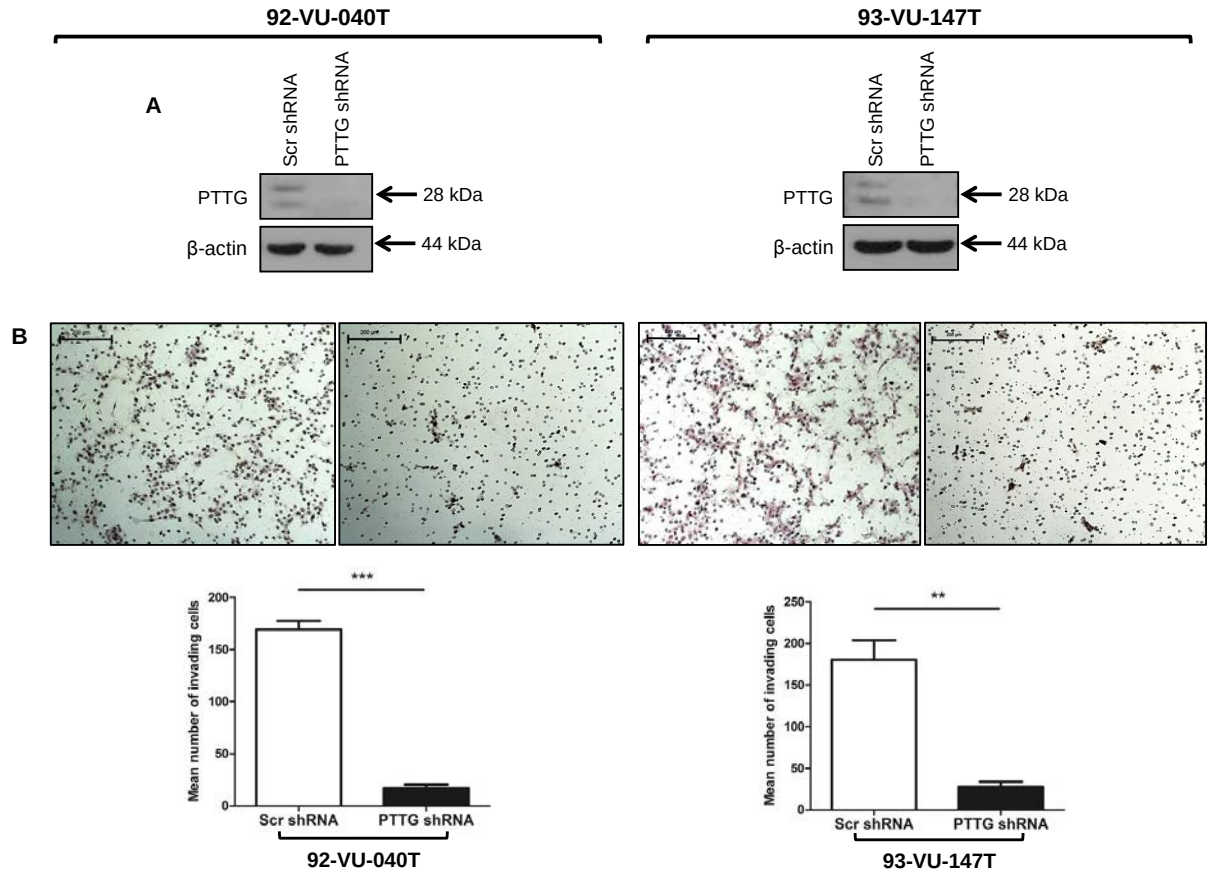


*Figure 7.1 Impaired cell invasion with PTTG depletion.* ***A*** *– Western blots demonstrating successful knockdown of PTTG in 92-VU-040T and 93-VU-147T cells stably transduced with PTTG shRNA.* ***B*** *– Representative 2D Boyden chamber assay images showing the effect of PTTG knockdown on the invasiveness of 92-VU-040T and 93-VU-147T cells. 2D Boyden chamber assays were quantified and the mean number of invading cells displayed below (n=3 experiments). Scale bars = 200 μm. Data presented as mean ± SEM. ** p ≤0.01, *** p ≤0.001.*

### 7.3.2 PBF gene silencing reduces the invasiveness of 92-VU-040T and 93-VU-147T cells

We have previously identified that PBF induces invasion in a number of different cell lines (Watkins et al. 2010, Watkins et al. 2016). To determine whether PBF may also regulate invasion of HNSCC cells we performed additional 2D Boyden chamber invasion assays using 92-VU-040T and 93-VU-147T cells stably transduced to express PBF shRNA or a scrambled shRNA. Western blot analysis confirmed knockdown of endogenous PBF protein expression in both cell lines (Figure 7.2A). Furthermore, both PBF knockdown cell lines lost the ability

to induce cell invasion (Figure 7.2B), albeit to a lesser extent that that observed in the stable PTTG shRNA cell lines. PBF depletion in 92-VU-040T cells resulted in a ~68 % reduction in the mean number of invading cells (Figure 7.2B – left panel; 197 ± 7.11 vs. 64 ± 2.53, p=0.0001, n=3). In 93-VU-147T cells, a decrease in the mean number of invading cells of ~78 % was observed (Figure 7.2B – right panel; 153 ± 14.84 vs. 34 ± 4.38, p=0.0015, n=3).

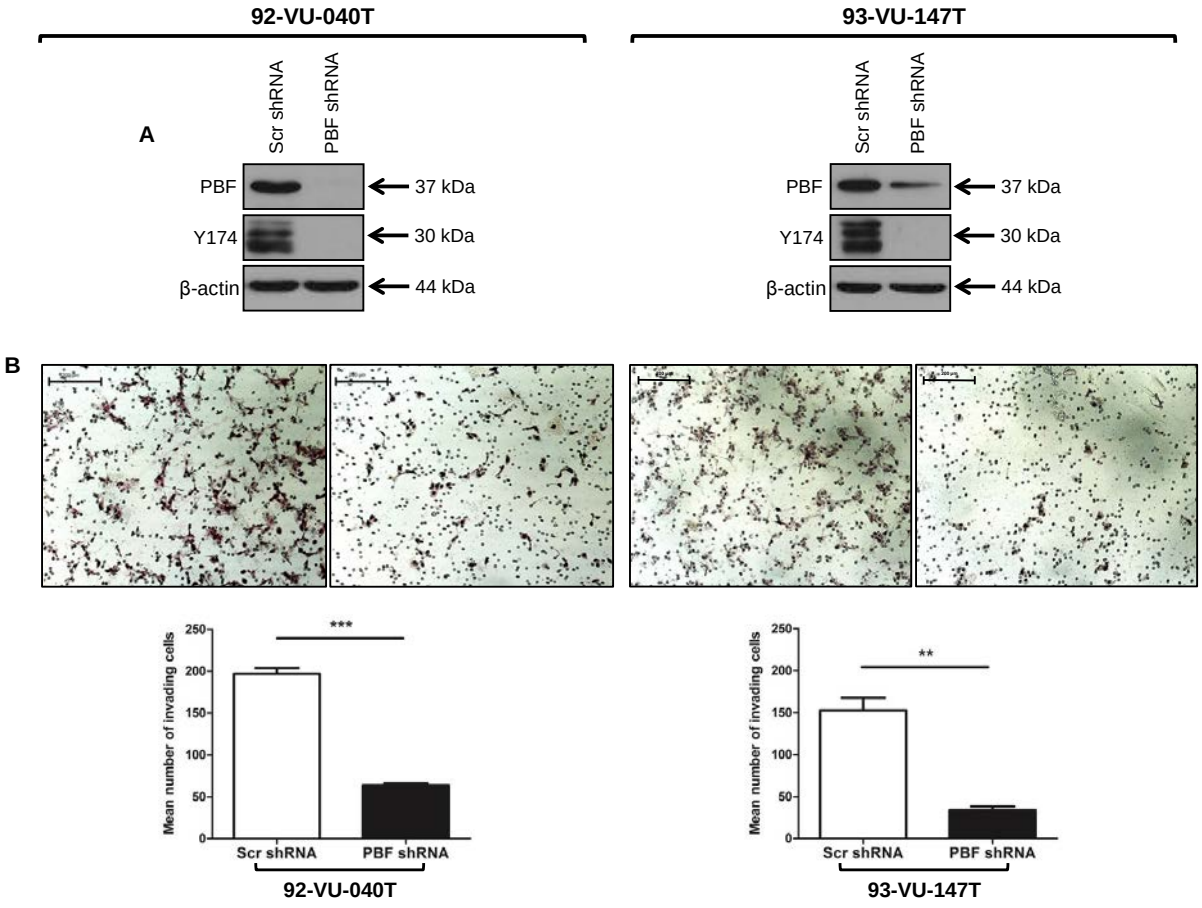


*Figure 7.2 Impaired cell invasion with PBF depletion.* ***A*** *– Western blots demonstrating successful knockdown of PBF in 92-VU-040T and 93-VU-147T cells stably transduced with PBF shRNA.* ***B*** *– Representative 2D Boyden chamber assay images showing the effect of PBF knockdown on the invasiveness of 92-VU-040T and 93-VU-147T cells. 2D Boyden chamber assays were quantified and the mean number of invading cells displayed below (n=3 experiments). Scale bars = 200 µm. Data presented as mean ± SEM. ** p ≤0.01, *** p ≤0.001.*

### 7.3.3 PTTG gene silencing impairs cell motility in 92-VU-040T and 93-VU-147T cells

As cell migration is an integral part of the cell invasion process, we next sought to determine the effects of PTTG gene silencing on 92-VU-040T and 93-VU-147T cell migration. To this end, classical wound healing assays were performed. Stably transduced 92-VU-040T and 93-VU-147T cells expressing either PTTG shRNA or scrambled shRNA were seeded in 6-well plates and incubated for 24 hours to allow the cells to form a confluent monolayer. A micropipette tip was then used to create a 'wound'. The doubling time for 92-VU-040T cells is approximately 20-25 hours, whereas, the doubling time for 93-VU-147T cells is 35-40 hours. For this reason, the wound area was imaged at 0, 4 and 8 hours for 92-VU-040T cells and at 0, 4, 8 and 24 hours for 93-VU-147T cells.

Stable 92-VU-040T and 93-VU-147T cells with reduced PTTG expression, as demonstrated by Western blot (Figure 7.3), displayed an impaired ability to migrate into the wound (Figure 7.4 and Figure 7.5). In the scrambled controls, the wound area was almost completely closed by 8 and 24 hours in 92-VU-040T (Figure 7.4A) and 93-VU-147T (Figure 7.5A) cells, respectively. In contrast, PTTG-depleted 92-VU-040T and 93-VU-147T cells were unable to migrate effectively to close the wound. Image J was used to further quantify wound closure at the various time points. PTTG knockdown resulted in a significant decrease in migratory ability of approximately 60 % in 92-VU-040T cells at 8 hours (Figure 7.4B; 54 % ± 5.51 vs. 22 % ± 3.93, $p<0.01$, $n=3$) and 30 % in 93-VU-147T cells at 24 hours (Figure 7.5B; 70 % ± 3.61 vs. 49 % ± 2.96, $p<0.001$, $n=3$), when compared to the scrambled controls.

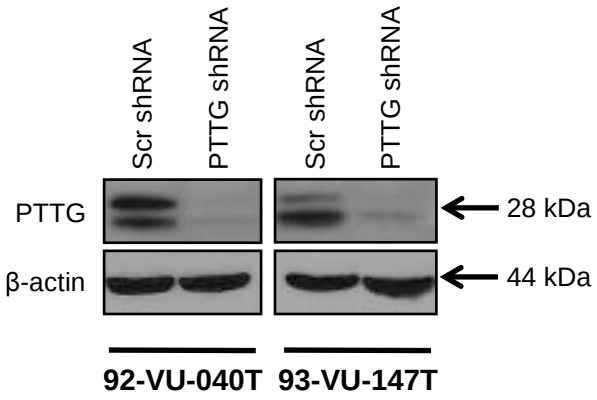


*Figure 7.3 Successful shRNA-mediated knockdown of PTTG protein expression. Western blots demonstrating successful knockdown of PTTG protein in 92-VU-040T and 93-VU-147T cells stably transduced with PTTG shRNA.*

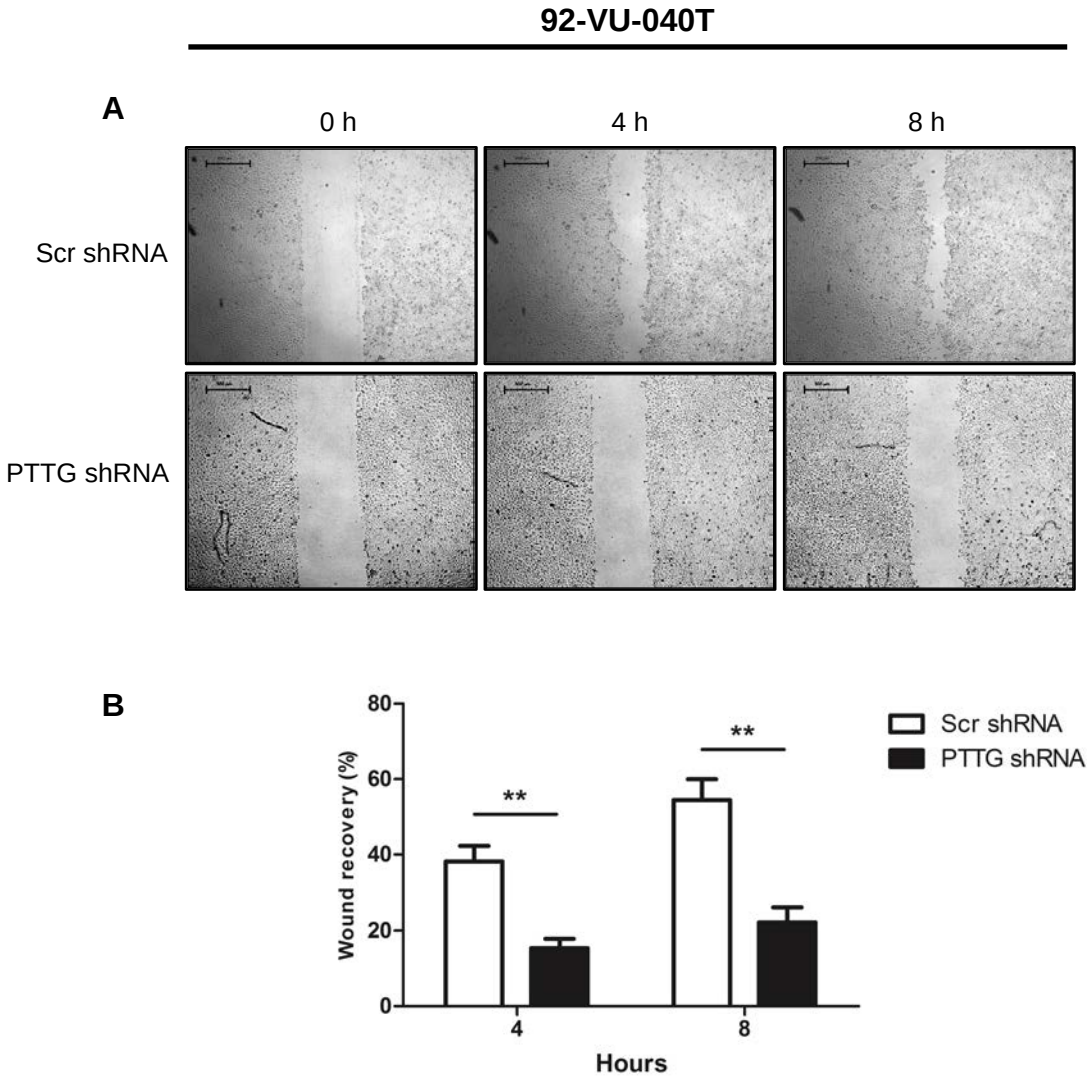


*Figure 7.4 Reduced cell motility with PTTG depletion in 92-VU-040T cells.* ***A*** *– Representative wound healing assay images, taken at 0, 4 and 8 hours after wound creation, showing the effect of PTTG knockdown on 92-VU-040T cell motility.* ***B*** *– Wound healing assays were quantified and the percentage wound recovery displayed below (n=3 experiments). Scale bars = 500 µm. Data presented as mean ± SEM. ** p ≤0.01.*

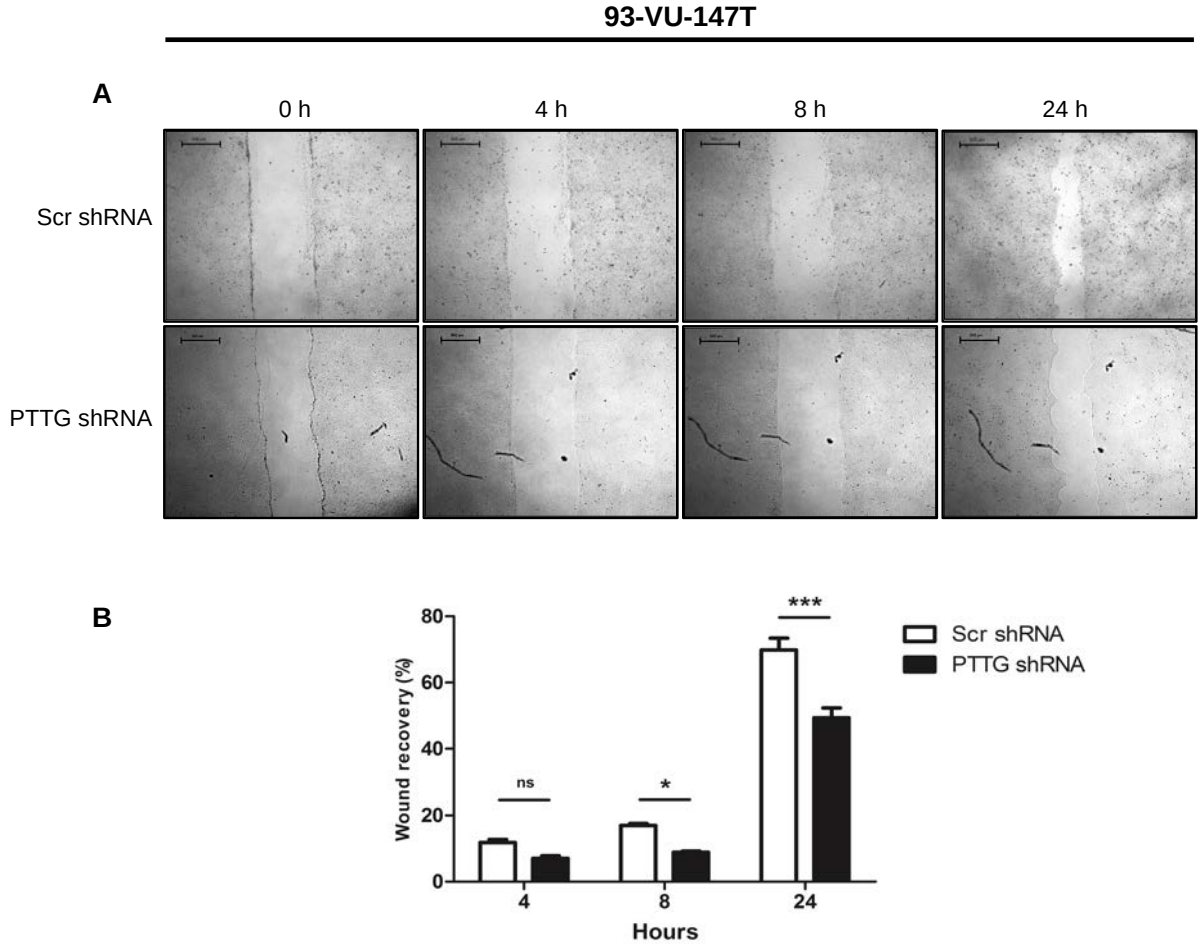


*Figure 7.5 Reduced cell motility with PTTG depletion in 93-VU-147T cells.* ***A*** *– Representative wound healing assay images, taken at 0, 4, 8 and 24 hours after wound creation, showing the effect of PTTG knockdown on 93-VU-147T cell motility.* ***B*** *– Wound healing assays were quantified and the percentage wound recovery displayed below (n=3 experiments). Scale bars = 500 µm. Data presented as mean ± SEM. ns = non-significant, * p ≤0.05, *** p ≤0.001.*

### 7.3.4 PBF gene silencing impairs cell motility in 92-VU-040T and 93-VU-147T cells

The effect of PBF knockdown was also assessed in stable 92-VU-040T and 93-VU-147T cells. PBF depletion, as confirmed by Western blot (Figure 7.6), was also associated with loss of migratory capacity in both cell lines (Figure 7.7A and Figure 7.8A). As demonstrated in Figure 7.7 and Figure 7.8, scrambled control cells migrated more effectively to close the wound when compared with the stable PBF shRNA cells. Further quantification of the wound areas found that PBF knockdown resulted in a ~36 % reduction in wound recovery in 92-VU-

040T cells after 8 hours (Figure 7.7B; 69 % ± 5.42 vs. 44 % ± 4.17, $p<0.01$, n=3) and a ~27 % reduction in wound recovery in 93-VU-147T cells after 24 hours (Figure 7.8B; 71 % ± 0.76 vs. 52 % ± 0.55, $p<0.001$, n=3).

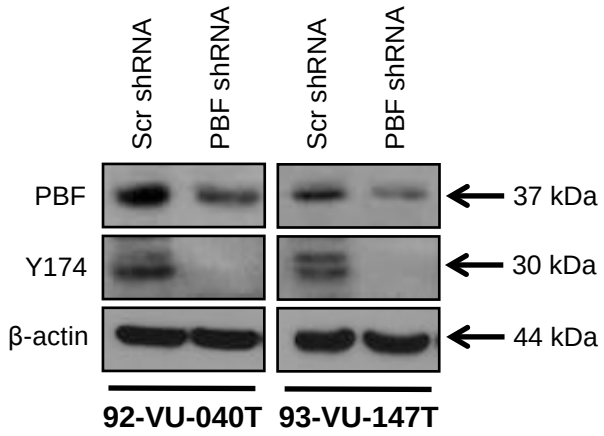


*Figure 7.6 Successful shRNA-mediated knockdown of PBF protein expression. Western blots demonstrating successful knockdown of PBF protein in 92-VU-040T and 93-VU-147T cells stably transduced with PBF shRNA.*

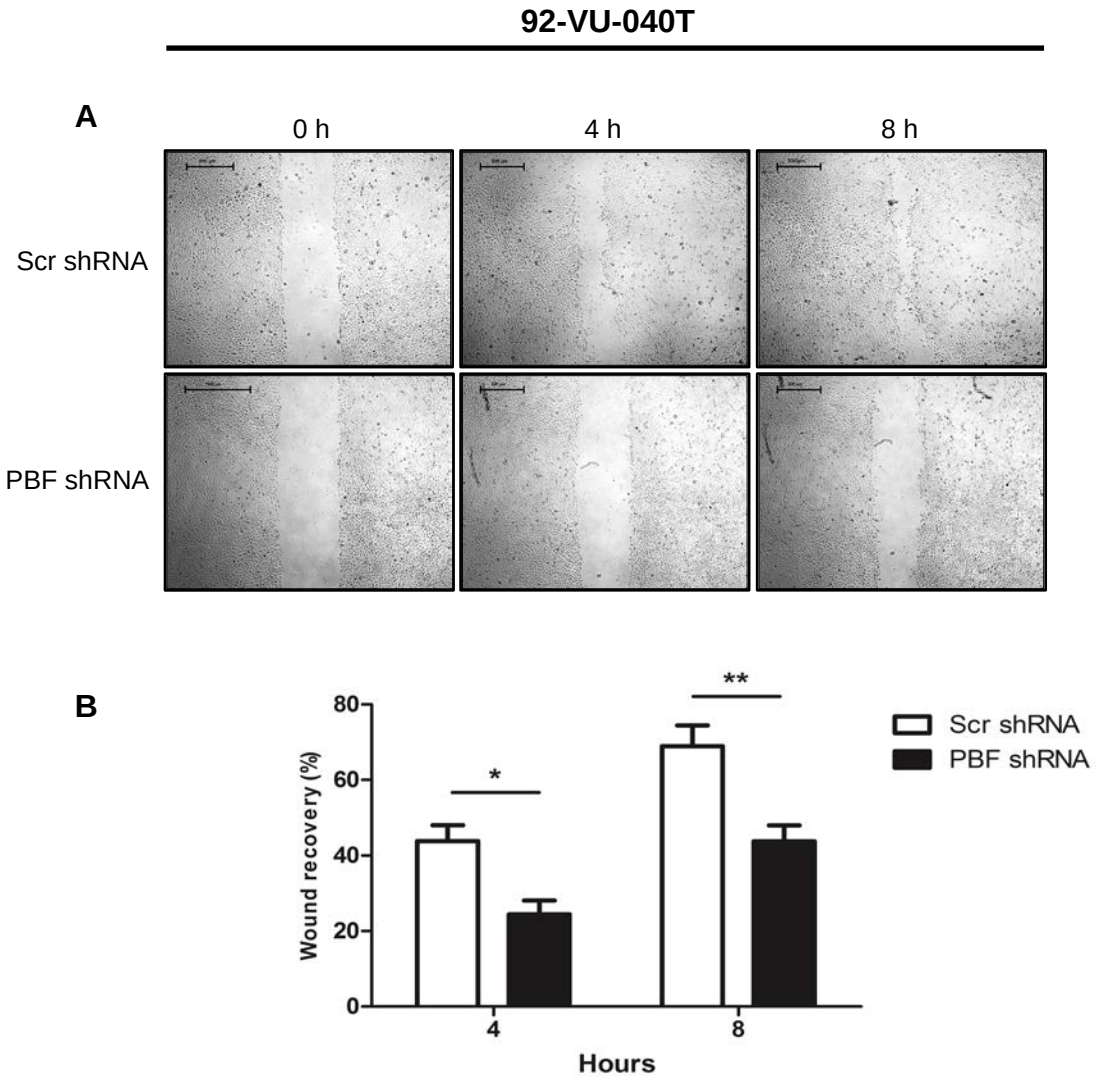


*Figure 7.7 Reduced cell motility with PBF depletion in 92-VU-040T cells.* ***A*** *– Representative wound healing assay images, taken at 0, 4 and 8 hours after wound creation, showing the effect of PBF knockdown on 92-VU-040T cell motility.* ***B*** *– Wound healing assays were quantified and the percentage wound recovery displayed below (n=3 experiments). Scale bars = 500 µm. Data presented as mean ± SEM. * p ≤0.05, ** p ≤0.01.*

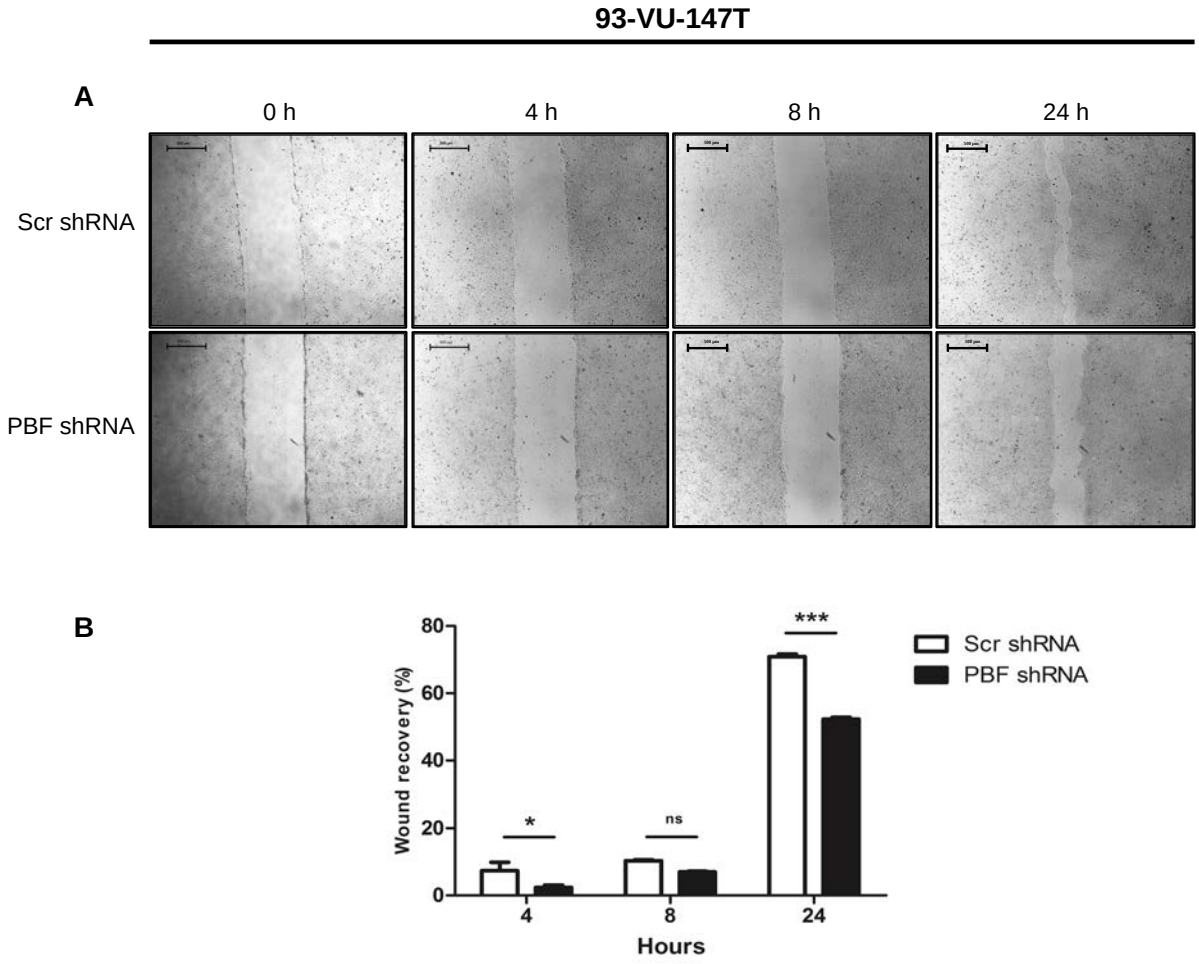


*Figure 7.8 Reduced cell motility with PBF depletion in 93-VU-147T cells.* ***A*** *– Representative wound healing assay images, taken at 0, 4, 8 and 24 hours after wound creation, showing the effect of PBF knockdown on 93-VU-147T cell motility.* ***B*** *– Wound healing assays were quantified and the percentage wound recovery displayed below (n=3 experiments). Scale bars = 500 µm. Data presented as mean ± SEM. ns = non-significant, * p ≤0.05, *** p ≤0.001.*

### 7.3.5 The reduced invasive and migratory capacities of stably transduced 92-VU-040T and 93-VU-147T cells are not due to altered cellular proliferation

At the time of seeding cells for 2D Boyden chamber cell invasion assays and wound healing assays, stably transduced 92-VU-040T and 93-VU-147T cells were also seeded for BrdU cell proliferation assays. BrdU assays were performed to determine whether changes in cellular proliferation associated with PTTG or PBF knockdown might affect interpretation of the cell invasion and migration assays. In 92-VU-040T ($p=0.02$, $n=3$) and 93-VU-147T ($p=0.02$, $n=3$) cells, stable knockdown of PTTG, led to a significant increase in cell proliferation, which was similar to that observed in previous chapters (Figure 7.9A). In contrast, stable PBF knockdown in 92-VU-040T ($p=0.006$, $n=3$) and 93-VU-147T ($p=0.003$, $n=3$) cells led to a decrease in cell proliferation, again, similar to that observed in previous chapters (Figure 7.9B).

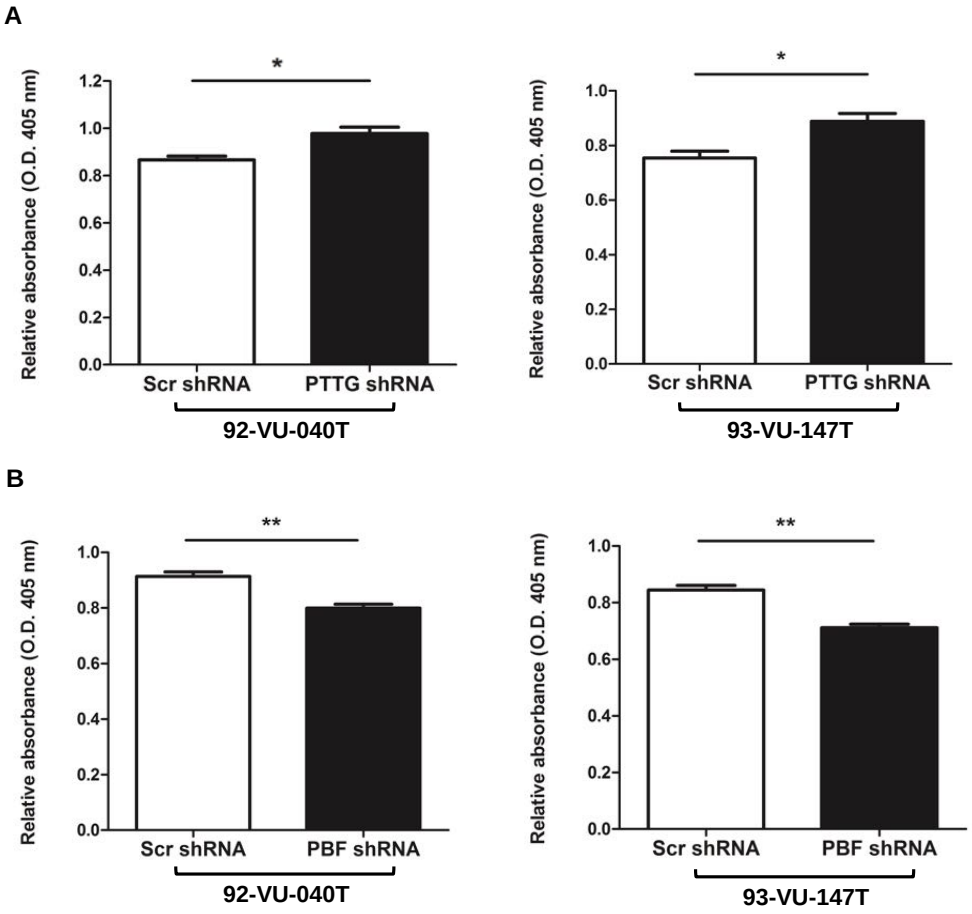


*Figure 7.9 The effect of PTTG and PBF gene silencing on cellular proliferation in 92-VU-040T and 93-VU-147T cells seeded for invasion and wound healing assays as assessed by BrdU assay. 92-VU-040T and 93-VU-147T cells stably transduced with either scrambled shRNA or PTTG shRNA (**A**), or scrambled shRNA and PBF shRNA (**B**) (n=3 with 8 replicates). Data presented as mean ± SEM. * p ≤0.05, ** p ≤0.01.*

### 7.3.6 PTTG gene silencing reduces the colony forming ability of 92-VU-040T and 93-VU-147T cells

Overexpression of PTTG has previously been shown to induce cell transformation *in vitro* (Pei, Melmed 1997, Boelaert et al. 2004, Stratford et al. 2005). To examine the influence of PTTG knockdown in our stable PTTG shRNA HNSCC cell lines, we performed colony formation assays. Although only preliminary experiments, PTTG knockdown led to a marked decrease in the number of colonies formed by both 92-VU-040T and 93-VU-147T stable PTTG shRNA cells when compared to the scrambled controls (Figure 7.10). Interestingly, in

PTTG shRNA-transduced 92-VU-040T cells, the colonies formed were strikingly larger than those formed by scrambled control-transduced 92-VU-040T cells.

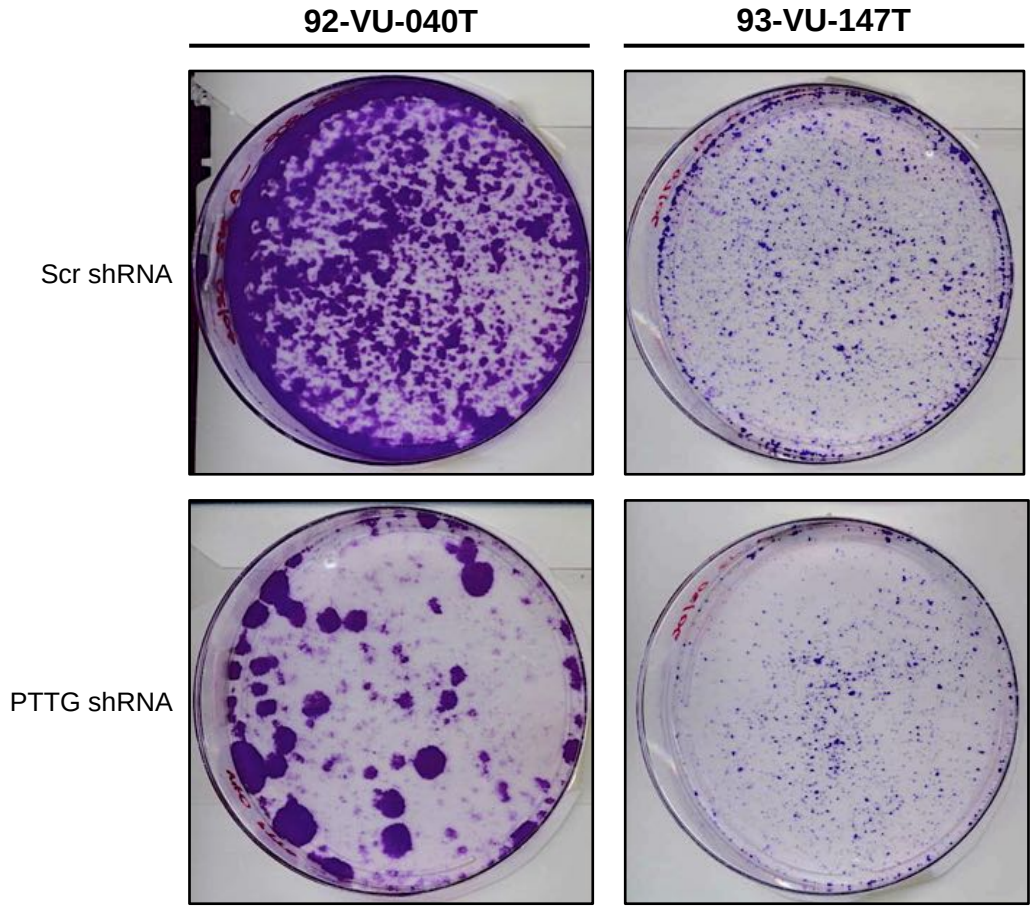


*Figure 7.10 Potentially impaired transforming ability of 92-VU-040T and 93-VU-147T cells upon depletion of PTTG. Representative colony formation assay images of 92-VU-040T and 93-VU-147T cells stably transduced with Scr shRNA or PTTG shRNA (n=3 experiments with 2 replicates).*

### 7.3.7 PBF gene silencing reduces the colony forming ability of 92-VU-040T and 93-VU-147T cells

Overexpression of PBF has also been documented to result in cell transformation *in vitro* (Stratford et al. 2005). We therefore examined the effect of stable PBF knockdown on colony formation in our PBF shRNA-expressing HNSCC cell lines. PBF depletion led to a marked

reduction in the number of colonies formed by 92-VU-040T and 93-VU-147T stable PBF shRNA cell lines when compared with scrambled control cells (Figure 7.11).

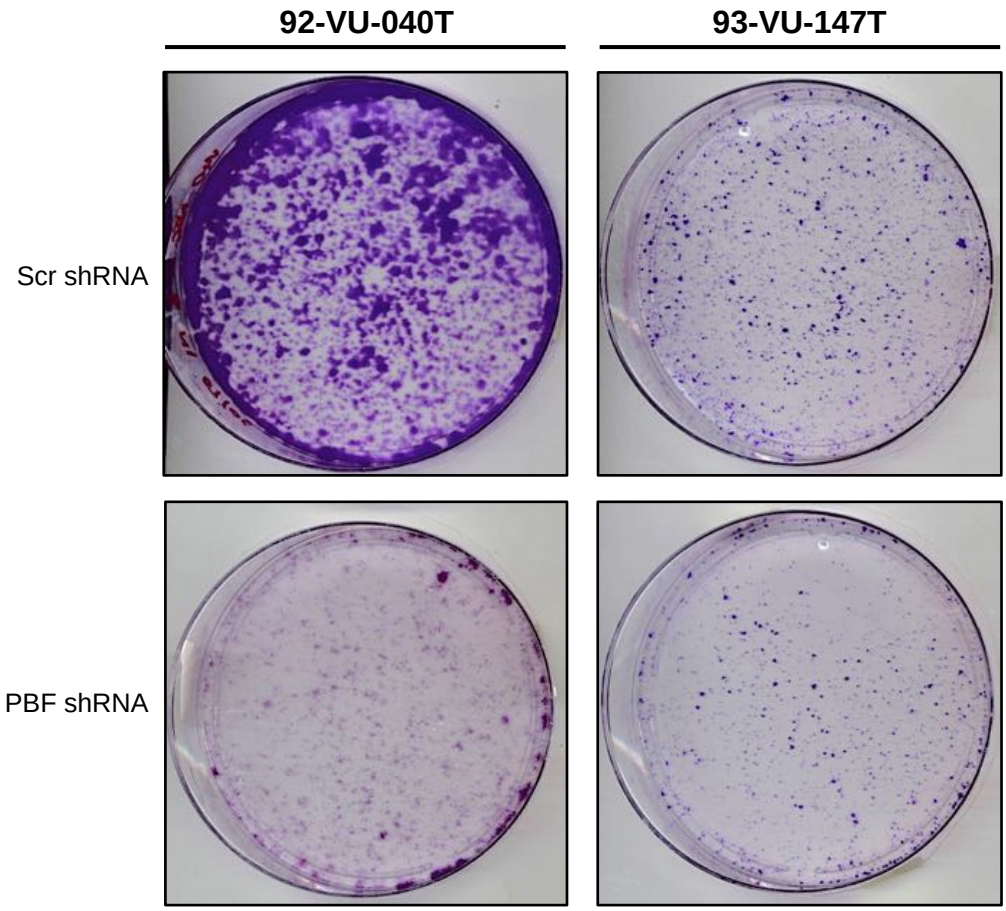


*Figure 7.11 Potentially impaired transforming ability of 92-VU-040T and 93-VU-147T cells upon depletion of PBF. Representative colony formation assay images of 92-VU-040T and 93-VU-147T cells stably transduced with Scr shRNA or PBF shRNA (n=3 experiments with 2 replicates).*

## 7.4 Discussion

### 7.4.1 PTTG and PBF gene silencing impairs 92-VU-040T and 93-VU-147T cell migration and invasion

Cell migration and invasion are imperative in the early stages of tumour metastasis. Previously, the proto-oncogene PTTG, and its binding partner, PBF, have been shown to induce potent cell migration and invasion in several tumour settings (Ito et al. 2008, Watkins

et al. 2010, Chen et al. 2015, Watkins et al. 2016). Similarly, in this chapter we have demonstrated that PTTG and PBF play an important role in regulating HNSCC cell motility and invasion. Silencing of PTTG or PBF in HPV-negative 92-VU-040T and HPV-positive 93-VU-147T cells, achieved through lentiviral transduction of gene-specific shRNAs, resulted in a marked reduction in the invasive capacity of both stable cell lines. In addition, stably transduced 92-VU-040T and 93-VU147T cells displayed impaired cell motility, as assessed by classical wound healing assays.

BrdU cell proliferation assays were performed in parallel to assess whether the observed decrease in cell invasiveness was the result of altered cellular proliferation in response to PTTG or PBF depletion. Both 92-VU-040T and 93-VU-147T cells with reduced PTTG expression displayed a modest but significant increase in cell proliferation of 1.1-fold and 1.2-fold, respectively. Therefore, the reduced cell invasion and migration, demonstrated by 2D Boyden chamber invasion assays and wound healing assays, in stable PTTG shRNA cell lines was unlikely to be a direct result of altered cell proliferation. In contrast, PBF knockdown led to a marginal 0.9-fold decrease in the rate of cell proliferation in both stable PBF shRNA cell lines. When compared to the degree of repression of invasion and migration in the stable cell lines, the reduction in cell proliferation is highly unlikely to be a major contributing factor.

Head and neck squamous cell carcinomas can be subdivided into two categories; HPV-positive and HPV-negative. Both are now recognised as distinct tumour subtypes and display vastly different biological and clinical outcomes (Gillison 2004, Ang et al. 2010). In recent years, HPV infection has been associated with enhanced head and neck tumour cell migration and invasion (Jung et al. 2013, Lee et al. 2015). However, we did not observe any significant differences in cellular invasion in scrambled shRNA-transduced HPV-positive 93-VU-147T cells as compared to scrambled shRNA-transduced HPV-negative 92-VU-040T cells.

Furthermore, no observable difference was noted between 93-VU-147T and 92-VU-040T cells transduced with either PTTG shRNA or PBF shRNA.

The tumour microenvironment, in addition to harbouring tumour cells, consists of a number of components, such as immune cells, fibroblasts, endothelial cells, growth factors, cytokines and collagen, all of which have a profound effect on the functional properties of the tumour cells, including their ability to effectively migrate and invade surrounding tissues (Petras et al. 2010). Therefore, the majority of 2D *in vitro* cell migration assays, including those used in the present study, have limited physiological relevance as they capture only specific aspects of the tumour microenvironment. This may, in part, help to explain the lack of observable differences between 93-VU-147T and 92-VU-040T cells.

These conflicting results may also be attributed to the fact that many of the studies examining the influence of HPV infection on HNSCC cell migration and invasion were performed in cell lines transfected with HPV E6 and/or E7, rather than using cell lines derived from HPV-positive tumours. Whilst this may overcome the inherent variability associated with use of cell lines derived from different patients and may thus enable direct comparison of the effects of HPV E6/E7, it may not provide a true representation of HPV infection. For example, the less-well characterised HPV oncoprotein, E5, is known to exert weak tumourigenic activity in a manner independent of E6 and E7 function (Leechanachai et al. 1992, Tsao et al. 1996). Furthermore, studies in HPV-related cervical and tonsillar squamous cell carcinoma have highlighted HPV DNA integration into the host genome as a critical event in HPV-induced carcinogenesis, affecting both viral and host gene expression (Wentzensen et al. 2004, Mooren et al. 2013).

It is becoming increasingly apparent that HPV-related HNSCCs are a biologically heterogeneous group and this is most likely reflected in HPV-positive cell lines too (Lechner

et al. 2013, Keck et al. 2015). Keck et al. recently analysed a clinically homogenous population of loco-regionally advanced HNSCCs, enriched for HPV-positive tumours, and revealed that HPV-related HNSCC could be further divided into two distinct subtypes based on gene expression profiles (Keck et al. 2015). HPV-positive HNSCC subgroups have also been identified based on unique epigenetic signatures and, importantly, were found to have differing prognostic features (Lechner et al. 2013). As a result, our findings will likely need to be challenged in a larger panel of HPV-positive and HPV-negative HNSCC cell lines, preferably those derived from the same tumour sub-site and with similar demographic and clinicopathological characteristics. However, whilst the use of clinically homogeneous cell lines may help to delineate the most common molecular mechanisms involved in the etiology of HNSCC, important insights into the complexity of this disease may be missed.

Despite a growing number of reports implicating PTTG and PBF in the regulation of cell motility, the mechanisms underlying their involvement in this process are yet to be clarified. Matrix metalloproteinases (MMP) represent an important class of proteolytic enzymes that mediate breakdown of the basement membrane and extracellular matrix, thereby paving the way for tumour cells to invade and metastasise. Among them, MMP-2 and MMP-9 have been identified as particularly important in tumour angiogenesis and metastasis, as they are responsible for the cleavage of type IV collagen, a key structural component of the basement membrane (Stamenkovic 2000). One potential mechanism by which PTTG is thought to promote tumour cell invasion is via modulation of MMP expression and secretion (Malik, Kakar 2006, Xia et al. 2013, Lin et al. 2015b). Conditioned medium from HEK293 cells transfected with PTTG was capable of inducing human umbilical vein endothelial cell (HUVEC) migration, invasion and tube formation (Malik, Kakar 2006). Importantly, pre-treatment with an anti-MMP-2 antibody significantly repressed these effects (Malik, Kakar

2006), suggesting modulation of MMP secretion by PTTG. In addition, expression of MMP-2, MMP-9 and MMP-13 have been shown to be significantly reduced in cutaneous squamous cell carcinoma and prostate cancer cell lines following RNAi-mediated PTTG knockdown, and was further associated with impaired cell migration and invasion (Xia et al. 2013, Lin et al. 2015b).

Given that these effects have been observed across several tumour types, PTTG modulation of MMPs, and their related signalling pathways, may represent a critical mechanism by which PTTG promotes tumour invasion and metastasis. With this in mind, it is perceivable that the observed reduction in invasiveness in our stable PTTG knockdown HNSCC cell lines is, at least in part, due to repressed MMP expression/secretion and warrants further investigation. Indeed, altered MMP-2 expression has been noted in oesophageal and oral squamous cell carcinoma cells following transfection with PTTG or PTTG-specific siRNA (Yan et al. 2009, Zhang et al. 2014). Furthermore, diminished secretion of tissue inhibitor of metalloproteinase (TIMP) family members, TIMP-1 and TIMP-2, has been recognised in oesophageal cancer cells overexpressing PTTG (Yan et al. 2009).

PTTG has also been linked to epithelial-to-mesenchymal transition. EMT was first identified as a crucial process that occurs during embryonic development but has since been associated with tumour progression and metastasis (Thiery et al. 2009). It is a multi-step process in which epithelial cells shed their epithelial characteristics and adopt a more mesenchymal phenotype. During this process, cell-to-cell adhesion is abrogated and cells undergo extensive cytoskeletal remodelling. As a consequence of these molecular alterations, the cells lose polarity and assume a spindle-like morphology, which ultimately enables tumour cell movement through the basement membrane and invasion of the surrounding lymphatic or blood vessels. PTTG overexpression in breast and ovarian cancer cells is

purported to be necessary for the acquisition of these spindle-like migratory properties (Shah, Kakar 2011a, Yoon et al. 2012). Overexpression of PTTG in breast cancer cells promoted invasion in trans-well invasion assays and was followed by suppression of the epithelial marker, E-cadherin, and a concomitant increase in expression of the mesenchymal markers, N-cadherin and vimentin (Yoon et al. 2012). Down-regulation of E-cadherin and induction of vimentin was also observed in ovarian cancer cells overexpressing PTTG (Shah, Kakar 2011a). In addition, the EMT transcription factors, Twist, Snail and Slug were found to be upregulation in these cells, further supporting a role for PTTG in the EMT process (Shah, Kakar 2011a). Although the influence of PTTG expression on EMT has not previously been examined in the setting of head and neck tumourigenesis, it may represent an additional pro-invasive mechanism employed by PTTG.

The mechanisms of PBF-induced cell migration and invasion, however, are only just being uncovered. Through extensive mass spectrometry we have identified the cytoskeletal protein, cortactin, as an interacting partner of PBF (Watkins et al. 2016). The principle role of cortactin is to regulate the actin-nucleating Arp2/3 complex (Weaver et al. 2001). When activated in response to external stimuli, cortactin directly activates the Arp2/3 complex and facilitates the Arp2/3-mediated stabilisation of F-actin filament branches (Weaver et al. 2001). In this manner, cortactin helps drive formation of specialised membrane protrusions at the leading edge of migrating cells (Ayala et al. 2008). Immunofluorescence and proximity ligation experiments confirmed co-localisation of PBF and cortactin, particularly at the leading edge (Watkins et al. 2016). Further co-immunoprecipitation assays confirmed direct binding between PBF and cortactin *in vitro* and identified Src-mediated phosphorylation of PBF at residue Y174 as critical to the functional interaction between these two proteins (Watkins et al. 2016). Importantly, 2D Boyden chamber invasion assays performed in a panel

of thyroid, breast and colorectal cancer cell lines demonstrated that depletion of cortactin protein expression ameliorated the ability of PBF to induce cell invasion (Watkins et al. 2016). This suggests that PBF induction of cell invasion is entirely driven by, and dependent on, the presence of functional cortactin.

Cortactin is frequently amplified in head and neck squamous cell carcinomas (~30 % of cases) (Schuuring et al. 1993, Schuuring 1995). Furthermore, overexpressed cortactin has been linked with advanced disease stage, tumour recurrence and disease-free survival in a series of human head and neck squamous cell carcinomas (Rodrigo et al. 2000), and has been reported to promote oesophageal cancer cell motility *in vitro*, as well as, tumour growth *in vivo* (Luo et al. 2006). Thus, it is plausible that attenuation of PBF protein expression in 92-VU-040T and 93-VU-147T cells indirectly abrogates cell invasion by impairing sequestration and subsequent activation of cortactin, by Src, at the plasma membrane.

Recent studies have identified a novel aspect of p53 function, namely in the regulation of cell migration and invasion. Stable expression of mutant forms of p53, frequently found in human cancers, has been shown to promote cell migration and invasion by boosting integrin and epidermal growth factor receptor (EGFR) trafficking to the plasma membrane (Muller et al. 2009). In addition, wild-type p53 has been demonstrated to suppress cancer cell invasion by promoting MDM2-mediated degradation of Slug, a key transcriptional repressor involved driving EMT (Wang et al. 2009). However, expression of mutant p53 was capable of repressing MDM2 expression, thereby allowing accumulation of Slug and subsequent induction of EMT (Wang et al. 2009). In murine models of HNSCC, loss of p53 is associated with a more aggressive, metastatic phenotype and results in rapid tumour formation in all mice (Ku et al. 2007). Furthermore, in an orthotopic murine model of oral squamous cell carcinoma, injection of mice with head and neck cancer cell lines harbouring various TP53

mutations leads to more aggressive tumour growth, increased incidence of lymph node metastases and reduced survival (Sano et al. 2011). Collectively, these studies suggest a potential anti-invasive function of p53 in the specific setting of head and neck cancer too. Indeed, p53 mutational status has been shown to modulate EMT in a panel of head and neck squamous cell carcinoma cell lines via NF-κB signalling (Lin et al. 2015a). In addition, microRNA-34a expression is frequently downregulated in head and neck cancers and leads to enhanced tumour growth, EMT and angiogenesis (Kumar et al. 2012, Sun et al. 2015). MicroRNA-34a is a known target of p53 and loss of p53 function, via mutation or inactivation, has been shown to result in a rise in microRNA-34a expression and Snail-dependent induction of EMT (Kim et al. 2011).

Therefore, based on these observations, the ability of PTTG and PBF to bind and modulate p53 protein stability may represent a final mechanism by which PTTG and PBF may promote HNSCC cell migration and invasion. However, it is important to note that the 93-VU-147T cell line contains a heterozygous mutation in the TP53 gene (c.770T>G, p.L257R), which renders p53 non-functional. However, they demonstrated a similar degree of reduced invasiveness in the absence of PTTG or PBF when compared with the 92-VU-040T cell line, which is wild-type for p53. It is therefore likely that additional mechanisms of PTTG-/PBF-induced cell migration and invasion are involved and may compensate for loss of p53 functionality in the 93-VU-147T cells.

Although beyond the scope of this body of work, it will be important to determine the precise mechanisms underlying PTTG- and PBF-induced invasion in head and neck cancer. It will also be necessary to determine the extent to which they interact to modulate HNSCC cell invasion. Many of the key functions of PTTG require its presence in the nucleus. PBF, which contains a bipartite nuclear localisation signal (NLS) sequence, was initially identified as an

interacting partner of PTTG (Chien, Pei 2000) This interaction was subsequently found to facilitate PTTG translocation from the cytoplasm to the nucleus (Chien, Pei 2000). Thus, it is possible that the reduction in cell invasion observed in our HNSCC cell lines following PBF knockdown is the result of a decrease in the nuclear transport and ensuing transcriptional activity of PTTG, rather than an independent effect of PBF gene silencing. Using mutant forms of PTTG and PBF, which are unable to interact with one another, may facilitate assessment of the precise contributions of both proto-oncogenes in HNSCC cell invasion.

### 7.4.2 PTTG and PBF gene silencing reduces the colony forming abilities of 92-VU-040T and 93-VU-147T cells

Previous investigations by our group and others have demonstrated overexpression of PTTG (Pei, Melmed 1997, Boelaert et al. 2004, Stratford et al. 2005) and PBF (Stratford et al. 2005) to induce mouse NIH3T3 fibroblast cell transformation *in vitro*. To determine the impact of PTTG or PBF knockdown on the transforming potential of HNSCC cell lines, we performed colony formation assays in our 92-VU-040T and 93-VU147T head and neck cell lines stably transduced with either PTTG-specific shRNA or PBF-specific shRNA. Preliminary experiments demonstrated a clear repression of the colony forming ability of both cell lines following PTTG and PBF gene silencing. Whilst these data indicate a role of PTTG and PBF in HNSCC cell survival and colony formation, they do not directly address their potential roles as potent transforming genes in HNSCC.

Anchorage dependence refers to the need for cells to be attached to, or in contact with, a stable surface in order for them to survive and initiate cell division. When grown in a monolayer, normal cells become growth arrested if they come into contact with each other at high density. This regulatory process is known as contact inhibition and is often dysregulated

during tumourigenesis, thereby enabling malignant transformed cells to grow in an anchorage-independent manner and without the need for stimulation by external triggers. The soft agar assay is a well-established *in vitro* assay used to evaluate this capability of transformed cells in response to various conditions. Therefore, in order to examine the transforming effects of PTTG and PBF in our stably transduced HNSCC cell lines, further soft agar assays will need to be performed.

### 7.4.3 Concluding Statements

Attenuation of PTTG or PBF protein expression abrogates cellular migration and invasion in HPV-negative and HPV-positive HNSCC cell lines. In addition, colony formation is impaired following PTTG and PBF knockdown. Overexpression of PTTG and/or PBF therefore present important aetiological events in the progression of HNSCC and may serve as therapeutic targets to prevent further development of metastatic disease.

# Chapter 8

# Final conclusions and future directions

The research presented in this thesis described investigations into the relationship between the functionally related proto-oncogenes PTTG and PBF and the tumour suppressor protein p53, with a particular focus on head and neck squamous cell carcinoma. Investigations were founded on the observation that p53 is frequently mutated in HNSCC tumours (Petitjean et al. 2007, Zhou et al. 2016) or is inactivated by other mechanisms, including HPV E6 oncoprotein expression (Scheffner et al. 1990), thus alluding to the importance of functionally active p53 in the suppression of HNSCC tumour initiation and progression. Given that PTTG and PBF are known to modulate p53 metabolism and function in several tumour settings (Bernal et al. 2002, Read et al. 2014, Read et al. 2016a, Read et al. 2016b) and the numerous reports demonstrating PTTG overexpression in head and neck cancer (Shibata et al. 2002, Zhou et al. 2005, Solbach et al. 2006, Ito et al. 2008, Yan et al. 2009, Zhang et al. 2013), we hypothesised that the interacting partners PBF and PTTG are overexpressed in HNSCC tumours and high tumoural expression significantly correlates with poor clinical outcome. We further hypothesised that PTTG and PBF bind to p53 and induce its rapid turnover in the setting of head and neck cancer, thereby disrupting its tumour suppressor activity and promoting HNSCC tumourigenesis and progression.

## 8.1 PTTG and PBF are overexpressed in HNSCC tumours

Overexpression of PTTG has been documented in numerous malignancies including breast (Solbach et al. 2004), pituitary (McCabe et al. 2003), thyroid (Boelaert et al. 2003a) and colon (Heaney et al. 2000) cancer. Several publications have also implicated PTTG in the pathogenesis of HNSCC, where high tumoural expression has been independently correlated with advanced tumour stage, lymph node involvement and reduced disease-free survival (Shibata et al. 2002, Solbach et al. 2006, Ito et al. 2008, Yan et al. 2009, Zhang et al. 2013),

thus suggesting that PTTG overexpression may be of prognostic significance in the setting of HNSCC. In order to address these previous findings, total RNA was extracted from matched fresh-frozen HNSCC normal and tumour tissue specimens and PTTG mRNA expression assessed by real-time quantitative PCR. In addition, PTTG protein expression was determined by immunohistochemistry using OPSCC tissue microarray (TMA) sections.

These studies confirmed that PTTG mRNA expression is significantly upregulated in HNSCC tumour tissue compared to matched normal tissue, with the greatest degree of overexpression evident in oropharyngeal tumours. Subsequent evaluation of PTTG protein expression in TMA sections revealed that a large proportion of patient samples were positive for PTTG staining and also highlighted a significant correlation between PTTG and HPV status, as illustrated by higher PTTG protein expression levels in HPV-positive OPSCC tumour samples.

The mechanisms regulating PTTG involvement in tumourigenesis have not been fully established. However Mora-Santos et al. have recently uncovered a putative PTTG phosphorylation site, threonine-60 (T60), which may be of particular importance with regard to PTTG oncogenic activity (Mora-Santos et al. 2013). We therefore generated a phospho-specific PTTG antibody to residue T60 to investigate PTTG T60 phosphorylation in the same series of TMA sections. Immunohistochemical examination revealed a significant association between PTTG-pT60 and OPSCC tumour sub-site, with higher PTTG-T60 protein expression observed in tonsillar carcinomas when compared with tumours originating from the base of the tongue. Interestingly, many studies have noted a higher prevalence of HPV infection in tonsillar carcinomas compared to other OPSCC sub-sites (Klussmann et al. 2001, Sethi et al. 2012). The observed correlation between PTTG-pT60 and tonsillar carcinoma therefore

provides further circumstantial support for a positive association between HPV and PTTG in OPSCC.

As a result of the heterogeneity displayed by HPV-negative and HPV-positive OPSCC cancers, current research is focused on identifying novel druggable targets, as well as biomarkers to help identify patients who are likely to respond to specific treatment strategies. As PTTG appears to be strongly associated with HPV status, manipulation of PTTG expression and/or function represents a promising future therapeutic target for the treatment of HPV-positive HNSCC. PTTG may also serve as a novel predictive biomarker to help identify HPV-positive HNSCC subpopulations that are likely to benefit from treatment de-intensification. Future research will involve confirming these findings in larger scale studies. Detailed assessment of the relationship between PTTG and HPV infection will also be required. It may be that PTTG cooperates with certain HPV oncoproteins to promote HPV-induced carcinogenesis. Alternatively, upregulation of PTTG expression may be an indirect effect mediated by a common regulatory mechanism, for example, the transcription factor Sp-1, has been implicated in the transcriptional regulation of both PTTG and HPV E6/E7 (Gloss, Bernard 1990, Clem et al. 2003).

Expression of PTTG's binding partner PBF has not previously been examined in HNSCC, although a recent unpublished GEO profile cDNA array analysis of 22 matched HNSCC tumour and normal tissues has hinted a potential upregulation of PBF. We therefore hypothesised that PBF is overexpressed in HNSCC tumours and that high PBF expression is associated with poor prognosis. To test this hypothesis, quantitative real-time PCR and immunohistochemistry techniques were used to assess PBF mRNA and protein expression in the same patient cohorts used to examine PTTG expression.

These studies demonstrated that PBF mRNA expression is significantly increased in HNSCC tumours when compared with matched normal tissues. Furthermore, a parallel increase in PBF and PTTG mRNA expression was apparent in these samples. Given that PBF is required for the nuclear translocation of PTTG and for its transcriptional activity (Chien, Pei 2000) and PBF mRNA expression is upregulated by PTTG in the thyroid (Stratford et al. 2005), induction of PBF expression may be a secondary effect mediated by PTTG. Alternatively, correlated PBF and PTTG expression may be a result of a common regulatory mechanism; for example, oestrogen is known to regulate expression of both PBF and PTTG (Heaney et al. 1999, Watkins et al. 2010, Xiang et al. 2012). Indeed abundant PBF protein expression was observed in 92 % of the OPSCC TMA specimens analysed and revealed a significant gender bias, with higher PBF protein expression levels in female patients, thus providing further support for the latter theory.

Surprisingly, neither PTTG nor PBF were associated with any of the prognostic factors assessed, including TNM stage and tumour recurrence. This was an unexpected finding as both proto-oncogenes have been reported to serve as prognostic markers in differentiated thyroid cancer (Boelaert et al. 2003a, Hsueh et al. 2013). It is entirely possible that PTTG and PBF expression/function is required in the early stages of HNSCC tumourigenesis and cease to be important once the tumour has progressed and become invasive. Future investigations could focus on examining expression of PTTG and PBF in precancerous lesions and tumour margins, alongside analysis of normal and tumour tissues. Determining whether PTTG and PBF may serve as prognostic markers in HNSCC will also require further evaluation in a much larger cohort of patient samples as our study was limited by the relatively small number of samples available.

## 8.2 Stable gene silencing in head and neck cancer cells by lentiviral vectors

The majority of HNSCC cell lines are extremely difficult to transfect using conventional transfection methods. Therefore, in order to explore the roles of PTTG and PBF in the pathogenesis of head and neck cancer, we generated lentiviral particles to deliver gene-specific shRNA into HPV-negative 92-VU-040T and HPV-positive 93-VU-147T HNSCC cell lines to effectively knockdown PTTG and PBF gene expression.

Lentiviral-based RNAi expression systems have emerged as a powerful tool to facilitate permanent target gene knockdown in primary, hard-to-transfect and non-dividing cells. However, the system has its drawbacks, especially in terms of generating functionally active shRNA molecules. This was indeed the case for PBF, whose expression was not significantly repressed in either HNSCC cell line following transduction with one of four different PBF shRNA target sequences generated in-house. We therefore purchased transduction-ready lentiviral particles, which were tailored to express one of three validated PBF gene-specific shRNA under the hCMV promoter, as it was found to be the most active promoter in both 92-VU-040T and 93-VU-147T cells. PBF expression was sufficiently reduced using this alternative RNAi expression system.

Having successfully knocked down expression of PTTG and PBF using both RNAi expression systems and having subsequently established clonal cell lines stably expressing PTTG or PBF shRNA, we next sought to determine the impact of PTTG and PBF depletion of HNSCC cell proliferation. PTTG knockdown resulted in a significant increase in the proliferation, whereas knockdown of PBF led to a significant decrease in the proliferation of 92-VU-040T and 93-VU-147T cells. Interestingly, the differences in the proliferative capacity of 92-VU-040T and 93-VU-147T cells following PTTG or PBF depletion correlated with BCL-2 mRNA expression levels; PTTG knockdown resulted in significant induction of BCL-

2, whereas, PBF knockdown led to significant repression of BCL-2, thereby implying that the observed differences in cell proliferation may be linked with altered apoptosis. However additional caspase 3/7 apoptosis assays would need to be performed to confirm or refute this theory.

## 8.3 The relationship between PTTG, PBF and p53

PTTG has previously been shown to be capable of binding to the tumour suppressor protein p53 both *in vitro* and *in vivo* (Bernal et al. 2002). Recent research conducted by our group has also uncovered a functional interaction between PBF and p53 in thyroid and colorectal cancer (Read et al. 2014, Read et al. 2016a, Read et al. 2016b). Given that both proto-oncogenes are known to functionally interact with p53 in other cancers, it was hypothesised that PTTG and PBF bind to p53 in the setting of head and neck cancer.

To explore their potential interactions *in vitro*, total cellular protein was extracted from transfected 92-VU-040T and 93-VU-147T cells and subjected to co-immunoprecipitation assays. In support of the hypothesis, p53 successfully co-immunoprecipitated with transfected PTTG-HA or PBF-HA and reciprocal assays confirmed direct and specific PTTG:p53 and PBF:p53 interactions in both HNSCC cell lines. Further co-immunoprecipitation assays demonstrated that the interaction between exogenous PBF and p53 was enhanced following PTTG depletion in stable 92-VU-040T and 93-VU-147T cell lines. On the other hand, PBF depletion resulted in impaired PTTG binding to p53 in stable 92-VU-040T and 93-VU-147T cell lines, therefore suggesting that the relative levels of PTTG and PBF expressed in the cell strongly influences their ability to interact with p53.

PTTG has previously been demonstrated to alter p53 stability. The interaction between PBF and p53 was also found to de-stabilise p53, inducing its ubiquitination and subsequent

proteasomal degradation in an MDM2-dependent manner (Read et al. 2014). In light of this research, we performed anisomycin half-life studies to determine the individual and combined effects of PTTG and PBF on p53 protein stability in 92-VU-040T and 93-VU-147T cells. Expression of PTTG or PBF alone resulted in a significant reduction if p53 stability, confirming our original hypothesis that PTTG and PBF alter p53 metabolism in HNSCC cells. Interestingly, this effect was further augmented following co-transfection with PTTG and PBF, thus suggesting that PTTG and PBF cooperate to induce turnover of p53.

To further explore the impact of the interaction between PTTG and PBF on p53 stability, anisomycin half-life assays were performed following co-transfection with wild-type PTTG or PBF and the existing mutants, PTTG BD- or PBF M1, which are incapable of binding one another. Interestingly, transfection with PTTG BD- and wild-type PBF resulted in a significant decrease in p53 stability, whereas transfection of wild-type PTTG and PBF M1 or PTTG BD- (Δ123-154) and PBF M1 (Δ149-180) led to stabilisation of p53. These results imply that modulation of p53 metabolism by PTTG and PBF is not necessarily contingent upon their interaction. Given that PBF phosphorylation at residue Y174 is essential for its interaction with, and trafficking of, numerous proteins (Smith et al. 2013, Watkins et al. 2016), PBF-mediated degradation of p53 may be dependent on PBF-Y174 phosphorylation status. Y174 phosphorylation may also impact on PTTG or p53 subcellular localisation and/or PTTG function. Additional anisomycin half-life assays would need to be conducted to determine the impact of abrogating PBF-Y174 phosphorylation on PBF- and PTTG-mediated p53 turnover. These experiments should also be performed in the presence of reduced endogenous PTTG and PBF expression or in cell lines devoid of PTTG and PBF to reduce potential interference from high background PTTG/PBF expression. It will also be important to determine the mechanism by which PTTG and PBF induce p53 turnover.

Taking into account the observed effects of PTTG and PBF expression on p53 interaction and stability, the impact of their depletion on the expression of a panel of p53-related genes was analysed, before and after irradiation-induced DNA damage. PTTG and PBF depletion led to significant dysregulation of a small number of p53-responsive genes, including BCL-2, RAD51 and BRCA1. Given that many of the genes analysed are usually induced in response to DNA damage in a p53-dependent manner, these data suggest that PTTG and PBF may have some impact on p53 transcriptional activity in 92-VU-040T and 93-VU-147T HNSCC cell lines. However, gene expression profiling would need to be conducted on a much larger panel of p53-responsive genes in future, as this would provide a more accurate account of the impact of PTTG and PBF expression on p53 transactivation function. It will also be important to determine whether the dysregulated gene expression is indeed p53-dependent. Luciferase reporter assays could be performed following PTTG or PBF overexpression to determine whether PTTG and PBF are capable of directly repressing p53 transcriptional activity. Furthermore, the levels of p53-responsive gene expression could be assessed in PTTG and PBF depleted 92-VU-040T and 93-VU-147T cells, both in the presence and absence of p53 siRNA. Finally, the FISSR-PCR technique could be employed to quantify the level of genomic instability in these stable knockdown cell lines compared to Scr shRNA control cells.

## 8.4 PTTG and PBF depletion reduced the invasiveness of head and neck cancer cells

Cell migration and invasion form an important early step in the metastatic cascade. Previous research has demonstrated that PTTG and PBF are capable of inducing potent migration and invasion of several types of cancer cells (Ito et al. 2008, Watkins et al. 2010, Chen et al. 2015, Watkins et al. 2016). Given that PTTG and PBF are frequently overexpressed in HNSCC, which is a highly aggressive malignancy, it was hypothesised that downregulation of each proto-oncogene may impair the inherent invasiveness of 92-VU-040T and 93-VU-147T HNSCC cells. To test this hypothesis, 2D Boyden chamber invasion assays and classical wound healing assays were utilised. In accordance with our hypothesis, attenuation of PTTG or PBF expression led to a marked reduction in the invasive capacity of 92-VU-040T and 93-VU-147T cells, thus implicating PTTG and PBF in the regulation of HNSCC cell invasion and migration. Furthermore, colony formation assays performed in PTTG or PBF depleted cells demonstrated clear suppression of the colony forming ability of both cell lines, also indicating a role for PTTG and PBF in HNSCC cell survival.

Unfortunately, determining the precise mechanisms by which PTTG and PBF promote HNSCC cell migration and invasion, or colony formation, was beyond the scope of this thesis and warrants further exploration. Aside from its well-established roles, p53 has been implicated in the processes of cell migration, invasion and epithelial-to-mesenchymal transition (Muller et al. 2009, Wang et al. 2009, Mukhopadhyay et al. 2010, Lin et al. 2015a). As we have provided evidence demonstrating that PTTG and PBF functionally interact with p53 in HNSCC cells, it is possible that PTTG and PBF promote HNSCC migration and invasion via modulation of p53-dependent mechanisms. However, 93-VU-147T cells harbour a heterozygous p53 mutation (c.770T>G, p.L257R), so it is possible that additional p53-

independent mechanisms may be involved. Further experiments may involve repeating these assays in the presence and absence of p53 siRNA to assess whether PTTG and PBF are acting upstream of p53 to regulate cell migration and invasion. 2D Boyden chamber invasion assays should also be performed following transfection with specific mutant forms of PTTG or PBF as this may shed light on the regions that are important in inducing invasion and may provide additional information regarding potential modes of action.

## 8.5 Concluding statements

The research presented in this thesis has demonstrated that the proto-oncogenes PTTG and PBF are overexpressed in HNSCC tumour tissue compared to matched normal tissue specimens. High tumoural PTTG protein expression was significantly associated with HPV status. Furthermore, PBF displayed a significant gender bias, with higher PBF protein expression levels in female patients. However, despite evidence implicating PTTG, and now PBF too, in head and neck cancer, the precise mechanisms by which they may promote HNSCC tumourigenesis remain to be elucidated. Work carried out in this thesis has established that PTTG and PBF functionally interact with and cooperate to reduce p53 protein stability in HPV-negative and HPV-positive HNSCC cells. Furthermore, attenuation of PTTG or PBF expression in these cell lines led to dysregulated expression of p53-related genes, both before and after treatment with ionising radiation. Affected genes were involved in important cellular processes, including DNA damage repair and apoptosis and, as such, may serve to promote genomic instability and HNSCC cell survival. Additional studies revealed that depletion of PTTG or PBF significantly repressed migration and invasion, and also impaired colony formation in HPV-positive and HPV-negative HNSCC cells. The frequent overexpression of PTTG and PBF in HNSCC tumours may therefore be of aetiological

importance, with regard to tumour progression and both proto-oncogenes may serve as therapeutic targets in the prevention or treatment of metastatic disease. Given that PTTG expression strongly correlated with HPV-positive HNSCC, PTTG may represent a novel predictive biomarker for the further stratification of HPV-positive HNSCC patients based on their likely response to specific treatment strategies. Differential PTTG expression may also prove useful in identifying HPV-positive HNSCC patients who are likely to benefit from treatment de-intensification.

Overall, this research has provided novel insights into the roles of PTTG and PBF in HNSCC tumour initiation and progression, through modulation of p53 activity and function.

# Chapter 9

# References

Agrawal, N., Frederick, M.J., Pickering, C.R., Bettegowda, C., Chang, K., Li, R.J., Fakhry, C., Xie, T.X., Zhang, J., Wang, J., Zhang, N., El-Naggar, A.K., Jasser, S.A., Weinstein, J.N., Trevino, L., Drummond, J.A., Muzny, D.M., Wu, Y., Wood, L.D., Hruban, R.H., Westra, W.H., Koch, W.M., Califano, J.A., Gibbs, R.A., Sidransky, D., Vogelstein, B., Velculescu, V.E., Papadopoulos, N., Wheeler, D.A., Kinzler, K.W. & Myers, J.N. 2011, "Exome sequencing of head and neck squamous cell carcinoma reveals inactivating mutations in NOTCH1", *Science,* 333(6046): 1154-1157.

Andersen, A.S., Sølling, K., Sophie, A., Ovesen, T. & Rusan, M. 2014, "The interplay between HPV and host immunity in head and neck squamous cell carcinoma", *Int. J. Cancer,* 134(12):2755-2763.

Ang, K.K., Berkey, B.A., Tu, X., Zhang, H.Z., Katz, R., Hammond, E.H., Fu, K.K. & Milas, L. 2002, "Impact of epidermal growth factor receptor expression on survival and pattern of relapse in patients with advanced head and neck carcinoma", *Cancer Res.,* 62(24):7350-7356.

Ang, K.K., Harris, J., Wheeler, R., Weber, R., Rosenthal, D.I., Nguyen-Tân, P.F., Westra, W.H., Chung, C.H., Jordan, R.C., Lu, C., Kim, H., Axelrod, R., Silverman, C.C., Redmond, K.P. & Gillison, M.L. 2010, "Human Papillomavirus and Survival of Patients with Oropharyngeal Cancer", *N Engl J Med,* vol. 363, no. 1, pp. 24-35.

Angeletti, P.C., Kim, K., Fernandes, F.J. & Lambert, P.F. 2002, "Stable replication of papillomavirus genomes in Saccharomyces cerevisiae", *J. Virol.,* 76(7):3350-3358.

Arenz, A., Ziemann, F., Mayer, C., Wittig, A., Dreffke, K., Preising, S., Wagner, S., Klussmann, J., Engenhart-Cabillic, R. & Wittekindt, C. 2014, "Increased radiosensitivity of HPV-positive head and neck cancer cell lines due to cell cycle dysregulation and induction of apoptosis", *Strahlenther. Onkol.,* 190(9):839-846.

Argiris, A., Karamouzis, M.V., Raben, D. & Ferris, R.L. 2008, "Head and neck cancer", *The Lancet,* 371(9625):1695-1709.

Attner, P. 2013, "HPV prevalence in the different subsites of the oropharynx", *J. Clin. Oncol.,* 31(15_suppl):6037.

Ayala, I., Baldassarre, M., Giacchetti, G., Caldieri, G., Tete, S., Luini, A. & Buccione, R. 2008, "Multiple regulatory inputs converge on cortactin to control invadopodia biogenesis and extracellular matrix degradation", *J. Cell Sci.,* 121(3):369-378.

Basu, A. & Haldar, S. 1998, "The relationship between BcI2, Bax and p53: consequences for cell cycle progression and cell death", *Mol. Hum. Reprod.,* 4(12):1099-1109.

Bau, D., Mau, Y. & Shen, C. 2006, "The role of BRCA1 in non-homologous end-joining", *Cancer Lett.,* 240(1):1-8.

Baumann, P. & West, S.C. 1998, "Role of the human RAD51 protein in homologous recombination and double-stranded-break repair", *Trends. Biochem. Sci.,* 23(7):247-251.

Bernal, J.A., Luna, R., Espina, Á, Lázaro, I., Ramos-Morales, F., Romero, F., Arias, C., Silva, A., Tortolero, M. & Pintor-Toro, J.A. 2002, "Human securin interacts with p53 and modulates p53-mediated transcriptional activity and apoptosis", *Nat. Genet.,* 32(2):306-311.

Bernal, J., Roche, M., Mendez-Vidal, C., Espina, A., Tortolero, M. & Pintor-Toro, J. 2008, "Proliferative potential after DNA damage and non-homologous end joining are affected by loss of securin", *Cell Death Differ.,* 15(1):202-212.

Bernal, J.A. & Hernandez, A. 2007, "p53 stabilization can be uncoupled from its role in transcriptional activation by loss of PTTG1/securin", *J. Biochem.,* 141(5):737-745.

Bernstein, E., Caudy, A.A., Hammond, S.M. & Hannon, G.J. 2001, "Role for a bidentate ribonuclease in the initiation step of RNA interference", *Nature,* 409(6818):363-366.

Bertrand, J., Pottier, M., Vekris, A., Opolon, P., Maksimenko, A. & Malvy, C. 2002, "Comparison of antisense oligonucleotides and siRNAs in cell culture and in vivo", *Biochem. Bioph. Res. Co.,* 296(4):1000-1004.

Betiol, J., Villa, L. & Sichero, L. 2013, "Impact of HPV infection on the development of head and neck cancer", *Braz. J. Med. Biol. Res.,* 46(3):217-226.

Bhalavat, R., Fakih, A., Mistry, R. & Mahantshetty, U. 2003, "Radical radiation vs surgery plus post-operative radiation in advanced (resectable) supraglottic larynx and pyriform sinus cancers: a prospective randomized study", *Eur. J. Surg. Oncol.,* 29(9):750-756.

Blot, W.J., McLaughlin, J.K., Winn, D.M., Austin, D.F., Greenberg, R.S., Preston-Martin, S., Bernstein, L., Schoenberg, J.B., Stemhagen, A. & Fraumeni, J.F.,Jr 1988, "Smoking and drinking in relation to oral and pharyngeal cancer", *Cancer Res.,* 48(11):3282-3287.

Boelaert, K., Smith, V., Stratford, A., Kogai, T., Tannahill, L., Watkinson, J., Eggo, M., Franklyn, J. & McCabe, C. 2007, "PTTG and PBF repress the human sodium iodide symporter", *Oncogene,* 26(30):4344-4356.

Boelaert, K., McCabe, C., Tannahill, L., Gittoes, N., Holder, R., Watkinson, J., Bradwell, A., Sheppard, M. & Franklyn, J. 2003a, "Pituitary tumor transforming gene and fibroblast growth factor-2 expression: potential prognostic indicators in differentiated thyroid cancer", *J. Clin. Endocrinol. Metab.,* 88(5):2341-2347.

Boelaert, K., Yu, R., Tannahill, L., Stratford, A., Khanim, F., Eggo, M., Moore, J., Young, L., Gittoes, N. & Franklyn, J. 2004, "PTTG's C-terminal PXXP motifs modulate critical cellular processes in vitro", *J. Mol. Endocrinol.,* 33(3):663-677.

Boelaert, K., Tannahill, L.A., Bulmer, J.N., Kachilele, S., Chan, S.Y., Kim, D., Gittoes, N.J., Franklyn, J.A., Kilby, M.D. & McCabe, C.J. 2003b, "A potential role for PTTG/securin in the developing human fetal brain", *FASEB,* 17(12):1631-1639.

Bork, P., Doerks, T., Springer, T.A. & Snel, B. 1999, "Domains in plexins: links to integrins and transcription factors", *Trends Biochem. Sci.,* 24(7):261-263.

Boyle, J.O., Hakim, J., Koch, W., van der Riet, P., Hruban, R.H., Roa, R.A., Correo, R., Eby, Y.J., Ruppert, J.M. & Sidransky, D. 1993, "The incidence of p53 mutations increases with progression of head and neck cancer", *Cancer Res.*, 53(19):4477-4480.

Brehm, A., Miska, E.A., McCance, D.J., Reid, J.L., Bannister, A.J. & Kouzarides, T. 1998, "Retinoblastoma protein recruits histone deacetylase to repress transcription", *Nature*, 391(6667):597-601.

Brummelkamp, T.R., Bernards, R. & Agami, R. 2002, "A system for stable expression of short interfering RNAs in mammalian cells", *Science*, 296(5567):550-553.

Cadoni, G., Boccia, S., Petrelli, L., Di Giannantonio, P., Arzani, D., Giorgio, A., De Feo, E., Pandolfini, M., Gallì, P. & Paludetti, G. 2012, "A review of genetic epidemiology of head and neck cancer related to polymorphisms in metabolic genes, cell cycle control and alcohol metabolism.", *Acta otorhinolaryngol. Ital.*, 32(1):1-11.

Cahill, D.P., Lengauer, C., Yu, J., Riggins, G.J., Willson, J.K., Markowitz, S.D., Kinzler, K.W. & Vogelstein, B. 1998, "Mutations of mitotic checkpoint genes in human cancers", *Nature*, 392(6673):300-303.

Camp, R.L., Charette, L.A. & Rimm, D.L. 2000, "Validation of tissue microarray technology in breast carcinoma", *Lab. Invest.*, 80(12):1943-1949.

Cancer Genome Atlas Network 2015, "Comprehensive genomic characterization of head and neck squamous cell carcinomas", *Nature*, 517(7536):576-582.

Cancer Genome Atlas Research Network 2012, "Comprehensive genomic characterization of squamous cell lung cancers", *Nature*, 489(7417):519-525.

Cancer Research UK 2016, *Oral Cancer Incidence Statistics: Cancer Research UK.* [Homepage of Cancer Research UK.], [Online]. Available: http://www.cancerresearchuk.org/health-professional/cancer-statistics/statistics-by-cancer-type/oral-cancer [2013, April/28].

Carvalho, L., Yu, J., Schwartsmann, G., McLeod, H.L. & Fleshman, J.W. 2011, "RNA expression of the molecular signature genes for metastasis in colorectal cancer.", *Oncol. Rep.*, 25(5):1321.

Cerami, E., Gao, J., Dogrusoz, U., Gross, B., Sumer, S., Aksoy, B., Jacobsen, A., Byrne, C., Heuer, M. & Larsson, E. 2012, "The cBio cancer genomics portal: an open platform for exploring multidimensional cancer genomics data.", *Cancer Discov.*, 2(5):401.

Chambers, A.F., Groom, A.C. & MacDonald, I.C. 2002, "Dissemination and growth of cancer cells in metastatic sites", *Nat. Rev. Cancer*, 2(8):563-572.

Chaturvedi, A.K., Anderson, W.F., Lortet-Tieulent, J., Curado, M.P., Ferlay, J., Franceschi, S., Rosenberg, P.S., Bray, F. & Gillison, M.L. 2013, "Worldwide trends in incidence rates for oral cavity and oropharyngeal cancers", *J. Clin. Oncol.*, 31(36)4550-4559.

Chaturvedi, A.K., Engels, E.A., Anderson, W.F. & Gillison, M.L. 2008, "Incidence Trends for Human Papillomavirus–Related and –Unrelated Oral Squamous Cell Carcinomas in the United States", *J. Clin. Oncol.*, 26(4):612-619.

Chen, B., Hou, Z., Li, C. & Tong, Y. 2015, "MiRNA-494 inhibits metastasis of cervical cancer through Pttg1", *Tumor Biol.*, 36(9):7143-7149.

Chen, Z., Storthz, K.A. & Shillitoe, E.J. 1997, "Mutations in the long control region of human papillomavirus DNA in oral cancer cells, and their functional consequences", *Cancer Res.*, 57(8):1614-1619.

Chesnokova, V., Zonis, S., Rubinek, T., Yu, R., Ben-Shlomo, A., Kovacs, K., Wawrowsky, K. & Melmed, S. 2007, "Senescence mediates pituitary hypoplasia and restrains pituitary tumor growth", *Cancer Res.*, 67(21):10564-10572.

Chien, W. & Pei, L. 2000, "A novel binding factor facilitates nuclear translocation and transcriptional activation function of the pituitary tumor-transforming gene product", *J. Biol. Chem.*, 275(25):19422-19427.

Chung, C.H., Parker, J.S., Karaca, G., Wu, J., Funkhouser, W.K., Moore, D., Butterfoss, D., Xiang, D., Zanation, A. & Yin, X. 2004, "Molecular classification of head and neck squamous cell carcinomas using patterns of gene expression", *Cancer Cell*, 5(5):489-500.

Chung, C.H., Parker, J.S., Ely, K., Carter, J., Yi, Y., Murphy, B.A., Ang, K.K., El-Naggar, A.K., Zanation, A.M., Cmelak, A.J., Levy, S., Slebos, R.J. & Yarbrough, W.G. 2006, "Gene expression profiles identify epithelial-to-mesenchymal transition and activation of nuclear factor-kappaB signaling as characteristics of a high-risk head and neck squamous cell carcinoma", *Cancer Res.*, 66(16):8210-8218.

Clem, A.L., Hamid, T. & Kakar, S.S. 2003, "Characterization of the role of Sp1 and NF-Y in differential regulation of PTTG/securin expression in tumor cells", *Gene*, 322:113-121.

Colella, G., Izzo, G., Carinci, F., Campisi, G., Muzio, L.L., D'Amato, S., Mazzotta, M., Cannavale, R., Ferrara, D. & Minucci, S. 2011, "Expression of sexual hormones receptors in oral squamous cell carcinoma", *Int. J. Immunopathol. Pharmacol.*, 24(2 suppl):129-132.

Colgan, D., Murthy, K., Zhao, W., Prives, C. & Manley, J. 1998, "Inhibition of poly (A) polymerase requires p34cdc2/cyclin B phosphorylation of multiple consensus and non consensus sites", *EMBO*, 17(4):1053-1062.

Dahlgren, L., Mellin, H., Wangsa, D., Heselmeyer Haddad, K., Björnestål, L., Lindholm, J., Munck Wikland, E., Auer, G., Ried, T. & Dalianis, T. 2003, "Comparative genomic hybridization analysis of tonsillar cancer reveals a different pattern of genomic imbalances in human papillomavirus positive and negative tumors", *Int. J. Cancer*, 107(2):244-249.

Deltcheva, E., Chylinksi, K., Sharma, C.M., Gonzales, K., Chao, Y., Pirzada, Z.A., Eckert, M.R., Vogel, J. & Charpentier, E. 2011, "CRISPR RNA maturation by trans-encoded small RNA and host factor RNase III", *Nature*, 471(7340):602-607.

Denaro, N., Lo Nigro, C., Natoli, G., Russi, E., Adamo, V. & Merlano, M. 2011, "The role of p53 and MDM2 in head and neck cancer", *ISRN Otolaryngol.*, 2011:931813.

Dok, R., Kalev, P., Van Limbergen, E.J., Asbagh, L.A., Vazquez, I., Hauben, E., Sablina, A. & Nuyts, S. 2014, "p16INK4a impairs homologous recombination-mediated DNA repair in human papillomavirus-positive head and neck tumors", *Cancer Res.*, 74(6):1739-1751.

Dominguez, A., Ramos-Morales, F., Romero, F., Rios, R.M., Dreyfus, F., Tortolero, M. & Pintor-Toro, J.A. 1998, "hpttg, a human homologue of rat pttg, is overexpressed in hematopoietic neoplasms. Evidence for a transcriptional activation function of hPTTG.", *Oncogene*, 17(17):2187-93.

Doorbar, J., Quint, W., Banks, L., Bravo, I.G., Stoler, M., Broker, T.R. & Stanley, M.A. 2012, "The biology and life-cycle of human papillomaviruses", *Vaccine*, 30:F55-F70.

Dropulić, B. 2011, "Lentiviral vectors: their molecular design, safety, and use in laboratory and preclinical research", *Hum. Gene Ther.*, 22(6):649-657.

D'Souza, G., Kreimer, A.R., Viscidi, R., Pawlita, M., Fakhry, C., Koch, W.M., Westra, W.H. & Gillison, M.L. 2007, "Case–Control Study of Human Papillomavirus and Oropharyngeal Cancer", *N. Engl. J. Med.*, 356(19):1944-1956.

Egloff, A.M., Rothstein, M.E., Seethala, R., Siegfried, J.M., Grandis, J.R. & Stabile, L.P. 2009, "Cross-talk between estrogen receptor and epidermal growth factor receptor in head and neck squamous cell carcinoma", *Clin. Cancer. Res.*, 15(21):6529-6540.

Fakhry, C., Westra, W.H., Li, S., Cmelak, A., Ridge, J.A., Pinto, H., Forastiere, A. & Gillison, M.L. 2008, "Improved survival of patients with human papillomavirus-positive head and neck squamous cell carcinoma in a prospective clinical trial", *J. Nat. Cancer Inst.*, 100(4):261-269.

Ferlay, J., Soerjomataram, I., Dikshit, R., Eser, S., Mathers, C., Rebelo, M., Parkin, D.M., Forman, D. & Bray, F. 2015, "Cancer incidence and mortality worldwide: sources, methods and major patterns in GLOBOCAN 2012", *Int. J. Cancer*, 136(5):E359-E386.

Ferris, R.L., Blumenschein, G.J., Fayette, J., Guigay, J., Colevas, A.D., Licitra, L., Harrington, K., Kasper, S., Vokes, E.E., Even, C., Worden, F., Saba, N.F., Iglesias, D.L.C., Haddad, R., Rordorf, T., Kiyota, N., Tahara, M., Monga, M., Lynch, M., Geese, W.J., Kopit, J., Shaw, J.W., Gillison, M.L. 2016, "Nivolumab for recurrent squamous-cell carcinoma of the head and neck", *N. Engl. J. Med.*, 375(19):1856-1867.

Foulkes, W.D., Brunet, J.S., Sieh, W., Black, M.J., Shenouda, G. & Narod, S.A. 1996, "Familial risks of squamous cell carcinoma of the head and neck: retrospective case-control study", *BMJ*, 7059:716-721.

Frame, S. & Cohen, P. 2001, "GSK3 takes centre stage more than 20 years after its discovery", *Biochem. J.*, 359:1-16.

Franceschi, S., Talamini, R., Barra, S., Barón, A.E., Negri, E., Bidoli, E., Serraino, D. & La Vecchia, C. 1990, "Smoking and Drinking in Relation to Cancers of the Oral Cavity, Pharynx, Larynx, and Esophagus in Northern Italy", *Cancer Res.*, 50(20):6502-6507.

Frenzel, A., Grespi, F., Chmelewskij, W. & Villunger, A. 2009, "Bcl2 family proteins in carcinogenesis and the treatment of cancer", *Apoptosis*, 14(4):584-596.

Fröhling, S. & Döhner, H. 2008, "Chromosomal abnormalities in cancer", *N. Engl. J. Med.*, 359(7):722-734.

Gao, J., Aksoy, B.A., Dogrusoz, U., Dresdner, G., Gross, B., Sumer, S.O., Sun, Y., Jacobsen, A., Sinha, R., Larsson, E., Cerami, E., Sander, C. & Schultz, N. 2013, "Integrative analysis of complex cancer genomics and clinical profiles using the cBioPortal", *Sci. Signal.*, 6(269):pl1.

Giacinti, C. & Giordano, A. 2006, "RB and cell cycle progression", *Oncogene*, 25(38):5220-5227.

Gibson, S.A., Pellenz, C., Hutchison, R.E., Davey, F.R. & Shillitoe, E.J. 2000, "Induction of apoptosis in oral cancer cells by an anti-bcl-2 ribozyme delivered by an adenovirus vector", *Clinical cancer research : an official journal of the Am. Assoc. Cancer Res.*, 6(1):213-222.

Gil-Bernabe, A.M., Romero, F., Limon-Mortes, M.C. & Tortolero, M. 2006, "Protein phosphatase 2A stabilizes human securin, whose phosphorylated forms are degraded via the SCF ubiquitin ligase", *Mol. Cell. Biol.*, 26(11):4017-4027.

Gillison, M.L. 2004, "Human papillomavirus-associated head and neck cancer is a distinct epidemiologic, clinical, and molecular entity", *Semin. Oncol.*, 31(6):744-54.

Gillison, M.L., D'Souza, G., Westra, W., Sugar, E., Xiao, W., Begum, S. & Viscidi, R. 2008, "Distinct risk factor profiles for human papillomavirus type 16-positive and human papillomavirus type 16-negative head and neck cancers", *J. Nat. Cancer Inst.*, 100(6):407-420.

Gillison, M.L., Koch, W.M., Capone, R.B., Spafford, M., Westra, W.H., Wu, L., Zahurak, M.L., Daniel, R.W., Viglione, M., Symer, D.E., Shah, K.V. & Sidransky, D. 2000, "Evidence for a Causal Association Between Human Papillomavirus and a Subset of Head and Neck Cancers", *J. Nat. Cancer Inst.*, 92(9):709-720.

Gloss, B. & Bernard, H.U. 1990, "The E6/E7 promoter of human papillomavirus type 16 is activated in the absence of E2 proteins by a sequence-aberrant Sp1 distal element", *J. Virol.*, 64(11):5577-5584.

Goessel, G., Quante, M., Hahn, W.C., Harada, H., Heeg, S., Suliman, Y., Doebele, M., von Werder, A., Fulda, C., Nakagawa, H., Rustgi, A.K., Blum, H.E. & Opitz, O.G. 2005, "Creating oral squamous cancer cells: a cellular model of oral-esophageal carcinogenesis", *PNAS*, 102(43):15599-15604.

Gorr, I.H., Boos, D. & Stemmann, O. 2005, "Mutual inhibition of separase and Cdk1 by two-step complex formation", *Mol. Cell*, 19(1):135-141.

Graham, F., Smiley, J., Russell, W. & Nairn, R. 1977, "Characteristics of a human cell line transformed by DNA from human adenovirus type 5", *J. Gen. Virol.*, 36(1):59-72.

Greenbaum, D., Colangelo, C., Williams, K. & Gerstein, M. 2003, "Comparing protein abundance and mRNA expression levels on a genomic scale", *Genome. Biol.*, 4:117.

Guo, Y., Xiao, P., Lei, S., Deng, F., Xiao, G.G., Liu, Y., Chen, X., Li, L., Wu, S., Chen, Y., Jiang, H., Tan, L., Xie, J., Zhu, X., Liang, S. & Deng, H. 2008, "How is mRNA expression predictive for protein expression? A correlation study on human circulating monocytes", *Acta Biochim. Biophys. Sin.*, 40(5):426-436.

Haddad, R.I. & Shin, D.M. 2008, "Recent advances in head and neck cancer", *N. Engl. J. Med.*, 359(11):1143-1154.

Hamid, T. & Kakar, S.S. 2004, "PTTG/securin activates expression of p53 and modulates its function", *Molecular cancer*, 3(1):1.

Hamid, T., Malik, M.T. & Kakar, S.S. 2005, "Ectopic expression of PTTG1/securin promotes tumorigenesis in human embryonic kidney cells", *Mol. Cancer*, 4(1):3.

Hammond, S.M., Bernstein, E., Beach, D. & Hannon, G.J. 2000, "An RNA-directed nuclease mediates post-transcriptional gene silencing in Drosophila cells", *Nature*, 404(6775):293-296.

Hashibe, M., Brennan, P., Benhamou, S., Castellsague, X., Chen, C., Curado, M.P., Dal Maso, L., Daudt, A.W., Fabianova, E., Fernandez, L., Wunsch-Filho, V., Franceschi, S., Hayes, R.B., Herrero, R., Koifman, S., La Vecchia, C., Lazarus, P., Levi, F., Mates, D., Matos, E., Menezes, A., Muscat, J., Eluf-Neto, J., Olshan, A.F., Rudnai, P., Schwartz, S.M., Smith, E., Sturgis, E.M., Szeszenia-Dabrowska, N., Talamini, R., Wei, Q., Winn, D.M., Zaridze, D., Zatonski, W., Zhang, Z.F., Berthiller, J. & Boffetta, P. 2007, "Alcohol drinking in never users of tobacco, cigarette smoking in never drinkers, and the risk of head and neck cancer: pooled analysis in the International Head and Neck Cancer Epidemiology Consortium", *J. Nat. Cancer Inst.*, 99(10):777-789.

Heaney, A.P., Horwitz, G.A., Wang, Z., Singson, R. & Melmed, S. 1999, "Early involvement of estrogen-induced pituitary tumor transforming gene and fibroblast growth factor expression in prolactinoma pathogenesis", *Nature Med.*, 5(11):1317-1321.

Heaney, A.P., Singson, R., McCabe, C.J., Nelson, V., Nakashima, M. & Melmed, S. 2000, "Expression of pituitary-tumour transforming gene in colorectal tumours", *The Lancet*, 355(9205):716-719.

Heaney, A.P., Fernando, M. & Melmed, S. 2002, "Functional role of estrogen in pituitary tumor pathogenesis", *J. Clin. Invest.*, 109(2):277-283.

Heck, J.E., Berthiller, J., Vaccarella, S., Winn, D.M., Smith, E.M., Shan'gina, O., Schwartz, S.M., Purdue, M.P., Pilarska, A., Eluf-Neto, J., Menezes, A., McClean, M.D., Matos, E., Koifman, S., Kelsey, K.T., Herrero, R., Hayes, R.B., Franceschi, S., Wunsch-Filho, V., Fernandez, L., Daudt, A.W., Curado, M.P., Chen, C., Castellsague, X., Ferro, G., Brennan, P., Boffetta, P. & Hashibe, M. 2010, "Sexual behaviours and the risk of head and neck cancers: a pooled analysis in the International Head and Neck Cancer Epidemiology (INHANCE) consortium", *Int. J. Epidemiol.,* 39(1):166-181.

Hellmuth, S., Pohlmann, C., Brown, A., Bottger, F., Sprinzl, M. & Stemmann, O. 2015, "Positive and negative regulation of vertebrate separase by Cdk1-cyclin B1 may explain why securin is dispensable", *J. Biol. Chem.,* 290(12):8002-8010.

Hermsen, M.A.J.A., Joenje, H., Arwert, F., Welters, M.J.P., Braakhuis, B.J.M., Bagnay, M., Westerveld, A. & Slater, R. 1996, "Centromeric breakage as a major cause of cytogenetic abnormalities in oral squamous cell carcinoma", *Gen. Chromosomes Canc.,* 15(1)1-9.

Holt, L.J., Krutchinsky, A.N. & Morgan, D.O. 2008, "Positive feedback sharpens the anaphase switch", *Nature,* 454(7202):353-357.

Homer, J. 2016, "Surgery in head and neck cancer: United Kingdom National Multidisciplinary Guidelines", *J. Laryngol. Otol.,* 130(suppl 2):S68.

Hsueh, C., Lin, J., Chang, Y., Hsueh, S., Chao, T., Yu, J., Jung, S., Tseng, N., Sun, J. & Kuo, S. 2013, "Prognostic Significance of Expression of Pituitary Tumour-Transforming Gene-Binding Factor in Papillary Thyroid Carcinoma", *Clin. Endocrinol.,* 78:303.

Huh, K., Zhou, X., Hayakawa, H., Cho, J., Libermann, T.A., Jin, J., Wade Harper, J. & Munger, K. 2007, "Human Papillomavirus Type 16 E7 Oncoprotein Associates with the Cullin 2 Ubiquitin Ligase Complex, Which Contributes to Degradation of the Retinoblastoma Tumor Suppressor", *J. Virol.,* 81(18):9737-9747.

Ishida, H., Wada, K., Masuda, T., Okura, M., Kohama, K., Sano, Y., Nakajima, A., Kogo, M. & Kamisaki, Y. 2007, "Critical role of estrogen receptor on anoikis and invasion of squamous cell carcinoma", *Cancer Sci.,* 98(5):636-643.

Ishikawa, H., Heaney, A.P., Yu, R., Horwitz, G.A. & Melmed, S. 2001, "Human Pituitary Tumor-Transforming Gene Induces Angiogenesis 1", *J. Clin. Endocrinol. Metab.,* 86(2):867-874.

Ito, T., Shimada, Y., Kan, T., David, S., Cheng, Y., Mori, Y., Agarwal, R., Paun, B., Jin, Z., Olaru, A., Hamilton, J.P., Yang, J., Abraham, J.M., Meltzer, S.J. & Sato, F. 2008, "Pituitary tumor-transforming 1 increases cell motility and promotes lymph node metastasis in esophageal squamous cell carcinoma", *Cancer Res.,* 68(9):3214-3224.

Jallepalli, P.V., Waizenegger, I.C., Bunz, F., Langer, S., Speicher, M.R., Peters, J., Kinzler, K.W., Vogelstein, B. & Lengauer, C. 2001, "Securin is required for chromosomal stability in human cells", *Cell,* 105(4):445-457.

Jemal, A., Bray, F., Center, M.M., Ferlay, J., Ward, E. & Forman, D. 2011, "Global cancer statistics", *CA Cancer J. Clin.,* 61(2):69-90.

Jinek, M., Chylinski, K., Fonfara, I., Hauer, M., Doudna, J.A. & Charpentier, E. 2012, "A programmable dual-RNA-guided DNA endonuclease in adaptive bacterial immunity", *Science,* 337(6096):816-821.

Jinek, M., East, A., Cheng, A., Lin, S., Ma, E. & Doudna, J. 2013, "RNA-programmed genome editing in human cells", *Elife,* 2:e00471.

Jung, C., Yoo, J., Jang, Y.J., Kim, S., Chu, I., Yeom, Y.I., Choi, J.Y. & Im, D. 2006, "Adenovirus mediated transfer of siRNA against PTTG1 inhibits liver cancer cell growth in vitro and in vivo", *Hepatology,* 43(5):1042-1052.

Jung, Y., Kato, I. & Kim, H.C. 2013, "A novel function of HPV16-E6/E7 in epithelial–mesenchymal transition", *Biochem. Bioph. Res. Co.,* 435(3):339-344.

Kajitani, N., Satsuka, A., Kawate, A. & Sakai, H. 2012, "Productive lifecycle of human papillomaviruses that depends upon squamous epithelial differentiation", *Front Microbiol.,* 3(152):5.

Kakar, S.S. & Jennes, L. 1999, "Molecular cloning and characterization of the tumor transforming gene (TUTR1): a novel gene in human tumorigenesis", *Cytogenet. Cell Genet.,* 84(3-4):211-216.

Kastan, M.B., Onyekwere, O., Sidransky, D., Vogelstein, B. & Craig, R.W. 1991, "Participation of p53 protein in the cellular response to DNA damage", *Cancer Res.,* 51(23):6304-6311.

Keck, M.K., Zuo, Z., Khattri, A., Stricker, T.P., Brown, C.D., Imanguli, M., Rieke, D., Endhardt, K., Fang, P., Bragelmann, J., DeBoer, R., El-Dinali, M., Aktolga, S., Lei, Z., Tan, P., Rozen, S.G., Salgia, R., Weichselbaum, R.R., Lingen, M.W., Story, M.D., Ang, K.K., Cohen, E.E., White, K.P., Vokes, E.E. & Seiwert, T.Y. 2015, "Integrative analysis of head and neck cancer identifies two biologically distinct HPV and three non-HPV subtypes", *Clin. Cancer Res.,* 21(4):870-881.

Keren, S., Shoude, Z., Lu, Z. & Beibei, Y. 2014, "Role of EGFR as a prognostic factor for survival in head and neck cancer: a meta-analysis", *Tumor Biol.,* 35(3):2285-2295.

Khan, Z., Khan, A.A., Prasad, G.B., Khan, N., Tiwari, R.P. & Bisen, P.S. 2016, "Growth inhibition and chemo-radiosensitization of head and neck squamous cell carcinoma (HNSCC) by surviving-siRNA lentivirus", *Radiother. Oncol.,* 118(2):359-368.

Khouja, M.H., Baekelandt, M., Sarab, A., Nesland, J.M. & Holm, R. 2010, "Limitations of tissue microarrays compared with whole tissue sections in survival analysis", *Oncol. Lett.,* 1(5):827-831.

Kim, D., Pemberton, H., Stratford, A.L., Buelaert, K., Watkinson, J.C., Lopes, V., Franklyn, J.A. & McCabe, C.J. 2005, "Pituitary tumour transforming gene (PTTG) induces genetic instability in thyroid cells", *Oncogene,* 24(30):4861-4866.

Kim, C.S., Ying, H., Willingham, M.C. & Cheng, S.Y. 2007a, "The pituitary tumor-transforming gene promotes angiogenesis in a mouse model of follicular thyroid cancer", *Carcinogenesis,* 28(5):932-939.

Kim, D.S., Franklyn, J.A., Smith, V.E., Stratford, A.L., Pemberton, H.N., Warfield, A., Watkinson, J.C., Ishmail, T., Wakelam, M.J. & McCabe, C.J. 2007b, "Securin induces genetic instability in colorectal cancer by inhibiting double-stranded DNA repair activity", *Carcinogenesis,* 28(3):749-759.

Kim, N.H., Kim, H.S., Li, X.Y., Lee, I., Choi, H.S., Kang, S.E., Cha, S.Y., Ryu, J.K., Yoon, D., Fearon, E.R., Rowe, R.G., Lee, S., Maher, C.A., Weiss, S.J. & Yook, J.I. 2011, "A p53/miRNA-34 axis regulates Snail1-dependent cancer cell epithelial-mesenchymal transition", *J. Cell Biol.,* 195(3)417-433.

Kimple, R.J., Smith, M.A., Blitzer, G.C., Torres, A.D., Martin, J.A., Yang, R.Z., Peet, C.R., Lorenz, L.D., Nickel, K.P., Klingelhutz, A.J., Lambert, P.F. & Harari, P.M. 2013, "Enhanced radiation sensitivity in HPV-positive head and neck cancer", *Cancer Res.,* 73(15):4791-4800.

Klussmann, J.P., Weissenborn, S.J., Wieland, U., Dries, V., Kolligs, J., Jungehuelsing, M., Eckel, H.E., Dienes, H.P., Pfister, H.J. & Fuchs, P.G. 2001, "Prevalence, distribution, and viral load of human papillomavirus 16 DNA in tonsillar carcinomas", *Cancer,* 92(11):2875-2884.

Kreimer, A.R., Clifford, G.M., Boyle, P. & Franceschi, S. 2005, "Human papillomavirus types in head and neck squamous cell carcinomas worldwide: a systematic review", *Cancer Epidemiol. Biomarkers Prev.,* 14(2):467-475.

Krol, J., Loedige, I. & Filipowicz, W. 2010, "The widespread regulation of microRNA biogenesis, function and decay", *Nat. Rev. Genet.,* 11(9):597-610.

Ku, T.K., Nguyen, D.C., Karaman, M., Gill, P., Hacia, J.G. & Crowe, D.L. 2007, "Loss of p53 expression correlates with metastatic phenotype and transcriptional profile in a new mouse model of head and neck cancer", *Mol. Cancer Res.,* 5(4):351-362.

Kumar, B., Yadav, A., Lang, J., Teknos, T.N. & Kumar, P. 2012, "Dysregulation of microRNA-34a expression in head and neck squamous cell carcinoma promotes tumor growth and tumor angiogenesis", *PloS one,* 7(5)e37601.

Lahtvee, P., Sánchez, B.J., Smialowska, A., Kasvandik, S., Elsemman, I.E., Gatto, F. & Nielsen, J. 2017, "Absolute quantification of protein and mRNA abundances demonstrate variability in gene-specific translation efficiency in yeast", *Cell systems.,* [Epub ahead of print].

Lechner, M., Fenton, T., West, J., Wilson, G., Feber, A., Henderson, S., Thirlwell, C., Dibra, H.K., Jay, A. & Butcher, L. 2013, "Identification and functional validation of HPV-mediated hypermethylation in head and neck squamous cell carcinoma", *Genome Med.*, 5(2):1.

Lee, I., Seonga, C. & Choe, I.S. 1999, "Cloning and expression of human cDNA encoding human homologue of pituitary tumor transforming gene", *Biochem. Mol. Biol. Int.*, 47(5):891-897.

Lee, S.H., Lee, C., Rigas, N.K., Kim, R.H., Kang, M.K., Park, N. & Shin, K. 2015, "Human papillomavirus 16 (HPV16) enhances tumor growth and cancer stemness of HPV-negative oral/oropharyngeal squamous cell carcinoma cells via miR-181 regulation", *Papillomavirus Res.*, 1:116-125.

Leechanachai, P., Banks, L., Moreau, F. & Matlashewski, G. 1992, "The E5 gene from human papillomavirus type 16 is an oncogene which enhances growth factor-mediated signal transduction to the nucleus", *Oncogene*, 7(1):19-25.

Leemans, C.R., Braakhuis, B.J. & Brakenhoff, R.H. 2011, "The molecular biology of head and neck cancer", *Nat. Rev. Cancer*, 11(1):9-22.

Levine, A.J. & Oren, M. 2009, "The first 30 years of p53: growing ever more complex", *Nat. Rev. Cancer*, 9(10):749-758.

Lewy, G.D., Ryan, G.A., Read, M.L., Fong, J.C., Poole, V., Seed, R.I., Sharma, N., Smith, V.E., Kwan, P.P. & Stewart, S.L. 2013, "Regulation of Pituitary Tumor Transforming Gene (PTTG) Expression and Phosphorylation in Thyroid Cells", *Endocrinology*, 154(11):4408-4422.

Li, L., Han, L., Yu, M., Zhou, Q., Xu, J. & Li, P. 2015, "Pituitary tumor-transforming gene 1 enhances metastases of cervical cancer cells through miR-3666-regulated ZEB1", *Tumor Biol.*, [Epub ahead of print]:1-7.

Li, C., Wang, Y., Wang, S., Wu, B., Hao, J., Fan, H., Ju, Y., Ding, Y., Chen, L., Chu, X., Liu, W., Ye, X. & Meng, S. 2013, "Hepatitis B virus mRNA-mediated miR-122 inhibition upregulates PTTG1-binding protein, which promotes hepatocellular carcinoma tumor growth and cell invasion", *J. Virol.*, 87(4):2193-2205.

Li, L., Lin, X., Khvorova, A., Fesik, S.W. & Shen, Y. 2007, "Defining the optimal parameters for hairpin-based knockdown constructs", *RNA*, 13(10):1765-1774.

Liang, H.Q., Wang, R.J., Diao, C.F., Li, J.W., Su, J.L. & Zhang, S. 2015, "The PTTG1-targeting miRNAs miR-329, miR-300, miR-381, and miR-655 inhibit pituitary tumor cell tumorigenesis and are involved in a p53/PTTG1 regulation feedback loop", *Oncotarget*, 6(30):29413-29427.

Liao, L.J., Hsu, Y.H., Yu, C.H., Chiang C.P., Jhan, J.R., Chang, L.C., Lin, J.J., Lou, P.J. 2011, "Association of pituitary tumor transforming gene expression with early oral

tumourigenesis and malignant progression of precancerous lesions", *Head Neck,* 33(5):719-726.

Licitra, L., Perrone, F., Bossi, P., Suardi, S., Mariani, L., Artusi, R., Oggionni, M., Rossini, C., Cantu, G., Squadrelli, M., Quattrone, P., Locati, L.D., Bergamini, C., Olmi, P., Pierotti, M.A. & Pilotti, S. 2006, "High-risk human papillomavirus affects prognosis in patients with surgically treated oropharyngeal squamous cell carcinoma", *J. Clin. Oncol.,* 24(36):5630-5636.

Limon-Mortes, M.C., Mora-Santos, M., Espina, A., Pintor-Toro, J.A., Lopez-Roman, A., Tortolero, M. & Romero, F. 2008, "UV-induced degradation of securin is mediated by SKP1-CUL1-beta TrCP E3 ubiquitin ligase", *J. Cell Sci.,* 121(11):1825-1831.

Lin, Y., Clair, J.M., Luo, J., Sharma, S., Dubinett, S. & John, M.S. 2015a, "p53 modulates NF-κB mediated epithelial-to-mesenchymal transition in head and neck squamous cell carcinoma", *Oral Oncol.,* 51(10):921-928.

Lin, Y., Tian, Y., Wang, J., Jiang, Y., Luo, Y. & Chen, Y. 2015b, "Pituitary tumor-transforming gene 1 regulates invasion of prostate cancer cells through MMP13", *Tumor Biol.,* [Epub ahead of print]:1-6.

Lo, J., Yu, C., Chiou, S., Huang, C., Jan, C., Lin, S., Liu, C., Hu, W. & Yu, Y. 2011, "The epithelial-mesenchymal transition mediator S100A4 maintains cancer-initiating cells in head and neck cancers", *Cancer Res.,* 71(5):1912-1923.

Lo, Y.M., Chan, A.T., Chan, L.Y., Leung, S.F., Lam, C.W., Huang, D.P. & Johnson, P.J. 2000, "Molecular prognostication of nasopharyngeal carcinoma by quantitative analysis of circulating Epstein-Barr virus DNA", *Cancer Res.,* 60(24):6878-6881.

Lo, Y.M., Chan, L.Y., Lo, K.W., Leung, S.F., Zhang, J., Chan, A.T., Lee, J.C., Hjelm, N.M., Johnson, P.J. & Huang, D.P. 1999, "Quantitative analysis of cell-free Epstein-Barr virus DNA in plasma of patients with nasopharyngeal carcinoma", *Cancer Res.,* 59(6):1188-1191.

Lohavanichbutr, P., Houck, J., Fan, W., Yueh, B., Mendez, E., Futran, N., Doody, D.R., Upton, M.P., Farwell, D.G. & Schwartz, S.M. 2009, "Genomewide gene expression profiles of HPV-positive and HPV-negative oropharyngeal cancer: potential implications for treatment choices", *Arch. Otolaryngol. Head Neck Surg.,* 135(2):180-188.

Longo, M.C., Berninger, M.S. & Hartley, J.L. 1990, "Use of uracil DNA glycosylase to control carry-over contamination in polymerase chain reactions", *Gene,* 93(1):125-128.

Losada, A., Hirano, M., Hirano, T. 2002, "Cohesin release is required for sister chromatid resolution, but not for condensin-mediated compaction, at the onset of mitosis", *Genes Dev.,* 16(23):3004-3016.

Louie, K.S., Mehanna, H., Sasieni, P. 2015 "Trends in head and neck cancers in England from 1995 to 2011 and projections up to 2025", *Oral Oncol.,* 51(4):341-348.

Lui, V.W., Hedberg, M.L., Li, H., Vangara, B.S., Pendleton, K., Zeng, Y., Lu, Y., Zhang, Q., Du, Y., Gilbert, B.R., Freilino, M., Sauerwein, S., Peyser, N.D., Xiao, D., Diergaarde, B., Wang, L., Chiosea, S., Seethala, R., Johnson, J.T., Kim, S., Duvvuri, U., Ferris, R.L., Romkes, M., Nukui, T., Kwok-Shing Ng, P., Garraway, L.A., Hammerman, P.S., Mills, G.B. & Grandis, J.R. 2013, "Frequent mutation of the PI3K pathway in head and neck cancer defines predictive biomarkers", *Cancer Discov.*, 3(7):761-769.

Lukits, J., Remenar, E., Rásó, E., Ladányi, A., Kásler, M. & Tímár, J. 2007, "Molecular identification, expression and prognostic role of estrogen-and progesterone receptors in head and neck cancer", *Int. J. Oncol.*, 30(1):155-160.

Luo, M.L., Shen, X.M., Zhang, Y., Wei, F., Xu, X., Cai, Y., Zhang, X., Sun, Y.T., Zhan, Q.M., Wu, M. & Wang, M.R. 2006, "Amplification and overexpression of CTTN (EMS1) contribute to the metastasis of esophageal squamous cell carcinoma by promoting cell migration and anoikis resistance", *Cancer Res.*, 66(24):11690-11699.

Lyakhovich, A. & Shekhar, M.P.V. 2003, "Supramolecular complex formation between Rad6 and proteins of the p53 pathway during DNA damage-induced response", *Mol. Cell Biol.*, 23(7):2463-2475.

Lynch, P.J. 2006, "Head lateral mouth anatomy.jpg", *Wikimedia Commons: Creative Commons Attribution 2.5 Generic*.

Makarova, K.S., Grishin, N.V., Shabalina, S.A., Wolf, Y.I. & Koonin, E.V. 2006, "A putative RNA-interference-based immune system in prokaryotes: computational analysis of the predicted enzymatic machinery, functional analogies with eukaryotic RNAi, and hypothetical mechanisms of action", *Biol. Direct*, 1:7.

Mali, P., Yang, L., Esvelt, K.M., Aach, J., Guell, M., DiCarlo, J.E., Norville, J.E. & Church, G.M. 2013, "RNA-guided human genome engineering via Cas9", *Science*, 339(6121):823-826.

Malik, M.T. & Kakar, S.S. 2006, "Regulation of angiogenesis and invasion by human Pituitary tumor transforming gene (PTTG) through increased expression and secretion of matrix metalloproteinase-2 (MMP-2)", *Mol. Cancer*, 5:61.

McCabe, C., Boelaert, K., Tannahill, L., Heaney, A., Stratford, A., Khaira, J., Hussain, S., Sheppard, M., Franklyn, J. & Gittoes, N. 2002, "Vascular endothelial growth factor, its receptor KDR/Flk-1, and pituitary tumor transforming gene in pituitary tumors", *J. Clin. Endocrinol. Metab.*, 87(9):4238-4244.

McCabe, C. & Gittoes, N. 1999, "PTTG--a new pituitary tumour transforming gene", *J. Endocrinol.*, 162(2):163-166.

McCabe, C., Khaira, J., Boelaert, K., Heaney, A., Tannahill, L., Hussain, S., Mitchell, R., Olliff, J., Sheppard, M. & Franklyn, J. 2003, "Expression of pituitary tumour transforming gene (PTTG) and fibroblast growth factor 2 (FGF 2) in human pituitary adenomas: relationships to clinical tumour behaviour", *Clin. Endocrinol.*, 58(2):141-150.

Mcintyre, G.J., Arndt, A.J., Gillespie, K.M., Mak, W.M. & Fanning, G.C. 2011, "A comparison of multiple shRNA expression methods for combinatorial RNAi", *Genet. Vaccines Ther.*, 9:9.

McKay, J.D., Truong, T., Gaborieau, V., Chabrier, A., Chuang, S., Byrnes, G., Zaridze, D., Shangina, O., Szeszenia-Dabrowska, N. & Lissowska, J. 2011, "A genome-wide association study of upper aerodigestive tract cancers conducted within the INHANCE consortium", *PLoS Genet.*, 7(3):e1001333.

McManus, M.T., Petersen, C.P., Haines, B.B., Chen, J. & Sharp, P.A. 2002, "Gene silencing using micro-RNA designed hairpins", *RNA*, 8(6):842-850.

Mehanna, H., Evans, M., Beasley, M., Chatterjee, S., Dilkes, M., Homer, J., O'Hara, J., Robinson, M., Shaw, R. & Sloan, P. 2016, "Oropharyngeal cancer: United Kingdom National Multidisciplinary Guidelines", *J. Laryngol. Otol.*, 130(suppl 2):S90.

Mehanna, H., West, C., Nutting, C. & Paleri, V. 2010, "Head and neck cancer–Part 2: Treatment and prognostic factors", *BMJ*, 341(c4690):721-725.

Mehanna, H., Beech, T., Nicholson, T., El Hariry, I., McConkey, C., Paleri, V. & Roberts, S. 2012, "Prevalence of human papillomavirus in oropharyngeal and nonoropharyngeal head and neck cancer—systematic review and meta analysis of trends by time and region", *Head Neck*, 35(5):747-55.

Melloni, G.E., Ogier, A.G., de Pretis, S., Mazzarella, L., Pelizzola, M., Pelicci, P.G. & Riva, L. 2014, "DOTS-Finder: a comprehensive tool for assessing driver genes in cancer genomes", *Genome Med.*, 6(6):1.

Mirghani, H., Amen, F., Blanchard, P., Moreau, F., Guigay, J., Hartl, D. & Lacau St Guily, J. 2015, "Treatment de escalation in HPV positive oropharyngeal carcinoma: Ongoing trials, critical issues and perspectives", *Int. J. Cancer*, 136(7):1494-1503.

Montini, E., Cesana, D., Schmidt, M., Sanvito, F., Ponzoni, M., Bartholomae, C., Sergi Sergi, L., Benedicenti, F., Ambrosi, A. & Di Serio, C., Doglioni, C., von Kalle, C. & Naldini, L. 2006, "Hematopoietic stem cell gene transfer in a tumor-prone mouse model uncovers low genotoxicity of lentiviral vector integration", *Nat. Biotechnol.*, 24(6):687-696.

Mooren, J.J., Kremer, B., Claessen, S.M., Voogd, A.C., Bot, F.J., Peter Klussmann, J., Huebbers, C.U., Hopman, A.H., Ramaekers, F. & Speel, E.M. 2013, "Chromosome stability in tonsillar squamous cell carcinoma is associated with HPV16 integration and indicates a favorable prognosis", *Int. J. Cancer*, 132(8):1781-1789.

Mora-Santos, M., Castilla, C., Herrero-Ruiz, J., Giráldez, S., Limón-Mortés, M.C., Sáez, C., Japón, M.Á, Tortolero, M. & Romero, F. 2013, "A single mutation in Securin induces chromosomal instability and enhances cell invasion", *Eur. J. Cancer*, 49(2):500-510.

Mora-Santos, M., Limon-Mortes, M.C., Giraldez, S., Herrero-Ruiz, J., Saez, C., Japon, M.A., Tortolero, M. & Romero, F. 2011, "Glycogen synthase kinase-3beta (GSK3beta) negatively

regulates PTTG1/human securin protein stability, and GSK3beta inactivation correlates with securin accumulation in breast tumors", *J. Biol. Chem.,* 286(34):30047-30056.

Mu, Y., OBA, K., Yanase, T., Ito, T., Ashida, K., Goto, K., Morinaga, H., Ikuyama, S., Takayanagi, R. & Nawata, H. 2003, "Human Pituitary Tumor Transforming Gene (hPTTG) Inhibits Human Lung Cancer A549 Cell Growth through Activation of p21WAF1/CIP1", *Endocr. J.,* 50(6):771-781.

Mukhopadhyay, U.K., Mooney, P., Jia, L., Eves, R., Raptis, L. & Mak, A.S. 2010, "Doubles game: Src-Stat3 versus p53-PTEN in cellular migration and invasion", *Mol. Cell. Biol.,* 30(21):4980-4995.

Muller, P.A., Caswell, P.T., Doyle, B., Iwanicki, M.P., Tan, E.H., Karim, S., Lukashchuk, N., Gillespie, D.A., Ludwig, R.L. & Gosselin, P. 2009, "Mutant p53 drives invasion by promoting integrin recycling", *Cell,* 139(7):1327-1341.

Munger, K., Scheffner, M., Huibregtse, J.M. & Howley, P.M. 1992, "Interactions of HPV E6 and E7 oncoproteins with tumour suppressor gene products", *Cancer Surv.,* 12:197-217.

Munger, K., Werness, B.A., Dyson, N., Phelps, W.C., Harlow, E. & Howley, P.M. 1989, "Complex formation of human papillomavirus E7 proteins with the retinoblastoma tumor suppressor gene product", *EMBO,* 8(13):4099-4105.

Naldini, L. 1998, "Lentiviruses as gene transfer agents for delivery to non-dividing cells", *Curr. Opin. Biotechnol.,* 9(5):457-463.

Negri, E., Boffetta, P., Berthiller, J., Castellsague, X., Curado, M.P., Maso, L.D., Daudt, A.W., Fabianova, E., Fernandez, L. & Wünsch Filho, V. 2009, "Family history of cancer: pooled analysis in the International Head and Neck Cancer Epidemiology Consortium", *Int. J. Cancer,* 124(2):394-401.

Nickoloff, B., Qin, J., Chaturvedi, V., Denning, M., Bonish, B. & Miele, L. 2002, "Jagged-1 mediated activation of notch signaling induces complete maturation of human keratinocytes through NF-κB and PPARγ.", *Cell Death Differ,* 9(8):842-55.

Nicolas, M., Wolfer, A., Raj, K., Kummer, J.A., Mill, P., van Noort, M., Hui, C., Clevers, H., Dotto, G.P. & Radtke, F. 2003, "Notch1 functions as a tumor suppressor in mouse skin", *Nature Genet.,* 33(3):416-421.

Nutting, C. 2016, "Radiotherapy in head and neck cancer management: United Kingdom National Multidisciplinary Guidelines", *J. Laryngol. Otol.,* 130(suppl 2):S66.

Old, L.J., Boyse, E.A., Oettgen, H.F., Harven, E.D., Geering, G., Williamson, B. & Clifford, P. 1966, "Precipitating antibody in human serum to an antigen present in cultured burkitt's lymphoma cells", *PNAS,* 56(6):1699-1704.

Park, J.W., Nickel, K.P., Torres, A.D., Lee, D., Lambert, P.F. & Kimple, R.J. 2014, "Human papillomavirus type 16 E7 oncoprotein causes a delay in repair of DNA damage", *Radiother. Oncol.,* 113(3):337-344.

Patel, S.G. & Shah, J.P. 2005, "TNM staging of cancers of the head and neck: striving for uniformity among diversity", *CA Cancer J. Clin.,* 55(4):242-258.

Pei, L. 2000, "Activation of mitogen-activated protein kinase cascade regulates pituitary tumor-transforming gene transactivation function", *J. Biol. Chem.,* 275(40):31191-31198.

Pei, L. & Melmed, S. 1997, "Isolation and characterization of a pituitary tumor-transforming gene (PTTG)", *Mol. Endocrinol.,* 11(4):433-441.

Pei, L. 2001, "Identification of c-myc as a down-stream target for pituitary tumor-transforming gene", *J. Biol. Chem.,* 276(11):8484-8491.

Perry, M.E. 1994, "The specialised structure of crypt epithelium in the human palatine tonsil and its functional significance", *J. Anat.,* 185(pt 1):111-127.

Petitjean, A., Mathe, E., Kato, S., Ishioka, C., Tavtigian, S.V., Hainaut, P. & Olivier, M. 2007, "Impact of mutant p53 functional properties on TP53 mutation patterns and tumor phenotype: lessons from recent developments in the IARC TP53 database; Database version: R18, April 2016", *Hum. Mutat.,* 28(6):622-629.

Petras, K. & Ostman, A. 2010, "Hallmarks of cancer: interactions with the tumour stroma", *Exp. Cell Res.,* 316:1324-1331.

Price, G., Roche, M., Crowther, R. & Wright, R. 2010, "Profile of head and neck cancers in England: incidence, mortality and survival".

Price, K.A. & Cohen, E.E. 2012, "Current treatment options for metastatic head and neck cancer", *Curr. Treat. Options Oncol.,* 13(1):35-46.

Purdue, M.P., Hashibe, M., Berthiller, J., La Vecchia, C., Dal Maso, L., Herrero, R., Franceschi, S., Castellsague, X., Wei, Q., Sturgis, E.M., Morgenstern, H., Zhang, Z.F., Levi, F., Talamini, R., Smith, E., Muscat, J., Lazarus, P., Schwartz, S.M., Chen, C., Neto, J.E., Wunsch-Filho, V., Zaridze, D., Koifman, S., Curado, M.P., Benhamou, S., Matos, E., Szeszenia-Dabrowska, N., Olshan, A.F., Lence, J., Menezes, A., Daudt, A.W., Mates, I.N., Pilarska, A., Fabianova, E., Rudnai, P., Winn, D., Ferro, G., Brennan, P., Boffetta, P. & Hayes, R.B. 2009, "Type of alcoholic beverage and risk of head and neck cancer--a pooled analysis within the INHANCE Consortium", *Am. J. Epidemiol.,* 169(2):132-142.

Pyeon, D., Newton, M.A., Lambert, P.F., den Boon, J.A., Sengupta, S., Marsit, C.J., Woodworth, C.D., Connor, J.P., Haugen, T.H., Smith, E.M., Kelsey, K.T., Turek, L.P. & Ahlquist, P. 2007, "Fundamental differences in cell cycle deregulation in human papillomavirus-positive and human papillomavirus-negative head/neck and cervical cancers", *Cancer Res.,* 67(10):4605-4619.

Que, L., Zhao, D., Tang, X., Liu, J., Zhang, X., Zhan, Y. & Zhang, L. 2015 "Effects of lentivirus-mediated shRNA targeting integrin-linked kinase in oral squamous cell carcinoma", *Oncol. Rep.,* 35(1):89-98.

Ramaswamy, S., Ross, K.N., Lander, E.S. & Golub, T.R. 2003, "A molecular signature of metastasis in primary solid tumors", *Nature Genet.,* 33(1):49-54.

Ramos-Morales, F., Domínguez, Á, Romero, F., Luna, R., Multon, M., Pintor-Toro, J.A. & Tortolero, M. 2000, "Cell cycle regulated expression and phosphorylation of hpttg proto-oncogene product", *Oncogene,* 19(3):403-9.

Rampias, T., Pectasides, E., Prasad, M., Sasaki, C., Gouveris, P., Dimou, A., Kountourakis, P., Perisanidis, C., Burtness, B., Zaramboukas, T., Rimm, D., Fountzilas, G. & Psyrri, A. 2013, "Molecular profile of head and neck squamous cell carcinomas bearing p16 high phenotype", *Ann. Oncol.,* 24(8):2124-2131.

Rangarajan, A., Talora, C., Okuyama, R., Nicolas, M., Mammucari, C., Oh, H., Aster, J.C., Krishna, S., Metzger, D., Chambon, P., Miele, L., Aguet, M., Radtke, F. & Dotto, G.P. 2001, "Notch signaling is a direct determinant of keratinocyte growth arrest and entry into differentiation", *EMBO,* 20(13):3427-3436.

Read, M.L., Fong, J.C.W., Imruetaicharoenchoke, W., Modasia, B., Nieto, H.R., Fletcher, A., Thompson, R., Bacon, A., Mallick, U., Hackshaw, A., Watkinson, J.C., Boelaert, K., Turnell, A.S., Smith, V.E. & McCabe, C.j. 2016a, "Elevated PTTG and PBF predicts poor patient outcome and modulates DNA damage response genes in thyroid cancer", *Oncogene,* under revision.

Read, M.L., Lewy, G.D., Fong, J.C.W., Sharma, N., Seed, R.I., Smith, V.E., Gentilin, E., Warfield, A., Eggo, M.C. & Knauf, J.A. 2011, "Proto-oncogene PBF/PTTG1IP regulates thyroid cell growth and represses radioiodide treatment", *Cancer Res.,* 71(19):6153-6164.

Read, M.L., Seed, R.I., Fong, J.C., Modasia, B., Ryan, G.A., Watkins, R.J., Gagliano, T., Smith, V.E., Stratford, A.L. & Kwan, P.K. 2014, "The PTTG1-Binding Factor (PBF/PTTG1IP) regulates p53 activity in thyroid cells", *Endocrinology,* 155(4):1222-1234.

Read, M.L., Seed, R.I., Modasia, B., Kwan, P.P., Sharma, N., Smith, V.E., Watkins, R.J., Bansal, S., Gagliano, T. & Stratford, A.L. 2016b, "The proto oncogene PBF binds p53 and is associated with prognostic features in colorectal cancer", *Mol. Carcinog.,* 55(1):15-26.

Reed, A.L., Califano, J., Cairns, P., Westra, W.H., Jones, R.M., Koch, W., Ahrendt, S., Eby, Y., Sewell, D., Nawroz, H., Bartek, J. & Sidransky, D. 1996, "High frequency of p16 (CDKN2/MTS-1/INK4A) inactivation in head and neck squamous cell carcinoma", *Cancer Res.,* 56(16):3630-3633.

Reynolds, A., Leake, D., Boese, Q., Scaringe, S., Marshall, W.S. & Khvorova, A. 2004, "Rational siRNA design for RNA interference", *Nat. Biotech.,* 22(3):326-330.

Rieckmann, T., Tribius, S., Grob, T.J., Meyer, F., Busch, C., Petersen, C., Dikomey, E. & Kriegs, M. 2013, "HNSCC cell lines positive for HPV and p16 possess higher cellular radiosensitivity due to an impaired DSB repair capacity", *Radiother. Oncol.*, 107(2):242-246.

Rodrigo, J.P., Garcia, L.A., Ramos, S., Lazo, P.S. & Suarez, C. 2000, "EMS1 gene amplification correlates with poor prognosis in squamous cell carcinomas of the head and neck", *Clin. Cancer Res.*, 6(8):3177-3182.

Roland, N., Porter, G., Fish, B. & Makura, Z. 2016, "Tumour assessment and staging: United Kingdom National Multidisciplinary Guidelines", *J. Laryngol. Otol.*, 130(suppl 2):S53.

Romero, F., Gil-Bernabe, A.M., Saez, C., Japon, M.A., Pintor-Toro, J.A. & Tortolero, M. 2004, "Securin is a target of the UV response pathway in mammalian cells", *Mol. Cell. Biol.* 24(7):2720-2733.

Romero, F., Multon, M.C., Ramos-Morales, F., Dominguez, A., Bernal, J.A., Pintor-Toro, J.A. & Tortolero, M. 2001, "Human securin, hPTTG, is associated with Ku heterodimer, the regulatory subunit of the DNA-dependent protein kinase", *Nucleic Acids Res.*, 29(6):1300-1307.

Rosen, D.G., Huang, X., Deavers, M.T., Malpica, A., Silva, E.G. & Liu, J. 2004, "Validation of tissue microarray technology in ovarian carcinoma", *Mod. Pathol.*, 17(7):790-797.

Rothenberg, S.M. & Ellisen, L.W. 2012, "The molecular pathogenesis of head and neck squamous cell carcinoma", *J. Clin. Invest.*, 122(6):1951-1957.

Rubin Grandis, J., Melhem, M.F., Gooding, W.E., Day, R., Holst, V.A., Wagener, M.M., Drenning, S.D. & Tweardy, D.J. 1998, "Levels of TGF-alpha and EGFR protein in head and neck squamous cell carcinoma and patient survival", *J. Nat. Cancer Inst.*, 90(11):824-832.

Saez, C., Japon, M.A., Ramos-Morales, F., Romero, F., Segura, D.I., Tortolero, M. & Pintor-Toro, J.A. 1999, "hpttg is over-expressed in pituitary adenomas and other primary epithelial neoplasias.", *Oncogene*, 18(39):5473.

Salehi, F., Kovacs, K., Scheithauer, B.W., Lloyd, R.V. & Cusimano, M. 2008, "Pituitary tumor-transforming gene in endocrine and other neoplasms: a review and update", *Endocr. Relat. Cancer*, 15(3):721-743.

Sano, D., Xie, T.X., Ow, T.J., Zhao, M., Pickering, C.R., Zhou, G., Sandulache, V.C., Wheeler, D.A., Gibbs, R.A., Caulin, C. & Myers, J.N. 2011, "Disruptive TP53 mutation is associated with aggressive disease characteristics in an orthotopic murine model of oral tongue cancer", *Clin. Cancer Res.*, 17(21):6658-6670.

Scheffner, M., Huibregtse, J.M., Vierstra, R.D. & Howley, P.M. 1993, "The HPV-16 E6 and E6-AP complex functions as a ubiquitin-protein ligase in the ubiquitination of p53", *Cell*, 75(3):495-505.

Scheffner, M., Werness, B.A., Huibregtse, J.M., Levine, A.J. & Howley, P.M. 1990, "The E6 oncoprotein encoded by human papillomavirus types 16 and 18 promotes the degradation of p53", *Cell,* 63(6):1129-1136.

Scherer, W.F., Syverton, J.T. & Gey, G.O. 1953, "Studies on the propagation in vitro of polymyelitis viruses: IV viral multiplication in a stable strain of human malignant epithelial cells (strain Hela) derived from an epidermoid carcinoma of the cervix", *J. Exp. Med.,* 97(5):695-710.

Schuuring, E. 1995, "The involvement of the chromosome 11q13 region in human malignancies: cyclin D1 and EMS1 are two new candidate oncogenes-a review", *Gene,* 159(1):83-96.

Schuuring, E., Verhoeven, E., Litvinov, S. & Michalides, R.J. 1993, "The product of the EMS1 gene, amplified and overexpressed in human carcinomas, is homologous to a v-src substrate and is located in cell-substratum contact sites", *Mol. Cell. Biol.,* 13(5):2891-2898.

Schwartz, S.M., Daling, J.R., Doody, D.R., Wipf, G.C., Carter, J.J., Madeleine, M.M., Mao, E.J., Fitzgibbons, E.D., Huang, S., Beckmann, A.M., McDougall, J.K. & Galloway, D.A. 1998, "Oral cancer risk in relation to sexual history and evidence of human papillomavirus infection", *J. Nat. Cancer Inst.,* 90(21):1626-1636.

Sethi, S., Ali Fehmi, R., Franceschi, S., Struijk, L., van Doorn, L., Quint, W., Albashiti, B., Ibrahim, M. & Kato, I. 2012, "Characteristics and survival of head and neck cancer by HPV status: a cancer registry based study", *Int. J. Cancer,* 131(5):1179-1186.

Shah, P.P., Fong, M.Y. & Kakar, S.S. 2012, "PTTG induces EMT through integrin αVβ3-focal adhesion kinase signaling in lung cancer cells", *Oncogene,* 31(26):3124-3135.

Shah, P.P. & Kakar, S.S. 2011a, "Pituitary tumor transforming gene induces epithelial to mesenchymal transition by regulation of Twist, Snail, Slug, and E-cadherin", *Cancer Lett.,* 311(1):66-76.

Shah, P.P. & Kakar, S.S. 2011b, "Regulation of integrins AlphaV Beta3 and focal adhesion kinase signaling by PTTG in induction of EMT", *Cancer Res.,* 71(8):3431-3431.

Shah, O.J., Ghosh, S. & Hunter, T. 2003, "Mitotic regulation of ribosomal S6 kinase 1 involves Ser/Thr, Pro phosphorylation of consensus and non-consensus sites by Cdc2", *The J. Biol. Chem.,* 278(18):16433-16442.

Shao, X., Tandon, R., Samara, G., Kanki, H., Yano, H., Close, L.G., Parsons, R. & Sato, T. 1998, "Mutational analysis of the PTEN gene in head and neck squamous cell carcinoma", *Int. J. Cancer,* 77(5):684-688.

Sharma, A., Singh, K. & Almasan, A. 2012, "Histone H2AX phosphorylation: a marker for DNA damage", *Methods Mol. Biol.,* 920:613-626.

Shatalova, E.G., Klein-Szanto, A.J., Devarajan, K., Cukierman, E. & Clapper, M.L. 2011, "Estrogen and cytochrome P450 1B1 contribute to both early-and late-stage head and neck carcinogenesis", *Cancer Prev. Res.,* 4(1):107-115.

Sheleg, S.V., Peloponese, J.M., Chi, Y.H., Li, Y., Eckhaus, M. & Jeang, K.T. 2007, "Evidence for cooperative transforming activity of the human pituitary tumor transforming gene and human T-cell leukemia virus type 1 Tax", *J. Virol.,* 81(15):7894-7901.

Shibata, Y., Haruki, N., Kuwabara, Y., Nishiwaki, T., Kato, J., Shinoda, N., Sato, A., Kimura, M., Koyama, H., Toyama, T., Ishiguro, H., Kudo, J., Terashita, Y., Konishi, S. & Fujii, Y. 2002, "Expression of PTTG (Pituitary Tumor Transforming Gene) in Esophageal Cancer", *Jpn. J. Clin. Oncol.,* 32(7):233-237.

Shieh, S., Ikeda, M., Taya, Y. & Prives, C. 1997, "DNA damage-induced phosphorylation of p53 alleviates inhibition by MDM2", *Cell,* 91(3):325-334.

Shillitoe, E. & Noonan, S. 2000, "Strength and specificity of different gene promoters in oral cancer cells", *Oral Oncol.,* 36(2):214-220.

Siegel, R.L., Miller, K.D. & Jemal, A. 2016, "Cancer statistics, 2016", *CA Cancer J. Clin.,* 66(1):7-30.

Smeets, S.J., van der Plas, M., Schaaij Visser, T., van Veen, E.A., van Meerloo, J., Braakhuis, B.J., Steenbergen, R.D. & Brakenhoff, R.H. 2011, "Immortalization of oral keratinocytes by functional inactivation of the p53 and pRb pathways", *Int. J. Cancer,* 128(7):1596-1605.

Smith, V.E., Read, M.L., Turnell, A.S., Watkins, R.J., Watkinson, J.C., Lewy, G.D., Fong, J.C.W., James, S.R., Eggo, M.C. & Boelaert, K. 2009, "A novel mechanism of sodium iodide symporter repression in differentiated thyroid cancer", *J. Cell. Sci.,* 122(18):3393-3402.

Smith, V., Sharma, N., Watkins, R., Read, M., Ryan, G., Kwan, P., Martin, A., Watkinson, J., Boelaert, K. & Franklyn, J. 2013, "Manipulation of PBF/PTTG1IP phosphorylation status; a potential new therapeutic strategy for improving radioiodine uptake in thyroid and other tumors", *J. Clin. Endocrinol. Metab.,* 98(7):2876-2886.

Sok, J.C., Coppelli, F.M., Thomas, S.M., Lango, M.N., Xi, S., Hunt, J.L., Freilino, M.L., Graner, M.W., Wikstrand, C.J., Bigner, D.D., Gooding, W.E., Furnari, F.B. & Grandis, J.R. 2006, "Mutant epidermal growth factor receptor (EGFRvIII) contributes to head and neck cancer growth and resistance to EGFR targeting", *Clin. Cancer Res.,* 12:5064-5073.

Solbach, C., Roller, M., Fellbaum, C., Nicoletti, M. & Kaufmann, M. 2004, "PTTG mRNA expression in primary breast cancer: a prognostic marker for lymph node invasion and tumor recurrence", *Breast,* 13(1):80-81.

Solbach, C., Roller, M., Eckerdt, F., Peters, S. & Knecht, R. 2006, "Pituitary tumor-transforming gene expression is a prognostic marker for tumor recurrence in squamous cell carcinoma of the head and neck", *BMC Cancer,* 6:242.

Song, J., Giang, A., Lu, Y., Pang, S. & Chiu, R. 2008, "Multiple shRNA expressing vector enhances efficiency of gene silencing", *BMB Rep.,* 41(5):358-362.

Song, X., Xia, R., Li, J., Long, Z., Ren, H., Chen, W. & Mao, L. 2014, "Common and complex Notch1 mutations in Chinese oral squamous cell carcinoma", *Clin. Cancer Res.,* 20(3):701-710.

Stamenkovic, I. 2000, "Matrix metalloproteinases in tumor invasion and metastasis", *Semin. Cancer Biol.,* 10(6):415-33.

Stephens, P.J., Tarpey, P.S., Davies, H., Van Loo, P., Greenman, C., Wedge, D.C., Nik-Zainal, S., Martin, S., Varela, I. & Bignell, G.R. 2012, "The landscape of cancer genes and mutational processes in breast cancer", *Nature,* 486(7403):400-404.

Stock, M., Schäfer, H., Fliegauf, M. & Otto, F. 2004, "Identification of Novel Target Genes of the Bone Specific Transcription Factor Runx2", *J. Bone Miner. Res.,* 19(6):959-972.

Stransky, N., Egloff, A.M., Tward, A.D., Kostic, A.D., Cibulskis, K., Sivachenko, A., Kryukov, G.V., Lawrence, M.S., Sougnez, C., McKenna, A., Shefler, E., Ramos, A.H., Stojanov, P., Carter, S.L., Voet, D., Cortes, M.L., Auclair, D., Berger, M.F., Saksena, G., Guiducci, C., Onofrio, R.C., Parkin, M., Romkes, M., Weissfeld, J.L., Seethala, R.R., Wang, L., Rangel-Escareno, C., Fernandez-Lopez, J.C., Hidalgo-Miranda, A., Melendez-Zajgla, J., Winckler, W., Ardlie, K., Gabriel, S.B., Meyerson, M., Lander, E.S., Getz, G., Golub, T.R., Garraway, L.A. & Grandis, J.R. 2011, "The mutational landscape of head and neck squamous cell carcinoma", *Science,* 333(6046):1157-1160.

Stratford, A.L., Boelaert, K., Tannahill, L.A., Kim, D.S., Warfield, A., Eggo, M.C., Gittoes, N.J.L., Young, L.S., Franklyn, J.A. & McCabe, C.J. 2005, "Pituitary tumor transforming gene binding factor: a novel transforming gene in thyroid tumorigenesis", *J. Clin. Endocronol. Metab.,* 90(7):4341-4349.

Sumara, I., Vorlaufer, E., Stukenberg, P.T., Kelm, O., Redemann, N., Nigg, E.A. & Peters, J. 2002, "The dissociation of cohesin from chromosomes in prophase is regulated by Polo-like kinase", *Mol. Cell,* 9(3):515-525.

Sun, Z., Hu, W., Xu, J., Kaufmann, A.M. & Albers, A.E. 2015, "MicroRNA-34a regulates epithelial-mesenchymal transition and cancer stem cell phenotype of head and neck squamous cell carcinoma in vitro", *Int. J. Oncol.,* 47(4):1339-1350.

Sun, W., Gaykalova, D.A., Ochs, M.F., Mambo, E., Arnaoutakis, D., Liu, Y., Loyo, M., Agrawal, N., Howard, J., Li, R., Ahn, S., Fertig, E., Sidransky, D., Houghton, J., Buddavarapu, K., Sanford, T., Choudhary, A., Darden, W., Adai, A., Latham, G., Bishop, J., Sharma, R., Westra, W.H., Hennessey, P., Chung, C.H. & Califano, J.A. 2014, "Activation of the NOTCH pathway in head and neck cancer", *Cancer Res.,* 74(4):1091-1104.

Talora, C., Sgroi, D.C., Crum, C.P. & Dotto, G.P. 2002, "Specific down-modulation of Notch1 signaling in cervical cancer cells is required for sustained HPV-E6/E7 expression and late steps of malignant transformation", *Genes Dev.,* 16(17):2252-2263.

Tfelt-Hansen, J., Yano, S., Bandyopadhyay, S., Carroll, R., Brown, E.M. & Chattopadhyay, N. 2004, "Expression of pituitary tumor transforming gene (PTTG) and its binding protein in human astrocytes and astrocytoma cells: function and regulation of PTTG in U87 astrocytoma cells", *Endocrinology,* 145(9):4222-4231.

Thiery, J.P., Acloque, H., Huang, R.Y. & Nieto, M.A. 2009, "Epithelial-mesenchymal transitions in development and disease", *Cell,* 139(5):871-890.

Thompson, A.D. & Kakar, S.S. 2005, "Insulin and IGF-1 regulate the expression of the pituitary tumor transforming gene (PTTG) in breast tumor cells", *FEBS Lett.,* 579(14):3195-3200.

Tong, Y., Tan, Y., Zhou, C. & Melmed, S. 2007, "Pituitary tumor transforming gene interacts with Sp1 to modulate G1/S cell phase transition", *Oncogene,* 26(38):5596-5605.

Torre, L.A., Bray, F., Siegel, R.L., Ferlay, J., Lortet-Tieulent, J. & Jemal, A. 2015, "Global cancer statistics, 2012", *CA Cancer J. Clin.,* 65(2):87-108.

Travasso, C. 2013, "Betel quid chewing is responsible for half of oral cancer cases in India, finds study", *BMJ,* 347:f7536.

Tsao, Y.P., Li, L.Y., Tsai, T.C. & Chen, S.L. 1996, "Human papillomavirus type 11 and 16 E5 represses p21(WafI/SdiI/CipI) gene expression in fibroblasts and keratinocytes", *J. Virol.,* 70(11):7535-7539.

van Houten, V.M.M., Snijders, P.J.F., van den Brekel, M.W.M., Kummer, J.A., Meijer, C.J.L.M., van Leeuwen, B., Denkers, F., Smeele, L.E., Snow, G.B. & Brakenhoff, R.H. 2001, "Biological evidence that human papillomaviruses are etiologically involved in a subgroup of head and neck squamous cell carcinomas", *Int. J. Cancer,* 93(2):232-235.

van Monsjou, H.S., Wreesmann, V.B., van den Brekel, Michiel WM & Balm, A.J. 2013, "Head and neck squamous cell carcinoma in young patients", *Oral Oncol.,* 49(12):1097-1102.

Vander Broek, R., Mohan, S., Eytan, D., Chen, Z. & Van Waes, C. 2015, "The PI3K/Akt/mTOR axis in head and neck cancer: functions, aberrations, cross talk, and therapies", *Oral Dis.,* 21(7):815-825.

Varela-Lema, L., Taioli, E., Ruano-Ravina, A., Barros-Dios, J.M., Anantharaman, D., Benhamou, S., Boccia, S., Bhisey, R.A., Cadoni, G. & Capoluongo, E. 2008, "Meta-analysis and pooled analysis of GSTM1 and CYP1A1 polymorphisms and oral and pharyngeal cancers: a HuGE-GSEC review", *Genet. Med.,* 10(6):369-384.

Vogelstein, B., Lane, D. & Levine, A.J. 2000, "Surfing the p53 network", *Nature,* 408(6810):307.

Waizenegger, I.C., Hauf, S., Meinke, A. & Peters, J. 2000, "Two distinct pathways remove mammalian cohesin from chromosome arms in prophase and from centromeres in anaphase", *Cell,* 103(3):399-410.

Waldman, T., Kinzler, K.W. & Vogelstein, B. 1995, "p21 is necessary for the p53-mediated G1 arrest in human cancer cells", *Cancer Res.,* 55(22):5187-5190.

Walter, V., Yin, X., Wilkerson, M.D., Cabanski, C.R., Zhao, N., Du, Y., Ang, M.K., Hayward, M.C., Salazar, A.H. & Hoadley, K.A. 2013, "Molecular subtypes in head and neck cancer exhibit distinct patterns of chromosomal gain and loss of canonical cancer genes", *PloS one,* 8(2):e56823.

Wang, S., Wang, W., Chang, Y., Wu, C., Chao, Y., Kao, S., Yuan, A., Lin, C., Yang, S. & Chan, W. 2009, "p53 controls cancer cell invasion by inducing the MDM2-mediated degradation of Slug", *Nat. Cell. Biol.,* 11(6):694-704.

Wang, X.J., Li, Y., Huang, H., Zhang, X.J., Xie, P.W., Hu, W., Li, D.D. & Wang, S.Q. 2013, "A simple and robust vector-based shRNA expression system used for RNA interference", *PLoS One,* 8(2):e56110.

Wang, X., Deng, X. & Li, L. 2014, "MicroRNA-584 functions as a tumor suppressor and targets PTTG1IP in glioma", *Int. J. Clin. Exp. Pathol.,* 7(12):8573-8582.

Wang, Z., Yu, R. & Melmed, S. 2001, "Mice lacking pituitary tumor transforming gene show testicular and splenic hypoplasia, thymic hyperplasia, thrombocytopenia, aberrant cell cycle progression, and premature centromere division", *Mol. Endocrinol.,* 15(11):1870-1879.

Wang, X., Duan, W., Li, X., Liu, J., Li, D., Ye, L., Qian, L., Yang, A., Xu, Q., Liu, H., Fu, Q., Wu, E., Ma, Q. & Shen, X. 2015, "PTTG regulates the metabolic switch of ovarian cancer cells via the c-myc pathway", *Oncotarget,* 6(38):40959-40969.

Wang, Z. & Melmed, S. 2000, "Pituitary tumor transforming gene (PTTG) transforming and transactivation activity", *J. Biol. Chem.,* 275(11):7459-7461.

Watkins, R.J., Imuretaicharoenchoke, W., Sharma, N., Poole, L.V., Gentillin, E., Bansal, S., Bosseboeuf, E., Fletcher, R., Nieto, H.R., Mallick, U., Hackshaw, A., Mehanna, H., Boelaert, K., Read, M.L., Smith, E.V. & and McCabe, C.J. 2016, "Pro-invasive effect of proto-oncogene PBF is modulated by an interaction with cortactin", *J. Clin. Endocrinol. Metab.,* [Epub ahead of print].

Watkins, R.J., Read, M.L., Smith, V.E., Sharma, N., Reynolds, G.M., Buckley, L., Doig, C., Campbell, M.J., Lewy, G. & Eggo, M.C. 2010, "Pituitary tumor transforming gene binding factor: a new gene in breast cancer", *Cancer Res.,* 70(9):3739.

Weaver, A.M., Karginov, A.V., Kinley, A.W., Weed, S.A., Li, Y., Parsons, J.T. & Cooper, J.A. 2001, "Cortactin promotes and stabilizes Arp2/3-induced actin filament network formation", *Curr. Biol.,* 11(5):370-374.

Wentzensen, N., Vinokurova, S. & von Knebel Doeberitz, M. 2004, "Systematic review of genomic integration sites of human papillomavirus genomes in epithelial dysplasia and invasive cancer of the female lower genital tract", *Cancer Res.,* 64(11):3878-3884.

White, J.S., Weissfeld, J.L., Ragin, C.C.R., Rossie, K.M., Martin, C.L., Shuster, M., Ishwad, C.S., Law, J.C., Myers, E.N., Johnson, J.T. & Gollin, S.M. 2006, "The Influence of Clinical and Demographic Risk Factors on the Establishment of Head and Neck Squamous Cell Carcinoma Cell Lines", *Oral Oncol.,* 43(7):701-712.

Wolf, G.T., Hong, W.K., Fisher, S.G., Urba, S., Endicott, J.W., Close, L., Fisher, S.R., Toohill, R.J., Karp, D. & Miller, D.M. 1991, "Induction chemotherapy plus radiation compared with surgery plus radiation in patients with advanced laryngeal cancer", *N. Engl. J. Med.,* 324(24):1685-1690.

Wyss, A., Hashibe, M., Chuang, S.C., Lee, Y.C., Zhang, Z.F., Yu, G.P., Winn, D.M., Wei, Q., Talamini, R., Szeszenia-Dabrowska, N., Sturgis, E.M., Smith, E., Shangina, O., Schwartz, S.M., Schantz, S., Rudnai, P., Purdue, M.P., Eluf-Neto, J., Muscat, J., Morgenstern, H., Michaluart, P.,Jr, Menezes, A., Matos, E., Mates, I.N., Lissowska, J., Levi, F., Lazarus, P., La Vecchia, C., Koifman, S., Herrero, R., Hayes, R.B., Franceschi, S., Wunsch-Filho, V., Fernandez, L., Fabianova, E., Daudt, A.W., Dal Maso, L., Curado, M.P., Chen, C., Castellsague, X., de Carvalho, M.B., Cadoni, G., Boccia, S., Brennan, P., Boffetta, P. & Olshan, A.F. 2013, "Cigarette, cigar, and pipe smoking and the risk of head and neck cancers: pooled analysis in the International Head and Neck Cancer Epidemiology Consortium", *Am. J. Epidemiol.,* 178(5):679-690.

Xia, Y., Li, M., Fu, D., Xu, S., Li, Z., Liu, D. & Tian, Z. 2013, "Effects of PTTG Down-regulation on Proliferation and Metastasis of the SCL-1 Cutaneous Squamous Cell Carcinoma Cell Line", *Asian Pac. J. Cancer Prev.,* 14(11):6245-6248.

Xiang, C., Gao, H., Meng, L., Qin, Z., Ma, R., Liu, Y., Jiang, Y., Dang, C., Jin, L. & He, F. 2012, "Functional variable number of tandem repeats variation in the promoter of proto oncogene PTTG1IP is associated with risk of estrogen receptor positive breast cancer", *Cancer Sci.,* 103(6):1121-1128.

Xie, X., Piao, L., Bullock, B.N., Smith, A., Su, T., Zhang, M., Teknos, T.N., Arora, P.S. & Pan, Q. 2013, "Targeting HPV16 E6-p300 interaction reactivates p53 and inhibits the tumorigenicity of HPV-positive head and neck squamous cell carcinoma", *Oncogene,* 33(8):1037-46.

Xu, C., Kim, N. & Gumbiner, B.M. 2009, "Regulation of protein stability by GSK3 mediated phosphorylation", *Cell Cycle,* 8(24):4032-4039.

Yan, S., Zhou, C., Lou, X., Xiao, Z., Zhu, H., Wang, Q., Wang, Y., Lu, N., He, S., Zhan, Q., Liu, S. & Xu, N. 2009, "PTTG Overexpression Promotes Lymph Node Metastasis in Human Esophageal Squamous Cell Carcinoma", *Cancer Res.,* 69(8):3283-3290.

Yaspo, M., Aaltonen, J., Horelli-Kuitunen, N., Peltonen, L. & Lehrach, H. 1998, "Cloning of a novel human putative type Ia integral membrane protein mapping to 21q22. 3", *Genomics,* 49(1):133-136.

Ying, H., Suzuki, H., Furumoto, H., Walker, R., Meltzer, P., Willingham, M.C. & Cheng, S.Y. 2003, "Alterations in genomic profiles during tumor progression in a mouse model of follicular thyroid carcinoma", *Carcinogenesis,* 24(9):1467-1479.

Yoon, C.H., Kim, M.J., Lee, H., Kim, R.K., Lim, E.J., Yoo, K.C., Lee, G.H., Cui, Y.H., Oh, Y.S., Gye, M.C., Lee, Y.Y., Park, I.C., An, S., Hwang, S.G., Park, M.J., Suh, Y. & Lee, S.J. 2012, "PTTG1 oncogene promotes tumor malignancy via epithelial to mesenchymal transition and expansion of cancer stem cell population", *J. Biol. Chem.,* 287(23):19516-19527.

Yu, R., Heaney, A.P., Lu, W., Chen, J. & Melmed, S. 2000a, "Pituitary tumor transforming gene causes aneuploidy and p53-dependent and p53-independent apoptosis", *J. Biol. Chem.,* 275(47):36502-36505.

Yu, R., Lu, W., Chen, J., McCabe, C.J. & Melmed, S. 2003, "Overexpressed pituitary tumor-transforming gene causes aneuploidy in live human cells", *Endocrinology,* 144(11):4991-4998.

Yu, R., Ren, S., Horwitz, G.A., Wang, Z. & Melmed, S. 2000b, "Pituitary tumor transforming gene (PTTG) regulates placental JEG-3 cell division and survival: evidence from live cell imaging", *Mol. Endocrinol.,* 14(8):1137-1146.

Zhang, E., Liu, S., Xu, Z., Huang, S., Tan, X., Sun, C. & Lu, L. 2014, "Pituitary tumor-transforming gene 1 (PTTG1) is overexpressed in oral squamous cell carcinoma (OSCC) and promotes migration, invasion and epithelial–mesenchymal transition (EMT) in SCC15 cells", *Tumor Biol.,* 35(9):8801-8811.

Zhang, J., Yang, Y., Chen, L., Zheng, D. & Ma, J. 2013, "Overexpression of pituitary tumor transforming gene (PTTG) is associated with tumor progression and poor prognosis in patients with esophageal squamous cell carcinoma", *Acta Histochem., 116(3):435-9.*

Zhang, S., Shan, W., Yuan, L., Liu, Y. & Sun, L. 2016, "Effects of silencing PTTG expression by small interference RNA", *Eur. Rev. Med. Pharmacol. Sci.,* 20(13):2835-2841.

Zhang, X., Horwitz, G.A., Prezant, T.R., Valentini, A., Nakashima, M., Bronstein, M.D. & Melmed, S. 1999, "Structure, expression, and function of human pituitary tumor-transforming gene (PTTG)", *Mol. Endocrinol.,* 13(1):156-166.

Zheng, Y., Guo, J., Zhou, J., Lu, J., Chen, Q., Zhang, C., Qing, C., Koeffler, H.P. & Tong, Y. 2015, "FoxM1 transactivates PTTG1 and promotes colorectal cancer cell migration and invasion", *BMC Med. Gen.,* 8(1):49.

Zhou, C., Liu, S., Zhou, X., Xue, L., Quan, L., Lu, N., Zhang, G., Bai, J., Wang, Y. & Liu, Z. 2005, "Overexpression of human pituitary tumor transforming gene (hPTTG), is regulated by β catenin/TCF pathway in human esophageal squamous cell carcinoma", *Int. J. Cancer,* 113(6):891-898.

Zhou, G., Liu, Z. & Myers, J.N. 2016, "TP53 Mutations in Head and Neck Squamous Cell Carcinoma and Their Impact on Disease Progression and Treatment Response", *J. Cell. Biochem.*, [Epub ahead of print].

Zhou, Y., Mehta, K.R., Choi, A.P., Scolavino, S. & Zhang, X. 2003a, "DNA damage-induced inhibition of securin expression is mediated by p53", *J. Biol. Chem.,* 278(1):462.

Zhou, Y., Mehta, K.R., Choi, A.P., Scolavino, S. & Zhang, X. 2003b, "DNA damage-induced inhibition of securin expression is mediated by p53", *J. Biol. Chem,* 278(1):462-470.

Zimmermann, H., Degenkolbe, R., Bernard, H. & O'Connor, M.J. 1999, "The human papillomavirus type 16 E6 oncoprotein can down-regulate p53 activity by targeting the transcriptional coactivator CBP/p300", *J. Virol.*, vol. 73(8):6209-6219.

Zou, H., McGarry, T.J., Bernal, T. & Kirschner, M.W. 1999, "Identification of a vertebrate sister-chromatid separation inhibitor involved in transformation and tumorigenesis", *Science*, 285(5426):418-422.

Zur, A. & Brandeis, M. 2001, "Securin degradation is mediated by fzy and fzr, and is required for complete chromatid separation but not for cytokinesis", *EMBO,* 20(4):792-801.

# Chapter 10

# Appendix A

## 10.1 Sequences and locations of the PTTG shRNAs generated for use with the BLOCK-iT™ lentiviral RNAi expression system

The following figure shows the locations of the two PTTG shRNA target (sense) sequences within the PTTG cDNA sequence, designed for use with the BLOCK-iT™ lentiviral RNAi expression system. Sequences are highlighted and bold, and are also given in the table below. The 3' UTR is highlighted in yellow, the 5' UTR highlighted in grey and the translation initiation/termination sites highlighted in black.

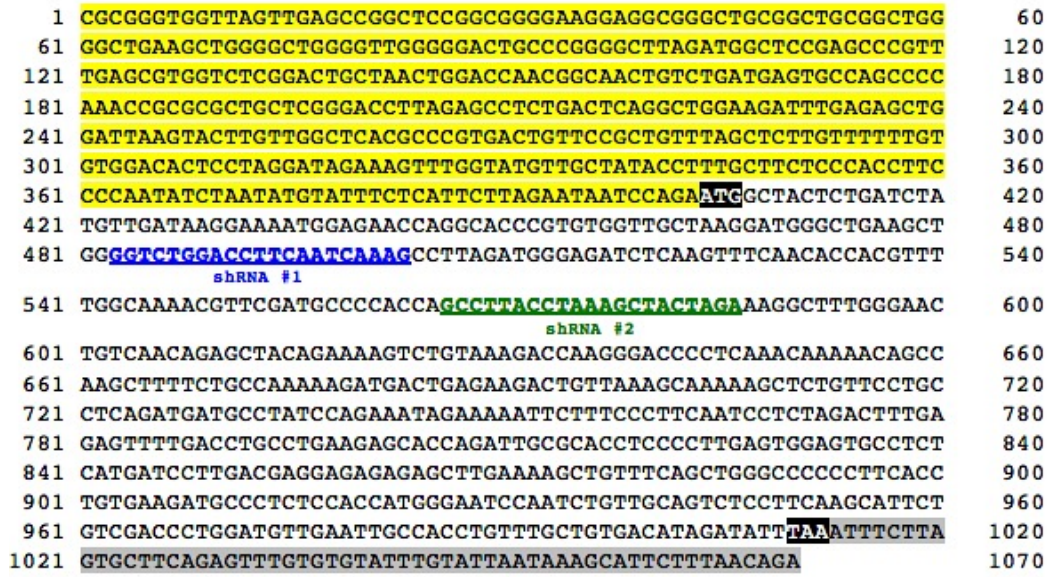


| shRNA ID | Sense sequence | Anti-sense sequence |
|---|---|---|
| PTTG shRNA #1 | 5'- GGTCTGGACCTTCAATCAAAG -3' | 5'- CTTTGATTGAAGGTCCAGACC -3' |
| PTTG shRNA #2 | 5'- GCCTTACCTAAAGCTACTAGA -3' | 5'- TCTAGTAGCTTTAGGTAAGGC -3' |

## 10.2 Sequences and locations of the PBF shRNAs generated for use with the BLOCK-iT™ lentiviral RNAi expression system

The following figure shows the locations of the four PBF shRNA target (sense) sequences within the PBF cDNA sequence, designed for use with the BLOCK-iT™ lentiviral RNAi expression system. Sequences are highlighted and bold, and are also given in the table below. The 3' UTR is highlighted in yellow, the 5' UTR highlighted in grey and the translation initiation/termination sites highlighted in black.

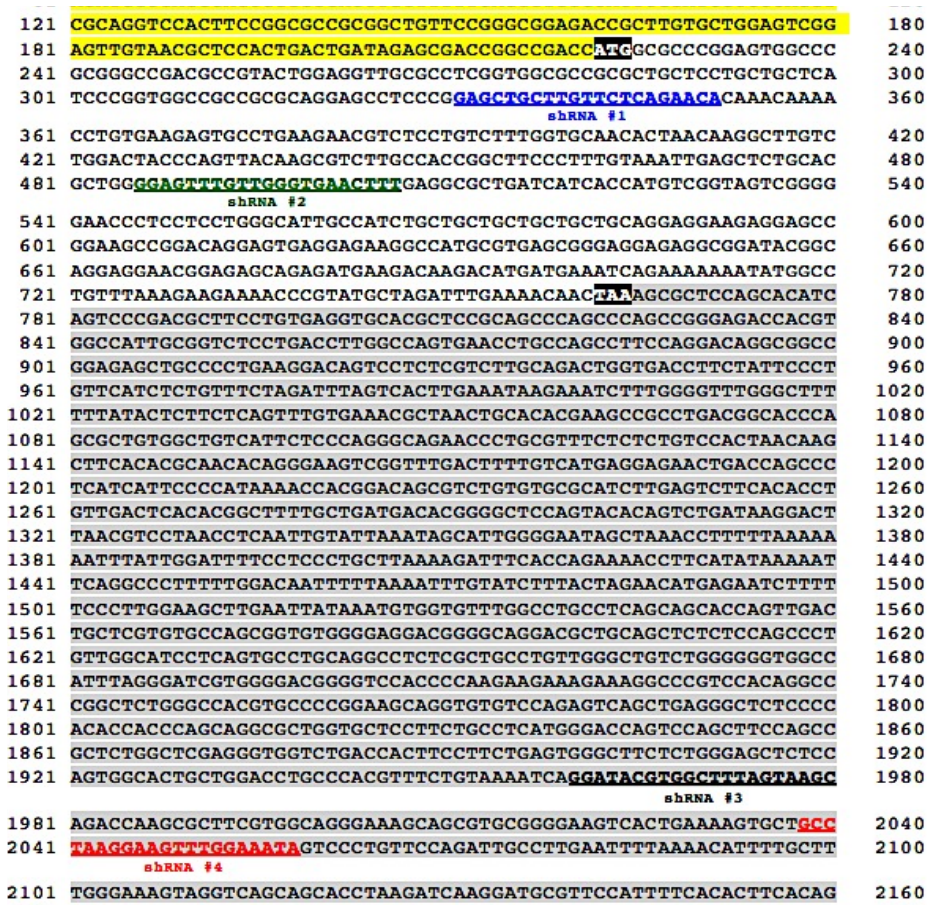


| shRNA ID | Sense sequence | Anti-sense sequence |
|---|---|---|
| PBF shRNA #1 | 5'- GAGCTGCTTGTTCTCAGAACA -3' | 5'- TGTTCTGAGAACAAGCAGCTC -3' |
| PBF shRNA #2 | 5'- GGAGTTTGTTGGGTGAACTTT -3' | 5'- AAAGTTCACCCAACAAACTCC -3' |
| PBF shRNA #3 | 5'- GCCTAAGGAAGTTTGGAAATA -3' | 5'- TATTTCCAAACTTCCTTAGGC -3' |
| PBF shRNA #4 | 5'- GGATACGTGGCTTTAGTAAGC -3' | 5'- GCTTACTAAAGCCACGTATCC -3' |

## 10.3 Sequences and locations of the SMARTvector 2.0 lentiviral PBF shRNAs

The following figure shows the locations of the three PBF shRNA target (sense) sequences within the PBF cDNA sequence. Sequences are highlighted and bold, and are also given in the table below. The 3' UTR is highlighted in yellow, the 5' UTR highlighted in grey and the translation initiation/termination sites highlighted in black.

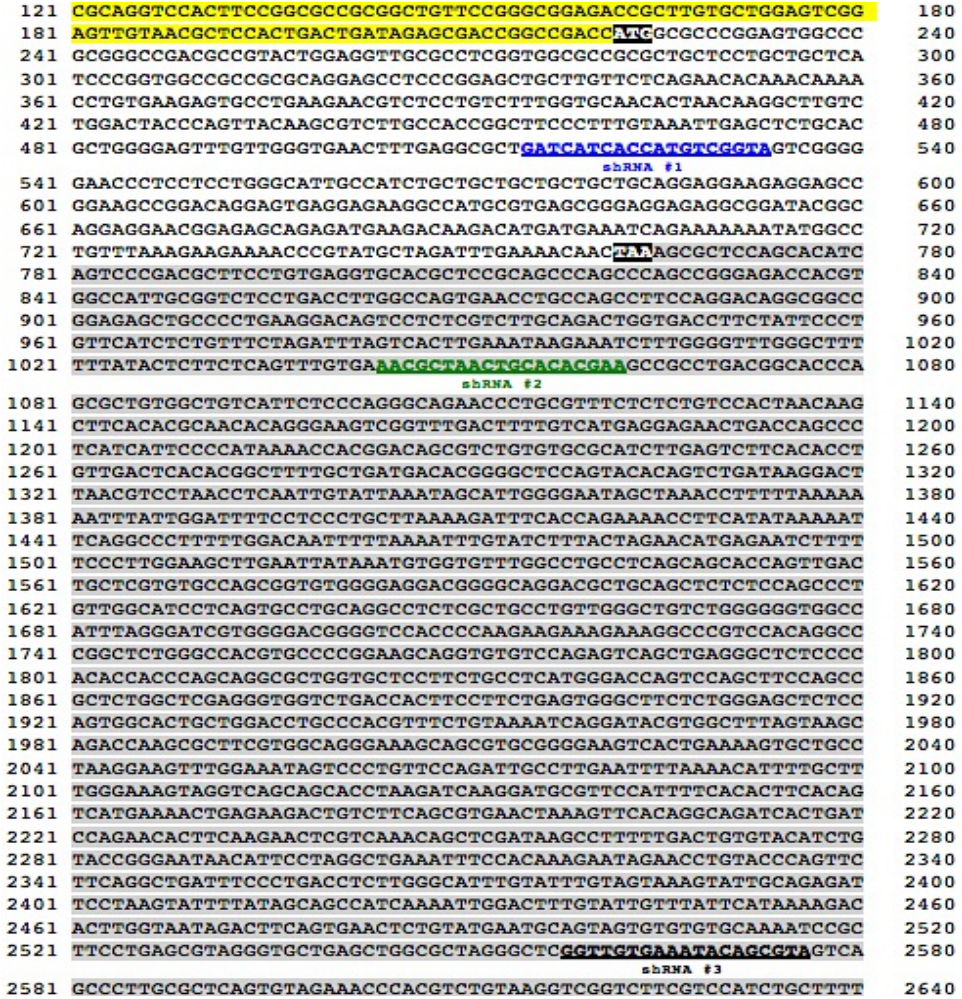


| shRNA ID | Target sequence |
|---|---|
| PBF shRNA #1 | 5'- GATCATCACCATGTCGGTA-3' |
| PBF shRNA #2 | 5'- AACGCTAACTGCACACGAA-3' |
| PBF shRNA #3 | 5'- GGTTGTGAAATACAGCGTA-3' |

# Chapter 11

# Bibliography

## 11.1 Publications relating to thesis

Read ML*, Seed RI*, Fong JC, Modasia B, Ryan GA, Watkins RJ, Gagliano T, Smith VE, Stratford AL, Kwan PK, Sharma N, Dixon OM, Watkinson JC, Boelaert K, Franklyn JA, Turnell AS, McCabe CJ. **The PTTG-binding factor (PBF/PTTG1IP) regulates p53 activity in thyroid cells.** *Endocrinology*. 2014 Apr; 155(4): 1222-34. *M.L.R and R.I.S are joint first authors.

Read ML*, Seed RI*, Modasia B, Kwan PK, Sharma N, Smith VE, Watkins RJ, Bansal S, Gagliano T, Stratford AL, Ismail T, Wakelam MJ, Kim DS, Ward ST, Boelaert K, Franklyn JA, Turnell AS, McCabe CJ. **The proto-oncogene PBF binds p53 and is associated with prognostic features in colorectal cancer.** *Mol. Carcinog.* 2016 Jan; 55(1): 15-26. *M.L.R and R.I.S contributed equally to this work.

Read ML*, Fong JCW*, Imruetaicharoenchoke W, Modasia B, Nieto H, Fletcher A, Thompson R, Bacon A, Mallick U, Hackshaw A, Watkinson JC, Boelaert K, Turnell AS, Smith VE, McCabe CJ. **Elevated PTTG and PBF predicts poor patient outcome and modulates DNA damage response genes in thyroid cancer.** *Oncogene.* 2016 – under revision. *M.L.R and R.I.S contributed equally to this work.

Imruetaicharoenchoke W, Watkins RJ, Modasia B, Poole VL, Nieto HR, Fletcher A, Thompson RJ, Boelaert K, Read ML, Smith VE, McCabe CJ. **Functional consequences of the first reported mutations of the proto-oncogene PTTG1IP/PBF.** *Endocr. Relat. Cancer.* 2016 – under revision.

## 11.2 Presentations

1. Poster presentation at British Thyroid Association meeting 2013
2. Poster presentation at International Federation of Head and Neck Oncologic Societies 5th World Congress meeting 2014
3. Poster presentation at the Wellcome Trust final year PhD student's meeting 2014
4. Poster presentation at British Endocrine Society meeting 2015